




8-2017

Discovery of Novel Tubulin Inhibitors and Selective Survivin Inhibitors for Advanced Melanoma and Total Synthesis of Bioactive 20S-hydroxyvitamin D3

Qinghui Wang
University of Tennessee Health Science Center

Follow this and additional works at: <https://dc.uthsc.edu/dissertations>

 Part of the [Medicinal and Pharmaceutical Chemistry Commons](#), [Neoplasms Commons](#), and the [Pharmaceutics and Drug Design Commons](#)

Recommended Citation

Wang, Qinghui (<http://orcid.org/0000-0002-9587-790X>), "Discovery of Novel Tubulin Inhibitors and Selective Survivin Inhibitors for Advanced Melanoma and Total Synthesis of Bioactive 20S-hydroxyvitamin D3" (2017). *Theses and Dissertations (ETD)*. Paper 452. <http://dx.doi.org/10.21007/etd.cghs.2017.0446>.

This Dissertation is brought to you for free and open access by the College of Graduate Health Sciences at UTHSC Digital Commons. It has been accepted for inclusion in Theses and Dissertations (ETD) by an authorized administrator of UTHSC Digital Commons. For more information, please contact jwelch30@uthsc.edu.

Discovery of Novel Tubulin Inhibitors and Selective Survivin Inhibitors for Advanced Melanoma and Total Synthesis of Bioactive 20S-hydroxyvitamin D3

Abstract

According to the statistics from American Cancer Society, the 5-year survival rate for patients with advanced melanoma is as low as 5%. Treatment of advanced melanoma, therefore, represents an unmet medical need. In this dissertation, I will show the effort to develop new generations of bioavailable tubulin inhibitors targeting the colchicine binding site and selective small-molecule survivin inhibitors for treating advanced melanoma. Extensive structure-activity relationship (SAR) studies of lead molecules ABI-231 and UC-112 have been performed.

Chapter 1 will introduce the current situation of advanced or metastatic melanoma, its clinical drug treatments, as well as problems in current drug treatments. Microtubule dynamics and survivin will be discussed as promising therapeutic targets for developing anticancer drugs. 20S-hydroxyvitamin D3 (20S-OH-D3) will be introduced as a promising anti-inflammatory scaffold.

Chapter 2 will disclose the SAR study of ABI-231, a previously reported potent tubulin inhibitor from our lab. In this chapter, a new synthetic method was developed to enable the synthesis of ABI-231 analogues modifying the indole moiety. The novel synthetic method involved the synthesis of a key diamine intermediate and imidazoline formation. From the new synthetic method, thirty ABI-231 analogues were synthesized and tested for activities. Among all analogues, 10ab with a 4-methyl-3-indole moiety and 10bb with a 4-indole moiety showed the most potent antiproliferative activities against a panel of melanoma cell lines. 10ab and 10bb had IC₅₀s of 2.2 and 3.0 nM, respectively. The SAR result revealed that modification of the indole moiety in ABI-231 was beneficial to activity.

In Chapter 3, we will describe our effort to develop the SAR study of ABI-231 focusing on modification of the 3,4,5-TMP moiety. This is selected since it is one of the most common moieties in current tubulin inhibitors targeting the colchicine binding site. To circumvent the use of potentially explosive azide reported in Chapter 2, an alternative was established to efficiently generate ABI-231 analogues. This new synthetic method involved Suzuki coupling and Grignard reactions to modify the 3,4,5-TMP moiety and to produce target compounds in gram-scale. Among the eight analogues synthesized, the one containing an unique 3-methoxybenzo[4,5]-dioxene moiety had the strongest antiproliferative activity against a panel of melanoma cell lines with an average IC₅₀ of 1.9 nM. To our best knowledge, it represents the most successful instance of isosterically modifying the 3,4,5-TMP moiety in CA-4 derivatives.

Chapter 4 will highlight our effort to synthesize reverse ABI (RABI) analogues for SAR study. In this chapter, a novel and concise synthetic route was established to access RABI scaffold. RABI scaffold was constructed through a Grignard reaction/Suzuki-Miyaura coupling reaction strategy. From this new synthetic method, twelve novel RABI analogues were synthesized. Compared to MX-RABI (the previously reported most potent RABI), several new RABI analogues showed significantly improved cytotoxicities. In particular, analogue 15i with a 4-indazole moiety showed the most potent antiproliferative activity against a panel of melanoma cell lines and had an average IC₅₀ of 0.8 nM. This is the first sub-nM anti-tubulin compound in the related scaffolds.

Chapter 5 will reveal our latest SAR study of UC-112, a previously reported selective survivin inhibitor. Fourteen UC-112 analogues modifying the benzyloxy moiety of UC-112 were synthesized. Their corresponding SAR result demonstrated that indole moiety was the most favorable (analogue 12a). Subsequent structural optimization of 12a by introducing either mono-substituent or di-substituent to the indole moiety led to the synthesis of another twenty-four new UC-112 analogues. Several substituted indole analogues showed equipotency to that of UC-112 and MX-106. Importantly, new indole analogues

exhibited significant abilities to overcome multidrug-resistance mediated by Pgp overexpression.

Chapter 6 is characterized by the establishment of a total synthetic method of 20SOH-D3 which showed comparable antiproliferative activity to 1,25 α -dihydroxyvitamin D3 without hypercalcemic toxic effect upto a concentration of 60 μ g/kg in vivo. The total synthesis of 20S-OH-D3 involved parallel generation of key intermediates from ergocalciferol. The vitamin D3 core structure was constructed through Wittig-Horner coupling reaction. Deprotection of SEM and TBS was achieved in one step. 20S-OH-D3 was furnished in sixteen steps with an overall yield of 0.4%.

Document Type

Dissertation

Degree Name

Doctor of Philosophy (PhD)

Program

Pharmaceutical Sciences

Research Advisor

Wei Li, Ph.D.

Keywords

medicinal chemistry, microtubule inhibitor, survivin inhibitor, synthetic chemistry, total synthesis, vitamin D3

Subject Categories

Diseases | Medicinal and Pharmaceutical Chemistry | Medicine and Health Sciences | Neoplasms |
Pharmaceutics and Drug Design | Pharmacy and Pharmaceutical Sciences

**Discovery of Novel Tubulin Inhibitors and Selective Survivin Inhibitors for
Advanced Melanoma and Total Synthesis of Bioactive 20S-hydroxyvitamin D3**

A Dissertation
Presented for
The Graduate Studies Council
The University of Tennessee
Health Science Center

In Partial Fulfillment
Of the Requirements for the Degree
Doctor of Philosophy
From The University of Tennessee

By
Qinghui Wang
August 2017

Portions of Chapter 6 © 2015 by Elsevier.
All other material © 2017 by Qinghui Wang.
All rights reserved.

ACKNOWLEDGEMENTS

First and foremost, I wish to express my special appreciation to my advisor, Dr. Wei Li, who opened a door for me to join his group in the third year of my graduate study. This is an unforgettable favor in my whole life. Dr. Li has been supportive from all perspectives including course learning and research conducting. In the last more than three years, he kept navigating me toward the right direction wherever he thought was right; he also endowed me the freedom to pursue what I proposed. He has set an outstanding example of being a supervisor, researcher, and individual.

My gratitude is also extended to Dr. Subhash C. Chauhan, Dr. Duane D. Miller, Dr. Bob M. Moore, and Dr. Fatima Rivas (from St. Jude Children's Research Hospital) for serving as my committee members. Their discussion and ideas are invaluable throughout my research. In addition, special thank is addressed to Dr. Duane D. Miller for his meaningful discussion during every group meeting.

I would especially thank my labmate Kinsie E. Arnst and Dr. Yi Xue for obtaining *in vitro* biological data for the synthesized tubulin inhibitors and survivin regulators. I am also grateful to the following persons for helping my research from different perspectives: Dr. Yuxi Wang and Dr. Jinliang Yang at Sichuan University for generating many co-crystal structures of tubulin inhibitors in complex with tubulin protein, Zining Lei and Dr. Zhe-sheng Chen at St. John's University for acquiring biological data on P-gp overexpressed cell lines in survivin project, Dr. Andrzej T. Slominski and Mr. Tae-kang Kim at University of Alabama for helping on the vitamin D3 project. I am also indebted to the current and former members of Dr. Wei Li's group.

Last, thanks to my parents for their unconditional support in my life. Special thanks to my wife Chenghong Meng. Without her encouragement, this thesis would never be finished. Thanks to my sweetheart Clair and Elvin for bringing joy to my life.

ABSTRACT

According to the statistics from American Cancer Society, the 5-year survival rate for patients with advanced melanoma is as low as 5%. Treatment of advanced melanoma, therefore, represents an unmet medical need. In this dissertation, I will show the effort to develop new generations of bioavailable tubulin inhibitors targeting the colchicine binding site and selective small-molecule survivin inhibitors for treating advanced melanoma. Extensive structure-activity relationship (SAR) studies of lead molecules ABI-231 and UC-112 have been performed.

Chapter 1 will introduce the current situation of advanced or metastatic melanoma, its clinical drug treatments, as well as problems in current drug treatments. Microtubule dynamics and survivin will be discussed as promising therapeutic targets for developing anticancer drugs. 20*S*-hydroxyvitamin D3 (20*S*-OH-D3) will be introduced as a promising antiinflammatory scaffold.

Chapter 2 will disclose the SAR study of ABI-231, a previously reported potent tubulin inhibitor from our lab. In this chapter, a new synthetic method was developed to enable the synthesis of ABI-231 analogues modifying the indole moiety. The novel synthetic method involved the synthesis of a key diamine intermediate and imidazoline formation. From the new synthetic method, thirty ABI-231 analogues were synthesized and tested for activities. Among all analogues, **10ab** with a 4-methyl-3-indole moiety and **10bb** with a 4-indole moiety showed the most potent antiproliferative activities against a panel of melanoma cell lines. **10ab** and **10bb** had IC₅₀s of 2.2 and 3.0 nM, respectively. The SAR result revealed that modification of the indole moiety in ABI-231 was beneficial to activity.

In Chapter 3, we will describe our effort to develop the SAR study of ABI-231 focusing on modification of the 3,4,5-TMP moiety. This is selected since it is one of the most common moieties in current tubulin inhibitors targeting the colchicine binding site. To circumvent the use of potentially explosive azide reported in Chapter 2, an alternative was established to efficiently generate ABI-231 analogues. This new synthetic method involved Suzuki coupling and Grignard reactions to modify the 3,4,5-TMP moiety and to produce target compounds in gram-scale. Among the eight analogues synthesized, the one containing an unique 3-methoxybenzo[4,5]-dioxene moiety had the strongest antiproliferative activity against a panel of melanoma cell lines with an average IC₅₀ of 1.9 nM. To our best knowledge, it represents the most successful instance of isosterically modifying the 3,4,5-TMP moiety in CA-4 derivatives.

Chapter 4 will highlight our effort to synthesize reverse ABI (RABI) analogues for SAR study. In this chapter, a novel and concise synthetic route was established to access RABI scaffold. RABI scaffold was constructed through a Grignard reaction/Suzuki-Miyaura coupling reaction strategy. From this new synthetic method, twelve novel RABI analogues were synthesized. Compared to MX-RABI (the previously reported most potent RABI), several new RABI analogues showed significantly

improved cytotoxicities. In particular, analogue **15i** with a 4-indazole moiety showed the most potent antiproliferative activity against a panel of melanoma cell lines and had an average IC_{50} of 0.8 nM. This is the first sub-nM anti-tubulin compound in the related scaffolds.

Chapter 5 will reveal our latest SAR study of UC-112, a previously reported selective survivin inhibitor. Fourteen UC-112 analogues modifying the benzyloxy moiety of UC-112 were synthesized. Their corresponding SAR result demonstrated that indole moiety was the most favorable (analogue **12a**). Subsequent structural optimization of **12a** by introducing either mono-substituent or di-substituent to the indole moiety led to the synthesis of another twenty-four new UC-112 analogues. Several substituted indole analogues showed equipotency to that of UC-112 and MX-106. Importantly, new indole analogues exhibited significant abilities to overcome multidrug-resistance mediated by P-gp overexpression.

Chapter 6 is characterized by the establishment of a total synthetic method of 20S-OH-D3 which showed comparable antiproliferative activity to 1,25 α -dihydroxyvitamin D3 without hypercalcemic toxic effect upto a concentration of 60 $\mu\text{g}/\text{kg}$ *in vivo*. The total synthesis of 20S-OH-D3 involved parallel generation of key intermediates from ergocalciferol. The vitamin D3 core structure was constructed through Wittig-Horner coupling reaction. Deprotection of SEM and TBS was achieved in one step. 20S-OH-D3 was furnished in sixteen steps with an overall yield of 0.4%.

TABLE OF CONTENTS

CHAPTER 1. INTRODUCTION	1
Advanced Melanoma	1
Drug Treatment for Advanced Melanoma.....	1
Targeted therapy	3
BRAF inhibitors.....	3
MEK inhibitor.....	3
C-kit inhibitor.....	4
Immune checkpoint inhibitors	5
Anti CTLA4 antibodies.....	5
Anti PD-1 antibodies.....	5
Chemotherapy	6
Challenges in targeted therapy and immunotherapy.....	6
Tubulin Inhibitors for Treatment of Cancer	7
Microtubule dynamics as a therapeutic target.....	7
Binding sites in tubulin	7
Tubulin inhibitors approved by FDA or in clinical development.....	9
Challenges in developing microtubule targeting agents as anticancer agents	9
Targeting colchicine binding site in tubulin for development of anticancer agents ..	11
Survivin as a Therapeutic Target for Cancer Treatment.....	11
Survivin as a therapeutic target.....	11
Major survivin inhibitors	13
Challenges in developing survivin inhibitors as anticancer agents	13
Vitamin D3 for Cancer Treatment	13
1 α ,25-dihydroxyvitamin D3 and its limit.....	13
20S-hydroxyvitamin D3 as a promising therapy for cancers.....	15
Discussion.....	15
CHAPTER 2. STRUCTURE-ACTIVITY RELATIONSHIP STUDY OF ABI-231 LEADS TO IMPROVED ACTIVITIES AGAINST MICROTUBULE POLYMERIZATION	20
Introduction.....	20
Experimental Section	21
General chemistry	21
Chemical synthesis.....	23
Cell culture and reagents.....	31
Cytotoxicity assay.....	31
Chemistry.....	32
Results.....	35
<i>In vitro</i> growth inhibitory effects of ABI-231 analogues with 3-indolylys	35
<i>In vitro</i> growth inhibitory effects of ABI-231 analogues with rotation of indolylys...40	40
Discussion.....	40

CHAPTER 3. STRUCTURAL MODIFICATION OF THE 3,4,5-TRIMETHOXYPHENYL MOIETY IN ABI-231 LEADS TO IMPROVED ANTIPROLIFERATIVE ACTIVITIES.....	44
Introduction.....	44
Experimental Section.....	46
General chemistry.....	46
Chemical synthesis.....	46
Cell culture and reagents.....	54
Cytotoxicity assay.....	55
Chemistry.....	55
Results.....	57
Discussion.....	60
CHAPTER 4. DESIGN AND SYNTHESIS OF NOVEL RABI ANALOGUES AS POTENT ANTITUBULINS.....	62
Introduction.....	62
Experimental Section.....	64
General chemistry.....	64
Chemical synthesis.....	64
Cell culture and reagents.....	71
Cytotoxicity assay.....	71
Chemistry.....	72
Results.....	72
Discussion.....	75
CHAPTER 5. DESIGN, SYNTHESIS AND STRUCTURE-ACTIVITY RELATIONSHIP STUDY OF NOVEL UC-112 ANALOGUES.....	80
Introduction.....	80
Experimental Section.....	81
General chemistry.....	81
Chemical synthesis.....	81
Cell culture and reagents.....	93
Cytotoxicity assay.....	94
Cytotoxicity against P-gp overexpressed cell lines by MTT assay.....	94
Liver microsomes stability assay.....	95
Chemistry.....	96
Results.....	96
<i>In vitro</i> growth inhibitory effects of UC-112 analogues with modification of benzyloxy moiety.....	96
<i>In vitro</i> growth inhibitory effects of UC-112 analogues with mono-substitution on the indole moiety.....	100
<i>In vitro</i> growth inhibitory effects of UC-112 analogues with di-substituents on the indole moiety.....	100
Inhibitory effect against P-gp overexpressed cell lines.....	103
<i>In vitro</i> metabolic stability study.....	103

Discussion.....	106
CHAPTER 6. TOTAL SYNTHESIS OF BIOLOGICAL ACTIVE 20S-HYDROXYVITAMIN D3.....	108
Introduction.....	108
Experimental Section.....	110
General chemistry.....	110
Chemical synthesis.....	110
Chemistry.....	116
Results.....	121
Discussion.....	121
CHAPTER 7. SUMMARY AND FUTURE DIRECTION	125
LIST OF REFERENCES.....	131
VITA.....	149

LIST OF TABLES

Table 2-1.	<i>In vitro</i> growth inhibitory effects (nM) of ABI-231 analogues with 3-indolyls (n=3)	37
Table 2-2.	<i>In vitro</i> growth inhibitory effects (nM) of ABI-231 analogues with rotation of indolyls (n=3)	38
Table 2-3.	Crystallographic data and structure refinement statistics for 10ab	42
Table 3-1.	<i>In vitro</i> growth inhibitory effects (nM) of ABI-231 analogues modifying the 3,4,5-TMP moiety (n=3)	59
Table 4-1.	<i>In vitro</i> growth inhibitory effects (nM) of RABI analogues (n=3)	76
Table 5-1.	<i>In vitro</i> growth inhibitory effects (μ M) of UC-112 analogues with modification of benzyloxy moiety (n=3)	99
Table 5-2.	<i>In vitro</i> growth inhibitory effects (μ M) of UC-112 analogues with mono-substituent on the indole moiety (n=3)	101
Table 5-3.	<i>In vitro</i> growth inhibitory effects (μ M) of UC-112 analogues with di-substituents on the indole moiety (n=3)	102
Table 5-4.	<i>In vitro</i> growth inhibitory effects of indole analogues in P-gp overexpressed cell line M14/MDR1 (n=3)	104
Table 5-5.	<i>In vitro</i> growth inhibitory effects of 10f, 10i, 10l and 10o in P-gp overexpressed cell lines (n=3)	105
Table 5-6.	<i>In vitro</i> microsomal stabilities of compounds 10f, 10i, 10l and 10o	107
Table 7-1.	<i>In vitro</i> growth inhibitory effect of proposed analogue and its intermediates	130

LIST OF FIGURES

Figure 1-1. Biological driver of melanoma	2
Figure 1-2. Binding sites in tubulin	8
Figure 1-3. Microtubule-stabilizing agents.....	10
Figure 1-4. Microtubule-destabilizing agents.....	10
Figure 1-5. Colchicine binding site inhibitors in clinical trials	12
Figure 1-6. Structures of the major survivin inhibitors	14
Figure 1-7. Molecule modeling result of ABI-231 in tubulin (PDB: 3HKD)	17
Figure 1-8. Proposed modification of UC-112 by reducing the flexibility of benzyloxy moiety	19
Figure 2-1. Examples of microtubule inhibitors that target colchicine binding sites in tubulin.....	22
Figure 2-2. Synthesis of an intermediate for 2-methyl-3-indole ABI-231 analogue.....	38
Figure 2-3. Co-crystal structure of 10ab in complex with tubulin	43
Figure 3-1. Examples of microtubule inhibitors with 3,4,5-TMP moieties targeting colchicine binding sites in tubulin.....	45
Figure 4-1. Examples of microtubule inhibitors binding to the colchicine binding sites in tubulin	63
Figure 4-2. Hypothesis: modifying the benzene in RABI to indole can increase activity.....	63
Figure 4-3. Synthesis of RABI scaffolds and proposed mechanism toward the observed major product.....	77
Figure 4-4. Synthesis of an intermediate for ABI-231 analogue.....	79
Figure 4-5. Structure and IC50 comparisons between ABI-231 and 15a, 15b and 15i...79	
Figure 5-1. Example of reported survivin inhibitors	82
Figure 5-2. Structures of UC-112 analogues with modification of benzyloxy moiety ...	99
Figure 6-1. Marketed vitamin D analogs and noncalcemic 20S-(OH)D3	109

Figure 6-2. Preferred conformation of the intermediate (compound 12) calculated with density function theory with 6-31G** baseset.....	122
Figure 6-3. ¹ H-NMR comparison of 20 <i>S</i> -(OH)D3 obtained via UVB irradiation and total synthesis	123
Figure 7-1. Docking study of proposed ABI-231 analogues in co-crystal structure of 4-methyl-3-indole analogue in complex with tubulin	129

LIST OF ABBREVIATIONS

ABC	ATP binding cassette
ABI	2-aryl-4-benzoyl-imidazoles
ADC	antibody-drug conjugate
ADP	adenosine triphosphate
ATCC	American type culture collection
ATP	adenosine triphosphate
CA-4	combretastatin A-4
CA-4P	combretastatin A-4 phosphate
CBSI	colchicine binding site inhibitor
CDK	cyclin-dependent kinase
CYP	cytochrome P450
DCM	dichloromethane
DMEM	Dulbecco's modified eagle's medium
DMF	dimethylformamide
DMSO	dimethyl sulfoxide
DNA	deoxyribonucleic acid
EtOAc	ethyl acetate
FDA	food and drug administration
GDP	guanosine diphosphate
GTP	guanosine triphosphate
HPLC	high performance liquid chromatography
IAP	inhibitor of apoptosis protein
IC50	concentration of 50% growth inhibition
MAP	mitogen-activated protein kinase
MDR1	multidrug resistance protein 1
MRP	multidrug resistance associated protein
MTA	microtubule-targeting agent
mTOR	mammalian target of rapamycin
PAT	phenyl-aminothiazole
PBS	phosphate-buffered saline
PD-1	programmed cell death-1
P-gp	P-glycoprotein
PI3K	phosphatidylinositol 3-kinase
PFS	progression-free survival
RABI	reverse 2-aryl-4-benzoyl-imidazoles
RAF	rapidly accelerated fibrosarcoma
RTK	receptor tyrosine kinase
SAR	structure-activity relationships
Sma	second mitochondria-derived activator of caspases
SMART	4-substituted methoxy benzoylaryl-thiazoles
THF	tetrahydrofuran
TLC	thin layer chromatography
TMS	trimethyl silane

VDR	vitamin D3 receptor
XIAP	X-linked inhibitor of apoptosis
1,25(OH) ₂ D3	1 α ,25-dihydroxyvitamin D3
2-ME	2-methoxyestradiol
20S-(OH)D3	20S-hydroxyvitamin D3
25-(OH)D3	25-hydroxyvitamin D3

CHAPTER 1. INTRODUCTION

Advanced Melanoma

Melanoma is the least common form of skin cancers and accounts for only about 5% in cases. It is, however, the deadliest form of all skin cancers and is responsible for approximately 80% deaths of patients with skin cancers. According to the statistics from the American Cancer Society, it is estimated that approximately 87,110 new cases of melanoma will be diagnosed and about 9,730 deaths will result from melanoma in 2017 [1]. There are five stages in melanoma progress: stages 0-IV. Melanoma begins within a single lesion but can spread to nearby lymph nodes and distant organs such as the lung, liver, or brain. Melanoma in stage IV is named advanced or metastatic melanoma. For patients who are at the very early stage of melanoma, the 5-year survival rate is over 98%. Surgery is an effective treatment for patients having melanoma with a low thickness in the skin (Breslow depths of up to 1.0 mm) [2]. For patients with advanced melanoma, the 5-year survival rate is 5-19% [3].

In nearly 90% cases of melanoma, mitogen-activated protein kinase (MAPK) pathway kinases were reported as activated [4]. MAPK pathway (**Figure 1-1**) is composed of a variety of kinases linking the extracellular signals to the DNA in the nucleus. MAPK pathway plays an important role in controlling diverse cellular functions including cell growth, differentiation, proliferation and apoptosis [5]. RAS is a G protein attached to the inner membrane. Upon receiving the activation signals from upstream kinases, GDP on the RAS can be detached. Free RAS can bind to GTP to form RAS-GTP complex and become activated. On one hand, the RAS-GTP complex can activate BRAF. Activated BRAF subsequently induces the phosphorylations of MEK and ERK in a sequential fashion. Phosphorylated ERK can then translocate into the nucleus to exert a series of cell-regulating functions [6-8]. On the other hand, the RAS-GTP complex can stimulate the phosphoinositide 3-kinase (PI3K) which phosphorylates phospholipid phosphatidylinositol 4,5-bisphosphate (PIP₂) to phospholipid phosphatidylinositol 3,4,5-trisphosphate (PIP₃). The intracellular signaling propagator PIP₃ can promote the phosphorylation of the well-known oncogene AKT. Elevated phosphorylation of AKT activates the downstream serine/threonine kinase mTOR, a protein that is of great importance in regulating cell growth, metabolism, and proliferation [9-11]. Phosphorylated AKT and activated mTOR are related to the death of melanoma patients. It is reported that nearly 70% of the malignant melanoma cases have elevated levels of phosphorylated AKT and activated mTOR [12, 13].

Drug Treatment for Advanced Melanoma

Currently, drug treatments for melanoma can be divided into three categories: targeted therapy, chemotherapy, and immunotherapy.

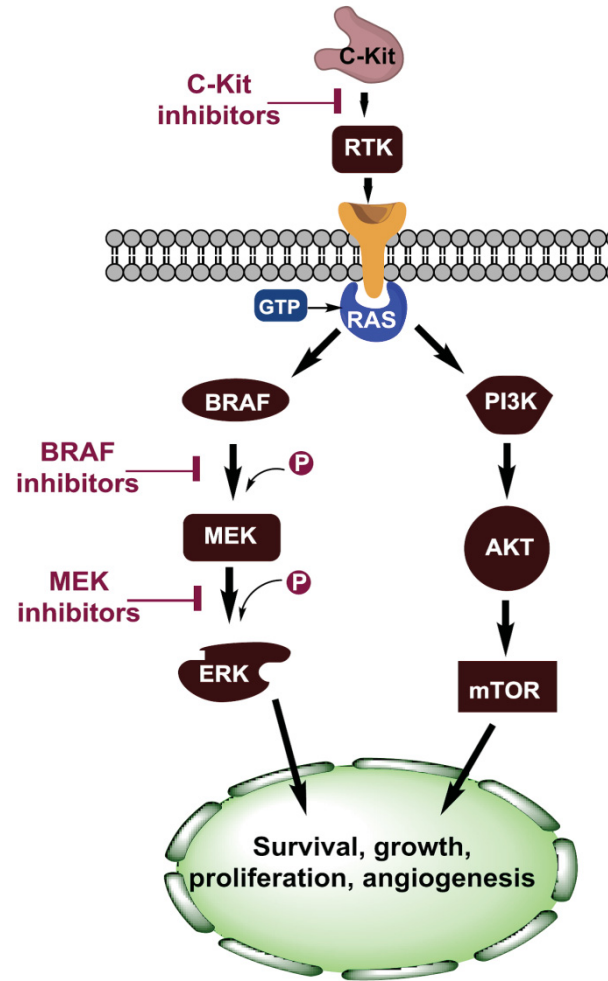


Figure 1-1. Biological driver of melanoma

Targeted therapy



BRAF inhibitors

RAF is a serine/threonine-specific protein kinase. The RAF family consists of four family members: ARAF, BRAF, CRAF and RAF1 [14]. BRAF is an oncogenic driver, which has been demonstrated in both *in vitro* and *in vivo* models [15-17]. It was shown in 2002 that nearly 50% of melanomas harbored BRAF mutations. 90% of the mutations replaced valine at amino acid 600 with glutamate (V600E) while a small portion of mutations substituted the valine with lysine, arginine or aspartic acid (V600K, V600R/D) [15]. These mutations in the BRAF gene was demonstrated to be responsible for the activation of MAPK pathway [18].

Vemurafenib, the first BRAF inhibitor, was approved by the FDA in 2011. It is applied for the treatment of metastatic or unresectable melanoma harboring the BRAF V600E mutation. Unlike nonspecific kinase inhibitors such as sorafenib, in a preclinical study vemurafenib was revealed to selectively bind to the activated mutant kinase BRAF at the ATP-binding site of V600E to inactivate the ERK phosphorylation [19]. An *in vivo* BRAF V600E xenograft animal model study suggested that vemurafenib markedly impeded tumor growth in the absence of significant toxicity. In phase I and II clinical studies, vemurafenib treatment significantly reduced the tumor size, improved overall survival rate, and enhanced progression-free survival in melanoma patients harboring BRAF V600E mutation. It was also reported that the median overall survival reached 13.6 months on average [20, 21]. For patients harboring BRAF V600K or non-V600K mutation, no complete or partial response was observed after treated with vemurafenib. Most frequently observed side effects for vemurafenib treatment in Phase II and III studies included but were no limited to fatigue, rash, and arthralgia [22].

Another FDA approved selective BRAF inhibitor is dabrafenib (approved in 2013). Darafenib has a similar response rate and survival rate to that of vemurafenib. Darafenib differs from vemurafenib in adverse effect profile. Whilst drug-specific side effects for darafenib include fever, specific side effects for vemurafenib involve photosensitivity and aminotransferase elevations [22]. In addition, dabrafenib is less likely to induce arthralgia and squamous cell carcinoma than vemurafenib [23].

MEK inhibitor

MEK1/2 is a serine/tyrosine/threonine kinase. It is a downstream target of the MAPK pathway. This cascade is activated and phosphorylated by RAF kinase at serines 22 and 218 in the activation loop [24]. The abilities of RAF subtypes to activate MEK follow the sequence of BRAF > RAF1 > ARAF > CRAF [25, 26]. Activated MEK subsequently stimulates the phosphorylation of ERK. Inhibition of MEK can obstruct cell proliferation and promote apoptosis [27]. Trametinib and cobimetinib are FDA approved MEK inhibitors. Other MEK1/2 inhibitors such as selumetinib, sinimetinib (MEK162), PD-0325901, TAK733, pimasertib, and RO4987655 are currently under clinical development.

Trametinib (GSK1120212) is the first MEK1/2 inhibitor approved by the FDA (approved in 2013). It is applied for treatment of metastatic melanoma with BRAF V600E/K mutation. Trametinib is a non-competitive MEK1/2 inhibitor and specifically binds to an allosteric binding site instead of the ATP site in MEK. Compared to BRAF inhibitors vemurafenib and dabrafenib, trametinib was less effective to improve median PFS and to trigger complete or partial response [28, 29] but was less likely to cause significant toxicities [30]. In particular, trametinib did not induce cutaneous squamous cell carcinoma. In a phase III trial that enrolled 322 patients, trametinib significantly prolonged the median PFS and overall survival of the patients with BRAF-mutated melanoma compared to chemotherapy treatments such as paclitaxel, or dacarbazine (DTIC) [31].

Cobimetinib is another MEK1/2 inhibitor approved by the FDA recently (2015). It is mainly used as a combinational therapy with vemurafenib to treat patients with BRAF-mutated metastatic melanoma. In phase III clinical trial that enrolled 495 patients with advanced melanoma, the combination of cobimetinib and vemurafenib significantly improved the median progression-free survival compared to vemurafenib alone [32].

Selumetinib is a MEK1/2 inhibitor that was in a phase II clinical trial. The *in vitro* assay displayed that selumetinib specifically bond to an adjacent allosteric binding site next to the ATP site in MEK1/2. Selumetinib showed potent antiproliferative activity in melanoma cell lines with BRAF V600E mutation and arrested the cell cycle in G1-phase [33-35]. In a phase I clinical study, selumetinib was found to markedly inactivate phosphorylation of ERK [33]. Nevertheless, in a phase II clinical study, selumetinib was unable to induce significant objective response. Current effort on selumetinib is, therefore, focusing on improving its clinical efficacy by combining with a BRAF inhibitor [36].

C-kit inhibitor

C-Kit, a receptor tyrosine kinase protein encoded by the Kit gene, is expressed in mature melanocytes. C-Kit binds to its ligand stem cell factor to trigger several signaling pathways including the MAPK pathway, the PI3K/AKT pathway, and the JAK-STAT pathway. In melanoma, 55% of the c-Kit mutated cells contain the substitution of L576P and K642E [37]. Recent studies reveal that c-Kit can induce melanocyte proliferation and melanoma survival through activation of the MAPK pathway [38].

Imatinib mesylate is an ATP-competitive inhibitor of c-Kit. In a Phase II study, imatinib was demonstrated to show significant antitumor activity, particularly in patients with advanced melanoma harboring c-Kit abreactions [39]. It was pointed out that metastatic melanoma with c-Kit mutations responded more strikingly to imatinib than metastatic melanoma with c-Kit amplifications [40]. An in-depth investigation is currently undergoing to explore the effect of imatinib on c-Kit mutated advanced melanoma.

Nilotinib, a tyrosine kinase inhibitor, was reported to be effective in imatinib-resistant gastrointestinal stromal tumors. Recently, in a phase II clinical trial, nilotinib

showed a lasting response in patients with metastatic melanoma harboring c-Kit mutations [41]. In another phase II study that enrolled patients with metastatic melanoma harboring c-Kit mutations, nilotinib tremendously improved one-year survival rate of patients and triggered durable response without causing severe adverse effects [41, 42].

Immune checkpoint inhibitors

Cancer cells can develop various mechanisms to evade the surveillance of the immune system. The mechanisms include but are not limited to releasing of inhibitory cytokines, recruiting immunosuppressive immune cells and upregulating immune checkpoints [43]. Therefore, inhibition of the immune checkpoints should re-enable the immune system to detect and kill cancer cells. To date, reported targetable checkpoints for melanoma treatment include but are not limited to programmed cell death 1 (PD1) and cytotoxic T-lymphocyte antigen 4 (CTLA4). PD-1 and CTLA-4 are both negative regulators of T cell activation.

Anti CTLA4 antibodies

Ipilimumab is discovered as a CTLA-4 checkpoint inhibitor. It was approved by the FDA in 2011 for the treatment of unresectable or metastatic melanoma. In contrast to a treatment group receiving placebo, ipilimumab treatment significantly prolonged PFS in patients with stage III melanoma [44]. Improved overall survival and median PFS were also observed for ipilimumab treatment [45]. However, due to the excessive immune activity caused by ipilimumab, mild to severe adverse effects were present in patients treated with ipilimumab [45, 46].

Tremelimumab, another anti CTLA-4 antibody, is currently under clinical development. In a phase I/II clinical trial that recruited patients with metastatic melanoma, less significant toxicity was observed for patients receiving tremelimumab than patients treated with ipilimumab[47]. However, tremelimumab did not markedly improve the overall survival in a phase III study when compared to conventional chemotherapy [48].

Anti PD-1 antibodies

Nivolumab is a monoclonal antibody specific for human PD1. It was approved by the FDA in 2014 for the treatment of advanced melanoma. In a phase I study that nivolumab was applied to treat patients with advanced melanoma, significant clinical efficacy and manageable safety profile were observed. Nivolumab gave an overall survival rate of 32%. 1-year, 2-year, 3-year and 4-year overall survival rates for nivolumab treatment were 63%, 48%, 42% and 32%, respectively. Immune-related grade $\frac{3}{4}$ adverse effects were present in 14% of the patients. In a phase III trial, nivolumab was effective for metastatic melanoma that was previously treated with ipilimumab. Nivolumab accomplished significantly higher overall survival rate than chemotherapy treatment [49].

Pembrolizumab (lambrolizumab or MK-3475) is another anti PD-1 antibody approved by the FDA in 2014. Pembrolizumab has a high affinity to the IgG4 isotype. In a phase I trial that recruited 135 patients with advanced melanoma, the highest response rate (~52%) was observed in the highest dose arm. A median duration progression-free survival of > 7 months was seen. 13% of the regimen showed grade3/4 adverse events. Manageable adverse effects were accompanied with pembrolizumab treatment [50]. A clinical trial enrolling 411 patients indicated that pembrolizumab had an overall response rate of 34%, a median progression-free survival of 5.5 months, and an overall survival rate of 69% at one-year. For patients with metastatic melanoma who were refractory to ipilimumab treatment, pembrolizumab was more effective than chemotherapy to prolong progression-free survival [51].

Chemotherapy

Traditional chemotherapeutics used for treating melanoma mainly include dacarbazine, temozolomide. While these drugs are very effective for treating melanoma at the early stages, their clinical effect is not satisfactory when applied to treat advanced melanoma. The tumor is prone to acquire resistance over the course of cancer treatment when dacarbazine or temozolomide is used. Furthermore, chemotherapy can cause broad drug-related side effects such as fatigue, hair loss, appetite loss, diarrhea and peripheral neuropathy. Therefore, in modern cancer treatment, chemotherapy is a less preferred strategy to targeted therapy and immunotherapy.

Challenges in targeted therapy and immunotherapy

Discovery of the oncogenic mutation in BRAF at codon 600 in the MAPK signaling pathway has revolutionized the treatment of advanced or metastatic melanoma in the last ten years. Several inhibitors targeting the BRAF mutation V600E or its downstreams (ERK and MEK) have been approved by the FDA to treat advanced stage melanoma. The years 2011 and 2014 have witnessed the approvals of immune checkpoint inhibitors ipilimumab and pembrolizumab. Both targeted therapy and immunotherapy have brought more substantial clinical benefits than traditional chemotherapies in treating metastatic melanoma. However, there are profound problems within targeted therapy and immunotherapy.

Despite the fact that targeted therapies such as BRAF inhibitors (vemurafenib and dabrafenib) and MEK inhibitor (trametinib) bring substantial initial tumor regression, drug resistance can be acquired in nearly 50% patients after a period of 6–8 months` treatment [52, 53]. The mechanism of resistance can be divided into three categories: intrinsic, acquired, and adaptive resistance [54]. While intrinsic resistance is characterized by no response to therapy, acquired resistance is typified by initially significant response followed by drug tolerance and progressive disease [54]. The major resistant mechanism is the reactivation of the MAPK pathway. The tumor can re-trigger the MAPK pathway by activating the downstream MEK1/2 kinase or upstream RAS

kinase mutation, elevating the CRAF level, amplifying the BRAF, overexpressing the RAF1 or MAP3K8-(COT)-kinase, ERK1/2 mutation, upregulating the RTK, as well as mutating the PI3K pathway gene [55-61]. The mechanism of resistance was discussed in detail in recent reviews [62-65]. Although combinational therapies of BRAF inhibitors and MEK inhibitors, for instance, vemurafenib and trametinib or dabrafenib and trametinib, were demonstrated to be more effective for improving median PFS than dabrafenib or vemurafenib monotherapy [66], drug resistance remains a significant problem with combinational therapies [67, 68].

Unlike targeted therapy, immune checkpoint inhibitors do not have the problem of drug resistance, but they can cause immune-related adverse events (irAEs). IrAEs are distinct from adverse events brought by chemotherapy or targeted therapy. These unique adverse events result from unrestrained T cell activation and include dermatologic, gastrointestinal, hepatic and endocrine toxicities. These toxicities can be reversed, however, if not managed timely, they can upgrade to high-grade adverse events and even to life-threatening situations [69].

Tubulin Inhibitors for Treatment of Cancer

Microtubule dynamics as a therapeutic target

Microtubules are key elements in eukaryotic cells. They are involved in many critical cellular functions, such as cell division, cell shape maintenance, vesicles transportation, and motility regulation. Formed from polymerized α/β -tubulin heterodimers, microtubules are responsible for the generation of mitotic spindle and induction of the movement of chromosomes during cellular mitosis [70-72]. Disruption of microtubule dynamics causes cell cycle arrest in the G2/M phase, leading to mitotic catastrophe and ultimately cellular apoptosis. Given the important role of microtubules in cell growth and division, tubulin dynamics has been a fertile target for developing anticancer drugs [73-75].

Binding sites in tubulin

At least four binding sites on tubulin have been reported to date: the taxane site, the laulimalide site, the vinca site, and the colchicine site (**Figure 1-2**). A number of approved tubulin inhibitors interact with the taxane site (e.g. paclitaxel, docetaxel, and epothilones) or the vinca site (e.g. vinblastine, vincristine) in tubulin. They have been highly successful in the clinical treatment for many cancer types including ovarian, lung, and breast cancers [76-79]. However, the clinical use of these drugs is often associated with several limitations. First, these drugs are usually good substrates for a number of ATP-binding cassette (ABC) transporters, including P-glycoprotein (P-gp or MDR1), breast cancer resistance protein (BCRP), and multidrug resistant proteins (MRP1,

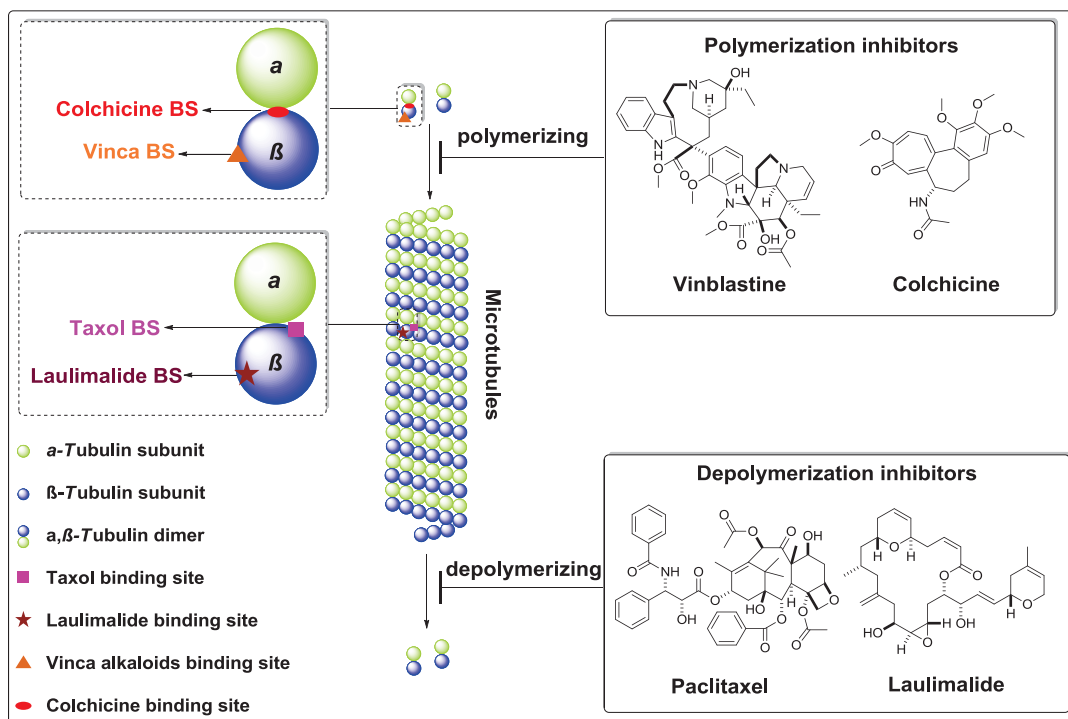


Figure 1-2. Binding sites in tubulin

Reprinted with permission from Bentham Science Publishers. Wu XX, Wang QH, Li W. Recent Advances in Heterocyclic Tubulin Inhibitors Targeting the Colchicine Binding Site. *Anti-cancer agents in medicinal chemistry*, 2016, 16:1325-1338.

MRP2). Thus multidrug resistance often develops in patients upon an extended period of drug administration [80-82]. Second, these drugs have very poor aqueous solubility; harmful surfactants such as Cremophor EL are usually required in their formulations [83]. Finally, overexpression of β -tubulin isoforms (especially the β -III tubulin isoform) and certain mutations in tubulin are associated with the development of resistance for most of these agents [84-87].

Tubulin inhibitors approved by FDA or in clinical development

Based on their effects on the microtubule structures at high concentrations, microtubule-targeting agents (MTAs) can be divided into two categories: microtubule stabilizers and microtubule destabilizers. **Figure 1-3** and **Figure 1-4** list some notable examples of the microtubule-stabilizing agents and microtubule-destabilizing agents, respectively.

Challenges in developing microtubule targeting agents as anticancer agents

Taxanes and vinca alkaloids have achieved great success in clinical treatment for a variety of cancers in the last decades; however, acquired drug resistance develops over the course of clinical administration and represented a significant obstacle [88]. Mechanistically, cancer cells evade cytotoxic MTAs mainly through the following pathways: (1) Overexpression of tubulin β -III isotype. Strong clinical evidence supported that overexpression of tubulin β -III isotype was responsible for drug resistance to either microtubule stabilizer or microtubule destabilizer in patients with different tumor types [89]. Overexpression of tubulin β -III might also inherently promote microtubule dynamics and prevent cells from proceeding to anaphase [90]. (2) Upregulation of MRP1, MRP2 or MDR1 gene. MDR1 gene is responsible for the encoding of P-gp [72]. P-gp mediated drug efflux has been reported as the major mechanism mediated drug-resistance to taxanes in many types of tumors [91]. (3) Overexpressed microtubule-regulating proteins. It was demonstrated that increased expression of microtubule-regulating proteins can stabilize microtubules and contribute to the occurrence of multidrug resistance [72]. (4) Changes in cytoskeletal proteins. Mutation in γ -actin was revealed to induce vinblastine-resistance [92]. In addition, downregulation of γ -actin was also related to drug resistance in childhood leukemia [93]. (5) Tubulin mutations. Certain mutations in tubulin are also known to confer resistance to CBSIs. For example, a K350N mutation in tubulin induces conformational change to the colchicine binding site and results in 2-ME2 resistance [94]. Besides these mechanisms, there were other factors that might mediate drug resistance to tubulin inhibitors [72, 95]. However, it does not mean that these mechanisms induce resistance exclusively, in fact, these mechanisms often work collectively.

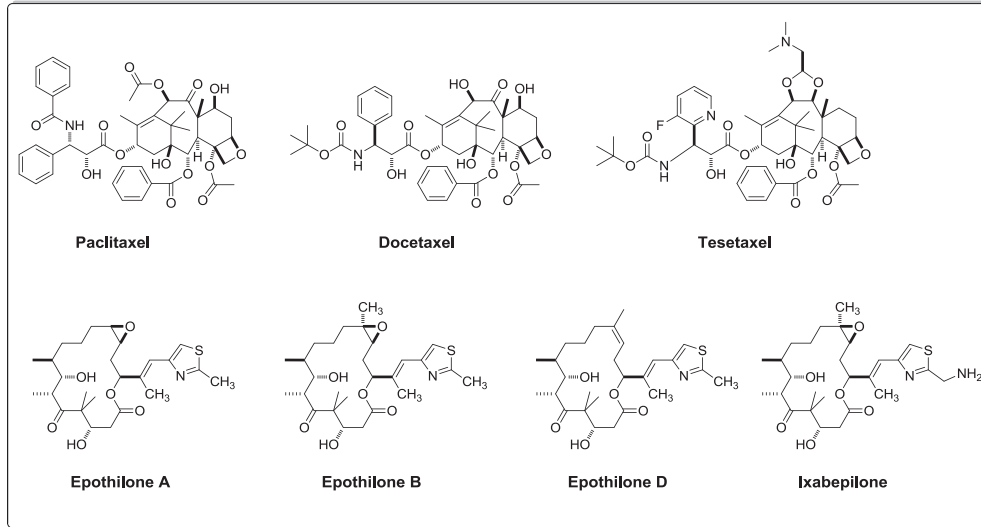


Figure 1-3. Microtubule-stabilizing agents

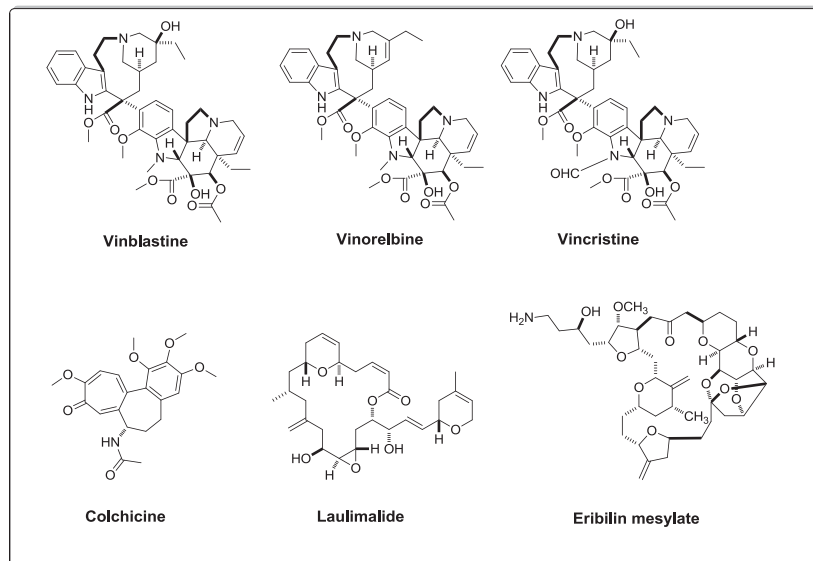


Figure 1-4. Microtubule-destabilizing agents

Targeting colchicine binding site in tubulin for development of anticancer agents

The colchicine binding site, one of the many well-documented binding sites in tubulin, locates at the interface between α and β -tubulin monomers [96]. Colchicine binding site inhibitors (CBSIs) mechanistically decrease cellular motility, alter cell morphology, impair protein assembly, and arrest mitosis [97, 98]. A number of preclinical studies have proven that CBSIs are effective to suppress the overexpression of β -tubulin isotype β -III tubulin. CBSIs are also demonstrated to surmount drug-resistance mediated by P-gp, MRP1, MRP2 [99-101]. Thus, despite the fact that there are currently no FDA-approved tubulin inhibitors interacting with the colchicine binding site [96, 102], colchicine binding site represents a great promise and has been extensively investigated. There are many CBSIs have entered clinical trials for cancer treatment, for instance, ABT-751, ZD6126, CA-4P, AVE8062, OXi4503 and NPI-2358 [103], some of which are listed in **Figure 1-5**.

Survivin as a Therapeutic Target for Cancer Treatment

Survivin as a therapeutic target

Due to its important role in anti-apoptosis, cell proliferation, and angiogenesis, survivin is regarded as a highly promising therapeutic target for the development of anticancer agents [104].

Survivin is the smallest member of the family of Inhibitor of Apoptosis Proteins (IAPs). Survivin is almost absent in normal tissues but is highly overexpressed in tumors [105]; it is therefore considered as a significant cancer specific biomarker [106]. Although the anti-apoptotic effect of survivin is well accepted, the mechanism regarding to how survivin mediates inhibition of apoptosis remains debatable. On one hand, it is believed that like other IAP family members survivin can directly bind to caspases and subsequently block their apoptotic activities [107, 108]. On the other hand, it was reported that survivin exerted its anti-apoptotic effect by indirectly inhibiting caspases. It has been demonstrated that survivin can bind to XIAP, another member of IAPs, to protect XIAP from ubiquitination and degradation. This eventually blocks activation of caspase-9 and apoptosis [109]. Additionally, survivin is shown to bind to the mitochondrial protein SMAC and antagonize its pro-apoptotic ability [110]. Overexpression of survivin is reported to associate with multidrug resistance as well as radiation resistance [111, 112]. Resistance to therapies such as cisplatin and vincristine can be developed easier in tumor cells with high expression of survivin than in tumor cells with low expression of survivin [113].

Selective expression of survivin in tumor cells is validated; the benefit of down-regulating survivin expression to treat cancer is therefore obvious. Current strategies employed to block the anti-apoptotic ability of survivin in tumor cells include but are not

limited to introducing recombinant cell-permeable dominant-negative survivin protein [114, 115], obstructing protein translation using antisense oligonucleotides [116], and small-molecule survivin antagonists [117, 118].

Major survivin inhibitors

To date, a few survivin inhibitors have been developed [119-129], the majority of which are listed in **Figure 1-6**.

Challenges in developing survivin inhibitors as anticancer agents

Only a small amount of survivin inhibitors has been reported in the last decade, it is therefore not illustrative enough to unlock the potential of survivin for anticancer drug development. Despite the fact that the crystal structure of survivin was obtained in early of the 2000s [130], targeting survivin for direct binding affinity is challenging because no druggable site in survivin has been disclosed to date [130]. Due to that survivin interacts with many other molecules such as Hsp90, Smac, caspases, and INCENP, it is therefore difficult to specify the drug target and evaluate the drug efficacy. Furthermore, although the level of survivin in benign cells is dramatically lower than in malignant tumor cells, it is of significant importance to evaluate the lasting effect of shutting off survivin by survivin inhibitors in normal tissue [105].

Vitamin D3 for Cancer Treatment

1 α ,25-dihydroxyvitamin D3 and its limit

Vitamin D3 is mainly obtained from photoconversion of 7-dehydrocholesterol on the skin. After photoconversion, 7-dehydrocholesterol is converted to pre-vitamin D3 that is subsequently isomerized to vitamin D3. The storage form of vitamin D3, 25-hydroxyvitamin D3 (25-OH-D3), is generated through metabolism of vitamin D3 in the liver by 25-hydroxylase (CYP2R1 or CYP27A1) [131]. 25-OH-D3 is metabolized by 1 α -hydroxylase (CYP27B1) in the kidney to form the active form of vitamin D3, 1 α ,25-dihydroxyvitamin D3 [1,25(OH)₂D3, calcitriol] [132]. 1,25(OH)₂D3 exerts its extensive biological functions through activation of nuclear vitamin D receptor (VDR), which is distributed in almost all tissues of the body. Those biological functions include but are not limited to antiproliferative effects [133-135], induction of apoptosis [136, 137], antiinflammation [138-140], antiangiogenesis [140, 141] and antimetastatic effects [142, 143]. The 1,25(OH)₂D3 represents a promising scaffold for cancer treatment; however, applications of 1,25(OH)₂D3 for treatment were greatly hampered by hypercalcemia at pharmacological concentrations [144].

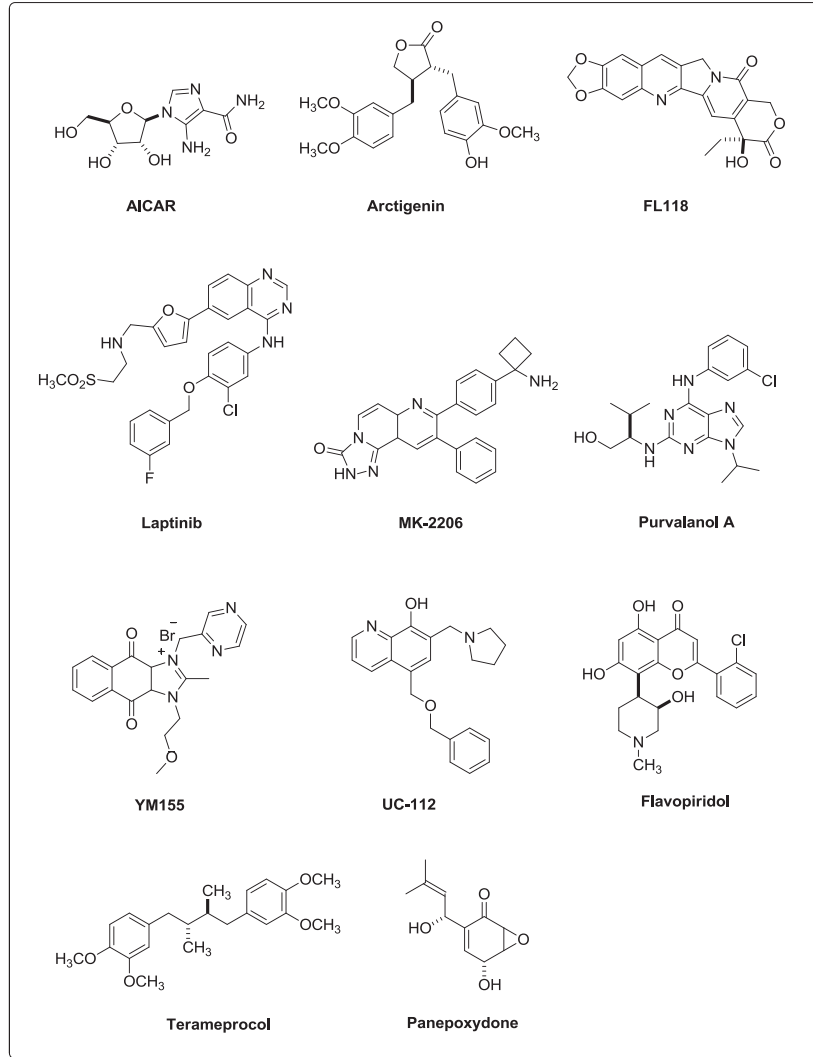


Figure 1-6. Structures of the major survivin inhibitors

20S-hydroxyvitamin D3 as a promising therapy for cancers

Mammalian cytochrome P450 side-chain cleavage enzyme (P450_{scc} or CYP11A1) cleaves the side chain of cholesterol to produce pregnenolone (precursor of all steroids) [145, 146]. P450_{scc} also hydroxylates vitamin D3 in a sequential fashion [146-150] starting from C20 to form 20S-hydroxyvitamin D3 [20S-(OH)D3] which is subsequently converted to di- and trihydroxy metabolites [147, 149-152]. Functional studies showed that 20S-(OH)D3 not only stimulated keratinocyte differentiation program but also inhibited NF- κ B activity in human keratinocytes [153]. In addition, 20S-(OH)D3 has shown antiinflammatory activities, strong antiproliferative effects, antileukemia and tumorostatic effects [153-157], protective effects against ultra-violet B (UVB) induced damage [158], as well as antifibrotic activity *in vivo* [159]. These activities are mediated either through activation of the VDR [153, 160] or inhibition of ROR α and ROR γ transcriptional activities [161]. More importantly, while 20S-(OH)D3 has comparable antiproliferative potency with 1,25(OH)₂D3 which has strong hypercalcemic toxicity at a concentration of 1 μ g/kg, 20S-(OH)D3 is not hypercalcemic at concentrations as high as 60 μ g/kg [154, 156, 158, 162]. However, to obtain proper quantity of 20S-(OH)D3 amenable for medicinal chemistry program is challenging. Therefore, a chemical synthesis that can prepare the amount of 20S-(OH)D3 and enable SAR investigation of this scaffold is of prime importance.

Discussion

Targeted therapy and immune therapy have achieved substantial success in treating metastatic melanoma. Since 2010, BRAF inhibitors (vemurafenib and dabrafenib), MEK1/2 inhibitors (trametinib and cobimetinib), anti PD-1 antibodies (nivolumab and pembrolizumab) and anti CTLA4 antibody (Ipilimumab) have been approved by the FDA for the treatment of advanced melanoma. Nevertheless, patients with advanced melanoma rapidly acquire drug-resistance after a 6-month treatment with targeted therapy. Clinical responses to immune therapy are sometimes reported to be unsatisfactory [163]. IrAEs resulted from unrestrained T cell activation are challenging and might be fatal if not managed timely [164, 165].

Unlike anticancer chemical alone, an antibody-drug conjugate (ADC) resorts to its monoclonal antibody to selectively target antigen on the surface of a tumor instead of normal tissue. As a result, ADC can minimize drug exposure to healthy cells and shows significantly less systemic toxicities or off-target side effect than anticancer chemical alone. Development of a successful ADC is challenging. There are demanding requirements for not only antigen on the surface of tumor but also each part of the ADC. ADC consists of anticancer chemical (payload or warhead), stable monoclonal antibodies, as well as synthetic linkers. The antigen should be mostly if not exclusively expressed in tumor instead of healthy tissue. The antibody should be selective to the antigen on the tumor to exclude off-target effect to healthy tissue. The antibody is also expected to have favorable stability in blood circulation in order to minimize the

destruction of ADC and maximize the concentration of payload that reaches the tumor. This stability requirement also applies to the synthetic linker.

As the cytotoxic part, the payload is crucial in ADC. Currently, two types of cytotoxic chemicals are mainly subjected to the construction of ADCs: DNA-damaging agents and microtubule inhibitors. Generally, the payload is required to show cytotoxicity in sub-nanomolar range because (1) only limited percentile of injected antibody can be localized to solid tumor (0.003–0.08% injected dose per gram of tumor); (2) there are limited quantities of antigens on tumor surface; (3) the drug-to-antibody ratio is low (3.5-4) [166-168]. Although the available pool of cytotoxic chemical is large, the conjugable toxins with “super” potency (sub-nanomolar) are of a limited amount. Thus, the discovery of highly potent inhibitors for different targets is still warranted. In addition, the ability of toxin to circumvent multidrug-resistance is desirable in order to prolong the clinical use.

Because of the critical role of microtubules in many cellular functions, disruption of microtubule dynamics is regarded as an attractive strategy for cancer treatment. MTAs including paclitaxel, docetaxel, and vincristine have achieved great success in the last decade. However, drug resistance resulting from ABC transporters or overexpression of β -III tubulin/ MAPs is a major problem for taxanes and vinca alkaloids. Drug discovery based on MTAs has experienced long-term infertility due to significant off-target toxicity. The interest in MTAs is not revived until the FDA approved trastuzumab emtansine in February 2013. Trastuzumab emtansine is applied to the treatment of HER2-positive metastatic breast cancer and is a MTA-based ADC.

ABI-231 is a potent CBSI discovered by our group in 2012 [169]. It has an average IC_{50} of 5.2 nM against a panel of melanoma and prostate cancer cell lines. It targets the colchicine binding site in tubulin and mechanistically inhibits the microtubule polymerization. Importantly, this molecule is effective in drug-resistant cell lines mediated by overexpression of P-gp and tubulin β -III isotype. ABI-231, therefore, represents a promising scaffold for developing anti-cancer agents and is worthy in-depth investigation. However, the in-depth SAR investigation of this promising scaffold is hampered by an inefficient synthetic method, through which ABI-231 was achieved within five steps with an overall yield of 0.28%. Hence, an efficient synthetic method that can rapidly generate ABI-231 analogues for SAR evaluation is needed. According to the reported molecular modeling (**Figure 1-7**) [169], ABI-231 forms three H-bonding interactions with tubulin protein. The interactions include the H-bond between methoxy and α -THR179 residue, H-bond between NH on imidazole and β -VAL238 as well as NH on indole with β -ASN167. The molecular modeling suggests the existence of an unoccupied pocket in the vicinity of the indole of ABI-231. We hypothesize that by introducing a small functional group to the indole of ABI-231 the ligand-receptor interaction can be strengthened. With this hypothesis in mind, we have established new generations of synthetic methods to access a variety of novel ABI-231 analogues and RABI analogues. ABI-231 analogues with more potent antiproliferative activities than ABI-231 have been achieved by introducing substituent to the indole moiety or by

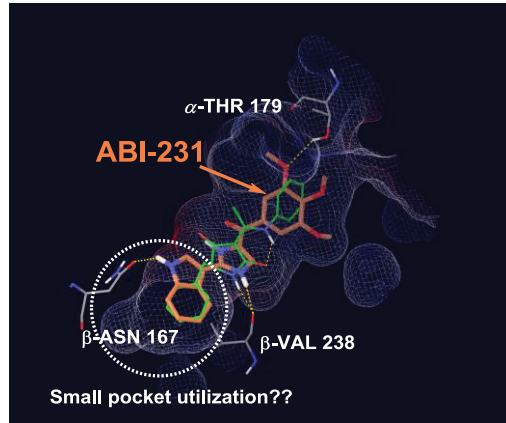


Figure 1-7. Molecule modeling result of ABI-231 in tubulin (PDB: 3HKD)

isosterically modifying the 3,4,5-trimethoxyphenyl (3,4,5-TMP) in ABI-231. The first RABI analogue with sub-nM activity has also been obtained. These efforts will be shown in Chapter 2 to 4.

UC-112 is discovered as a selective survivin inhibitor through virtual screening by our group in 2014 [126]. It has a low micromolar range IC_{50} against a panel of melanoma cancer cell lines and is selective to survivin over other IAP family members such as XIAP, cIAP-1, cIAP-2 and livin. A significant tumor growth inhibitory efficacy is observed for UC-112 at a dose of 20mg/kg in an A375 human melanoma xenograft model *in vivo*. Subsequent SAR study of UC-112 has manifested that modifying either the 8-hydroquinoline or the pyrrolidine is detrimental to the activity; introducing hydrophobic substituent to the para-position of the benzyloxy is beneficial to the activity. We hypothesize that the benzyl ether moiety in UC-112 might be too flexible and reducing the flexibility of this benzyloxy tail can increase the antiproliferative activity of this scaffold (**Figure 1-8**). With these hypotheses in mind, we have synthesized thirty-six UC-112 analogues replacing the benzyloxy in UC-112 with different moieties. Most of the new analogues show more potent activities than prototype UC-112. Importantly, the new analogues display significant abilities to circumvent P-gp mediated drug-resistance. The effort on investigating SAR of UC-112 will be shown in Chapter 5.

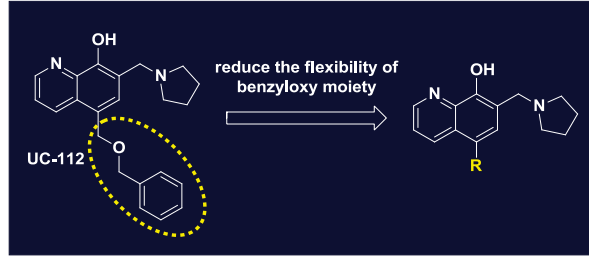


Figure 1-8. Proposed modification of UC-112 by reducing the flexibility of benzyloxy moiety

CHAPTER 2. STRUCTURE-ACTIVITY RELATIONSHIP STUDY OF ABI-231 LEADS TO IMPROVED ACTIVITIES AGAINST MICROTUBULE POLYMERIZATION

Introduction

Microtubules are cylindrical polymers that are of great importance for many cellular functions in the normal cells such as cell division, cell shape maintenance, and cell motility. Microtubules are dynamically involved in the formation of the mitotic spindle and play a critical role in the proliferation of cancer cells [91, 170, 171]. For these reasons, microtubule dynamic is among the most promising therapeutic targets for the development of cancer treatment [171]. MTAs can interfere with the microtubular functions to disrupt the formation of the mitotic spindle, eventually leading to mitotic arrest at the metaphase/anaphase transition. Numerous MTAs have been discovered in the last decades and several of them have been approved by the FDA for the treatment of different cancer types, such as breast cancer, lung cancer, ovarian cancer, etc. [172]. MTAs are generally classified into two categories based on their effect on microtubule at high concentrations: microtubule-stabilizing and microtubule-destabilizing agents. Microtubule-stabilizing agents bind to tubulin polymer and enhance microtubule polymerization. Microtubule-stabilizing agents include, for instance, epothilone, ixabepilone, paclitaxel, and docetaxel. Microtubule-destabilizing agents inhibit polymerization of microtubule and contain such as colchicine, combretastatins A-4 (CA-4) and vinca alkaloids [173].

The MTAs have achieved great success in cancer treatment in the last decade. Drug-resistance is, however, acquired over the course of treatment and becomes a tremendous obstacle. Since 22 million new cancer cases are estimated to be diagnosed worldwide in the coming two decades, the importance of developing anticancer agents to treat resistant phenotypes is apparent [174, 175]. Mechanisms to mediate drug-resistance against MTAs include but are not limited to overexpression of membrane-bound drug efflux proteins such as P-gp, overexpression of β -tubulin isotypes, and microtubule mutations [72, 176]. Epothilones are natural products isolated from the *Sorangium cellulosum* strain of the *myxobacterium sorangium cellulosum*. Some of the epothilones have been approved by the FDA for cancer treatment while some are currently at late stages of clinical trials. Different from taxanes and vinca alkaloids, epothilones are not substrates of ATP-binding cassette (ABC) transporters and are able to inhibit the overexpression of tubulin β -III isotype [177-179].

As one of the many well-documented binding sites in tubulin, colchicine binding site locates at the interface between α and β -tubulin heterodimers [96]. CBSIs mechanistically decrease cellular motility, alter cell morphology, impair protein assembly, and arrest mitosis [97, 98]. Colchicine, a secondary metabolite isolated from natural source, binds to the colchicines binding site in tubulin. Colchicine has wide-scope mechanisms of action. It, unfortunately, shows systemic toxicities and induces multiorgan dysfunction in a clinical trial for cancer treatment [97]. Other than colchicine

and its derivatives, a number of other CBSIs have also been discovered in the last decade. Encouragingly, extensive preclinical studies have proven that CBSIs are effective to suppress overexpression of tubulin β -III isotype and surmount drug-resistance mediated by P-gp, MRP1, MRP2 [99-101].

In our preceding investigations, we have described the discovery of SMART scaffold. SMARTs exhibited nanomolar range antiproliferative activity against a panel of cancer cell lines (**Figure 2-1**) [180]. Replacing the substituted benzenes in SMARTs with anilines provided the PATs. The PATs showed equipotency to that of SMARTs. Subsequent structural modification of the SMART scaffold by replacing the sulfur in thiazole with NH resulted in the discovery of ABI-I/II (2-aryl-4-benzoyl-imidazole) pharmacophores. ABI-I/II showed not only potent activity but also improved bioavailability in comparison with SMARTs (shown in **Figure 2-1**) [181, 182]. Follow-up modification of the ABI-I/II gave ABI-III pharmacophore (**Figure 2-1**) [169, 183]. From the perspective of chemical structure, ABI-IIIs differed from ABI-I/II in having bicyclic heterocycles, which are versatile moieties in medicinal chemistry program [184]. From the perspective of bioactivity, ABI-IIIs exhibited more potent antiproliferative activity (IC_{50} s as low as single-digit nanomolar range) than ABI-I/II. Rotation of the imidazole ring in ABI-I/II led to the establishment of reverse ABIs (RABIs, shown in **Figure 2-1**). RABIs had average IC_{50} s as low as 14 nM [185]. Substituting the imidazole and carbonyl linker in ABI-IIIs with bicyclic heterocycles provided the IBIs (shown in **Figure 2-1**). IBIs displayed similar potency to that of ABI-IIIs. All SMARTs, ABIs, RABIs and IBIs have been demonstrated to share the same mechanism of action: binding to the colchicine binding site in tubulin and inhibiting the tubulin polymerization. Importantly, they were all effective to multidrug-resistant cell lines and can overcome P-gp mediated drug resistance [169, 182, 183]. Among these SMARTs, ABIs, RABIs and IBIs, ABI-231 (shown in **Figure 2-1**) displayed the optimum activity and had an average IC_{50} value of 5.2 nM against a panel of cancer cell lines. Molecular modeling study revealed the existence of unoccupied pockets in the vicinity of the indole moiety of ABI-231. This pocket might serve as an opportunity to strengthen the ligand-protein interaction [169]. With this hypothesis in mind, we are prompted to conduct comprehensive SAR study of ABI-231 by introducing “indole rotation” and different functional groups to the indole moiety.

Experimental Section

General chemistry

Tetrahydrofuran was distilled from sodium-benzophenone. All other solvents and chemical reagents were obtained from commercial sources and directly used without further purification. Glassware was oven-dried before use. All reactions were performed under an argon atmosphere. TLC was performed on silica gel 60 GF254 and monitored under UV light or visualized using phosphomolybdic acid reagent. Flash chromatography

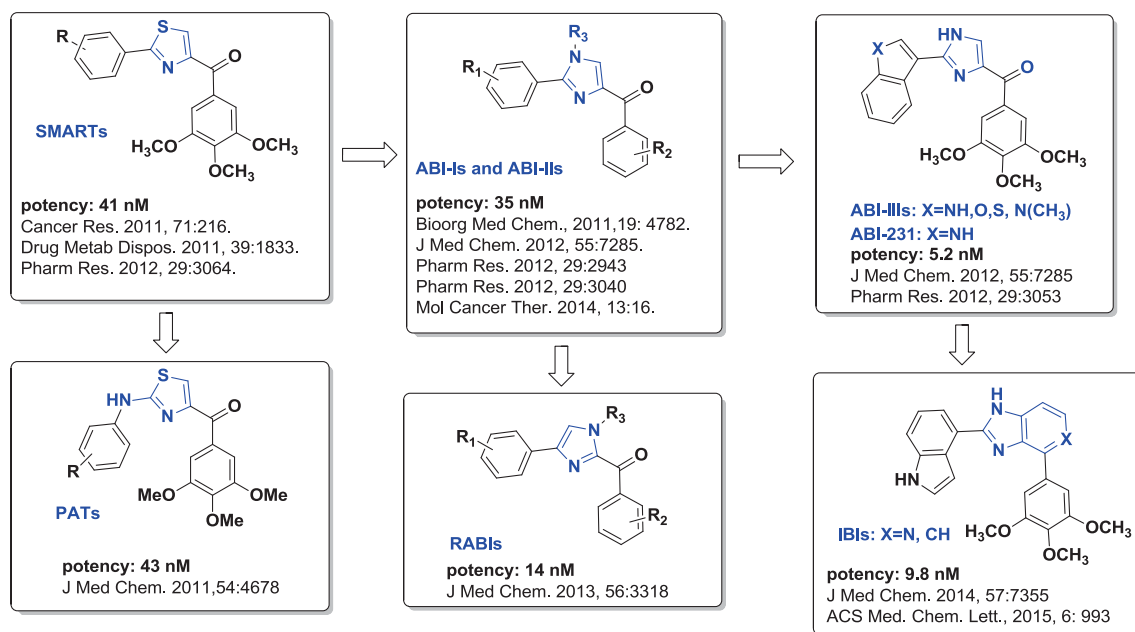


Figure 2-1. Examples of microtubule inhibitors that target colchicine binding sites in tubulin

was performed on 230-400 mesh silica gel (Fisher Scientific). Melting points were recorded on a MPA100 Automated Melting Point Apparatus. NMR spectra were obtained on a Bruker Ascend 400 (Billerica, MA) spectrometer or a Varian Inova-500 spectrometer (Agilent Technologies, Santa Clara, CA). HR-MS were obtained on Waters Acquity UPLC linked to Waters Acquity Photodiode Array Detector and Waters Acquity Single Quadrupole Mass Detector. Chemical shifts are given in ppm with tetramethylsilane (TMS) as an internal reference. All coupling constants (J) are given in Hertz (Hz).

Chemical synthesis

Synthesis of 3-((tert-butyldimethylsilyl)oxy)-3-(3,4,5-trimethoxyphenyl)propane-1,2-diol (2). To a solution of 3,4,5-trimethoxybenzaldehyde (30 g, 0.153 mol) in anhydrous THF (100 mL) at 0 °C under argon was added vinylmagnesium bromide solution (168 ml, 0.168 mol, 1.0 M in THF) dropwise, the resulting mixture was stirred for an hour. On completion reaction was quenched with saturated NH_4Cl . The mixture was then extracted with ethyl acetate, washed with brine and dried with anhydrous Na_2SO_4 . The combined extracts were evaporated under vacuum to give crude oil which was used directly for next step without purification. Imidazole (15.6 g, 0.229 mol) and *tert*-butyldimethylsilyl chloride (34.4 g, 0.229 mol) was sequentially added to a solution of the above crude oil in dichloromethane (150 mL) in a round bottom flask with stirring under argon. The resulting suspension was stirred for 2 hours. Water was then added and the mixture was extracted with dichloromethane, washed with brine and dried with anhydrous Na_2SO_4 . The combined extracts were evaporated to give crude oil mixture which was purified by flash chromatography on silica. Elution with hexane/ethyl acetate (10:0-10:1) gave racemic mixture **2** as yellowish oil (44.1 g, 85%).

Synthesis of 3-((tert-butyldimethylsilyl)oxy)-3-(3,4,5-trimethoxyphenyl)propane-1,2-diol (3). To a solution of the compound **2** (44.0 g, 0.13 mol) in acetone (150 mL) was added *N*-methylmorpholine *N*-oxide (22.9 g, 0.195 mol) and osmium tetroxide (40 mg, 0.157 mmol) in *tert*-butanol (5 mL) at room temperature with stirring. After 48 hour, acetone was removed under vacuum, water and ethyl acetate was then added and the organic phase was separated, washed with brine and dried with Na_2SO_4 . Evaporation under vacuum gave the oily residue which was purified with flash chromatography on silica. Elution with hexane/ethyl acetate (2:1-1:1) gave diol **3** as colorless oil (45.1 g, 93%).

Synthesis of 3-((tert-butyldimethylsilyl)oxy)-3-(3,4,5-trimethoxyphenyl)propane-1,2-diyl dimethanesulfonate (4). To a solution of compound **3** (45.0 g, 0.12 mol) and Methanesulfonyl chloride (23.4 ml, 0.30 mol) in anhydrous dichloromethane (100 mL) in a round bottom flask at 0 °C under argon, trimethylamine (36.9 ml, 0.26 mol) was added dropwise with vigorous stirring. The resulting mixture was stirred for overnight, water was then added and the reaction mixture was extracted with dichloromethane, washed with brine and dried with

anhydrous Na₂SO₄. The combined extracts were evaporated under vacuum to give the oily crude which was purified with flash chromatography on silica. Pure mesylates **4** was eluted out with hexane/ethyl acetate (3:1-2:1) as colorless oil (45.2 g, 71%). ¹H NMR (400 MHz, Chloroform-*d*) δ 6.61 – 6.56 (m, 2H), 4.93 (dd, *J* = 19.9, 5.3 Hz, 1H), 4.79 (ddd, *J* = 7.0, 4.8, 2.4 Hz, 1H), 4.53 – 4.41 (m, 1H), 4.36 (dd, *J* = 11.5, 2.4 Hz, 1H), 3.89 – 3.77 (m, 9H), 3.04 – 2.75 (m, 6H), 0.90 (d, *J* = 5.0 Hz, 9H), 0.12 (d, *J* = 13.5 Hz, 3H), -0.07 (d, *J* = 1.4 Hz, 3H). HRMS: calculated for C₂₀H₃₇O₁₀S₂Si [M+H]⁺ 529.1597, found 529.1562.

Synthesis of tert-butyl(2,3-diazido-1-(3,4,5-trimethoxyphenyl)propoxy)dimethylsilane (5). To a solution of mesylates **4** (45.0 g, 0.085 mol) in anhydrous *N,N*-dimethylformamide (100 mL) in a round bottom flask under argon, sodium azide (30 g, 0.46 mol) was added in portions with stirring. The resulting mixture was refluxed for overnight. The precipitate was filtered off and washed with dichloromethane. The combined filtration was evaporated under vacuum to give the oily crude which was purified with flash chromatography on silica. Pure azides **5** was eluted out with hexane/ethyl acetate (4:1-3:1) as colorless oil (20.8 g, 58%). ¹H NMR (400 MHz, Chloroform-*d*) δ 6.55 (d, *J* = 9.6 Hz, 2H), 4.64 (dd, *J* = 6.3, 4.7 Hz, 1H), 3.85 (dd, *J* = 2.4, 1.5 Hz, 9H), 3.61 – 3.04 (m, 3H), 0.90 (d, *J* = 1.0 Hz, 9H), 0.10 (d, *J* = 9.4 Hz, 3H), -0.13 (d, *J* = 4.1 Hz, 3H). HRMS: calculated for C₁₈H₃₁N₆O₄Si [M+H]⁺ 423.2176, found 423.2177.

Synthesis of 3-((tert-butyl)dimethylsilyloxy)-3-(3,4,5-trimethoxyphenyl)propane-1,2-diamine (6). A suspension of azides **5** (20.0 g, 0.047 mol) and 10% Pd/C (0.2 g) in ethylacetate-methanol (1:1, 50 ml) was hydrogenated overnight, the reaction mixture was filtered off and washed with dichloromethane-methanol (1:1). The combined filtration was evaporated under vacuum to give the oily crude which was purified with flash chromatography on silica. Pure diamine **7** was eluted out with dichloromethane/methanol (15:0-15:1) as slightly yellowish oil (10.6 g, 61%). ¹H NMR (400 MHz, Chloroform-*d*) δ 6.51 (d, *J* = 13.4 Hz, 2H), 4.45 (dd, *J* = 34.5, 5.1 Hz, 1H), 3.83 (d, *J* = 1.2 Hz, 9H), 2.97 – 2.46 (m, 3H), 0.90 (d, *J* = 10.8 Hz, 9H), 0.04 (d, *J* = 8.5 Hz, 3H), -0.17 (d, *J* = 8.5 Hz, 3H). HRMS: calculated for C₁₈H₃₅N₂O₄Si [M+H]⁺ 371.2366, found 371.2369.

General procedure for Boc protection of indolecarboxyaldehydes 7aa-7at and 7ba-7be. To a solution of the indoles (1.34 mmol) and 4-dimethylaminopyridine (65 mg, 0.54 mol) in anhydrous dichloromethane (5 mL) under argon was added *di-tert*-butyl dicarbonate (351 mg, 1.61 mmol) with stirring. After 1 hour, water was then added and the reaction mixture was extracted with dichloromethane, washed with brine and dried with Na₂SO₄. Evaporation under vacuum gave the crude solid residue which was purified with flash chromatography on silica. Elution with hexane/ethyl acetate (10:1-3:1) gave pure boc-protected indolecarboxyaldehydes **7aa-7at** and **7ba-7be** as white to yellowish solids.

General procedure for cyclolization to form imidazoline 8aa-8at and 8ba-8be. A solution of compound **6** (370 mg, 1.0 mmol) and boc-protected indole (1.1 mmol) in

anhydrous dichloromethane (10 mL) was stirred for one hour under argon, then *N*-bromosuccinimide (151 mg, 0.85 mmol) was added at ice temperature and reaction was warmed to room temperature. After 4 hours, the reaction was quenched with saturated sodium thiosulfate solution and extracted with dichloromethane for three times, washed with brine and dried with Na₂SO₄. The combined extracts were evaporated to give crude oil, which was purified with flash chromatography on silica. Elution with dichloromethane/ethyl acetate (10:1-1:2) gave diastereomers **8aa-8at** and **8ba-8be** as transparent oil.

General procedure for removal of TBS protecting group. To a stirred solution of compound **8aa-8at** (0.5 mmol) in THF (5.0 mL) was added *tetra-n*-butylammonium fluoride (1.0 M in THF, 1.0 ml, 1.0 mmol) under argon. The reaction was quenched with water, extracted with ethyl acetate for three times, washed with brine and dried with Na₂SO₄. The combined extracts were evaporated to give crude oil, which was purified with flash chromatography on silica. Elution with ethyl acetate/methanol (1:0 – 5:1) afforded pure compound **9aa-9at** and **9ba-9be** as colorless oil.

General procedure for synthesis of 10ab-10at and 10ba-10be. To a stirred solution of compound **9** (0.3 mmol) in anhydrous dichloromethane (1.0 mL) was added trifluoroacetic acid (1.0 mL) under argon at room temperature. After 1 hour, solvent was removed under vacuum to give crude solid which was directly used for next step without purification. To a stirred solution of the above crude in anhydrous dimethyl sulfoxide (2.0 mL) under argon was added 2-iodoxybenzoic acid (252 mg, 0.9 mmol) at room temperature. The reaction mixture was stirred for overnight, extracted with ethyl acetate for three times, washed with brine and dried with Na₂SO₄. The combined extracts were evaporated to give crude solid, which was purified with flash chromatography on silica. Elution with hexane/ethyl acetate (4:1) gave pure compound **15** as yellowish solid.

General procedure for synthesis of 10au-10aw and 10ay. To a stirred solution of compound **10af** or **10ak** or **10ao** or **10as** (0.05 mmol) in EtOAc-MeOH (3 mL, 1:1) was added catalytic equivalent of 10% Pd/C (0.0025 mmol) under argon at room temperature. The reaction was then charged with hydrogen and monitored by TLC. Until the disappearance of starting material, the reaction mixture was filtered through celite and washed with EtOAc. The combined solvents were evaporated to give crude solid, which was purified with flash chromatography on silica. Elution with Hexanes/ethyl acetate (1:1-1:4) gave pure compound **10au-10aw** and **10ay** as yellowish solid.

Synthesis of 10ax. To a stirred solution of compound **10aq** in dioxane (1 mL) was added saturated LiOH solution (1mL) and reaction was heated at 50°C until the disappearance of starting material. The solvent was removed under reduced pressure and the crude was purified with flash chromatography on silica. Elution with DCM/MeOH (20:1-5:1) gave pure compound **10ax** as yellowish solid.

(2-(2-phenyl-1H-indol-3-yl)-1H-imidazol-4-yl)(3,4,5-trimethoxyphenyl)methanone (10aa). obtained as a yellowish solid. ¹H NMR (400 MHz, Methylene Chloride-*d*₂) δ 8.15 – 8.06 (m, 1H), 7.79 (s, 1H), 7.59 – 7.53 (m, 2H),

7.47 – 7.41 (m, 4H), 7.22 (dddd, $J = 20.6, 8.1, 7.1, 1.2$ Hz, 3H), 3.89 (s, 6H), 3.87 (s, 3H). ^{13}C NMR (101 MHz, Methylene Chloride- d_2) δ 183.45, 153.73, 142.58, 138.59, 136.68, 133.65, 132.38, 129.72, 129.63, 129.13, 128.11, 123.63, 121.59, 121.06, 111.94, 111.89, 107.17, 61.19, 56.78. HRMS: calculated for $\text{C}_{27}\text{H}_{24}\text{N}_3\text{O}_4$ $[\text{M}+\text{H}]^+$ 454.1767, found 454.1771.

(2-(4-methyl-1H-indol-3-yl)-1H-imidazol-4-yl)(3,4,5-trimethoxyphenyl)methanone (10ab). obtained as a yellowish solid. ^1H NMR (400 MHz, Methylene Chloride- d_2) δ 7.78 (s, 1H), 7.36 (s, 1H), 7.22 (d, $J = 16.4$ Hz, 3H), 7.08 (t, $J = 7.6$ Hz, 1H), 6.93 – 6.84 (m, 1H), 3.88 (d, $J = 2.0$ Hz, 9H), 2.50 (s, 3H). ^{13}C NMR (101 MHz, Methylene Chloride- d_2) δ 184.41, 153.78, 148.55, 142.68, 137.13, 136.97, 135.76, 133.67, 133.22, 131.08, 127.41, 127.24, 125.09, 125.06, 123.30, 122.79, 110.14, 110.09, 107.17, 106.73, 106.69, 61.21, 56.82, 21.07. HRMS: calculated for $\text{C}_{22}\text{H}_{22}\text{N}_3\text{O}_4$ $[\text{M}+\text{H}]^+$ 392.1610, found 392.1603.

2-(4-fluoro-1H-indol-3-yl)-1H-imidazol-4-yl)(3,4,5-trimethoxyphenyl)methanone (10ac). obtained as a yellowish solid. ^1H NMR (400 MHz, Chloroform- d) δ 8.04 (s, 1H), 7.71 (s, 1H), 7.24 (d, $J = 8.1$ Hz, 1H), 7.19 (s, 2H), 7.14 (td, $J = 8.0, 5.2$ Hz, 1H), 6.91 (dd, $J = 12.7, 7.8$ Hz, 1H), 3.90 (d, $J = 1.1$ Hz, 9H). ^{13}C NMR (101 MHz, Chloroform- d) δ 181.51, 167.73, 156.38, 154.01, 153.47, 143.21, 139.62, 131.22, 130.90, 129.80, 128.82, 124.35, 111.77, 109.92, 107.33, 107.12, 106.31, 61.08, 56.46. HRMS: calculated for $\text{C}_{21}\text{H}_{19}\text{FN}_3\text{O}_4$ $[\text{M}+\text{H}]^+$ 396.1360, found 396.1364.

(2-(4-bromo-1H-indol-3-yl)-1H-imidazol-4-yl)(3,4,5-trimethoxyphenyl)methanone (10ad). obtained as a yellowish solid. (EtOAc). ^1H NMR (400 MHz, Methylene Chloride- d_2) δ 7.77 (s, 1H), 7.68 (s, 1H), 7.42 (d, $J = 8.1$ Hz, 1H), 7.34 (d, $J = 7.6$ Hz, 1H), 7.26 (s, 2H), 7.06 (t, $J = 7.9$ Hz, 1H), 3.91 (s, 6H), 3.87 (s, 3H). ^{13}C NMR (101 MHz, Methylene Chloride- d_2) δ 184.36, 153.80, 146.48, 142.67, 138.16, 133.68, 129.87, 125.75, 124.76, 123.88, 113.25, 112.31, 112.25, 107.15, 106.35, 61.20, 56.84. HRMS: calculated for $\text{C}_{21}\text{H}_{19}\text{BrN}_3\text{O}_4$ $[\text{M}+\text{H}]^+$ 456.0559, found 456.0560.

(2-(4-methoxy-1H-indol-3-yl)-1H-imidazol-4-yl)(3,4,5-trimethoxyphenyl)methanone (10ae). obtained as a yellowish solid. ^1H NMR (400 MHz, Chloroform- d) δ 9.91 (s, 1H), 8.75 (s, 1H), 7.90 (s, 1H), 7.41 (d, $J = 8.4$ Hz, 1H), 7.30 (s, 2H), 7.26 (s, 2H), 6.70 (d, $J = 8.4$ Hz, 1H), 4.26 (s, 3H), 4.01 (s, 3H), 4.00 (s, 6H). ^{13}C NMR (101 MHz, Chloroform- d) δ 181.65, 153.51, 151.42, 145.59, 143.17, 138.93, 131.25, 130.44, 128.59, 127.66, 124.71, 113.49, 107.27, 106.23, 102.57, 99.65, 61.05, 56.41, 56.09. HRMS: calculated for $\text{C}_{22}\text{H}_{22}\text{N}_3\text{O}_5$ $[\text{M}+\text{H}]^+$ 408.1559, found 408.1564.

(2-(4-(benzyloxy)-1H-indol-3-yl)-1H-imidazol-4-yl)(3,4,5-trimethoxyphenyl)methanone (10af). obtained as a yellowish solid. ^1H NMR (400 MHz, Methylene Chloride- d_2) δ 11.96 (s, 1H), 10.50 (s, 1H), 8.07 (d, $J = 2.6$ Hz, 1H), 7.58 – 7.51 (m, 2H), 7.47 – 7.21 (m, 5H), 7.11 (d, $J = 4.2$ Hz, 2H), 6.74 (p, $J = 4.7$ Hz, 1H), 5.48 (s, 2H), 4.25 – 3.89 (m, 6H), 3.87 (d, $J = 0.8$ Hz, 3H). ^{13}C NMR (101 MHz, Methylene Chloride- d_2) δ 183.51, 153.73, 151.84, 142.38, 139.56, 136.73, 134.10, 129.41, 129.04,

128.66, 126.85, 124.00, 114.88, 107.16, 107.09, 103.65, 71.70, 61.15, 56.78. HRMS: calculated for $C_{28}H_{26}N_3O_5$ $[M+H]^+$ 484.1872, found 484.1870.

(2-(5-methyl-1H-indol-3-yl)-1H-imidazol-4-yl)(3,4,5-trimethoxyphenyl)methanone (10ag). obtained as a yellowish solid. 1H NMR (400 MHz, Methylene Chloride- d_2) δ 8.03 (s, 1H), 7.88 (d, $J = 1.6$ Hz, 1H), 7.79 (s, 1H), 7.36 (dd, $J = 8.4, 1.5$ Hz, 1H), 7.27 (s, 2H), 7.09 (d, $J = 8.4$ Hz, 1H), 3.92 (d, $J = 1.6$ Hz, 6H), 3.88 (d, $J = 1.6$ Hz, 3H), 2.62 – 2.40 (m, 3H). ^{13}C NMR (101 MHz, Methylene Chloride- d_2) δ 184.33, 153.77, 149.36, 142.51, 135.52, 134.01, 131.13, 126.56, 125.50, 125.01, 120.34, 112.08, 107.14, 106.03, 61.22, 56.79, 21.80. HRMS: calculated for $C_{22}H_{22}N_3O_4$ $[M+H]^+$ 392.1610, found 392.1611.

(2-(5-fluoro-1H-indol-3-yl)-1H-imidazol-4-yl)(3,4,5-trimethoxyphenyl)methanone (10ah). obtained as a yellowish solid. 1H NMR (400 MHz, Methylene Chloride- d_2) δ 8.00 – 7.91 (m, 2H), 7.80 (s, 1H), 7.41 (dd, $J = 8.9, 4.5$ Hz, 1H), 7.30 (s, 2H), 7.01 (td, $J = 9.0, 2.5$ Hz, 1H), 3.92 (s, 6H), 3.88 (s, 3H). ^{13}C NMR (101 MHz, Methylene Chloride- d_2) δ 184.61, 160.45, 158.11, 153.75, 142.54, 134.00, 133.81, 127.77, 125.96, 125.85, 113.26, 113.17, 111.74, 111.48, 107.28, 106.92, 106.88, 106.21, 105.96, 61.22, 56.79. HRMS: calculated for $C_{21}H_{19}FN_3O_4$ $[M+H]^+$ 396.1360, found 396.1364.

(2-(5-chloro-1H-indol-3-yl)-1H-imidazol-4-yl)(3,4,5-trimethoxyphenyl)methanone (10ai). obtained as a yellowish solid. 1H NMR (400 MHz, Acetone- d_6) δ 10.93 (s, 1H), 8.64 (d, $J = 2.2$ Hz, 1H), 8.29 (s, 1H), 7.92 (s, 1H), 7.54 (d, $J = 8.7$ Hz, 2H), 7.23 (dd, $J = 8.7, 2.1$ Hz, 1H), 3.97 (s, 6H), 3.85 (s, 3H). ^{13}C NMR (101 MHz, Acetone- d_6) δ 183.80, 154.15, 142.94, 136.18, 136.03, 134.44, 127.60, 127.20, 126.71, 123.53, 121.78, 114.04, 114.00, 107.96, 107.57, 60.71, 56.67. HRMS: calculated for $C_{21}H_{19}ClN_3O_4$ $[M+H]^+$ 412.1064, found 412.1068.

(2-(5-bromo-1H-indol-3-yl)-1H-imidazol-4-yl)(3,4,5-trimethoxyphenyl)methanone (10aj). obtained as a yellowish solid. 1H NMR (400 MHz, Methylene Chloride- d_2) δ 8.44 (dd, $J = 1.9, 0.8$ Hz, 1H), 7.90 (s, 1H), 7.80 (s, 1H), 7.39 – 7.26 (m, 4H), 3.93 (s, 6H), 3.88 (s, 3H). ^{13}C NMR (101 MHz, Methylene Chloride- d_2) δ 184.63, 153.78, 148.24, 142.61, 135.92, 133.91, 127.33, 127.10, 126.19, 123.58, 114.77, 113.96, 107.29, 106.30, 61.23, 56.84. HRMS: calculated for $C_{21}H_{19}BrN_3O_4$ $[M+H]^+$ 456.0559, found 456.0555.

(2-(5-(benzyloxy)-1H-indol-3-yl)-1H-imidazol-4-yl)(3,4,5-trimethoxyphenyl)methanone (10ak). obtained as a yellowish solid. 1H NMR (400 MHz, Acetone- d_6) δ 10.69 (s, 1H), 8.24 (dd, $J = 9.5, 2.5$ Hz, 2H), 7.93 (s, 1H), 7.59 – 7.46 (m, 4H), 7.46 – 7.35 (m, 3H), 7.35 – 7.28 (m, 1H), 6.98 (dd, $J = 8.8, 2.5$ Hz, 1H), 5.16 (s, 2H), 3.95 (s, 6H), 3.82 (s, 3H). ^{13}C NMR (101 MHz, Acetone- d_6) δ 183.75, 155.14, 154.15, 142.92, 138.97, 134.58, 133.03, 132.88, 129.20, 128.58, 128.47, 127.12, 126.57, 126.40, 114.10, 113.23, 113.18, 107.92, 107.32, 105.98, 71.25, 60.71, 60.54, 56.69. HRMS: calculated for $C_{28}H_{26}N_3O_5$ $[M+H]^+$ 484.1872, found 484.1875.

(2-(6-methyl-1H-indol-3-yl)-1H-imidazol-4-yl)(3,4,5-trimethoxyphenyl)methanone (10al). obtained as a yellowish solid. ¹H NMR (400 MHz, Methylene Chloride-d₂) δ 8.06 (d, J = 8.2 Hz, 1H), 7.88 (s, 1H), 7.83 (s, 1H), 7.25 (s, 2H), 7.21 (s, 1H), 7.05 (d, J = 8.0 Hz, 1H), 3.87 (d, J = 3.0 Hz, 9H), 2.41 (s, 3H). ¹³C NMR (101 MHz, Methylene Chloride-d₂) δ 183.51, 153.86, 148.33, 142.82, 137.43, 133.85, 133.46, 132.01, 125.84, 123.74, 123.03, 120.50, 112.28, 107.08, 106.16, 61.20, 56.83, 21.90. HRMS: calculated for C₂₂H₂₂N₃O₄ [M+H]⁺ 392.1610, found 392.1613.

(2-(6-fluoro-1H-indol-3-yl)-1H-imidazol-4-yl)(3,4,5-trimethoxyphenyl)methanone (10am). obtained as a yellowish solid. ¹H NMR (400 MHz, Methylene Chloride-d₂) δ 8.27 – 8.17 (m, 1H), 7.88 (d, J = 2.1 Hz, 1H), 7.79 (d, J = 2.5 Hz, 1H), 7.30 (d, J = 2.1 Hz, 2H), 7.15 (dt, J = 9.6, 2.4 Hz, 1H), 6.98 (ddd, J = 9.6, 8.8, 2.4 Hz, 1H), 3.91 (d, J = 2.2 Hz, 6H), 3.87 (s, 3H). ¹³C NMR (101 MHz, Methylene Chloride-d₂) δ 184.67, 161.98, 159.62, 153.76, 148.67, 142.55, 137.37, 137.25, 134.00, 126.67, 126.64, 122.14, 122.10, 122.00, 110.09, 109.85, 107.27, 106.71, 98.65, 98.40, 61.23, 56.77. HRMS: calculated for C₂₁H₁₉FN₃O₄ [M+H]⁺ 396.1360, found 396.1357.

(2-(6-bromo-1H-indol-3-yl)-1H-imidazol-4-yl)(3,4,5-trimethoxyphenyl)methanone (10an). obtained as a yellowish solid. ¹H NMR (400 MHz, Methylene Chloride-d₂) δ 8.17 (d, J = 8.5 Hz, 1H), 7.87 (s, 1H), 7.80 (s, 1H), 7.59 (d, J = 1.9 Hz, 1H), 7.30 (d, J = 10.4 Hz, 3H), 3.90 (s, 6H), 3.88 (s, 3H). ¹³C NMR (101 MHz, Methylene Chloride-d₂) δ 184.48, 153.73, 148.37, 142.54, 137.94, 133.90, 126.73, 124.56, 124.45, 124.42, 122.51, 116.67, 115.32, 115.27, 107.20, 106.91, 61.21, 56.77. HRMS: calculated for C₂₁H₁₉BrN₃O₄ [M+H]⁺ 456.0559, found 456.0558.

(2-(6-(benzyloxy)-1H-indol-3-yl)-1H-imidazol-4-yl)(3,4,5-trimethoxyphenyl)methanone (10ao). obtained as a yellowish solid. ¹H NMR (400 MHz, Methylene Chloride-d₂) δ 9.54 (s, 1H), 8.21 (d, J = 8.6 Hz, 1H), 7.83 (d, J = 7.0 Hz, 2H), 7.49 – 7.20 (m, 7H), 7.00 – 6.84 (m, 2H), 4.98 (s, 2H), 3.86 (s, 3H), 3.84 (s, 6H). ¹³C NMR (101 MHz, Methylene Chloride-d₂) δ 183.92, 156.66, 153.75, 142.52, 137.89, 137.81, 133.88, 129.02, 128.41, 128.12, 124.92, 122.11, 120.08, 112.30, 107.17, 107.13, 96.74, 70.92, 61.17, 56.75. HRMS: calculated for C₂₈H₂₆N₃O₅ [M+H]⁺ 484.1872, found 484.1870.

(2-(6-methoxy-1H-indol-3-yl)-1H-imidazol-4-yl)(3,4,5-trimethoxyphenyl)methanone (10ap). obtained as a yellowish solid. ¹H NMR (400 MHz, Methylene Chloride-d₂) δ 8.12 (dd, J = 8.7, 0.6 Hz, 1H), 7.79 (d, J = 5.8 Hz, 2H), 7.27 (s, 2H), 6.94 (d, J = 2.2 Hz, 1H), 6.88 (dd, J = 8.8, 2.3 Hz, 1H), 3.91 (s, 6H), 3.87 (s, 3H), 3.83 (s, 3H). ¹³C NMR (101 MHz, Methylene Chloride-d₂) δ 184.25, 157.54, 153.75, 149.09, 142.51, 137.98, 133.96, 125.15, 121.60, 119.63, 111.53, 107.14, 106.61, 95.58, 95.52, 61.20, 56.78, 56.06. HRMS: calculated for C₂₂H₂₂N₃O₅ [M+H]⁺ 408.1559, found 408.1566.

Methyl 3-(4-(3,4,5-trimethoxybenzoyl)-1H-imidazol-2-yl)-1H-indole-6-carboxylate (10aq). obtained as a yellowish solid. ¹H NMR (400 MHz, DMSO-d₆) δ 13.21 (s, 1H), 11.98 (s, 1H), 8.52 (d, J = 8.4 Hz, 1H), 8.45 (s, 1H), 8.15 (s, 1H), 8.00 (s,

1H), 7.77 (d, J = 8.4 Hz, 1H), 7.49 (s, 2H), 3.91 (s, 6H), 3.88 (s, 3H), 3.79 (s, 3H). ¹³C NMR (101 MHz, DMSO-d₆) δ 182.97, 166.98, 152.62, 141.15, 135.65, 133.24, 129.07, 128.45, 127.98, 127.74, 127.50, 123.27, 120.91, 120.60, 117.93, 113.86, 106.82, 106.36, 60.14, 55.98, 51.84. HRMS: calculated for C₂₃H₂₂N₃O₆ [M+H]⁺ 436.1509, found 436.1506.

(2-(7-methyl-1H-indol-3-yl)-1H-imidazol-4-yl)(3,4,5-trimethoxyphenyl)methanone (10ar). obtained as a yellowish solid. ¹H NMR (400 MHz, Methylene Chloride-d₂) δ 8.09 (dt, J = 7.7, 0.9 Hz, 1H), 7.92 (s, 1H), 7.81 (s, 1H), 7.28 (s, 2H), 7.14 (dd, J = 8.1, 7.1 Hz, 1H), 7.05 (dt, J = 7.2, 1.0 Hz, 1H), 3.90 (s, 6H), 3.88 (s, 3H), 2.51 (s, 3H). ¹³C NMR (101 MHz, Methylene Chloride-d₂) δ 184.19, 153.74, 149.12, 142.49, 136.79, 136.65, 133.95, 126.24, 126.08, 124.99, 124.96, 123.86, 121.99, 121.95, 121.75, 118.53, 107.15, 107.08, 107.03, 61.18, 56.76, 16.91. HRMS: calculated for C₂₂H₂₂N₃O₄ [M+H]⁺ 392.1610, found 392.1615.

(2-(7-(benzyloxy)-1H-indol-3-yl)-1H-imidazol-4-yl)(3,4,5-trimethoxyphenyl)methanone (10as). obtained as a yellowish solid. ¹H NMR (400 MHz, Methylene Chloride-d₂) δ 9.29 (s, 1H), 7.95 (d, J = 2.9 Hz, 1H), 7.90 (d, J = 8.1 Hz, 1H), 7.84 (s, 1H), 7.54 – 7.47 (m, 2H), 7.44 – 7.33 (m, 3H), 7.30 (s, 2H), 7.15 (t, J = 7.9 Hz, 1H), 6.82 (dd, J = 7.8, 0.7 Hz, 1H), 5.24 (s, 2H), 3.90 (s, 6H), 3.87 (s, 3H). ¹³C NMR (101 MHz, Methylene Chloride-d₂) δ 183.55, 153.81, 146.12, 142.59, 137.54, 133.81, 129.15, 128.74, 128.43, 127.78, 126.94, 125.29, 122.36, 114.16, 107.82, 107.07, 104.86, 70.93, 61.17, 56.81. HRMS: calculated for C₂₈H₂₆N₃O₅ [M+H]⁺ 484.1872, found 484.1868.

(2-(7-methoxy-1H-indol-3-yl)-1H-imidazol-4-yl)(3,4,5-trimethoxyphenyl)methanone (10at). obtained as a yellowish solid. ¹H NMR (400 MHz, Methylene Chloride-d₂) δ 7.88 (s, 1H), 7.85 – 7.77 (m, 2H), 7.28 (s, 2H), 7.17 (t, J = 7.9 Hz, 1H), 6.74 (dd, J = 7.9, 0.8 Hz, 1H), 3.98 (s, 3H), 3.91 (s, 6H), 3.88 (s, 3H). ¹³C NMR (101 MHz, Methylene Chloride-d₂) δ 184.15, 153.77, 147.11, 142.55, 133.91, 127.59, 126.64, 125.67, 122.28, 113.43, 107.26, 107.12, 103.42, 61.20, 56.79, 56.01. HRMS: calculated for C₂₂H₂₂N₃O₅ [M+H]⁺ 408.1559, found 408.1556.

(2-(4-hydroxy-1H-indol-3-yl)-1H-imidazol-4-yl)(3,4,5-trimethoxyphenyl)methanone (10au). obtained as a yellowish solid. ¹H NMR (400 MHz, Methylene Chloride-d₂) δ 8.02 (s, 1H), 7.72 (d, J = 3.4 Hz, 1H), 7.31 – 7.14 (m, 3H), 7.07 (t, J = 7.5 Hz, 1H), 6.92 (d, J = 7.3 Hz, 1H), 6.58 (d, J = 7.7 Hz, 1H), 3.91 (s, 6H), 3.88 (s, 3H). HRMS: calculated for C₂₁H₂₀N₃O₅ [M+H]⁺ 394.1403, found 394.1405.

(2-(5-hydroxy-1H-indol-3-yl)-1H-imidazol-4-yl)(3,4,5-trimethoxyphenyl)methanone (10av). obtained as a yellowish solid. ¹H NMR (400 MHz, DMSO-d₆) δ 12.88 (d, J = 58.5 Hz, 1H), 11.48 – 10.98 (m, 1H), 8.84 (d, J = 12.5 Hz, 1H), 8.25 (d, J = 2.8 Hz, 1H), 7.89 (d, J = 3.5 Hz, 1H), 7.83 (q, J = 2.0, 1.3 Hz, 1H), 7.24 (dd, J = 8.6, 2.3 Hz, 1H), 7.18 (s, 1H), 6.69 (ddd, J = 11.2, 8.7, 2.5 Hz, 1H), 3.84 (dd, J = 47.9, 6.9 Hz, 9H). HRMS: calculated for C₂₁H₂₀N₃O₅ [M+H]⁺ 394.1403, found 394.1404.

(2-(6-hydroxy-1H-indol-3-yl)-1H-imidazol-4-yl)(3,4,5-trimethoxyphenyl)methanone (10aw). obtained as a yellowish solid. ^1H NMR (400 MHz, Methylene Chloride- d_2) δ 7.89 (s, 1H), 7.79 (s, 1H), 7.71 (dd, $J = 8.0, 0.9$ Hz, 1H), 7.27 (s, 2H), 7.09 (t, $J = 7.9$ Hz, 1H), 6.70 (dd, $J = 7.7, 0.8$ Hz, 1H), 3.92 (s, 6H), 3.88 (s, 3H). HRMS: calculated for $\text{C}_{21}\text{H}_{20}\text{N}_3\text{O}_5$ $[\text{M}+\text{H}]^+$ 394.1403, found 394.1401.

3-(4-(3,4,5-trimethoxybenzoyl)-1H-imidazol-2-yl)-1H-indole-6-carboxylic acid (10ax). obtained as a yellowish solid. ^1H NMR (400 MHz, DMSO- d_6) δ 13.79 – 13.14 (m, 1H), 12.38 (d, $J = 75.1$ Hz, 1H), 8.83 – 8.41 (m, 2H), 8.15 (s, 1H), 8.10 – 7.84 (m, 2H), 7.74 (dd, $J = 13.7, 8.4$ Hz, 1H), 7.20 (s, 1H), 3.86 (dd, $J = 50.2, 10.6$ Hz, 9H). HRMS: calculated for $\text{C}_{22}\text{H}_{20}\text{N}_3\text{O}_6$ $[\text{M}+\text{H}]^+$ 422.1352, found 422.1355.

(2-(1H-indol-2-yl)-1H-imidazol-4-yl)(3,4,5-trimethoxyphenyl)methanone (10ba). obtained as a yellowish solid. ^1H NMR (400 MHz, Chloroform- d) δ 10.31 (s, 1H), 8.18 (d, $J = 7.7$ Hz, 1H), 7.89 (s, 1H), 7.63 (t, $J = 8.9$ Hz, 2H), 7.51 (t, $J = 7.6$ Hz, 1H), 7.34 (d, $J = 8.2$ Hz, 1H), 7.27 (d, $J = 4.9$ Hz, 7H), 7.15 (ddd, $J = 8.0, 6.9, 1.0$ Hz, 1H), 3.99 (s, 3H), 3.91 (s, 6H). ^{13}C NMR (101 MHz, DMSO- d_6) δ 182.28, 152.72, 141.89, 141.11, 139.01, 136.94, 133.12, 129.21, 128.44, 127.86, 122.31, 120.75, 119.66, 111.90, 107.32, 106.16, 101.99, 100.14, 60.12, 56.00. HRMS: calculated for $\text{C}_{21}\text{H}_{20}\text{N}_3\text{O}_4$ $[\text{M}+\text{H}]^+$ 378.1454, found 378.1458.

(2-(1H-indol-4-yl)-1H-imidazol-4-yl)(3,4,5-trimethoxyphenyl)methanone (10bb). obtained as a yellowish solid. ^1H NMR (400 MHz, Chloroform- d) δ 11.06 (s, 1H), 8.80 (s, 1H), 7.94 (s, 1H), 7.69 (d, $J = 7.4$ Hz, 1H), 7.47 (dt, $J = 8.2, 0.9$ Hz, 1H), 7.33 (t, $J = 2.9$ Hz, 2H), 7.26 (d, $J = 1.7$ Hz, 1H), 7.20 (t, $J = 7.8$ Hz, 1H), 3.96 (s, 3H), 3.91 (s, 6H). ^{13}C NMR (101 MHz, Chloroform- d) δ 183.67, 153.30, 142.36, 136.84, 133.00, 126.16, 125.49, 121.97, 120.82, 119.18, 113.41, 106.78, 102.88, 61.15, 56.45. HRMS: calculated for $\text{C}_{21}\text{H}_{20}\text{N}_3\text{O}_4$ $[\text{M}+\text{H}]^+$ 378.1454, found 378.1453.

(2-(1H-indol-5-yl)-1H-imidazol-4-yl)(3,4,5-trimethoxyphenyl)methanone (10bc). obtained as a yellowish solid. ^1H NMR (400 MHz, Methylene Chloride- d_2) δ 9.34 (s, 1H), 8.28 (d, $J = 1.6$ Hz, 1H), 7.83 (dd, $J = 8.6, 1.7$ Hz, 1H), 7.80 (s, 1H), 7.51 (d, $J = 8.6$ Hz, 1H), 7.31 (dt, $J = 2.7, 1.2$ Hz, 1H), 7.26 (s, 2H), 6.61 (dt, $J = 3.0, 1.3$ Hz, 1H), 3.91 (s, 6H), 3.88 (s, 3H). ^{13}C NMR (101 MHz, Chloroform- d) δ 183.52, 153.35, 142.35, 137.06, 133.13, 128.33, 125.77, 120.90, 120.78, 119.55, 111.83, 106.70, 103.64, 61.15, 56.43. HRMS: calculated for $\text{C}_{21}\text{H}_{20}\text{N}_3\text{O}_4$ $[\text{M}+\text{H}]^+$ 378.1454, found 378.1459.

(2-(1H-indol-6-yl)-1H-imidazol-4-yl)(3,4,5-trimethoxyphenyl)methanone (10bd). obtained as a yellowish solid. ^1H NMR (400 MHz, Chloroform- d) δ 11.02 (s, 1H), 8.77 (s, 1H), 7.95 (s, 1H), 7.79 – 7.65 (m, 1H), 7.49 (d, $J = 8.1$ Hz, 1H), 7.36 (t, $J = 2.8$ Hz, 1H), 7.32 – 7.16 (m, 4H), 3.97 (s, 3H), 3.92 (s, 6H). ^{13}C NMR (101 MHz, Chloroform- d) δ 183.29, 153.36, 151.90, 142.38, 138.95, 136.83, 132.97, 131.17, 126.23, 125.52, 122.01, 120.72, 119.32, 113.51, 106.55, 102.84, 61.16, 56.45. HRMS: calculated for $\text{C}_{21}\text{H}_{20}\text{N}_3\text{O}_4$ $[\text{M}+\text{H}]^+$ 378.1454, found 378.1453.

(2-(1H-indol-7-yl)-1H-imidazol-4-yl)(3,4,5-trimethoxyphenyl)methanone (10be). obtained as a yellowish solid. ¹H NMR (400 MHz, Chloroform-d) δ 8.58 (s, 1H), 8.24 (d, J = 7.5 Hz, 1H), 7.93 (d, J = 3.6 Hz, 1H), 7.87 (dd, J = 7.8, 0.8 Hz, 1H), 7.72 (s, 2H), 7.60 (t, J = 7.7 Hz, 1H), 7.02 (d, J = 3.7 Hz, 1H), 3.97 (d, J = 0.9 Hz, 9H). ¹³C NMR (101 MHz, Chloroform-d) δ 186.04, 153.10, 143.96, 143.25, 142.87, 142.05, **132.31**, 132.01, 128.20, 125.87, 124.94, 123.97, 121.35, 120.31, 112.94, 110.91, 108.31, 61.14, 56.49. HRMS: calculated for C₂₁H₂₀N₃O₄ [M+H]⁺ 378.1454, found 378.1452.

Cell culture and reagents

Human melanoma carcinoma cell lines A375, M14, and WM-164 (American Type Culture Collection or ATCC, Manassas, VA, USA) were cultured in Dulbecco's modified Eagle's medium (DMEM) (Corning, Manassas, VA) supplemented with 10% (v/v) fetal bovine serum (FBS) (Atlanta Biologicals, Lawerenceville, GA) and 1% antibiotic/antimycotic mixture (Sigma-Aldrich, St. Louis MO). Murine melanoma B16F10 cells (ATCC, Manassas, VA, USA) were cultured in Minimum essential medium (Invitrogen, Carlsbad, CA), supplemented with 5% heat-inactivated Hyclone FBS (Thermo Scientific, Rockford, IL), 1% antibiotic-antimycotic mixture (Sigma-Aldrich, St. Louis MO), 1% Mem-sodium pyruvate (Invitrogen, Carlsbad, CA), 1% Mem-vitamin (Invitrogen, Carlsbad, CA), L-Glutamine (2mM final concentration) (Invitrogen, Carlsbad, CA), and 1% Mem NEAA (Invitrogen, Carlsbad, CA). All cell lines were authenticated by ATCC by short tandem repeat profiling. Cultures were maintained to 80-90% confluency at 37°C in a humidified atmosphere containing 5% CO₂. Compounds were dissolved in dimethyl sulfoxide (DMSO) (Sigma-Aldrich, St. Louis, MO) to make a stock solution of 20 mM. Compound solutions were freshly prepared by diluting stocks with cell culture medium before use.

Cytotoxicity assay

A375, M14, and WM-164 were seeded in 96-well plates at a concentration of 1,000–5,000 cells per well, depending on growth rate of the cell line. After overnight incubation, the media was replaced and cells were treated with the test compounds at 10 concentrations ranging from 0.03 nM to 1 μM plus a vehicle control for 72 h in four replicates. Following treatment, the MTS reagent (Promega, Madison, WI) was added to the cells and incubated in dark at 37°C for at least 1 hour. Absorbance at 490 nm was measured using a plate reader (DYNEX Technologies, Chantilly VA). Percentages of cell survival versus drug concentrations were plotted, and the IC₅₀ (concentration that inhibited cell growth by 50% of untreated control) values were obtained by nonlinear regression analysis using GraphPad Prism (GraphPad Software, San Diego, CA).

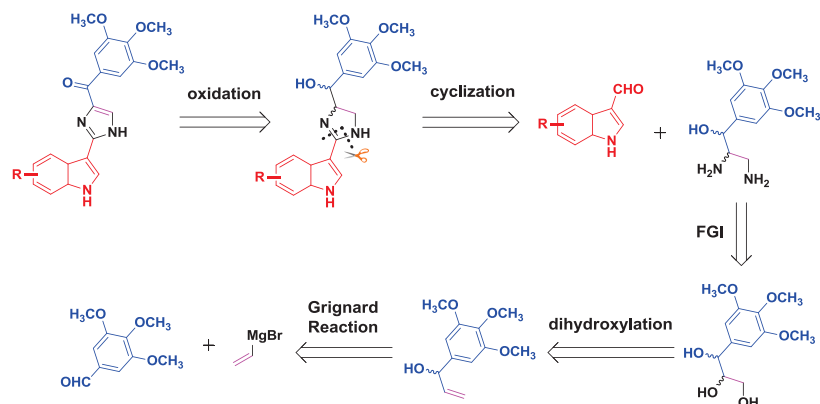
Chemistry

ABI-231 belongs to the third generation of ABIs developed in our lab. It is composite of a 3,4,5-trimethoxybenzoyl moiety, a 3-indole moiety, as well as a imidazole linker. In the previous SAR studies of ABI-I/II and RABI scaffold, attempts to improve their antiproliferative activities against cancer cell lines by modifying the 3,4,5-trimethoxybenzoyl moiety were not successful [169, 182, 185, 186]. Considering the structural similarity between ABI-231 and ABI-I/II, we hypothesize that the 3,4,5-trimethoxybenzoyl moiety is essential for the activity of ABI-231. Based on the molecular modeling result as shown in **Figure 1-7**, we also hypothesize that introduction of substituent to the indole can utilize the unoccupied pocket in the vicinity of the indole to enhance the binding affinity of the ABI-231 to tubulin protein. With these hypotheses in mind, we have synthesized ABI-231 analogues with modification of the indole moiety. Thirty new ABI-231 analogues are furnished.

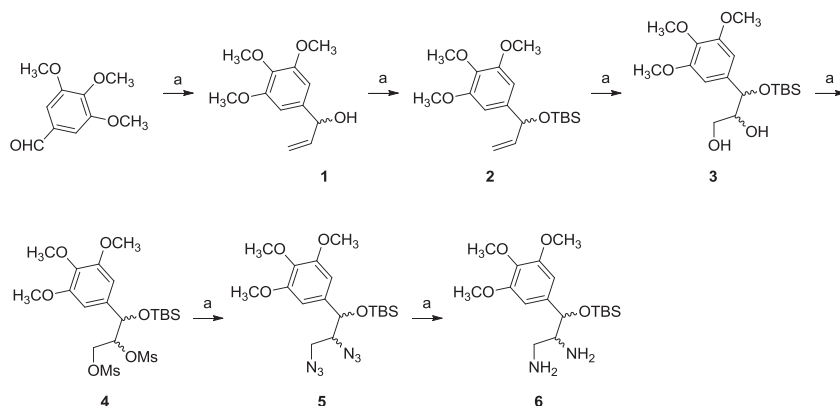
The previously published synthetic method accessed ABI-231 by resorting to an imidazole formation/nucleophilic substitution strategy. This method provided ABI-231 with an overall yield of 0.28% over five steps, which is not amenable for SAR investigation of ABI-231. Hence, to investigate the SAR of ABI-231, it is of imperativeness to establish a synthetic method that can efficiently and rapidly generate ABI-231 and its analogues. Our proposed synthetic strategy is illustrated in **Scheme 2-1**. To construct the ABI-231 scaffold, we resort to imidazoline cyclization. The imidazoline can be formed from a diamine intermediate **6** and indolylcarboxyaldehydes according to a reported methodology [187]. We envisage that the imidazoline formation can provide resourceful ABI-231 analogues with modifications of the indole moiety because indolylcarboxyaldehydes are broadly commercially available. In this proposed method, accumulation of a large quantity of the diamine intermediate **6** is crucial.

Diamine **6** can be derived from alkene **1** through a series of well-known and high-yielding functional group interconversions including Upjohn dihydroxylation, mesylation and hydrogenation. **6** was obtained in six steps as depicted in **Scheme 2-2**. Starting material 3,4,5-trimethoxybenzaldehyde was treated with Grignard reagent vinylmagnesium bromide to generate the racemic mixture **1**, which was protected with TBS to give **2** (87% for 2 steps). **2** was then subjected to Upjohn reaction in the presence of a catalytic equivalent of OsO₄ to form a mixture diastereoisomers **3** in 82% yield. Diazide **5** was synthesized in two steps by following reported procedures [188]: mesylation of the diol **3** yielded mesylates **4** in 86% yield; **4** was then refluxed with sodium azide in DMF carefully to give azides **5** in 67% yield. Hydrogenation of diazide **5** provided diamine **6** in 53% yield in the presence of Pd/C (10%).

Synthesis of ABI-231 analogues with substituted 3-indolylys was outlined in **Scheme 2-3**. Indolecarboxyaldehyde was protected with Boc to give **7**. **7** then reacted with diamine **6** in the presence of *N*-bromosuccinimide in DCM at ice temperature to form imidazoline **8**. **8** was subjected to the deprotection of TBS and Boc in the presence of TBAF and TFA to provide **9**. Simultaneous oxidation of imidazoline and secondary

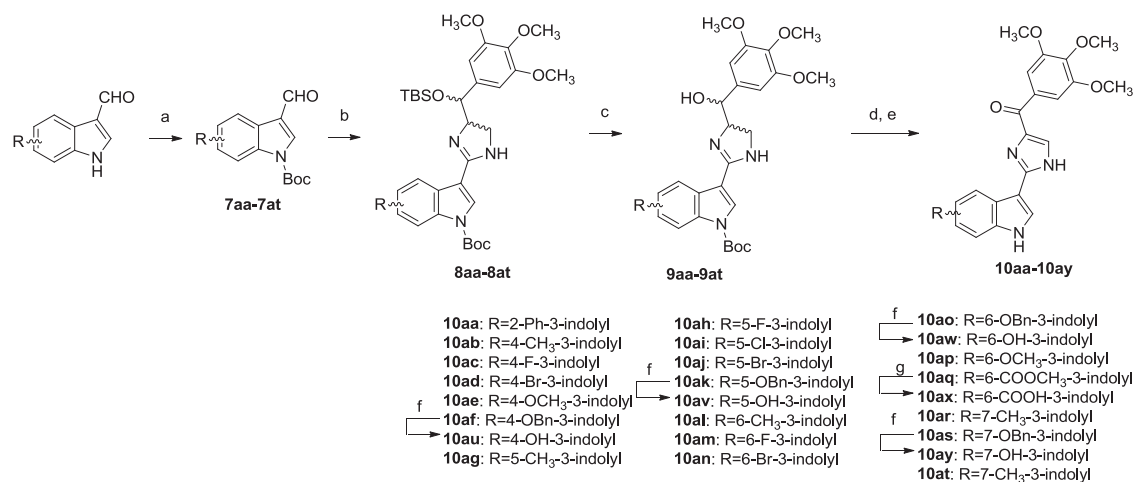


Scheme 2-1. Retrosynthetic analysis of ABI-231 and its analogues



Scheme 2-2. Synthesis of the intermediate 6

Reagents and conditions: (a): vinylmagnesium bromide, THF, 0°C to rt; (b): *tert*-butyldimethylsilyl chloride, imidazole, DCM, rt; (c): OsO₄, NMO, Acetone/*t*-BuOH, rt; (d): MsCl, TEA, DCM, rt; (e): NaN₃, DMF, reflux; (f): H₂, Pd/C (10%), EtOAc-MeOH, rt.



Scheme 2-3. Synthesis of ABI-231 analogues with 3-indolylys

Reagents and conditions: (a): (Boc)₂O, DMAP, DCM, rt; (b): NBS, DCM, 0°C to rt; (c): TBAF, THF, rt; (d): TFA, DCM, rt; (e): IBX, DMSO, rt; (f): H₂, Pd/C (10%), EtOAc-MeOH(1:1), rt; (g): LiOH, Dioxane-H₂O, r.t; 10-20% over 4 steps.

alcohol in **9** to imidazole and carbonyl was accomplished in the presence of 3.0-5.0 equivalents of 2-iodoxybenzoic acid (IBX) by referring to a reported method, in which imidazoline was oxidized to imidazole using 1.0 equivalent of IBX [189]. Analogues of ABI-231 **10a-10t** were given in 10-20% yield over four steps. Hydrogenation of **10af**, **10ak**, **10ao** and **10as** afforded **10au**, **10av**, **10aw** and **10ay**, respectively. Saponification of **10aq** provided **10ax**. Analogs **10ba-10be** with indole rotation were synthesized by following similar procedures as outlined in **Scheme 2-4**.

In summary, we have established an efficient synthetic route for ABI-231 and its analogues. This novel method necessitated the synthesis of a key diamine intermediate **6** and imidazoline formation. **6** was obtained from commercially available 3,4,5-trimethoxybenzaldehyde with an overall yield of 22% in six steps. Rapid generation of ABI-231 analogues modifying the indole moiety was successfully carried out through cyclization between **6** and commercially available indolylcarboxyaldehydes. Thirty ABI-231 analogues were prepared from **6** in four steps with an overall yield of 10-20%.

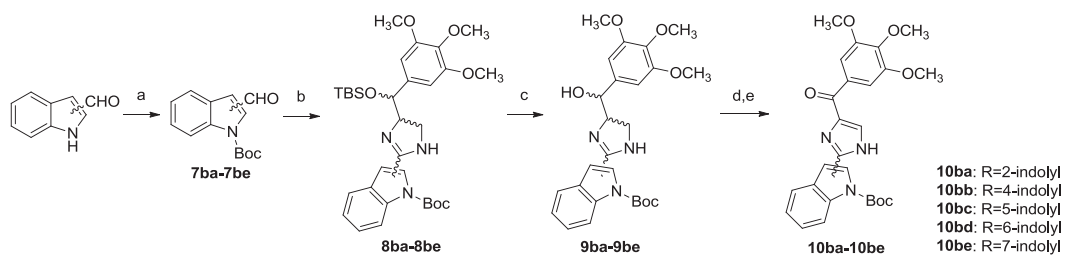
Results

All analogues of ABI-231 were evaluated for their cytotoxicities in human melanoma cell lines including A375, WM1641 and M14. Colchicine was used as a positive control. ABI-231 was used as a prototype for comparison. The antiproliferative effects of the compounds were evaluated by MTT assay. IC₅₀s were reported in nM and calculated from at least three independent experiments, each performed in duplicates. Their *in vitro* growth inhibitory effects were shown in **Table 2-1** and **Table 2-2**. ABI-231 had an average IC₅₀ value of 7.0 nM and was comparable to our previously reported data [169].

In vitro growth inhibitory effects of ABI-231 analogues with 3-indolyls

Substitution at the 2-position of the indole ring. Compared to the prototype ABI-231, analogue **10aa** with a bulky phenyl group on the 2-position of indole moiety showed markedly reduced activity. **10aa** had an average IC₅₀ value of more than 1 μM against a panel of melanoma cell lines. This indicated that only small substituent on the indole can be tolerated. It is worthy noting that attempts to synthesize analogues with electron-donating functional groups on the 2-position of indole were not successful. For example, the reaction as depicted in **Figure 2-2** was performed to obtain 2-methyl-3-indole analogue. This reaction can only provide the target imidazoline in less than 10% yield. The low yield of this reaction is probably due to that the electron-donating property of the 2-methyl can attenuate reactivity of the 3-carboxaldehyde.

Substitution at the 4-position of the indole ring. Six analogues including **10ab-10af** and **10au** were synthesized in this series. The best inhibitory effect was observed for 4-methyl analogue **10ab**. **10ab** exhibited 3-fold improvement of potency compared to



Scheme 2-4. Synthesis of ABI-231 analogues with rotation of indolylys

Reagents and conditions:(a): (Boc)₂O, DMAP, DCM, rt; (b): NBS, DCM, 0°C to rt; (c): TBAF, THF, rt; (d): TFA, DCM, rt; (e): IBX, DMSO, rt; 10-20% over 4 steps.

Table 2-1. *In vitro* growth inhibitory effects (nM) of ABI-231 analogues with 3-indolyis (n=3)

Compound	A375	M14	WM164
10aa	>1000	>1000	>1000
10ab	1.8 ± 0.2	1.7 ± 0.2	3.2 ± 0.3
10ac	7.2 ± 0.7	8.2 ± 0.9	44.5 ± 15.6
10ad	13.8 ± 1.7	10.4 ± 1.2	67.1 ± 14.5
10ae	>1000	>1000	>1000
10af	>1000	>1000	>1000
10au	9.2 ± 1.4	8.6 ± 0.8	19.1 ± 1.8
10ag	277.7 ± 36.3	177.4 ± 16.3	552.3 ± 108.3
10ah	19.2 ± 1.5	18.0 ± 1.3	80.9 ± 16.6
10ai	61.8 ± 9.3	64.9 ± 4.3	159.5 ± 24.1
10aj	164.2 ± 16.7	104.3 ± 5.9	441.7 ± 110.0
10ak	>1000	>1000	>1000
10av	>1000	>1000	>1000
10al	21.1 ± 3.9	21.7 ± 4.7	23.7 ± 6.1
10am	17.5 ± 3.0	5.8 ± 0.8	10.3 ± 1.2
10an	67.8 ± 10.5	41.2 ± 7.5	55.4 ± 7.4
10ao	>1000	>1000	>1000
10aw	>1000	>1000	>1000
10ap	793.4 ± 89.9	879.8 ± 88.2	>1000
10aq	>1000	196.1	>1000
10ax	>1000	>1000	>1000
10ar	13.1 ± 1.3	10.8 ± 1.0	61.3 ± 11.0
10as	>1000	>1000	>1000
10ay	>1000	>1000	>1000
10at	38.3 ± 3.7	34.1 ± 3.5	115.4 ± 25.0
ABI-231	8.1 ± 1.6	5.6 ± 0.9	7.2 ± 0.9
Colchicine	14.1 ± 2.2	16.6 ± 1.5	10.8 ± 1.9

Table 2-2. *In vitro* growth inhibitory effects (nM) of ABI-231 analogues with rotation of indolyls (n=3)

Compound	A375	M14	WM164
10ba	137.7 ± 23.7	72.3 ± 7.8	55.8 ± 9.5
10bb	3.6 ± 1.0	3.7 ± 0.8	1.6 ± 0.3
10bc	8.6 ± 3.3	18.5 ± 3.7	6.1 ± 1.2
10bd	8.0 ± 1.0	6.1 ± 1.1	3.8 ± 0.5
10be	285.5 ± 28.7	240.6 ± 21.1	435.8 ± 38.3
ABI-231	8.1 ± 1.6	5.6 ± 0.9	7.2 ± 0.9
Colchicine	14.1 ± 2.2	16.6 ± 1.5	10.8 ± 1.9

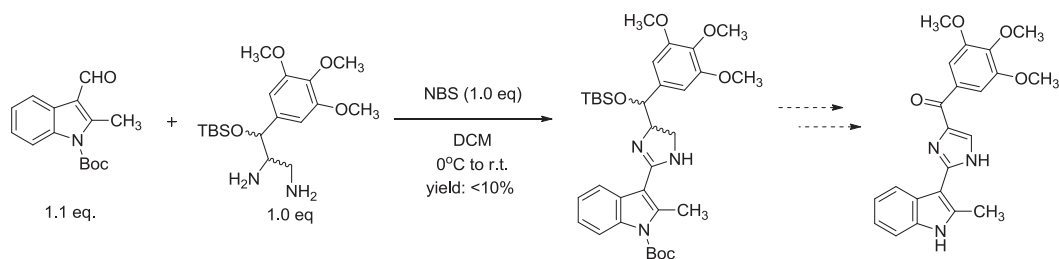


Figure 2-2. Synthesis of an intermediate for 2-methyl-3-indole ABI-231 analogue

prototype ABI-231 and had an average IC_{50} value of 2.2 nM against three melanoma cell lines. Analogue **10ac** with a small size halogen 4-F displayed equipotent antiproliferative activity to that of ABI-231 and had an average IC_{50} value of 7.7 nM. In contrast, analogue **10ad** having a large size halogen 4-bromo was 2-fold less potent than ABI-231 and had an average IC_{50} value of 12.1 nM. For analogues **10ae** with a 4-methoxy group and **10af** with a 4-benzyloxy group, remarkable reduction of activity were observed. Their IC_{50} s were more than 1 μ M. Analogue **10au** that derived from deprotection of **10af** showed restored antiproliferative activity from an average IC_{50} of more than 1 μ M to 12.3 nM. These findings illustrated the importance of the size of substituent on 4-position, which strongly correlated with our hypothesis that only small functional groups can be accommodated in the pocket in the vicinity of the indole moiety.

Substitution at the 5-position of the indole ring. In this series, the best activity was observed in the 5-fluoro analogue **10ah**. **10ah** had an average IC_{50} of 39.4 nM. Analogue **10ak** bearing a bulky benzyloxy showed completely lost antiproliferative activity. Overall, analogues with functional groups on 5-position of the indole in ABI-231 showed markedly decreased antiproliferative activities in comparison with 4-position substituted analogues. For example, 5-fluoro analogue **10ah** and 5-bromo analogue **10aj** were 2-fold and 10-fold less potent than **10ac** and **10ad**, respectively. 5-methyl analogue **10ag** and 5-hydroxy analogue **10av** possessed approximately 100-fold decreased antiproliferative activity compared to **10ab** and **10au**.

Substitution at the 6-position of the indole ring. In the series of 6-position substituted 3-indolyl analogues, the best activity was observed for the 6-fluoro analogue **10am**, which had an average IC_{50} of 11.2 nM. Similar to the series of 4-position substituted and 5-position substituted 3-indolyl analogues, analogues with bulky substituents such as **10ao**, **10ap**, **10aq** lost activities and all had IC_{50} s of more than 1 μ M. For halogen functional groups, fluoro was more favorable than bromo. Hydrogenation of the benzyloxy to hydroxy on the 6-position did not provide any significant activity improvement (**10aw**). 6-methyl analogue **10al** was 10-fold less potent than 4-methyl analogue **10ab** whilst it displayed approximately 10-fold higher potency than 5-methyl analogue **10ag**.

Substitution at the 7-position of the indole ring. Among the 7-position substituted 3-indolyl analogues, **10ar** with a methyl substitution possessed the most potent inhibitory effect (average IC_{50} = 28.4 nM). Interestingly, **10at** with a 7-methoxy substituent showed better anticancer activity (average IC_{50} = 62.6 nM) than analogues with methoxy on the other positions in the indole moiety.

To summarize the SAR of analogues with 3-indolyls, small substituents (e.g. methyl, fluoro) benefits the inhibitory effect while bulky groups (e.g. phenyl, benzyloxy, methoxy, bromo) abolishes the antiproliferative activities. In terms of the substituting positions of the functional group on the indole, the activity trend follows: 4- > 7- > 6- > 5-position.

***In vitro* growth inhibitory effects of ABI-231 analogues with rotation of indolyls**

Hwang et al have disclosed a series of indolyl-imidazopyridines as CBSIs in 2015 [190]. Their SAR study revealed that replacing the 2-indole with 4-, 5- or 6-indole significantly affected the antiproliferative activities. In view of the structural similarity between ABI-231 and indolyl-imidazopyridines, we hypothesize that rotating the 3-indole in ABI-231 to 2, 4, 5, 6, or 7-indole will have an influence on the activity. To test this hypothesis, five ABI-231 analogues were synthesized (**Scheme 2-4**) and their *in vitro* growth inhibitory effects were shown in **Table 2-2**. In this series, 5- and 6-indolyl analogues **10bc** and **10bd** showed comparable antiproliferative activities to that of ABI-231 and had average IC₅₀s of 11.1 and 6.0 nM, respectively. 2- and 7-indolyl analogues **10ba** and **10be** were significantly less potent than ABI-231. **10ba** and **10be** both had IC₅₀s of more than 100 nM. Replacement of the 3-indolyl in ABI-231 with 4-indolyl resulted in **10bb**. **10bb** showed approximately 1-fold improvement of activity compared to ABI-231 and had an average IC₅₀ of 3.0 nM against three melanoma cell lines.

To summarize the SAR of analogues with “indole rotation”, rotating the indole in ABI-231 affects the antiproliferative activities. Among **10ba-10be** and ABI-231, 4-indole analogue **10bb** shows the most potent activity and has an average IC₅₀ of 3.0 nM.

Discussion

Previously, our group has disclosed ABI-231 as a potent tubulin inhibitor. ABI-231 showed antiproliferative activity in the nanomolar range. Importantly, ABI-231 was not a substrate of P-gp and was effective to inhibit the expression of β -III tubulin isotype. Therefore, ABI-231 represents a promising scaffold. According to the published molecular modeling result of ABI-231, we hypothesize that introduction of a small substituent to the indole moiety on ABI-231 may strengthen its binding affinity to tubulin protein. We also hypothesize that rotation of the indole in ABI-231 will affect the activity based on the SAR result of indolyl-imidazopyridines published by Hwang et al.

To overcome the earlier limitations, a novel synthetic method is established for ABI-231 and its analogues. In this method, the core structure of ABI is furnished through an imidazoline formation from a crucial diamine intermediate and commercially available indolylcarboxyaldehydes; simultaneous oxidation of the alcohol and imidazoline to 4-carbonylimidazole in the presence of IBX is firstly reported. This new method is amicable for a gram-scale synthesis of ABI-231 and can rapidly generate ABI-231 analogues for SAR investigation. Thirty new ABI-231 analogues are accomplished from the newly established synthetic method. The SAR result demonstrates that small substituent such as methyl or fluoro is favorable, which is highly correlated with our hypothesis that only small functional group can be accommodated in the target pocket. Among the thirty analogues, **10ab** (4-methyl-3-indolyl analogue) and **10bb** (4-indolyl analogue) exhibit the most potent antiproliferative activities and have average IC₅₀s of 2.2 and 3.0 nM, respectively.

The X-ray crystal structure of the most potent analogue **10ab** in complex with tubulin has been successfully obtained by our collaborators at Sichuan University in China. The crystallographic data and structure refinement statistics for **10ab** is shown in **Table 2-3**. The co-crystal structure of **10ab** in complex with tubulin is shown in **Figure 2-3**. The result shows that **10ab** binds to the colchicine binding site locating at the interface of α and β -tubulin heterodimers. **10ab** forms three H-bond interactions with tubulin: the carbonyl with the residue β -Asp249 in a distance of 3.4 Å; the imidazole NH with the residue α -Thr179 in a distance of 2.9 Å; indole NH with residue β -Asn347 through a water “bridge”. The crystal structure suggests that a methylene or NH between the indole and imidazole moiety may force the indole moiety to move toward the β -Asn347 residue. This movement may allow the formation of a direct H-bond interaction between the indole and β -Asn347 without resorting to a water “bridge”. This is worthy investigating in future effort on structural modification of ABI-231.

In conclusion, we have established an efficient synthetic method for ABI-231 analogues modifying the indole moiety. Thirty new ABI-231 analogues have been synthesized. The most potent analogue **10ab** has an average IC_{50} of 2.2 nM and is 3.2-fold more potent than ABI-231.

Table 2-3. Crystallographic data and structure refinement statistics for 10ab

Ligand	10ab
X-ray source	SSRF-BL19U1
Data collection	
Wavelength (Å)	0.97853
Resolution range (Å)	50 – 2.80 (2.85 – 2.80) ^a
Space group	P 212121
Unit cell (Å, °)	105.2, 157.0, 182.6
Total reflections	503678
Unique reflections	75002
Multiplicity	6.7 (6.3)
Completeness (%)	100 (100)
Mean I/sigma (I)	19.3 (3.0)
Rmerge	0.109 (0.576)
Structure refinement	
R-factor/ R-free^b	0.2174/ 0.2567
RMS (bonds)	0.007
RMS (angles)	1.205
No. of atoms	17520
Macromolecules	17435
Ligand	60
Waters	25
Average B-factor	55.92
Macromolecules	55.91
Ligands (TAJ)	62.6
Waters	44.0
Ramachandran plot statistics	
Most favored regions (%)	92.3
Allowed regions (%)	7.5
Generously allowed regions (%)	0.2
Disallowed regions (%)	0.0

Note: ^a The values for the data in the highest resolution shell are shown in parentheses.

^b R-free = $\frac{\sum \text{Test} ||F_{\text{obs}}| - |F_{\text{calc}}||}{\sum \text{Test} |F_{\text{obs}}|}$, where “Test” is a test set of about 5% of the total reflections randomly chosen and set aside prior to refinement for the structure.

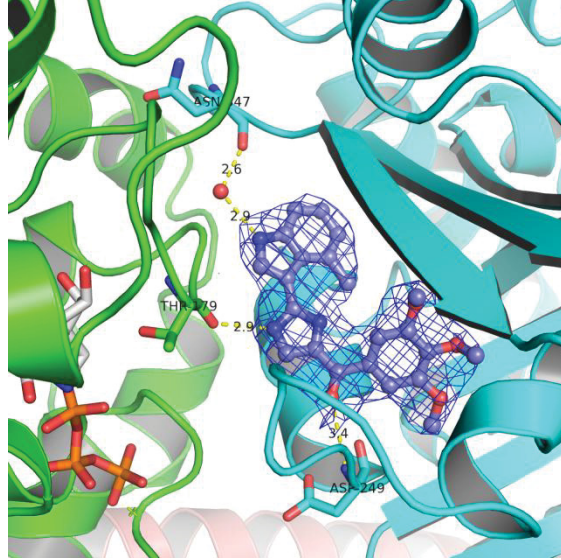


Figure 2-3. Co-crystal structure of 10ab in complex with tubulin

CHAPTER 3. STRUCTURAL MODIFICATION OF THE 3,4,5-TRIMETHOXYPHENYL MOIETY IN ABI-231 LEADS TO IMPROVED ANTIPROLIFERATIVE ACTIVITIES

Introduction

Inhibition of microtubules assembly from α and β -tubulin heterodimers is an attractive and effective target for developing anticancer therapy. MTAs interrupt the cell cycle and result in mitotic arrest at the metaphase/anaphase transition, and eventually induce apoptosis of cancer cells [91, 191]. Although MTAs have achieved great success in cancer treatment, acquired drug-resistance represented a significant obstacle [88]. Therefore, MTAs that are able to surmount multidrug-resistance mechanisms is imperatively needed for treatment of resistant phenotypes.

CBSIs have shown significant abilities to overcome P-gp or MRP-mediated drug resistance [99, 102]. A number of CBSIs are also proven to effectively inhibit the overexpression of tubulin β -III isotype in cancer cells [100]. Thus, colchicine binding site in tubulin represents a promising therapeutic target. Some of the notable examples of CBSIs are outlined in **Figure 3-1**. Of these CBSIs, they share a common moiety, 3,4,5-trimethoxyphenyl (3,4,5-TMP). 3,4,5-TMPs are structurally crucial for many CBSIs to exert their maximum antiproliferative activities [101, 102, 192, 193]. Attempts to modify 3,4,5-TMPs are reported not successful. In colchicine and its derivatives, 3,4,5-TMPs play important roles in increasing the binding affinities and maintaining the suitable molecular conformations [194]. 3,4,5-TMPs in CA-4 and its derivatives are also indispensable in a similar manner. Structural modifications of CA-4 and its derivatives are mainly performed on either the double bond linkage or the 3-hydroxy-4-methoxyphenyl moiety, but rarely on the 3,4,5-TMP moiety [101].

In the search for novel MTAs, we have previously described the discovery of a 2-aryl-4-benzoyl-imidazole (ABI-I) pharmacophore that had desirable drug-like properties and exhibited potent antiproliferative activity against a panel of cancer cell lines [182]. Subsequent structural modifications of the benzoyl moiety, the aryl moiety, as well as the imidazole fragment in the ABI-I scaffold, result in other pharmacophores, including ABI-IIs, ABI-IIIs, RABIs, and IIPs. ABI-231 belongs to ABI-IIIs and had an indole moiety. It shows the most potent antiproliferative activity and had an average IC_{50} value of 5.2 nM against a panel of cancer cell lines [169, 183, 185, 190]. ABI-231 is not a substrate of P-gp and displays a dramatic effect in inhibiting tubulin β -III isotype in a pancreatic cancer cell model with overexpression of different β -tubulin isotypes (unpublished data). ABI-231, therefore, is of great promise for developing anticancer therapy.

In Chapter 2, the co-crystal structure of the most potent 4-methyl-3-indole analogue in complex with tubulin suggests that there are extensive H-bond interactions between each moiety of the ABI-231 with the tubulin protein except for the 3,4,5-TMP moiety. The crystal structure also reveals that there is a methionine residue nearby the

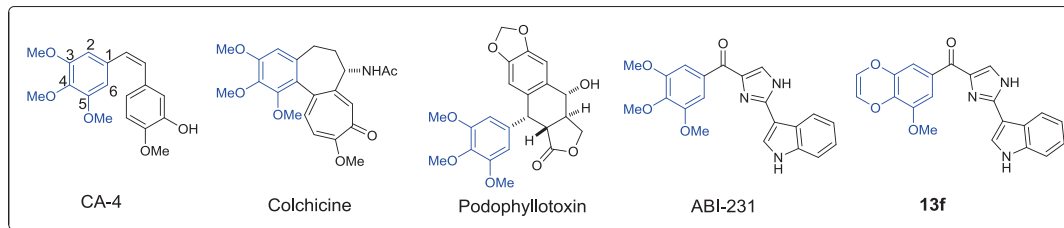


Figure 3-1. Examples of microtubule inhibitors with 3,4,5-TMP moieties targeting colchicine binding sites in tubulin

3,4,5-TMP moiety. We hypothesize that optimization of the 3,4,5-TMP moiety in ABI-231 can potentially introduce a hydrophobic interaction to the methionine residue in tubulin. With this hypothesis, we have carried out the SAR investigation of ABI-231 by modifying the 3,4,5-TMP moiety. In this chapter, we will disclose the establishment of a novel synthetic route to ABI-231 analogues modifying the 3,4,5-TMP moiety. This synthetic method involves a Suzuki coupling/Grignard reaction strategy and can efficiently generate ABI-231 analogues in gram-scale. This novel method can circumvent the involvement of potentially explosive azide reported in the last chapter. Among the eight synthesized ABI-231 analogues, the one containing a unique 3-methoxybenzo[4,5]-dioxene moiety exhibits the strongest antiproliferative activity against a panel of melanoma cell lines and has an average IC₅₀ of 1.9 nM. To our best knowledge, it represents the most successful instance of modifying the 3,4,5-TMP moiety in CA-4 derivatives isosterically. Currently, the mechanistic study and *in vivo* efficacy evaluation of these novel ABI-231 analogues are undergoing.

Experimental Section

General chemistry

Tetrahydrofuran was distilled from sodium-benzophenone. All other solvents and chemical reagents were obtained from commercial sources and directly used without further purification. Glassware was oven-dried before use. All reactions were performed under an argon atmosphere. TLC was performed on silica gel 60 GF254 and monitored under UV light or visualized using phosphomolybdic acid reagent. Flash chromatography was performed on 230-400 mesh silica gel (Fisher Scientific). Melting points were recorded on a MPA100 Automated Melting Point Apparatus. NMR spectra were obtained on a Bruker Ascend 400 (Billerica, MA) spectrometer or a Varian Inova-500 spectrometer (Agilent Technologies, Santa Clara, CA). HR-MS were obtained on Waters Acquity UPLC linked to Waters Acquity Photodiode Array Detector and Waters Acquity Single Quadrupole Mass Detector. Chemical shifts are given in ppm with tetramethylsilane (TMS) as an internal reference. All coupling constants (*J*) are given in Hertz (Hz).

Chemical synthesis

General procedure for synthesis of alkylated methyl benzoate 1a, 1b and 4.
To a solution of the methyl 3-methoxy-4,5-dihydroxybenzoate (2.5 mmol) in acetonitrile (10 mL) was added potassium carbonate (6.0 mmol) and dibromomethane (2.75 mmol) or 1,3-dibromopropane (2.75 mmol) or allyl bromide (6.0 mmol). The mixture was reflux for overnight and then cooled to room temperature; the precipitate was filtered off and washed with dichloromethane. The combined filtration was evaporated under vacuum to give the oily crude which was further purified with flash chromatography on silica.

Elution with hexane/ethyl acetate (5:1-2:1) gave **1a**, **1b** and **4** as colorless oil (yields: 42% for **1a**, 36% for **1b** and 93% for **4**).

Methyl 7-methoxybenzo[d][1,3]dioxole-5-carboxylate (1a). ¹H NMR (400 MHz, Chloroform-d) δ 7.32 (d, J = 1.4 Hz, 1H), 7.19 (d, J = 1.4 Hz, 1H), 6.04 (s, 2H), 3.93 (s, 3H), 3.87 (s, 3H). HRMS: calculated for C₁₀H₁₁O₅ [M+H]⁺ 211.0606, found 211.0607.

Methyl 9-methoxy-3,4-dihydro-2H-benzo[b][1,4]dioxepine-7-carboxylate (1b). ¹H NMR (400 MHz, Chloroform-d) δ 7.31 (d, J = 2.0 Hz, 1H), 7.25 (d, J = 2.0 Hz, 1H), 4.39 – 4.22 (m, 6H), 3.88 (s, 3H), 2.22 (q, J = 5.8 Hz, 2H), 1.35 (t, J = 7.1 Hz, 3H). HRMS: calculated for C₁₂H₁₅O₅ [M+H]⁺ 239.0919, found 239.0917.

Methyl 3,4-bis(allyloxy)-5-methoxybenzoate (4). ¹H NMR (400 MHz, Chloroform-d) δ 7.27 (s, 2H), 6.12 – 5.99 (m, 2H), 5.42 (dq, J = 17.3, 1.6 Hz, 1H), 5.34 – 5.24 (m, 2H), 5.17 (ddt, J = 10.3, 1.9, 1.1 Hz, 1H), 4.59 (ddt, J = 6.1, 5.0, 1.5 Hz, 4H), 3.87 (d, J = 0.7 Hz, 6H). HRMS: calculated for C₁₅H₁₉O₅ [M+H]⁺ 279.1232, found 279.1236.

General procedure for the synthesis of benzoic acids 2a, 2b and 7. To a solution of the methyl benzoate **1a**, **1b** or **6** (1.0 mmol) in dioxane (5 mL) was added solution of lithium hydroxide (1.5 mmol) in water (3ml). The mixture was stirred at 50°C until the TLC indicated the completion of the reaction. The solvents were removed under reduced pressure and the resulted residue was partitioned between water (10 ml) and DCM (10ml), pH value was adjusted to 5 using 1M HCl solution. The organic solvents were then combined, dried over Na₂SO₄, filtered and evaporated under reduced pressure. The crude was purified with flash chromatography on silica. Elution with hexane/ethyl acetate (4:1-1:1) gave **2a**, **2b** and **7** as colorless oil (yields: 88% for **2a**, 91% for **2b** and 84% for **7**).

7-methoxybenzo[d][1,3]dioxole-5-carboxylic acid (2a). ¹H NMR (400 MHz, Acetone-d₆) δ 11.11 (s, 1H), 7.34 (d, J = 1.5 Hz, 1H), 7.15 (d, J = 1.5 Hz, 1H), 6.10 (s, 2H), 3.93 (s, 3H). HRMS: calculated for C₉H₉O₅ [M+H]⁺ 197.0450, found 197.0451.

9-methoxy-3,4-dihydro-2H-benzo[b][1,4]dioxepine-7-carboxylic acid (2b). ¹H NMR (400 MHz, Chloroform-d) δ 10.87 (s, 1H), 7.39 (d, J = 2.0 Hz, 1H), 7.31 (d, J = 2.0 Hz, 1H), 4.41 (t, J = 5.8 Hz, 2H), 4.29 (t, J = 5.9 Hz, 2H), 3.90 (s, 3H), 2.25 (p, J = 5.8 Hz, 2H). HRMS: calculated for C₁₁H₁₃O₅ [M+H]⁺ 225.0763, found 225.0765.

8-methoxybenzo[b][1,4]dioxine-6-carboxylic acid (7). ¹H NMR (400 MHz, Acetone-d₆) δ 7.25 (d, J = 1.8 Hz, 1H), 6.91 (d, J = 1.8 Hz, 1H), 6.15 (d, J = 3.6 Hz, 1H), 6.12 (d, J = 3.6 Hz, 1H), 3.86 (s, 3H). HRMS: calculated for C₁₀H₉O₅ [M+H]⁺ 209.0450, found 209.0447.

General procedure for synthesis of benzoyl chloride 3a, 3b and 8. To a solution of the benzoic acid **2a**, **2b** or **7** (0.8 mmol) in DCM (5 mL) was added thionyl

chloride (1.5 ml). The mixture was stirred at 50°C for 3 hours. The solvents were then removed under reduced pressure and the corresponding crude benzoyl chloride was directly used for next step.

Synthesis of methyl methyl 3-methoxy-4,5-bis(prop-1-en-1-yloxy)benzoate (5). To a solution of **4** (279 mg, 1.0 mmol) in toluene (5 mL) was added carbonylchlorohydridotris(triphenylphosphine)ruthenium(II) (95 mg, 0.1 mmol). The mixture was refluxed for 36hr. Water was then added and the reaction mixture was extracted with ethyl acetate, washed with brine and dried with anhydrous Na₂SO₄. The combined extracts were evaporated under vacuum to give crude product which was purified with flash chromatography on silica. Elution with hexane/ethyl acetate (8:1-3:1) gave **5** as colorless oil (218 mg, 78%). ¹H NMR (400 MHz, Chloroform-*d*) δ 7.35 (s, 2H), 6.47 – 6.11 (m, 2H), 5.44 – 4.60 (m, 2H), 3.90 (d, *J* = 2.0 Hz, 6H), 1.80 – 1.55 (m, 6H). HRMS: calculated for C₁₅H₁₉O₅ [M+H]⁺ 279.1232, found 279.1234.

Synthesis of methyl 8-methoxybenzo[b][1,4]dioxine-6-carboxylate (6). To a solution of **5** (200 mg, 0.72 mmol) in toluene (5 mL) was added Grubbs' catalyst 2nd generation (95 mg, 0.072 mmol). The mixture was refluxed for 24hr. Water was then added and the reaction mixture was extracted with ethyl acetate, washed with brine and dried with anhydrous Na₂SO₄. The combined extracts were evaporated under vacuum to give crude product which was purified with flash chromatography on silica. Elution with hexane/ethyl acetate (8:1-3:1) gave **6** as colorless oil (131 mg, 82%). ¹H NMR (400 MHz, Chloroform-*d*) δ 7.14 (d, *J* = 1.9 Hz, 1H), 6.89 (d, *J* = 1.9 Hz, 1H), 5.91 (d, *J* = 3.6 Hz, 1H), 5.83 (d, *J* = 3.6 Hz, 1H), 3.81 (d, *J* = 0.9 Hz, 6H). HRMS: calculated for C₁₁H₁₁O₅ [M+H]⁺ 223.0606, found 223.0607.

Synthesis of 2,4,5-tribromo-1-((2-(trimethylsilyl)ethoxy)methyl)-1H-imidazole (9). To a stirred solution of 2,4,5-tribromoimidazole (9.5 g, 31.1 mmol) in anhydrous THF (100 mL) at ice temperature was added sodium hydride (1.5g, 40.6 mmol) in portions under argon. The mixture was stirred for 1 hr at this temperature and was added 2-(trimethylsilyl)ethoxymethyl chloride (6.7 ml, 35.8 mmol) dropwise. Reaction was then warmed to room temperature and stirred for another 1.5 hr. Water was then added at ice temperature carefully and the reaction mixture was extracted with ethyl acetate, washed with brine and dried with Na₂SO₄. The combined extracts were evaporated under vacuum to give the oily residue which was purified with flash chromatography on silica. Elution with hexane/ethyl acetate (10:0-10:1) gave **9** as slightly yellowish solid (12.6 g, 93%). ¹H NMR (400 MHz, Chloroform-*d*) δ 5.30 (s, 2H), 3.65 – 3.49 (m, 2H), 0.94 – 0.87 (m, 2H), -0.03 (s, 9H). HRMS: calculated for C₉H₁₆Br₃N₂OSi [M+H]⁺ 432.8582, found 432.8588.

Synthesis of 10 and 16. To a mixture of 1-(Phenylsulfonyl)-3-indolylboronic acid pinacol ester (5.0 g, 13.1 mmol) or **15**, **9** (6.8 g, 15.7 mmol), and sodium carbonate (2.8 g, 26.1 mmol) in toluene (50 ml), methanol (5 ml) and (2.5 ml) was added 2-dicyclohexylphosphino-2',4',6'-triisopropylbiphenyl (935 mg, 2.0 mmol) and tris(dibenzylideneacetone)dipalladium (600 mg, 0.66 mmol) under argon. The mixture was refluxed for overnight. Water was then added and the reaction mixture was extracted

with ethyl acetate, washed with brine and dried with anhydrous Na₂SO₄. The combined extracts were evaporated under vacuum to give crude product which was purified with flash chromatography on silica. Elution with hexane/ethyl acetate (15:1-4:1) gave **10** or **16** as pale-yellow solid (for **10**: 34% yield; for **16**: 31% yield).

3-(4,5-dibromo-1-((2-(trimethylsilyl)ethoxy)methyl)-1H-imidazol-2-yl)-1-(phenylsulfonyl)-1H-indole (10). ¹H NMR (400 MHz, Chloroform-d) δ 8.20 (s, 1H), 8.17 (dt, J = 7.7, 1.1 Hz, 1H), 8.05 – 8.00 (m, 1H), 7.92 – 7.85 (m, 2H), 7.58 – 7.51 (m, 1H), 7.47 – 7.36 (m, 3H), 7.32 (td, J = 7.7, 1.1 Hz, 1H), 5.35 (s, 2H), 3.80 – 3.68 (m, 2H), 1.09 – 0.98 (m, 2H), 0.05 (s, 9H). HRMS: calculated for C₂₃H₂₆Br₂N₃O₃SSi [M+H]⁺ 609.9831, found 609.9822.

4-(4,5-dibromo-1-((2-(trimethylsilyl)ethoxy)methyl)-1H-imidazol-2-yl)-1-(phenylsulfonyl)-1H-indole (16). ¹H NMR (400 MHz, Chloroform-d) δ 8.11 (dd, J = 8.4, 1.0 Hz, 1H), 7.86 (dd, J = 8.0, 1.4 Hz, 2H), 7.64 (d, J = 3.7 Hz, 1H), 7.57 – 7.50 (m, 2H), 7.41 (dt, J = 20.0, 7.8 Hz, 3H), 6.97 (d, J = 3.7 Hz, 1H), 5.25 (s, 2H), 3.49 (dd, J = 8.8, 7.6 Hz, 2H), 0.85 (dd, J = 8.8, 7.6 Hz, 2H), -0.06 (s, 9H). HRMS: calculated for C₂₃H₂₆Br₂N₃O₃SSi [M+H]⁺ 609.9831, found 609.9834.

General procedure for synthesis of 11a-11f, 17 and 23. To a stirred solution of compound **10** or **16** or **21** (1.0 mmol) in anhydrous THF (3.0 mL) under argon was added isopropylmagnesium chloride lithium chloride complex solution (1.3 M in THF, 0.92 ml, 1.2 mmol) at room temperature. The mixture was stirred for 1 hr and was added benzoyl chlorides (1.3 mmol) in anhydrous THF (mL). Reaction was kept stirring at room temperature for 1 hour and then refluxed for 30 minute. Saturated NH₄Cl solution was then added to quench the reaction. Reaction mixture was extracted with ethyl acetate, washed with brine and dried with Na₂SO₄. The combined extracts were evaporated under vacuum to give the crude product which was purified with flash chromatography on silica. Elution with hexane/ethyl acetate (10:1-3:1) gave pure **11a-11f**, **17** and **22** as pale-yellow to yellowish solids (yields: 31-48%).

(4-bromo-2-(1-(phenylsulfonyl)-1H-indol-3-yl)-1-((2-(trimethylsilyl)ethoxy)methyl)-1H-imidazol-5-yl)(2,3-dihydrobenzo[b][1,4]dioxin-6-yl)methanone (11a). ¹H NMR (400 MHz, Chloroform-d) δ 8.30 (s, 1H), 8.19 (ddd, J = 7.7, 1.3, 0.7 Hz, 1H), 8.05 (dt, J = 8.4, 1.0 Hz, 1H), 7.97 – 7.87 (m, 2H), 7.59 – 7.54 (m, 1H), 7.49 – 7.32 (m, 6H), 5.62 (s, 2H), 4.42 – 4.33 (m, 2H), 4.30 (dt, J = 5.7, 1.6 Hz, 2H), 3.64 – 3.53 (m, 2H), 0.98 – 0.90 (m, 2H), -0.07 (s, 9H). HRMS: calculated for C₃₂H₃₃BrN₃O₆SSi [M+H]⁺ 694.1043, found 694.1045.

Benzo[d][1,3]dioxol-5-yl(4-bromo-2-(1-(phenylsulfonyl)-1H-indol-3-yl)-1-((2-(trimethylsilyl)ethoxy)methyl)-1H-imidazol-5-yl)methanone (11b). ¹H NMR (400 MHz, Chloroform-d) δ 8.29 (s, 1H), 8.19 (ddd, J = 7.9, 1.4, 0.7 Hz, 1H), 8.05 (dt, J = 8.3, 1.0 Hz, 1H), 7.95 – 7.87 (m, 2H), 7.59 – 7.50 (m, 2H), 7.49 – 7.32 (m, 5H), 6.90 (dd, J = 8.2, 1.3 Hz, 1H), 6.10 (s, 2H), 5.62 (s, 2H), 3.66 – 3.50 (m, 2H), 0.99 – 0.90 (m, 2H), -0.06 (s, 9H). HRMS: calculated for C₃₁H₃₁BrN₃O₆SSi [M+H]⁺ 680.0886, found 680.0881.

(4-bromo-2-(1-(phenylsulfonyl)-1H-indol-3-yl)-1-((2-(trimethylsilyl)ethoxy)methyl)-1H-imidazol-5-yl)(8-methoxy-2,3-dihydrobenzo[b][1,4]dioxin-6-yl)methanone (11c). ¹H NMR (400 MHz, Chloroform-d) δ 8.34 (s, 1H), 8.15 (d, J = 7.8 Hz, 1H), 8.04 (dd, J = 8.4, 1.0 Hz, 1H), 7.97 – 7.89 (m, 2H), 7.56 (t, J = 7.4 Hz, 1H), 7.49 – 7.39 (m, 3H), 7.35 (td, J = 7.6, 1.1 Hz, 1H), 7.20 – 7.11 (m, 3H), 5.62 (s, 2H), 4.41 (dd, J = 3.8, 1.8 Hz, 2H), 4.30 (dd, J = 3.8, 1.8 Hz, 2H), 3.95 (s, 3H), 3.62 – 3.53 (m, 2H), 0.96 – 0.89 (m, 2H), -0.08 (s, 9H). HRMS: calculated for C₃₃H₃₅BrN₃O₇SSi [M+H]⁺ 724.1148, found 724.1144.

(4-bromo-2-(1-(phenylsulfonyl)-1H-indol-3-yl)-1-((2-(trimethylsilyl)ethoxy)methyl)-1H-imidazol-5-yl)(7-methoxybenzo[d][1,3]dioxol-5-yl)methanone (11d). ¹H NMR (400 MHz, Chloroform-d) δ 8.30 (s, 1H), 8.20 (ddd, J = 7.9, 1.4, 0.7 Hz, 1H), 8.05 (dt, J = 8.2, 1.0 Hz, 1H), 7.94 – 7.90 (m, 2H), 7.60 – 7.53 (m, 1H), 7.48 – 7.33 (m, 4H), 7.22 (d, J = 1.5 Hz, 1H), 7.12 (d, J = 1.5 Hz, 1H), 6.11 (s, 2H), 5.63 (s, 2H), 3.95 (s, 3H), 3.65 – 3.57 (m, 2H), 1.00 – 0.91 (m, 2H), -0.06 (s, 9H). HRMS: calculated for C₃₂H₃₃BrN₃O₇SSi [M+H]⁺ 710.0992, found 710.0999.

(4-bromo-2-(1-(phenylsulfonyl)-1H-indol-3-yl)-1-((2-(trimethylsilyl)ethoxy)methyl)-1H-imidazol-5-yl)(9-methoxy-3,4-dihydro-2H-benzo[b][1,4]dioxepin-7-yl)methanone (11e). ¹H NMR (400 MHz, Chloroform-d) δ 8.30 (s, 1H), 8.23 – 8.17 (m, 1H), 8.05 (dt, J = 8.4, 1.0 Hz, 1H), 7.94 – 7.89 (m, 2H), 7.60 – 7.53 (m, 1H), 7.49 – 7.32 (m, 4H), 7.22 (d, J = 2.0 Hz, 1H), 7.18 (d, J = 2.0 Hz, 1H), 5.63 (s, 2H), 4.46 (t, J = 5.7 Hz, 2H), 4.30 (t, J = 5.9 Hz, 2H), 3.93 (s, 3H), 3.64 – 3.56 (m, 2H), 2.28 (p, J = 5.8 Hz, 2H), 0.99 – 0.90 (m, 2H), -0.06 (s, 9H). HRMS: calculated for C₃₄H₃₇BrN₃O₇SSi [M+H]⁺ 738.1305, found 738.1313.

(4-bromo-2-(1-(phenylsulfonyl)-1H-indol-3-yl)-1-((2-(trimethylsilyl)ethoxy)methyl)-1H-imidazol-5-yl)(8-methoxybenzo[b][1,4]dioxin-6-yl)methanone (11f). ¹H NMR (400 MHz, Acetone-d₆) δ 8.54 (s, 1H), 8.35 (ddd, J = 8.0, 1.3, 0.7 Hz, 1H), 8.18 – 8.09 (m, 3H), 7.79 – 7.73 (m, 1H), 7.72 – 7.63 (m, 2H), 7.52 (ddd, J = 8.4, 7.3, 1.4 Hz, 1H), 7.44 (ddd, J = 8.2, 7.2, 1.1 Hz, 1H), 7.31 (d, J = 1.9 Hz, 1H), 6.92 (d, J = 1.9 Hz, 1H), 6.24 (d, J = 3.6 Hz, 1H), 6.20 (d, J = 3.6 Hz, 1H), 5.81 (s, 2H), 3.93 (s, 3H), 3.76 – 3.67 (m, 2H), 1.06 – 0.95 (m, 2H), 0.00 (s, 9H). HRMS: calculated for C₃₃H₃₃BrN₃O₇SSi [M+H]⁺ 722.0992, found 722.0989.

(4-bromo-2-(1-(phenylsulfonyl)-1H-indol-4-yl)-1-((2-(trimethylsilyl)ethoxy)methyl)-1H-imidazol-5-yl)(8-methoxybenzo[b][1,4]dioxin-6-yl)methanone (17). ¹H NMR (400 MHz, Chloroform-d) δ 8.16 (d, J = 8.3 Hz, 1H), 7.88 (dd, J = 8.4, 1.3 Hz, 2H), 7.68 (d, J = 3.7 Hz, 1H), 7.59 – 7.53 (m, 2H), 7.48 – 7.39 (m, 3H), 7.13 (d, J = 1.9 Hz, 1H), 6.96 (d, J = 3.7 Hz, 1H), 6.88 (d, J = 1.8 Hz, 1H), 6.00 (d, J = 3.6 Hz, 1H), 5.91 (d, J = 3.5 Hz, 1H), 5.50 (s, 2H), 3.90 (s, 3H), 3.34 – 3.27 (m, 2H), 0.76 – 0.67 (m, 2H), -0.15 (s, 9H). HRMS: calculated for C₃₃H₃₃BrN₃O₇SSi [M+H]⁺ 722.0992, found 722.0996.

(4-bromo-2-(4-methyl-1-(phenylsulfonyl)-1H-indol-3-yl)-1-((2-(trimethylsilyl)ethoxy)methyl)-1H-imidazol-5-yl)(8-methoxybenzo[b][1,4]dioxin-6-

yl)methanone (23). ^1H NMR (400 MHz, Chloroform- d) δ 7.92 – 7.83 (m, 4H), 7.54 (dd, $J = 8.3, 6.5$ Hz, 1H), 7.47 – 7.39 (m, 2H), 7.25 – 7.20 (m, 1H), 7.10 (d, $J = 1.9$ Hz, 1H), 7.01 (d, $J = 7.5$ Hz, 1H), 6.84 (s, 1H), 6.00 – 5.91 (m, 1H), 5.88 (dd, $J = 3.3, 1.8$ Hz, 1H), 5.36 (d, $J = 1.8$ Hz, 2H), 3.87 (d, $J = 1.7$ Hz, 3H), 3.39 – 3.29 (m, 2H), 2.18 (s, 3H), 0.79 – 0.66 (m, 2H), -0.14 (d, $J = 1.5$ Hz, 9H). HRMS: calculated for $\text{C}_{34}\text{H}_{35}\text{BrN}_3\text{O}_7\text{SSi}$ $[\text{M}+\text{H}]^+$ 736.1148, found 736.1155.

General procedure for synthesis of 12a-12f, 18 and 24. To a suspension of **11a-11f** or **17** or **23** (0.5 mmol), potassium carbonate (276 mg, 2.0 mmol), and triphenylphosphine (26 mg, 0.1 mmol) in *n*-BuOH (3 mL) was added palladium acetate (5.6 mg, 0.025 mmol). The mixture was heated to reflux for 4 hr. *n*-BuOH was removed under reduced pressure. The residue was partitioned between water (10 ml) and EtOAc (10ml). The combined organic solvents were then evaporated under reduced pressure. The crude was purified with flash chromatography on silica. Elution with hexane/ethyl acetate (10:1-3:1) gave pure **12a-12f, 18** and **24** as pale-yellow to yellowish solids (yields: 76-89%).

(2-(1H-indol-3-yl)-1-((2-(trimethylsilyl)ethoxy)methyl)-1H-imidazol-5-yl)(benzo[d][1,3]dioxol-5-yl)methanone (12b). ^1H NMR (400 MHz, Chloroform- d) δ 9.35 (s, 1H), 8.30 – 8.17 (m, 1H), 7.94 (d, $J = 2.8$ Hz, 1H), 7.74 (s, 1H), 7.51 (dd, $J = 8.1, 1.7$ Hz, 1H), 7.41 (dd, $J = 7.2, 1.7$ Hz, 2H), 7.29 – 7.18 (m, 3H), 6.91 (d, $J = 8.1$ Hz, 1H), 6.08 (s, 2H), 5.88 (s, 2H), 3.78 – 3.64 (m, 2H), 1.00 – 0.86 (m, 2H), -0.06 (s, 9H). HRMS: calculated for $\text{C}_{25}\text{H}_{28}\text{N}_3\text{O}_4\text{Si}$ $[\text{M}+\text{H}]^+$ 462.1849, found 462.1852.

(2-(1H-indol-3-yl)-1-((2-(trimethylsilyl)ethoxy)methyl)-1H-imidazol-5-yl)(8-methoxy-2,3-dihydrobenzo[b][1,4]dioxin-6-yl)methanone (12c). ^1H NMR (400 MHz, Chloroform- d) δ 9.24 (s, 1H), 8.19 (d, $J = 7.2$ Hz, 1H), 7.95 (s, 1H), 7.81 (s, 1H), 7.50 – 7.42 (m, 1H), 7.30 – 7.20 (m, 2H), 7.18 (d, $J = 2.0$ Hz, 1H), 7.11 (d, $J = 2.0$ Hz, 1H), 5.88 (s, 2H), 4.42 (dd, $J = 3.9, 1.7$ Hz, 2H), 4.33 (dd, $J = 3.7, 1.7$ Hz, 2H), 3.96 (s, 3H), 3.77 – 3.64 (m, 2H), 1.00 – 0.87 (m, 2H), -0.05 (s, 9H). HRMS: calculated for $\text{C}_{27}\text{H}_{32}\text{N}_3\text{O}_5\text{Si}$ $[\text{M}+\text{H}]^+$ 506.2111, found 506.2113.

(2-(1H-indol-3-yl)-1-((2-(trimethylsilyl)ethoxy)methyl)-1H-imidazol-5-yl)(7-methoxybenzo[d][1,3]dioxol-5-yl)methanone (12d). ^1H NMR (400 MHz, Chloroform- d) δ 8.79 (s, 1H), 8.35 – 8.25 (m, 1H), 8.03 (d, $J = 2.8$ Hz, 1H), 7.77 (s, 1H), 7.46 – 7.42 (m, 1H), 7.30 – 7.27 (m, 1H), 7.20 (d, $J = 1.5$ Hz, 1H), 7.13 (d, $J = 1.5$ Hz, 1H), 6.10 (s, 2H), 5.91 (s, 2H), 3.96 (s, 3H), 3.80 – 3.70 (m, 2H), 0.94 (d, $J = 8.3$ Hz, 2H), -0.05 (s, 9H). HRMS: calculated for $\text{C}_{26}\text{H}_{30}\text{N}_3\text{O}_5\text{Si}$ $[\text{M}+\text{H}]^+$ 492.1955, found 492.1957.

(2-(1H-indol-3-yl)-1-((2-(trimethylsilyl)ethoxy)methyl)-1H-imidazol-5-yl)(9-methoxy-3,4-dihydro-2H-benzo[b][1,4]dioxepin-7-yl)methanone (12e). ^1H NMR (400 MHz, Chloroform- d) δ 8.66 (s, 1H), 8.36 – 8.23 (m, 1H), 8.05 (d, $J = 2.8$ Hz, 1H), 7.79 (s, 1H), 7.51 – 7.40 (m, 1H), 7.33 – 7.24 (m, 4H), 7.22 (d, $J = 2.1$ Hz, 1H), 7.16 (d, $J = 2.0$ Hz, 1H), 5.92 (s, 2H), 4.44 (t, $J = 5.7$ Hz, 2H), 4.32 (t, $J = 5.9$ Hz, 2H), 3.92 (s, 3H), 3.81 – 3.71 (m, 2H), 2.34 – 2.20 (m, 2H), 1.00 – 0.91 (m, 2H), -0.04 (s, 9H). HRMS: calculated for $\text{C}_{28}\text{H}_{34}\text{N}_3\text{O}_5\text{Si}$ $[\text{M}+\text{H}]^+$ 520.2268, found 520.2272.

(2-(1H-indol-3-yl)-1-((2-(trimethylsilyl)ethoxy)methyl)-1H-imidazol-5-yl)(8-methoxybenzo[b][1,4]dioxin-6-yl)methanone (12f). ¹H NMR (400 MHz, Chloroform-d) δ 10.02 (d, J = 2.8 Hz, 1H), 8.36 – 8.27 (m, 1H), 7.94 (d, J = 2.8 Hz, 1H), 7.87 (s, 1H), 7.38 – 7.31 (m, 1H), 7.30 – 7.22 (m, 2H), 7.16 (d, J = 1.9 Hz, 1H), 6.95 (d, J = 1.9 Hz, 1H), 6.04 (d, J = 3.6 Hz, 1H), 5.98 – 5.88 (m, 3H), 3.92 (s, 3H), 3.83 – 3.67 (m, 2H), 1.03 – 0.89 (m, 2H), 0.00 (s, 9H). HRMS: calculated for C₂₇H₃₀N₃O₅Si [M+H]⁺ 504.1955, found 504.1952.

(2-(1H-indol-4-yl)-1-((2-(trimethylsilyl)ethoxy)methyl)-1H-imidazol-5-yl)(8-methoxybenzo[b][1,4]dioxin-6-yl)methanone (18). ¹H NMR (400 MHz, Chloroform-d) δ 8.47 (s, 1H), 7.76 (s, 1H), 7.55 (d, J = 8.2 Hz, 1H), 7.50 (d, J = 7.3 Hz, 1H), 7.34 – 7.29 (m, 2H), 7.15 (d, J = 1.8 Hz, 1H), 6.93 (d, J = 1.8 Hz, 1H), 6.73 (s, 1H), 6.01 (d, J = 3.6 Hz, 1H), 5.92 (d, J = 3.7 Hz, 1H), 5.78 (s, 2H), 3.91 (s, 3H), 3.43 – 3.33 (m, 2H), 0.80 – 0.73 (m, 2H), -0.13 (s, 9H). HRMS: calculated for C₂₇H₃₀N₃O₅Si [M+H]⁺ 504.1955, found 504.1965.

(8-methoxybenzo[b][1,4]dioxin-6-yl)(2-(4-methyl-1H-indol-3-yl)-1-((2-(trimethylsilyl)ethoxy)methyl)-1H-imidazol-5-yl)methanone (24). ¹H NMR (400 MHz, Chloroform-d) δ 9.17 (s, 1H), 7.36 (s, 1H), 7.21 (d, J = 8.2 Hz, 1H), 7.15 (s, 1H), 7.12 (d, J = 7.4 Hz, 1H), 6.94 (d, J = 7.2 Hz, 1H), 6.90 (q, J = 1.6 Hz, 1H), 6.01 (t, J = 2.4 Hz, 1H), 5.92 (t, J = 2.8 Hz, 1H), 5.46 (s, 2H), 3.91 (s, 3H), 3.31 (t, J = 8.1 Hz, 2H), 2.34 (s, 3H), 0.70 (t, J = 8.1 Hz, 2H), -0.14 (d, J = 1.5 Hz, 9H). HRMS: calculated for C₂₈H₃₂N₃O₅Si [M+H]⁺ 518.2111, found 518.2108.

General procedure for synthesis of 13a-13f, 19 and 25. To a solution of **12a-12f** or **18** or **24** in DCM (1 ml) was added trifluoroacetic acid (1 ml). The reaction was stirred for 2 hr and solvent was evaporated under reduced pressure. The residue was partitioned between saturated NaHCO₃ solution and EtOAc. The combined organic solvents were then evaporated under reduced pressure. The crude was purified with flash chromatography on silica. Elution with hexane/ethyl acetate (4:1-1:2) gave pure **13a-13f**, **19** and **25** as yellowish solids (yields: 79-92%).

(2-(1H-indol-3-yl)-1H-imidazol-5-yl)(2,3-dihydrobenzo[b][1,4]dioxin-6-yl)methanone (13a). ¹H NMR (400 MHz, DMSO-d₆) δ 13.14 (s, 1H), 11.62 (s, 1H), 8.47 – 8.36 (m, 1H), 8.30 – 8.17 (m, 1H), 7.87 (s, 1H), 7.68 (s, 2H), 7.48 (dt, J = 8.2, 0.9 Hz, 1H), 7.25 – 7.12 (m, 2H), 7.04 (d, J = 8.8 Hz, 1H), 4.52 – 4.27 (m, 4H). HRMS: calculated for C₂₀H₁₆N₃O₃ [M+H]⁺ 346.1192, found 346.1190.

(2-(1H-indol-3-yl)-1H-imidazol-5-yl)(benzo[d][1,3]dioxol-5-yl)methanone (13b). ¹H NMR (400 MHz, DMSO-d₆) δ 13.36 (s, 1H), 11.67 (s, 1H), 8.42 – 8.32 (m, 1H), 8.23 (d, J = 2.7 Hz, 1H), 7.92 (s, 1H), 7.81 (d, J = 7.1 Hz, 1H), 7.71 – 7.56 (m, 1H), 7.49 (dt, J = 8.2, 0.9 Hz, 1H), 7.19 (dtd, J = 17.2, 7.1, 1.3 Hz, 2H), 7.11 (d, J = 8.1 Hz, 1H), 6.18 (s, 2H). HRMS: calculated for C₁₉H₁₄N₃O₃ [M+H]⁺ 332.1035, found 332.1036.

(2-(1H-indol-3-yl)-1H-imidazol-5-yl)(8-methoxy-2,3-dihydrobenzo[b][1,4]dioxin-6-yl)methanone (13c). ¹H NMR (400 MHz, Chloroform-d) δ 8.02 (s, 1H), 7.92 (s, 1H), 7.81 (s, 1H), 7.40 (dd, J = 10.9, 7.7 Hz, 1H), 7.16 (dd, J = 7.0, 3.0 Hz, 3H), 7.07 (s, 1H), 4.41 – 4.32 (m, 2H), 4.32 – 4.22 (m, 2H), 3.91 (s, 3H). HRMS: calculated for C₂₁H₁₈N₃O₄ [M+H]⁺ 376.1297, found 376.1294.

(2-(1H-indol-3-yl)-1H-imidazol-5-yl)(7-methoxybenzo[d][1,3]dioxol-5-yl)methanone (13d). ¹H NMR (400 MHz, Chloroform-d) δ 8.16 – 8.07 (m, 1H), 7.90 (s, 1H), 7.74 (s, 1H), 7.46 – 7.37 (m, 1H), 7.25 – 7.20 (m, 3H), 7.14 (d, J = 1.5 Hz, 1H), 6.06 (s, 2H), 3.93 (s, 3H). HRMS: calculated for C₂₀H₁₆N₃O₄ [M+H]⁺ 362.1141, found 362.1136.

(2-(1H-indol-3-yl)-1H-imidazol-5-yl)(9-methoxy-3,4-dihydro-2H-benzo[b][1,4]dioxepin-7-yl)methanone (13e). ¹H NMR (400 MHz, Chloroform-d) δ 8.16 (dd, J = 6.5, 2.9 Hz, 1H), 7.87 (d, J = 3.0 Hz, 1H), 7.74 (d, J = 3.4 Hz, 1H), 7.62 – 7.48 (m, 1H), 7.42 (dt, J = 6.0, 3.0 Hz, 1H), 7.25 – 7.20 (m, 2H), 7.20 – 7.13 (m, 1H), 4.38 (t, J = 5.8 Hz, 2H), 4.34 – 4.23 (m, 2H), 3.89 (s, 3H), 2.24 (dd, J = 7.0, 4.5 Hz, 2H). HRMS: calculated for C₂₂H₂₀N₃O₄ [M+H]⁺ 390.1454, found 390.1457.

(2-(1H-indol-3-yl)-1H-imidazol-5-yl)(8-methoxybenzo[b][1,4]dioxin-6-yl)methanone (13f). ¹H NMR (400 MHz, DMSO-d₆) δ 13.02 (s, 1H), 11.55 (s, 1H), 8.40 (d, J = 7.8 Hz, 1H), 7.94 (s, 2H), 7.47 (d, J = 7.9 Hz, 1H), 7.16 (dtd, J = 16.1, 8.1, 7.6, 6.4 Hz, 2H), 6.30 (d, J = 9.2 Hz, 2H), 3.88 (s, 3H). HRMS: calculated for C₂₁H₁₆N₃O₄ [M+H]⁺ 374.1141, found 374.1142.

(2-(1H-indol-4-yl)-1H-imidazol-5-yl)(8-methoxybenzo[b][1,4]dioxin-6-yl)methanone (19). ¹H NMR (400 MHz, Chloroform-d) δ 10.59 (s, 1H), 8.51 (s, 1H), 7.90 (s, 1H), 7.68 (d, J = 7.2 Hz, 1H), 7.51 (d, J = 8.1 Hz, 1H), 7.38 (t, J = 2.9 Hz, 1H), 7.29 (d, J = 7.8 Hz, 1H), 7.25 (s, 1H), 7.19 (s, 1H), 7.01 (s, 1H), 6.01 (d, J = 3.6 Hz, 1H), 5.93 (d, J = 3.6 Hz, 1H), 3.90 (s, 3H). HRMS: calculated for C₂₁H₁₆N₃O₄ [M+H]⁺ 374.1141, found 374.1144.

(8-methoxybenzo[b][1,4]dioxin-6-yl)(2-(4-methyl-1H-indol-3-yl)-1H-imidazol-5-yl)methanone (25). ¹H NMR (400 MHz, Methylene Chloride-d₂) δ 9.11 (s, 1H), 7.74 (d, J = 2.0 Hz, 1H), 7.30 (s, 1H), 7.24 (d, J = 8.3 Hz, 1H), 7.19 (s, 1H), 7.10 (t, J = 7.8 Hz, 1H), 6.98 (s, 1H), 6.90 (d, J = 7.1 Hz, 1H), 6.00 (d, J = 2.7 Hz, 1H), 5.95 (t, J = 2.8 Hz, 1H), 3.83 (s, 3H), 2.47 (s, 3H). HRMS: calculated for C₂₂H₁₈N₃O₄ [M+H]⁺ 388.1297, found 388.1303.

Synthesis of 4-bromo-1-(phenylsulfonyl)-1H-indole (14). To a solution of 4-bromoindole (1.0 g, 5.1 mmol) in THF (10 ml) was added sodium hydride (314 mg, 7.6 mmol) in portions under ice temperature. After 1 hr, benzenesulfonyl chloride (0.81 ml, 6.1 mmol) was added dropwise. The reaction was stirred at room temperature for 2 hr. Water was then added and the reaction mixture was extracted with ethyl acetate, washed with brine and dried with anhydrous Na₂SO₄. The combined extracts were evaporated under vacuum to give crude product which was purified with flash chromatography on

silica. Elution with hexane/ethyl acetate (20:1-6:1) gave **14** as colorless solid (1.6 g, 93%). ¹H NMR (400 MHz, Chloroform-*d*) δ 7.96 (dd, *J* = 8.4, 0.8 Hz, 1H), 7.91 – 7.84 (m, 2H), 7.64 (d, *J* = 3.7 Hz, 1H), 7.57 – 7.50 (m, 1H), 7.44 (dd, *J* = 8.5, 7.1 Hz, 2H), 7.39 (d, *J* = 7.8 Hz, 1H), 7.18 (t, *J* = 8.0 Hz, 1H), 6.74 (d, *J* = 3.7 Hz, 1H). HRMS: calculated for C₁₄H₁₁BrNO₂S [M+H]⁺ 335.9694, found 335.9691.

Synthesis of 1-(phenylsulfonyl)-4-(4,4,5,5-tetramethyl-1,3,2-dioxaborolan-2-yl)-1H-indole (15). To a solution of **14** (0.86 g, 2.5 mmol) in dioxane (10 ml) was added bis(pinacolato)diboron (1.9 g, 7.5 mmol), potassium acetate (0.75 g, 7.5 mmol) and [1,1'-Bis(diphenylphosphino)ferrocene]dichloropalladium complex with dichloromethane (220 mg, 0.125 mmol). The mixture was heated to reflux for overnight. Dioxane was removed under reduced pressure and then water was partitioned between water and EtOAc. The combined extracts were evaporated under vacuum to give crude product which was purified with flash chromatography on silica. Elution with hexane/ethyl acetate (20:1) gave **15** as colorless solid (2.47 g, 86%). ¹H NMR (400 MHz, Chloroform-*d*) δ 8.11 (dt, *J* = 8.4, 0.9 Hz, 1H), 7.88 – 7.82 (m, 2H), 7.71 (dd, *J* = 7.2, 1.0 Hz, 1H), 7.60 (d, *J* = 3.7 Hz, 1H), 7.53 – 7.47 (m, 1H), 7.40 (dd, *J* = 8.5, 7.0 Hz, 2H), 7.32 (dd, *J* = 8.3, 7.3 Hz, 1H), 7.21 (d, *J* = 3.6 Hz, 1H), 1.35 (s, 12H). HRMS: calculated for C₂₀H₂₃BNO₄S [M+H]⁺ 384.1441, found 384.1438.

Synthesis of 21. Compound **21** was synthesized following our previously reported procedures [169].

Synthesis of 22. To a solution of **21** (1.0 g, 3.3 mmol) in THF (10 ml) was added *N*-bromosuccinimide (1.07 g, 6.0 mmol) in portions. The reaction was stirred for 1.5 hr, quenched with saturated Na₂S₂O₃ solution, and extracted with EtOAc. The combined extracts were evaporated under reduced pressure and dried under vacuum to give crude product. The crude was dissolved in anhydrous THF (10 mL) at ice temperature; sodium hydride (122 mg, 3.3 mmol) was added in portions under argon. The mixture was stirred for another 1 hr at this temperature and was added 2-(trimethylsilyl)ethoxymethyl chloride (0.62 ml, 3.3 mmol) dropwise. Reaction was then warmed to room temperature and stirred for 1.5 hr. Water was then added and the reaction mixture was extracted with ethyl acetate, washed with brine and dried with Na₂SO₄. The combined extracts were evaporated under vacuum to give the oily residue which was purified with flash chromatography on silica. Elution with hexane/ethyl acetate (10:0-10:1) gave **22** as pale-yellow solid (1.4 g, 70%).

Cell culture and reagents

Human melanoma carcinoma cell lines A375, M14, and RPMI7951 (American Type Culture Collection or ATCC, Manassas, VA, USA) were cultured in Dulbecco's modified Eagle's medium (DMEM) (Corning, Manassas, VA) supplemented with 10% (v/v) fetal bovine serum (FBS) (Atlanta Biologicals, Lawerenceville, GA) and 1% antibiotic/antimycotic mixture (Sigma-Aldrich, St. Louis MO). Murine melanoma B16F10 cells (ATCC, Manassas, VA, USA) were cultured in Minimum essential medium

(Invitrogen, Carlsbad, CA), supplemented with 5% heat-inactivated Hyclone FBS (Thermo Scientific, Rockford, IL), 1 % antibiotic-antimycotic mixture (Sigma-Aldrich, St. Louis MO), 1% Mem-sodium pyruvate (Invitrogen, Carlsbad, CA), 1% Mem-vitamin (Invitrogen, Carlsbad, CA), L-Glutamine (2mM final concentration) (Invitrogen, Carlsbad, CA), and 1% Mem NEAA (Invitrogen, Carlsbad, CA). All cell lines were authenticated by ATCC by short tandem repeat profiling. Cultures were maintained to 80-90% confluency at 37°C in a humidified atmosphere containing 5% CO₂. Compounds were dissolved in dimethyl sulfoxide (DMSO) (Sigma-Aldrich, St. Louis, MO) to make a stock solution of 20 mM. Compound solutions were freshly prepared by diluting stocks with cell culture medium before use.

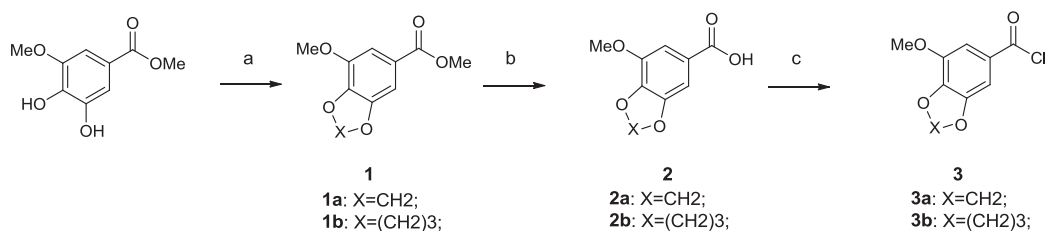
Cytotoxicity assay

A375, M14, and RPMI7951 were seeded in 96-well plates at a concentration of 1,000–5,000 cells per well, depending on growth rate of the cell line. After overnight incubation, the media was replaced and cells were treated with the test compounds at 10 concentrations ranging from 0.03 nM to 1 μM plus a vehicle control for 72 h in four replicates. Following treatment, the MTS reagent (Promega, Madison, WI) was added to the cells and incubated in dark at 37°C for at least 1 hour. Absorbance at 490 nm was measured using a plate reader (DYNEX Technologies, Chantilly VA). Percentages of cell survival versus drug concentrations were plotted, and the IC₅₀ (concentration that inhibited cell growth by 50% of untreated control) values were obtained by nonlinear regression analysis using GraphPad Prism (GraphPad Software, San Diego, CA).

Chemistry

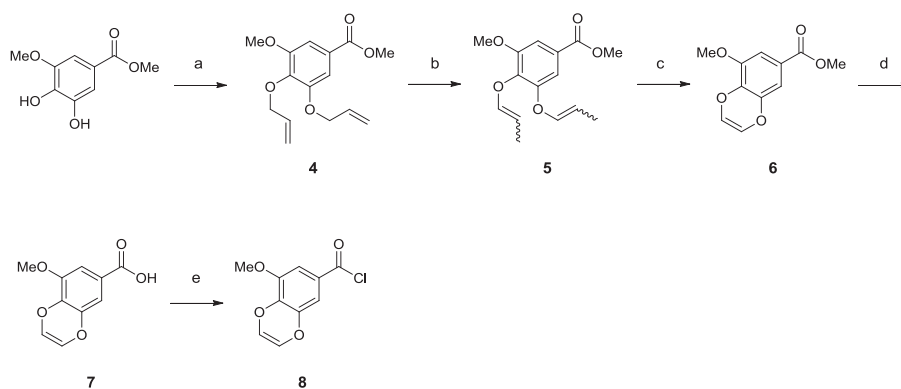
Scheme 3-1 showed the synthetic method we followed to access the commercially expensive or unavailable benzoyl chlorides. Commercially available methyl 3-methoxy-4,5-dihydroxybenzoate was treated with dibromomethane or 1,3-dibromopropane to form **1a** and **1b** in the presence of potassium carbonate. The cyclized benzoates were then hydrolyzed under basic condition to provide carboxylic acids **2a** and **2b**. **2a** and **2b** subsequently refluxed with thionyl chloride in DCM to generate benzoyl chlorides **3a** and **3b**, which were used directly for next step without purification.

Another commercially unavailable benzoyl chloride **8** was prepared following **Scheme 3-2**. Methyl 3-methoxy-4,5-dihydroxybenzoate refluxed together with allyl bromide in the presence of potassium carbonate to generate alkylated methyl benzoate **4**. An isomerization/ring closing metathesis strategy as reported in the literature [195] was followed to furnish the dioxene moiety in **6**. In brief, **4** was treated with a catalytic equivalent of (Ph₃P)₃Ru(CO)(Cl)H in toluene to provide **5**, which was subjected to Grubbs' reaction to afford **6**. Hydrolysis of the methyl ester under basic condition provided **7**, which was converted to benzoyl chloride **8** by refluxing with thionyl chloride. **8** was used directly for next step without purification.



Scheme 3-1. Synthesis of the benzoyl chlorides 3a-3b

Reagents and conditions: (a): dibromomethane or 1,3-dibromopropane, K₂CO₃, acetonitrile, reflux; (b): LiOH, dioxane-H₂O (2:1), 50°C; (c): SO₂Cl, DCM, reflux.



Scheme 3-2. Synthesis of the benzoyl chloride 8

Reagents and conditions: (a): allyl bromide, K₂CO₃, acetonitrile, reflux; (b): (Ph₃P)₃Ru(CO)(Cl)H, toluene, reflux; (c): Grubbs' catalyst 2nd generation, toluene, reflux; (d): LiOH, dioxane-H₂O(2:1), 50°C; (e): SO₂Cl, DCM, reflux.

ABI structure was constructed through a Suzuki coupling/Grignard reaction strategy as depicted in **Scheme 3-3**. In short, SEM-protected compound **9** was obtained from the treatment of 2,4,5-tribromoimidazole with SEMCl in the presence of sodium hydride. **9** coupled with 1-(Phenylsulfonyl)-3-indolylboronic acid pinacol ester in the presence of Pd₂(dba)₃ and 2-dicyclohexylphosphino-2',4',6'-triisopropylbiphenyl to provide **10** in 34% yield. It is worthy mentioning that Suzuki coupling reaction of this tribromo substrate under current condition was not regioselective. Coupling reactions happening on the 4- or 5-bromo were also observed. **10** was treated with *i*-PrMgCl(LiCl) and benzoyl chlorides to furnish compounds **11a-11f** in 31-48% yields. Bromo on the imidazole moiety and benzenesulfonyl were simultaneously removed in the presence of Pd(OAc)₂, PPh₃ and K₂CO₃ in *n*-BuOH under reflux condition, giving **12a-12f** in 76-89% yields. Deprotection of SEM using TFA in DCM finally provided ABI-231 analogues **13a-13f** in 79-92% yields.

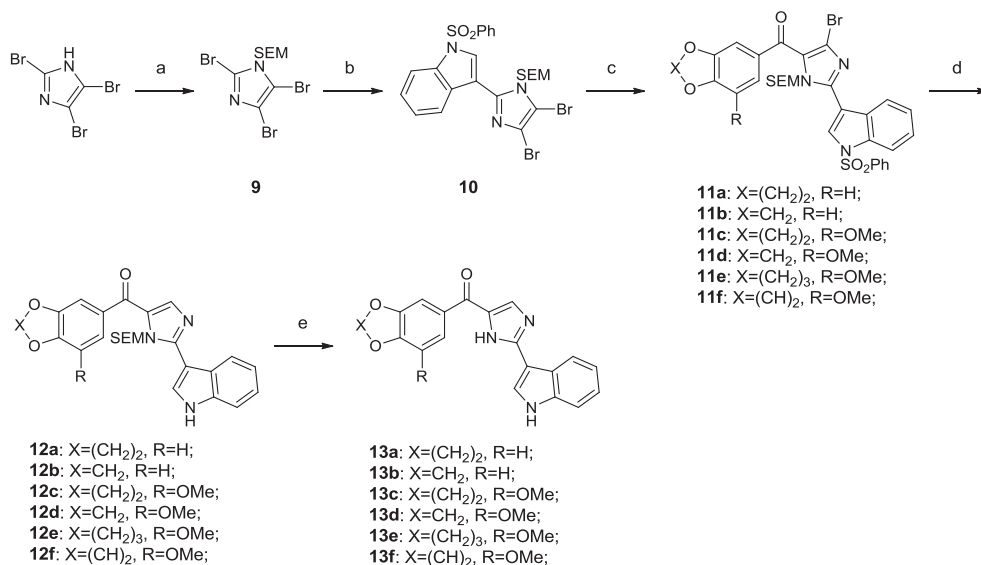
Analogue **19** was synthesized according to **Scheme 3-4**. In brief, 4-bromoindole was treated with benzenesulfonyl chloride in the presence of sodium hydride to provide **14** in 93% yield. **14** was then subjected Miyaura borylation catalyzed by Pd(pddf)₂Cl₂.CH₂Cl₂ to generate **15** in 86% yield. The boronic ester **15** was then subjected to Suzuki coupling, Grignard reaction and deprotections to eventually yield analog **19**.

To synthesize analog **25**, we followed the synthetic method as shown in **Scheme 3-5**. **20** was prepared by following a reported procedure [169]. Bromination of imidazole **20** using *N*-bromosuccinimide in THF was followed by protection in the presence of SEMCl and sodium hydride to afford intermediate **22** in 70% yield over two steps. **22** was then subject to Grignard reaction and deprotections to provide analogue **25**.

Results

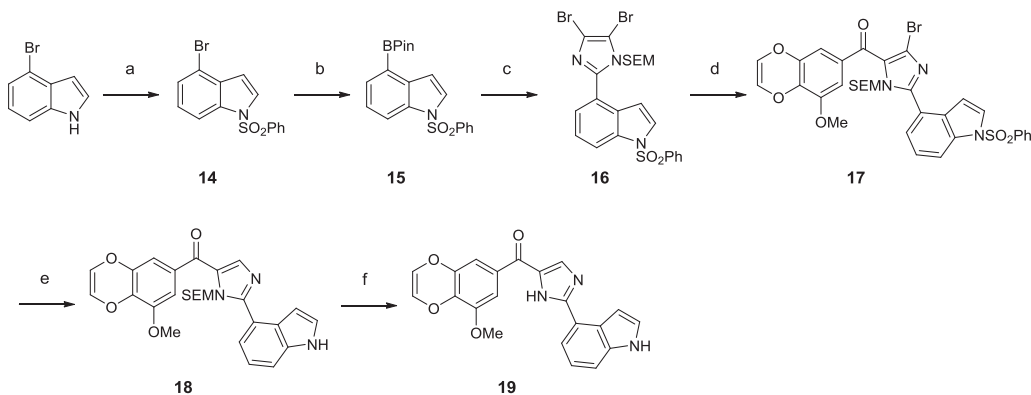
All analogues of ABI-231 were evaluated for their cytotoxicities in human melanoma cell lines including A375, WM1641 and M14. Colchicine was used as a positive control. The antiproliferative effects of the compounds were evaluated by MTT assay. IC₅₀s were reported in nM and calculated from at least three independent experiments, each performed in duplicates. *In vitro* growth inhibitory effects of the new analogues were shown in **Table 3-1**.

13a structurally replaced the 3,4,5-TMP in ABI-231 with a benzo[4,5]-dioxane moiety. It exhibited remarkable loss of cytotoxicity in several cell lines and had an average IC₅₀ of more than 150 nM. Shrinkage of the benzo[4,5]-dioxane to benzo[4,5]-dioxole resulted in analogue **13b**, which showed comparable antiproliferative activity to that of **13a**. In contrast to **13a**, 3-methoxy counterpart 3-methoxybenzo[4,5]-dioxane analogue **13c** showed dramatically increased inhibitory effect with an average IC₅₀ of 21 nM, suggesting the importance of the 3-methoxy in this scaffold. The same phenomenon was observed for **13d**. When 3-methoxy was introduced to benzo[4,5]-dioxole analogue



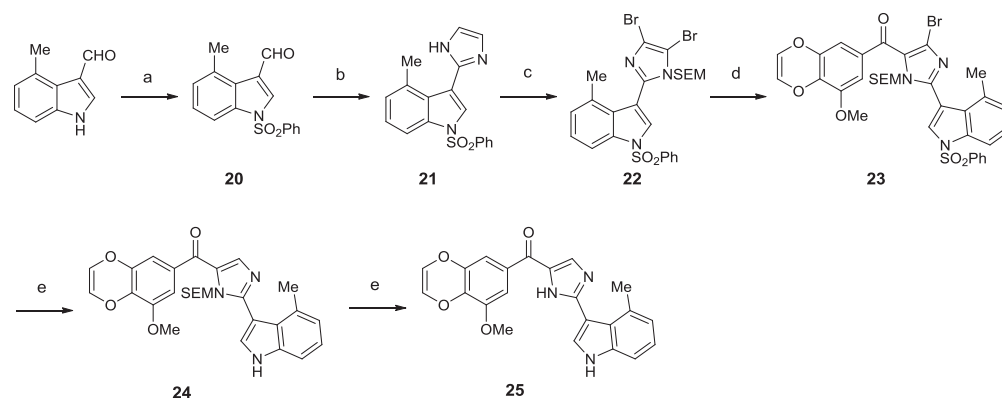
Scheme 3-3. Synthesis of the ABI-231 analogues 13a-13f

Reagents and conditions: (a): SEMCl, NaH, THF, 0°C to rt; (b): Pd₂(dba)₃, 2-dicyclohexylphosphino-2',4',6'-triisopropylbiphenyl, Na₂CO₃, toluene-MeOH-H₂O (20:4:1), reflux; (c): benzoyl chlorides, *i*-PrMgCl(LiCl), THF, rt to reflux; (d): Pd(OAc)₂, K₂CO₃, PPh₃, *n*-BuOH, reflux; (e): TFA, DCM, rt.



Scheme 3-4. Synthesis of 19

Reagents and conditions: (a): PhSO₂Cl, NaH, THF, 0°C to rt; (b): bis(pinacolato)diboron, Pd(dppf)₂.CH₂Cl₂, KOAc, dioxane, 80°C; (c): Pd₂(dba)₃, 2-dicyclohexylphosphino-2',4',6'-triisopropylbiphenyl, Na₂CO₃, toluene-MeOH-H₂O (20:4:1), reflux; (d): **8**, *i*-PrMgCl(LiCl), THF, rt to reflux; (e): Pd(OAc)₂, K₂CO₃, PPh₃, *n*-BuOH, reflux; (f): TFA, DCM, rt.



Scheme 3-5. Synthesis of 25

Reagents and conditions: (a): PhSO_2Cl , NaH , THF, 0°C to rt; (b): NH_4OH , glyoxal, ethanol, reflux; (c): NBS , THF, 0°C to rt; (d): **8**, $i\text{-PrMgCl}(\text{LiCl})$, THF, rt to reflux; (e): $\text{Pd}(\text{OAc})_2$, K_2CO_3 , PPh_3 , $n\text{-BuOH}$, reflux; (f): TFA, DCM, rt.

Table 3-1. *In vitro* growth inhibitory effects (nM) of ABI-231 analogues modifying the 3,4,5-TMP moiety (n=3)

Compound	A375	M14	RPMI7951
13a	158.7 ± 16.4	118.8 ± 14.3	213.7 ± 17.1
13b	190.6 ± 16.8	154.6 ± 10.4	235.6 ± 19.3
13c	21.0 ± 1.6	11.3 ± 0.8	29.2 ± 1.7
13d	3.5 ± 0.4	5.6 ± 0.6	5.6 ± 0.5
13e	32.2 ± 3.4	38.2 ± 3.5	47.7 ± 3.9
13f	1.1 ± 0.1	1.2 ± 0.2	3.3 ± 0.3
19	17.1 ± 1.1	13.8 ± 0.9	34.8 ± 2.2
25	6.1 ± 0.2	6.1 ± 0.2	8.8 ± 0.5
Colchicine	3.6 ± 0.2	4.8 ± 0.4	4.3 ± 0.6

13b, 3-methoxybenzo[4,5]-dioxole analogue **13d** was resulted in. **13d** had an average IC_{50} value of 5.0 nM and was comparable to that of ABI-231. It showed more than 30-fold enhancement of activity compared to **13b**. **13d** was ~2-fold more potent than **13c**. While 3-methoxy was crucial for the activities of ABI-231 analogues, the size of the cyclic rings on the phenyl moiety also mattered (**13c** vs **13d**). Increasing the five or six-membered rings to seven-membered ring resulted in 3-methoxybenzo[4,5]dioxepin analogue **13e**, which had an average IC_{50} value of 39.4 nM. Taken **13c**, **13d** and **13e** together, five-membered dioxole ring was preferred to both six-membered dioxane ring and seven-membered dioxepin ring. The likely explanation for this phenomenon is that the pocket in tubulin where the 3,4,5-TMP fit was so shallow that only small moieties (five or six-membered rings) instead of large moieties (seven-membered ring) can be accommodated. Among all the analogues modifying the 3,4,5-TMPs, **13f**, a unique 3-methoxybenzo[4,5]-dioxene analogue, exhibited the most potent antiproliferative activity and had an average IC_{50} of 1.9 nM against a panel of melanoma cell lines. This significant improvement of activity might result from an extra hydrophobic interaction between the double bond of the dioxene and the methionine residue nearby. The current effort is on obtaining the co-crystal structure of **13f** in complex with tubulin to clarify the additional interaction between dioxene moiety and tubulin.

Our previous SAR study of ABI-231 has demonstrated that ABI-231 analogues with a 4-indolyl or a 4-methyl-3-indolyl moiety showed the most potent antiproliferative activities. After optimization of the 3,4,5-TMP moiety, we, therefore, have produced analogues **19** and **25**. The purpose of synthesis of **19** and **25** is to investigate the combinational effect of the unique 3-methoxybenzo[4,5]-dioxene moiety with 4-indolyl moiety or 4-methyl-3-indolyl moiety. Surprisingly, the 4-indolyl analogue **19** exhibited ~11 folds reduced antiproliferative activity compared to **13f**. This might due to the disappearance of the H-bond interaction between the NH of 4-indolyl in **19** and α -THR179 or the absence of hydrophobic interaction between the dioxene moiety and methionine residue. Compared to **19**, the 4-methyl-3-indolyl analogue **25** showed much stronger antiproliferative activity and had an average IC_{50} of 7.0 nM.

To summarize the SAR, 3-methoxy is indispensable in the related scaffolds. Cyclizing 4,5-dimethoxy of the 3,4,5-TMP in ABI-231 to large heterocycle (e.g. dioxepin) is detrimental to inhibitory activity. **13f** with a unique 3-methoxybenzo[4,5]-dioxene moiety shows the most potent activity, indicating a possible hydrophobic interaction between the dioxene and nearby residue in tubulin.

Discussion

Reported CBSIs such as colchicine, CA-4, podophyllotoxin share a common character, the 3,4,5-TMP moiety. While most structural modifications of CA-4 focus on either the double bond linkage or the 3-hydroxy-4-methoxy benzene moiety, a rare modification has been conducted on the 3,4,5-TMP moiety.

ABI-231 showed potent antiproliferative activity and ability to surmount major drug-resistance mechanisms (e.g. overexpression of P-gp or tubulin β -III isotype). Thus, ABI-231 represents a promising scaffold for the development of anticancer agents. ABI-231 consists of 3,4,5-TMP, carbonyl, imidazole and indole moieties. In Chapter 2, we have shown our effort on investigating the SAR of ABI-231 by modifying the indole moiety. The co-crystal structure of the most potent 4-methyl-3-indole analogue reported in the last chapter indicates the existence of a methionine residue nearby the 3,4,5-TMP in tubulin. We assume that this methionine residue can serve as an opportunity to introduce a hydrophobic interaction to ABI-231 scaffold. With this hypothesis in mind, we have carried out the SAR investigation of ABI-231 by modifying the 3,4,5-TMP moiety.

We herein have established a concise alternative that can efficiently generate ABI-231 analogues in gram-scale. This method circumvents the involvement of a potentially explosive azide intermediate that is reported in Chapter 2. The novel strategy involves Suzuki coupling and Grignard reactions to yield eight new ABI-231 analogues. Among the eight analogues, analogue **13f** exhibits the strongest antiproliferative activity against a panel of melanoma cell lines. It has a unique 3-methoxybenzo[4,5]-dioxene moiety and an average IC_{50} of 1.9 nM. To the best of our knowledge, this analogue represents the most successful instance of isosterically modifying the 3,4,5-TMP moiety in CA-4 derivatives. To validate the significant potency of **13f**, obtaining the co-crystal structure of **13f** in complex with tubulin is currently undergoing.

In conclusion, we have established a concise synthetic method for ABI-231 analogues modifying the 3,4,5-TMP moiety. Eight new ABI-231 analogues are synthesized. The most potent analogue **13f** has an average IC_{50} of 1.9 nM and was 3.7-fold more potent than ABI-231.

CHAPTER 4. DESIGN AND SYNTHESIS OF NOVEL RABI ANALOGUES AS POTENT ANTITUBULINS

Introduction

Immunotherapy includes the adoptive cellular therapy and the monoclonal antibody. Immunotherapy has brought unprecedented improved survival rate for cancer patients in advanced stages and is advancing at an inspiring pace [45, 196]. However, cancer cells are able to develop multiple resistant mechanisms to circumvent the surveillance of normal host immune systems. The resistant mechanisms include but are not limited to tumor heterogeneity and metastasis, production of immune suppressive mediators, and down-modulating antigens [197, 198]. Current cancer treatments, therefore, still rely on targeted therapy and chemotherapy. Microtubules, the hollow cylinders, are composed of α and β -tubulin heterodimers. Microtubules are of great importance for a variety of cellular functions in all eukaryotes [199]. During mitosis, microtubules are responsible for the formation of mitotic spindles, which segregate sister chromatids into daughter cells [200]. Disruption of the microtubule dynamics can lead to the mitotic arrest and eventually apoptosis. Thus, microtubule dynamics are targetable for developing cancer therapy [91].

Most of the MTAs are summarized well in several reviews published recently [101, 102, 201, 202]. Due to their significant off-target effects, MTAs are infertile to produce an FDA-approved drug in the last years. Different from toxin alone, ADC utilizes its monoclonal antibody part to specifically expose the anticancer agent to cancerous cells rather than healthy cells; this results in limited undesirable off-target toxicity [203]. In February 2013, the FDA approved trastuzumab emtansine, a tubulin inhibitor based ADC, for the treatment of HER2 positive breast cancer.

In order to develop a successful ADC, it is of great cruciality for the payload to possess extremely potent cytotoxicity (typically IC_{50} in sub-nanomolar range) because minimal of the payloads (approximately 1-2%) can penetrate tumor cells [204]. In our previous search for potent anti-tubulins, a variety of scaffolds (**Figure 4-1**) including SMARTs, ABI-Is, ABI-IIIs and RABIs were designed, synthesized and biologically evaluated. The SAR has shown that replacement of the phenyl moieties in ABI-I/IIIs with indole moiety can improve the IC_{50} from double-digit nanomolar range to single-digit nanomolar range [169]. In view of the structural similarity between ABI-I/IIIs and RABIs, we hypothesize that replacing the benzene moiety in RABIs with indole moiety can significantly boost the cytotoxicity (**Figure 4-2**). With this hypothesis in mind, we herein report the establishment of a novel and concise synthetic route for RABI scaffold. Twelve new RABI analogues with modifications of the benzene moiety are synthesized and tested for biological activities.

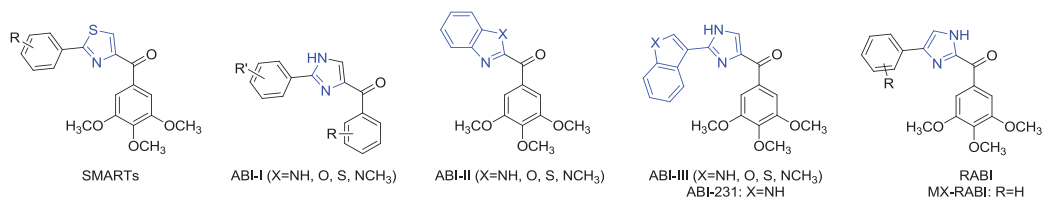


Figure 4-1. Examples of microtubule inhibitors binding to the colchicine binding sites in tubulin

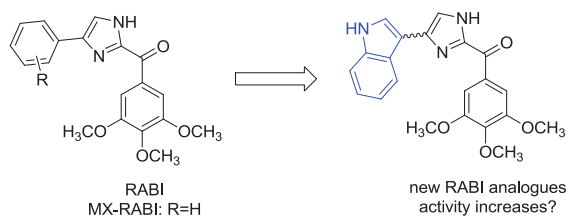


Figure 4-2. Hypothesis: modifying the benzene in RABI to indole can increase activity

Experimental Section

General chemistry

Tetrahydrofuran was distilled from sodium-benzophenone. All other solvents and chemical reagents were obtained from commercial sources and directly used without further purification. Glassware was oven-dried before use. All reactions were performed under an argon atmosphere. TLC was performed on silica gel 60 GF254 and monitored under UV light or visualized using phosphomolybdic acid reagent. Flash chromatography was performed on 230-400 mesh silica gel (Fisher Scientific). Melting points were recorded on a MPA100 Automated Melting Point Apparatus. NMR spectra were obtained on a Bruker Ascend 400 (Billerica, MA) spectrometer or a Varian Inova-500 spectrometer (Agilent Technologies, Santa Clara, CA). HR-MS were obtained on Waters Acquity UPLC linked to Waters Acquity Photodiode Array Detector and Waters Acquity Single Quadrupole Mass Detector. Chemical shifts are given in ppm with tetramethylsilane (TMS) as an internal reference. All coupling constants (J) are given in Hertz (Hz).

Chemical synthesis

General procedure for Boc protection. To a solution of indole or indazole or imidazole or pyrrolo[2,3-b]pyridine (1.34 mmol) and 4-dimethylaminopyridine (65 mg, 0.54 mol) in anhydrous dichloromethane (5 mL) under argon was added *di-tert*-butyl dicarbonate (351 mg, 1.61 mmol) while stirring. After 1 hour, water was added and the reaction mixture was extracted with dichloromethane, washed with brine and dried with Na_2SO_4 . Evaporation under vacuum gave the crude solid residue which was purified with flash chromatography on silica. Elution with hexane/ethyl acetate (10:1-3:1) gave pure boc-protected compounds as white to yellowish solids (55-94% yield).

Tert-butyl 4-bromo-1H-indazole-1-carboxylate (1b). ^1H NMR (400 MHz, Chloroform- d) δ 8.12 (d, $J = 2.0$ Hz, 1H), 8.08 (dd, $J = 8.1, 2.0$ Hz, 1H), 7.38 (dd, $J = 7.7, 2.0$ Hz, 1H), 7.35 – 7.28 (m, 1H), 1.69 (s, 9H). HRMS: calculated for $\text{C}_{12}\text{H}_{14}\text{BrN}_2\text{O}_2$ $[\text{M}+\text{H}]^+$ 297.0239, found 297.0241.

Tert-butyl 4-bromo-1H-pyrrolo[2,3-b]pyridine-1-carboxylate (1d). ^1H NMR (400 MHz, Chloroform- d) δ 8.30 – 8.20 (m, 1H), 7.64 (t, $J = 2.9$ Hz, 1H), 7.35 – 7.29 (m, 1H), 6.51 (t, $J = 2.9$ Hz, 1H), 1.62 (s, 9H). HRMS: calculated for $\text{C}_{12}\text{H}_{14}\text{BrN}_2\text{O}_2$ $[\text{M}+\text{H}]^+$ 297.0239, found 297.0237.

4-bromo-1-(phenylsulfonyl)indoline (2). ^1H NMR (400 MHz, Chloroform- d) δ 7.85 – 7.77 (m, 2H), 7.62 – 7.53 (m, 2H), 7.46 (dd, $J = 8.4, 7.1$ Hz, 2H), 7.14 – 7.03 (m, 2H), 3.95 (t, $J = 8.5$ Hz, 2H), 2.91 (t, $J = 8.5$ Hz, 2H). HRMS: calculated for $\text{C}_{14}\text{H}_{13}\text{BrNO}_2\text{S}$ $[\text{M}+\text{H}]^+$ 337.9850, found 337.9855.

5-bromoquinoline (5). ^1H NMR (400 MHz, Chloroform- d) δ 8.85 (dd, J = 4.2, 1.7 Hz, 1H), 8.40 (dt, J = 8.5, 1.2 Hz, 1H), 8.00 (dt, J = 8.5, 1.0 Hz, 1H), 7.71 (dd, J = 7.5, 1.1 Hz, 1H), 7.46 (dd, J = 8.5, 7.5 Hz, 1H), 7.37 (dd, J = 8.5, 4.2 Hz, 1H). HRMS: calculated for $\text{C}_9\text{H}_7\text{BrN}$ $[\text{M}+\text{H}]^+$ 207.9762, found 207.9763.

General procedure for synthesis of boronic ester 6a-6d, 7, 8, 9, 10a-10b, 11.

To a solution of bromide (1.0 mmol) in dioxane (10 mL) under argon was added bis(pinacolato)diboron (3.0 mmol), $\text{Pd}(\text{dppf})_2\cdot\text{CH}_2\text{Cl}_2$ (0.05 mmol), KOAc (3.0 mmol). The reaction was kept stirring at 90 °C overnight. Dioxane was removed under reduced pressure. Water was added and the reaction mixture was extracted with dichloromethane, washed with brine and dried with Na_2SO_4 . Evaporation under vacuum gave the crude solid residue which was purified with flash chromatography on silica. Elution with hexane/ethyl acetate (30:1-10:1) gave pure boronic esters as white to yellowish oil (31-87% yield).

Tert-butyl 4-(4,4,5,5-tetramethyl-1,3,2-dioxaborolan-2-yl)-1H-indole-1-carboxylate (6a). ^1H NMR (400 MHz, Chloroform- d) δ 8.26 (d, J = 8.3 Hz, 1H), 7.72 (dd, J = 7.2, 1.1 Hz, 1H), 7.63 (d, J = 3.7 Hz, 1H), 7.32 (dd, J = 8.3, 7.2 Hz, 1H), 7.15 – 7.06 (m, 1H), 1.68 (s, 9H), 1.39 (s, 12H). HRMS: calculated for $\text{C}_{19}\text{H}_{27}\text{BNO}_4$ $[\text{M}+\text{H}]^+$ 344.2033, found 344.2034.

Tert-butyl 4-(4,4,5,5-tetramethyl-1,3,2-dioxaborolan-2-yl)-1H-indazole-1-carboxylate (6b). ^1H NMR (400 MHz, Chloroform- d) δ 8.49 (d, J = 2.0 Hz, 1H), 8.19 (d, J = 8.4 Hz, 1H), 7.70 (dd, J = 7.0, 1.9 Hz, 1H), 7.48 – 7.40 (m, 1H), 1.65 (s, 9H), 1.31 (s, 12H). HRMS: calculated for $\text{C}_{18}\text{H}_{26}\text{BN}_2\text{O}_4$ $[\text{M}+\text{H}]^+$ 345.1986, found 345.1988.

Tert-butyl 4-(4,4,5,5-tetramethyl-1,3,2-dioxaborolan-2-yl)-1H-benzo[d]imidazole-1-carboxylate (6c). ^1H NMR (400 MHz, Chloroform- d) δ 8.55 (s, 1H), 8.08 (dd, J = 8.2, 1.3 Hz, 1H), 7.83 (dd, J = 7.3, 1.2 Hz, 1H), 7.37 (dd, J = 8.1, 7.3 Hz, 1H), 1.68 (s, 9H), 1.41 (s, 12H). HRMS: calculated for $\text{C}_{18}\text{H}_{26}\text{BN}_2\text{O}_4$ $[\text{M}+\text{H}]^+$ 345.1986, found 345.1987.

Tert-butyl 4-(4,4,5,5-tetramethyl-1,3,2-dioxaborolan-2-yl)-1H-pyrrolo[2,3-b]pyridine-1-carboxylate (6d). ^1H NMR (400 MHz, Chloroform- d) δ 8.48 (t, J = 3.5 Hz, 1H), 7.62 (t, J = 3.3 Hz, 1H), 7.51 (t, J = 3.6 Hz, 1H), 6.90 (t, J = 3.2 Hz, 1H), 1.63 (d, J = 2.8 Hz, 9H), 1.34 (d, J = 2.5 Hz, 12H). HRMS: calculated for $\text{C}_{18}\text{H}_{26}\text{BN}_2\text{O}_4$ $[\text{M}+\text{H}]^+$ 345.1986, found 345.1988.

1-(phenylsulfonyl)-4-(4,4,5,5-tetramethyl-1,3,2-dioxaborolan-2-yl)indoline (7). ^1H NMR (400 MHz, Chloroform- d) δ 7.77 (ddd, J = 17.2, 8.2, 1.1 Hz, 3H), 7.56 – 7.49 (m, 1H), 7.46 – 7.38 (m, 3H), 7.22 – 7.16 (m, 1H), 3.90 (t, J = 8.5 Hz, 2H), 3.11 (t, J = 8.5 Hz, 2H), 1.27 (s, 12H). HRMS: calculated for $\text{C}_{20}\text{H}_{25}\text{BNO}_4\text{S}$ $[\text{M}+\text{H}]^+$ 386.1597, found 386.1597.

Tert-butyl 6-(4,4,5,5-tetramethyl-1,3,2-dioxaborolan-2-yl)-1H-indole-1-carboxylate (9). ^1H NMR (400 MHz, Chloroform- d) δ 8.66 (s, 1H), 7.65 (dd, J = 7.8, 0.9

Hz, 1H), 7.62 (d, $J = 3.7$ Hz, 1H), 7.55 (dd, $J = 7.8, 0.8$ Hz, 1H), 6.59 – 6.51 (m, 1H), 1.68 (s, 9H), 1.26 (s, 12H). HRMS: calculated for $C_{19}H_{27}BNO_4$ $[M+H]^+$ 344.2033, found 344.2029.

Tert-butyl 3-(4,4,5,5-tetramethyl-1,3,2-dioxaborolan-2-yl)-1H-indole-1-carboxylate (10a). HRMS: calculated for $C_{19}H_{27}BNO_4$ $[M+H]^+$ 344.2033, found 344.2035.

Tert-butyl 4-methyl-3-(4,4,5,5-tetramethyl-1,3,2-dioxaborolan-2-yl)-1H-indole-1-carboxylate (10b). 1H NMR (400 MHz, Chloroform- d) δ 8.05 (d, $J = 8.5$ Hz, 1H), 8.01 (d, $J = 2.3$ Hz, 1H), 7.23 – 7.16 (m, 1H), 7.04 (dd, $J = 7.3, 2.1$ Hz, 1H), 2.71 (d, $J = 2.4$ Hz, 3H), 1.67 (d, $J = 2.3$ Hz, 9H), 1.40 – 1.34 (m, 12H). HRMS: calculated for $C_{20}H_{29}BNO_4$ $[M+H]^+$ 358.2190, found 358.2192.

5-(4,4,5,5-tetramethyl-1,3,2-dioxaborolan-2-yl)quinolone (11). 1H NMR (400 MHz, Chloroform- d) δ 9.10 (ddd, $J = 8.5, 1.8, 0.9$ Hz, 1H), 8.89 (dd, $J = 4.1, 1.7$ Hz, 1H), 8.18 (dt, $J = 8.4, 1.0$ Hz, 1H), 8.13 (dd, $J = 6.9, 1.3$ Hz, 1H), 7.69 (dd, $J = 8.4, 6.9$ Hz, 1H), 7.41 (dd, $J = 8.6, 4.2$ Hz, 1H), 1.39 (s, 12H). HRMS: calculated for $C_{15}H_{19}BNO_2$ $[M+H]^+$ 256.1509, found 256.1510.

Synthesis of 4-bromo-1-((2-(trimethylsilyl)ethoxy)methyl)-1H-imidazole (12). To a stirred solution of 4-bromoimidazole (25.0 g, 0.17 mol) in anhydrous THF (300 mL) at ice temperature was added sodium hydride (7.5 g, 0.187 mol) in portions under argon. The mixture was stirred for 1 hr at this temperature and was added 2-(trimethylsilyl)ethoxymethyl chloride (33.0 ml, 0.187 mol) dropwise. Reaction was then warmed to room temperature and stirred for another 2 hr. Water was then added at ice temperature carefully and the reaction mixture was extracted with ethyl acetate, washed with brine and dried with Na_2SO_4 . The combined extracts were evaporated under vacuum to give the oily residue which was purified with flash chromatography on silica. Elution with hexane/ethyl acetate (10:1) gave **12** as slightly yellowish oil (40.5 g, 86% yield). 1H NMR (400 MHz, Chloroform- d) δ 7.46 (s, 1H), 7.01 (s, 1H), 5.22 (s, 2H), 3.53 – 3.40 (m, 2H), 0.95 – 0.85 (m, 2H), -0.01 (s, 9H). HRMS: calculated for $C_9H_{18}BrN_2OSi$ $[M+H]^+$ 277.0372, found 277.0370.

Synthesis of (4-bromo-1-((2-(trimethylsilyl)ethoxy)methyl)-1H-imidazol-2-yl)(3,4,5-trimethoxyphenyl)methanone (13). To a stirring solution of compound **12** (2.77 g, 10.0 mmol) in anhydrous THF (15.0 mL) under argon was added isopropylmagnesium chloride lithium chloride complex solution (1.3 M in THF, 9.3 ml, 12.0 mmol) at room temperature. The mixture was stirred for 1 hr and was added freshly made 3,4,5-trimethoxybenzoyl chloride (2.76 g, 12.0 mmol) in anhydrous THF (15.0 mL). Reaction was kept stirring at room temperature for another 4 hr and then saturated NH_4Cl solution was added to quench the reaction. Reaction mixture was extracted with ethyl acetate, washed with brine and dried with Na_2SO_4 . The combined extracts were evaporated under vacuum to give the crude product which was purified with flash chromatography on silica. Elution with hexane/ethyl acetate (20:1-5:1) gave **13** as pale-yellow oil (1.1 g, 24% yield). 1H NMR (400 MHz, Chloroform- d) δ 7.72 (s, 2H), 7.40 (s,

1H), 5.81 (s, 2H), 3.97 (d, $J = 2.8$ Hz, 9H), 3.70 – 3.63 (m, 2H), 1.03 – 0.95 (m, 2H), 0.02 (s, 9H). HRMS: calculated for $C_{19}H_{28}BrN_2O_5Si$ $[M+H]^+$ 471.0951, found 471.0955.

General procedure for the synthesis of 14a-14k. To the mixture of 13 (1.0 mmol), boronate (1.1 mmol), sodium carbonate (2.0 mmol) tris(dibenzylideneacetone)dipalladium (0.05 mmol) and 2-dicyclohexylphosphino-2',4',6'-triisopropyl-1,1'-biphenyl (0.15 mmol) was added 6.25 mL mixed solvent $PhCH_3$ -MeOH- H_2O (20:4:1). After refluxed for 4 hr, water was added and the reaction mixture was extracted with ethyl acetate (3*10 mL), washed with brine and dried with Na_2SO_4 . Evaporation under vacuum gave the crude product which was purified with flash chromatography on silica. Elution with hexane/ethyl acetate (10:1-3:1) gave 14a-14k pale-yellow to yellowish solids or oil (yield: 27-74%).

Tert-butyl 3-(2-(3,4,5-trimethoxybenzoyl)-1-((2-(trimethylsilyl)ethoxy)methyl)-1H-imidazol-4-yl)-1H-indole-1-carboxylate (14a). 1H NMR (400 MHz, Chloroform- d) δ 8.15 (d, $J = 7.9$ Hz, 1H), 8.05 (d, $J = 8.3$ Hz, 1H), 7.97 (d, $J = 1.8$ Hz, 1H), 7.94 – 7.85 (m, 4H), 7.71 (d, $J = 1.9$ Hz, 1H), 7.55 – 7.47 (m, 1H), 7.46 – 7.34 (m, 3H), 7.29 (t, $J = 7.4$ Hz, 1H), 5.88 (d, $J = 1.9$ Hz, 2H), 3.96 (s, 9H), 3.74 – 3.62 (m, 2H), 1.04 – 0.95 (m, 2H), -0.02 (s, 9H). HRMS: calculated for $C_{32}H_{42}N_3O_7Si$ $[M+H]^+$ 608.2792, found 608.2799.

Tert-butyl 4-(2-(3,4,5-trimethoxybenzoyl)-1-((2-(trimethylsilyl)ethoxy)methyl)-1H-imidazol-4-yl)-1H-indole-1-carboxylate (14b). 1H NMR (400 MHz, Chloroform- d) δ 8.16 (d, $J = 8.2$ Hz, 1H), 7.95 (s, 2H), 7.80 (s, 1H), 7.72 – 7.58 (m, 2H), 7.41 (d, $J = 3.7$ Hz, 1H), 7.36 (t, $J = 7.9$ Hz, 1H), 5.91 (s, 2H), 3.97 (d, $J = 8.7$ Hz, 9H), 3.70 (dd, $J = 8.9, 7.5$ Hz, 2H), 1.69 (s, 9H), 0.99 (dd, $J = 8.9, 7.7$ Hz, 2H), -0.01 (s, 9H). HRMS: calculated for $C_{32}H_{42}N_3O_7Si$ $[M+H]^+$ 608.2792, found 608.2783.

Tert-butyl 4-methyl-3-(2-(3,4,5-trimethoxybenzoyl)-1-((2-(trimethylsilyl)ethoxy)methyl)-1H-imidazol-4-yl)-1H-indole-1-carboxylate (14d). 1H NMR (400 MHz, Chloroform- d) δ 8.12 (d, $J = 8.3$ Hz, 1H), 7.92 – 7.83 (m, 2H), 7.69 (t, $J = 1.7$ Hz, 1H), 7.52 – 7.45 (m, 1H), 7.25 (td, $J = 8.2, 1.9$ Hz, 1H), 7.02 (d, $J = 7.4$ Hz, 1H), 5.95 – 5.83 (m, 2H), 3.93 (s, 3H), 3.91 (s, 6H), 3.69 (td, $J = 8.9, 2.1$ Hz, 2H), 2.49 (s, 3H), 1.67 (s, 9H), 1.04 – 0.94 (m, 2H), -0.00 (s, 9H). HRMS: calculated for $C_{33}H_{44}N_3O_7Si$ $[M+H]^+$ 622.2949, found 622.2955.

(4-(quinolin-5-yl)-1-((2-(trimethylsilyl)ethoxy)methyl)-1H-imidazol-2-yl)(3,4,5-trimethoxyphenyl)methanone (14e). 1H NMR (400 MHz, Chloroform- d) δ 9.20 (ddd, $J = 8.6, 1.7, 0.8$ Hz, 1H), 8.95 (dd, $J = 4.1, 1.8$ Hz, 1H), 8.13 (dt, $J = 8.1, 1.2$ Hz, 1H), 7.96 (s, 2H), 7.82 – 7.73 (m, 2H), 7.72 (s, 1H), 7.39 (dd, $J = 8.6, 4.2$ Hz, 1H), 5.94 (s, 2H), 3.95 (s, 3H), 3.93 (s, 6H), 3.80 – 3.65 (m, 2H), 1.05 – 0.96 (m, 2H), -0.00 (s, 9H). HRMS: calculated for $C_{28}H_{34}N_3O_5Si$ $[M+H]^+$ 520.2268, found 520.2277.

(4-(1-(phenylsulfonyl)indolin-4-yl)-1-((2-(trimethylsilyl)ethoxy)methyl)-1H-imidazol-2-yl)(3,4,5-trimethoxyphenyl)methanone (14f). 1H NMR (400 MHz,

Chloroform-d) δ 7.88 – 7.82 (m, 5H), 7.67 (dd, $J = 8.0, 0.9$ Hz, 1H), 7.59 – 7.53 (m, 3H), 7.46 (dd, $J = 8.4, 7.1$ Hz, 2H), 7.31 (t, $J = 7.9$ Hz, 1H), 5.86 (s, 2H), 4.03 (d, $J = 8.4$ Hz, 2H), 3.99 (s, 3H), 3.94 (s, 6H), 3.70 – 3.65 (m, 2H), 3.27 (t, $J = 8.4$ Hz, 2H), 1.01 – 0.96 (m, 2H), 0.00 (s, 9H). HRMS: calculated for $C_{33}H_{40}N_3O_7SSi$ $[M+H]^+$ 650.2356, found 650.2351.

4-(2-(3,4,5-trimethoxybenzoyl)-1-((2-(trimethylsilyl)ethoxy)methyl)-1H-imidazol-4-yl)indolin-2-one (14h). 1H NMR (400 MHz, Chloroform-d) δ 9.06 (s, 1H), 7.87 (d, $J = 2.1$ Hz, 2H), 7.67 (d, $J = 2.1$ Hz, 1H), 7.56 (dd, $J = 8.1, 2.0$ Hz, 1H), 7.36 – 7.24 (m, 1H), 6.93 – 6.83 (m, 1H), 5.88 (d, $J = 2.1$ Hz, 2H), 3.99 (dd, $J = 4.8, 2.2$ Hz, 9H), 3.87 (s, 2H), 3.74 – 3.64 (m, 2H), 1.08 – 0.93 (m, 2H), 0.00 (s, 9H). HRMS: calculated for $C_{27}H_{34}N_3O_6Si$ $[M+H]^+$ 524.2217, found 524.2210.

Tert-butyl 4-(2-(3,4,5-trimethoxybenzoyl)-1-((2-(trimethylsilyl)ethoxy)methyl)-1H-imidazol-4-yl)-1H-benzo[d]imidazole-1-carboxylate (14j). 1H NMR (400 MHz, Chloroform-d) δ 8.63 (s, 1H), 8.48 (s, 1H), 8.15 (dd, $J = 7.8, 1.1$ Hz, 1H), 7.96 (s, 2H), 7.92 (dd, $J = 8.2, 1.1$ Hz, 1H), 7.45 (t, $J = 7.9$ Hz, 1H), 5.92 (s, 2H), 3.98 (s, 6H), 3.97 (s, 3H), 3.73 – 3.66 (m, 2H), 1.72 (s, 9H), 1.01 – 0.95 (m, 2H), -0.04 (s, 9H). HRMS: calculated for $C_{31}H_{41}N_4O_7Si$ $[M+H]^+$ 609.2745, found 609.2751.

Tert-butyl 4-(2-(3,4,5-trimethoxybenzoyl)-1-((2-(trimethylsilyl)ethoxy)methyl)-1H-imidazol-4-yl)-1H-pyrrolo[2,3-b]pyridine-1-carboxylate (14k). 1H NMR (400 MHz, Chloroform-d) δ 8.54 (dd, $J = 5.4, 2.2$ Hz, 1H), 7.95 (t, $J = 1.5$ Hz, 1H), 7.91 (t, $J = 1.6$ Hz, 2H), 7.68 (t, $J = 3.2$ Hz, 1H), 7.57 (dd, $J = 5.6, 2.2$ Hz, 1H), 7.29 (q, $J = 2.2, 1.4$ Hz, 1H), 5.91 (s, 2H), 4.00 (s, 3H), 3.96 (s, 6H), 3.75 – 3.68 (m, 2H), 1.70 (s, 9H), 1.05 – 0.98 (m, 2H), 0.00 (s, 9H). HRMS: calculated for $C_{31}H_{41}N_4O_7Si$ $[M+H]^+$ 609.2745, found 609.2740.

General procedure for synthesis of 15a-15k. For deprotection of protecting group $PhSO_2$ and SEM: To a solution of **14a-14k** (0.3 mmol) in MeOH (3 mL) was added 40% NaOH (1.0 mL). The mixture was refluxed for 2 hr, solvent was removed under reduced pressure. Water was added and the reaction mixture was extracted with ethyl acetate (3*10 mL). Combined solvent was evaporated under reduced pressure to provide crude product. To the crude was then added trifluoroacetic acid in dichloromethane (1:1, 2mL). After 2 hour, solvent was removed under reduced pressure. Saturated $NaHCO_3$ solution and ethyl acetate was then added and the organic phase was separated, washed with brine and dried with Na_2SO_4 . Evaporation under vacuum gave the solid residue which was purified with flash chromatography on silica. Elution with hexane/ethyl acetate (3:1-1:3) gave **15a-15k** as pale-yellow to yellowish solids (yield: 39-76% over two steps). For deprotection of Boc and SEM: To a solution of **14a-14k** (0.2 mmol) in dichloromethane (1.5 mL) was added trifluoroacetic acid (1.5 mL). The mixture was stirred for 2 hr. Solvent was removed under reduced pressure. Saturated $NaHCO_3$ solution and ethyl acetate was then added and the organic phase was separated, washed with brine and dried with Na_2SO_4 . Evaporation under vacuum gave the solid residue

which was purified with flash chromatography on silica. Elution with hexane/ethyl acetate (3:1-1:3) gave **15a-15k** as pale-yellow to yellowish solids (yield: 33-81%).

(4-(1H-indol-3-yl)-1H-imidazol-2-yl)(3,4,5-trimethoxyphenyl)methanone (15a). ¹H NMR (400 MHz, Methylene Chloride-d₂) δ 8.58 (s, 1H), 8.16 (s, 2H), 8.06 (s, 1H), 7.67 (s, 1H), 7.60 (d, J = 2.0 Hz, 1H), 7.48 (d, J = 8.1 Hz, 1H), 7.25 (dt, J = 22.6, 7.4 Hz, 2H), 3.97 (s, 6H), 3.90 (s, 3H). HRMS: calculated for C₂₁H₂₀N₃O₄ [M+H]⁺ 378.1454, found 378.1453.

(4-(1H-indol-4-yl)-1H-imidazol-2-yl)(3,4,5-trimethoxyphenyl)methanone (15b). ¹H NMR (400 MHz, Chloroform-d) δ 11.09 (d, J = 64.7 Hz, 1H), 8.56 (d, J = 64.0 Hz, 1H), 8.32 (s, 1H), 8.07 (s, 1H), 7.76 (dd, J = 27.3, 1.9 Hz, 1H), 7.65 (d, J = 7.3 Hz, 1H), 7.47 – 7.36 (m, 2H), 7.36 – 7.22 (m, 3H), 6.85 (t, J = 2.6 Hz, 1H), 4.00 (d, J = 10.8 Hz, 9H). HRMS: calculated for C₂₁H₂₀N₃O₄ [M+H]⁺ 378.1454, found 378.1451.

(4-(1H-indol-6-yl)-1H-imidazol-2-yl)(3,4,5-trimethoxyphenyl)methanone (15c), HRMS: calculated for C₂₁H₂₀N₃O₄ [M+H]⁺ 378.1454, found 378.1455.

(4-(4-methyl-1H-indol-3-yl)-1H-imidazol-2-yl)(3,4,5-trimethoxyphenyl)methanone (15d). ¹H NMR (400 MHz, Methylene Chloride-d₂) δ 7.98 (d, J = 2.1 Hz, 2H), 7.34 (d, J = 2.0 Hz, 1H), 7.30 (d, J = 2.1 Hz, 1H), 7.25 (d, J = 8.2 Hz, 1H), 7.15 – 7.04 (m, 1H), 6.89 (d, J = 7.1 Hz, 1H), 3.90 (s, 6H), 3.88 (s, 3H), 2.46 (s, 3H). HRMS: calculated for C₂₀H₂₂N₃O₄ [M+H]⁺ 392.1610, found 392.1606.

(4-(quinolin-5-yl)-1H-imidazol-2-yl)(3,4,5-trimethoxyphenyl)methanone (15e). ¹H NMR (400 MHz, Chloroform-d) δ 11.95 (s, 1H), 9.31 (ddd, J = 8.6, 1.7, 0.9 Hz, 1H), 8.98 (dd, J = 4.2, 1.7 Hz, 1H), 8.25 (s, 2H), 8.14 (dt, J = 8.0, 1.2 Hz, 1H), 7.81 – 7.67 (m, 2H), 7.62 (d, J = 2.4 Hz, 1H), 7.40 (dd, J = 8.7, 4.2 Hz, 1H), 3.94 (d, J = 15.7 Hz, 9H). HRMS: calculated for C₂₂H₂₀N₃O₄ [M+H]⁺ 390.1454, found 390.1455.

(4-(1-(phenylsulfonyl)indolin-4-yl)-1H-imidazol-2-yl)(3,4,5-trimethoxyphenyl)methanone (15f). ¹H NMR (400 MHz, Chloroform-d) δ 7.96 (s, 2H), 7.79 – 7.71 (m, 2H), 7.56 (d, J = 8.0 Hz, 1H), 7.52 – 7.45 (m, 1H), 7.38 (dd, J = 8.4, 7.1 Hz, 3H), 7.34 (s, 1H), 7.22 (t, J = 7.9 Hz, 1H), 3.93 (t, J = 8.4 Hz, 2H), 3.88 (s, 3H), 3.87 (s, 6H), 3.16 (dd, J = 16.8, 8.6 Hz, 2H). HRMS: calculated for C₂₇H₂₆N₃O₆S [M+H]⁺ 520.1542, found 520.1554.

(4-(indolin-4-yl)-1H-imidazol-2-yl)(3,4,5-trimethoxyphenyl)methanone (15g). ¹H NMR (400 MHz, Chloroform-d) δ 10.90 (d, J = 15.6 Hz, 1H), 8.23 (s, 1H), 8.05 (s, 1H), 7.55 – 7.41 (m, 1H), 7.27 (d, J = 7.8 Hz, 1H), 7.16 – 7.03 (m, 1H), 6.64 (dd, J = 7.9, 4.3 Hz, 1H), 3.98 (d, J = 5.3 Hz, 9H), 3.65 (dt, J = 11.5, 8.3 Hz, 2H), 3.40 (t, J = 8.3 Hz, 1H), 3.25 (t, J = 8.4 Hz, 1H). HRMS: calculated for C₂₁H₂₂N₃O₄ [M+H]⁺ 380.1610, found 380.1605.

4-(2-(3,4,5-trimethoxybenzoyl)-1H-imidazol-4-yl)indolin-2-one (15h). ¹H NMR (400 MHz, DMSO-d₆) δ 13.68 (s, 1H), 10.47 (s, 1H), 8.02 (d, J = 21.6 Hz, 3H),

7.54 (d, $J = 8.0$ Hz, 1H), 7.24 (t, $J = 7.9$ Hz, 1H), 6.76 (d, $J = 7.6$ Hz, 1H), 3.92 (s, 6H), 3.84 (s, 2H), 3.80 (s, 3H). HRMS: calculated for $C_{21}H_{20}N_3O_5$ $[M+H]^+$ 378.1454, found 378.1452.

(4-(1H-indazol-4-yl)-1H-imidazol-2-yl)(3,4,5-trimethoxyphenyl)methanone (15i). 1H NMR (400 MHz, DMSO- d_6) δ 13.80 (s, 1H), 13.18 (s, 1H), 8.82 (s, 1H), 8.29 (s, 1H), 8.13 (s, 2H), 7.72 (d, $J = 6.6$ Hz, 1H), 7.48 (dd, $J = 28.9, 7.4$ Hz, 2H), 3.97 (s, 6H), 3.87 (s, 3H). HRMS: calculated for $C_{20}H_{19}N_4O_4$ $[M+H]^+$ 379.1406, found 379.1409.

(4-(1H-benzo[d]imidazol-4-yl)-1H-imidazol-2-yl)(3,4,5-trimethoxyphenyl)methanone (15j). 1H NMR (400 MHz, Chloroform- d) δ 8.00 (s, 1H), 7.74 (d, $J = 24.9$ Hz, 3H), 7.63 – 7.24 (m, 2H), 7.23 – 7.13 (m, 1H), 3.83 (d, $J = 4.3$ Hz, 9H). HRMS: calculated for $C_{20}H_{19}N_4O_4$ $[M+H]^+$ 379.1406, found 379.1407.

(4-(1H-pyrrolo[2,3-b]pyridin-4-yl)-1H-imidazol-2-yl)(3,4,5-trimethoxyphenyl)methanone (15k). 1H NMR (400 MHz, DMSO- d_6) δ 14.05 – 13.58 (m, 1H), 11.68 (s, 1H), 8.39 – 8.19 (m, 2H), 8.11 (s, 2H), 7.57 (dd, $J = 29.4, 3.7$ Hz, 2H), 7.20 (s, 1H), 3.93 (s, 6H), 3.82 (s, 3H). HRMS: calculated for $C_{20}H_{19}N_4O_4$ $[M+H]^+$ 379.1406, found 379.1403.

Synthesis of (4-bromo-1-((2-(trimethylsilyl)ethoxy)methyl)-1H-imidazol-2-yl)(8-methoxybenzo[b][1,4]dioxin-6-yl)methanone (16). To a stirring solution of compound **12** (1.38 g, 5.0 mmol) in anhydrous THF (10.0 mL) under argon was added isopropylmagnesium chloride lithium chloride complex solution (1.3 M in THF, 4.6 ml, 6.0 mmol) at room temperature. The mixture was stirred for 1 hr and was added 3-methoxy[4,5]dioxene benzoyl chloride (1.5 g, 6.5 mmol) in anhydrous THF (7.0 mL). Reaction was kept stirring at room temperature for another 4 hr and then saturated NH_4Cl solution was added to quench the reaction. Reaction mixture was extracted with ethyl acetate, washed with brine and dried with Na_2SO_4 . The combined extracts were evaporated under vacuum to give the crude product which was purified with flash chromatography on silica. Elution with hexane/ethyl acetate (20:1-5:1) gave **16** as pale-yellow oil (0.74 g, 32% yield). 1H NMR (400 MHz, Chloroform- d) δ 7.59 (s, 1H), 7.44 (s, 1H), 7.36 – 7.30 (m, 1H), 5.98 (dd, $J = 3.7, 1.6$ Hz, 1H), 5.90 (dd, $J = 3.8, 1.5$ Hz, 1H), 5.79 – 5.70 (m, 2H), 3.96 – 3.82 (m, 3H), 3.61 (td, $J = 8.4, 1.4$ Hz, 2H), 1.00 – 0.90 (m, 2H), -0.01 (s, 9H). HRMS: calculated for $C_{19}H_{24}BrN_2O_5Si$ $[M+H]^+$ 467.0638, found 467.0644.

Synthesis of tert-butyl 4-(2-(8-methoxybenzo[b][1,4]dioxine-6-carbonyl)-1-((2-(trimethylsilyl)ethoxy)methyl)-1H-imidazol-4-yl)-3-methyl-1H-indole-1-carboxylate (17). To the mixture of **16** (467 mg, 1.0 mmol), **10b** (392 mg, 1.1 mmol), sodium carbonate (2.0 mmol) tris(dibenzylideneacetone)dipalladium (0.05 mmol) and 2-dicyclohexylphosphino-2',4',6'-triisopropyl-1,1'-biphenyl (0.15 mmol) was added 6.25 mL mixed solvent $PhCH_3$ -MeOH- H_2O (20:4:1). After refluxed for 4 hr, water was added and the reaction mixture was extracted with ethyl acetate (3*10 mL), washed with brine and dried with Na_2SO_4 . Evaporation under vacuum gave the crude product which was purified with flash chromatography on silica. Elution with hexane/ethyl acetate (10:1-3:1)

gave **17** as yellowish solid (376 mg, 61%). ¹H NMR (400 MHz, Chloroform-*d*) δ 8.25 (d, *J* = 8.3 Hz, 1H), 7.82 (d, *J* = 1.9 Hz, 1H), 7.62 (d, *J* = 1.9 Hz, 1H), 7.45 (s, 1H), 7.39 (d, *J* = 2.1 Hz, 1H), 7.33 (dd, *J* = 8.3, 7.4 Hz, 1H), 7.29 – 7.24 (m, 1H), 5.97 (d, *J* = 3.6 Hz, 1H), 5.92 – 5.86 (m, 3H), 3.88 (s, 3H), 3.71 – 3.64 (m, 2H), 2.06 (d, *J* = 1.3 Hz, 3H), 1.68 (s, 9H), 1.02 – 0.96 (m, 2H), 0.00 (s, 9H). HRMS: calculated for C₃₃H₄₀N₃O₇Si [M+H]⁺ 618.2636, found 618.2628.

Synthesis of (8-methoxybenzo[*b*][1,4]dioxin-6-yl)(4-(3-methyl-1H-indol-4-yl)-1H-imidazol-2-yl)methanone (18). To a solution of **17** (0.1 mmol) in dichloromethane (1.5 mL) was added trifluoroacetic acid (1.5 mL). The mixture was stirred for 2 hr. Solvent was removed under reduced pressure. Saturated NaHCO₃ solution and ethyl acetate was then added and the organic phase was separated, washed with brine and dried with Na₂SO₄. Evaporation under vacuum gave the solid residue which was purified with flash chromatography on silica. Elution with hexane/ethyl acetate (3:1-1:3) gave **18** as yellowish solid (28 mg, 74%). ¹H NMR (400 MHz, Chloroform-*d*) δ 11.36 (s, 1H), 8.30 (s, 1H), 7.85 (s, 1H), 7.63 (s, 1H), 7.40 (d, *J* = 22.8 Hz, 2H), 7.15 (dd, *J* = 24.1, 7.4 Hz, 2H), 6.98 (s, 1H), 5.95 (dd, *J* = 29.6, 3.5 Hz, 2H), 3.87 (s, 3H), 2.05 (s, 3H). HRMS: calculated for C₂₂H₁₈N₃O₄ [M+H]⁺ 388.1297, found 388.1301.

Cell culture and reagents

Human melanoma carcinoma cell lines A375, M14, and RPMI7951 (American Type Culture Collection or ATCC, Manassas, VA, USA) were cultured in Dulbecco's modified Eagle's medium (DMEM) (Corning, Manassas, VA) supplemented with 10% (v/v) fetal bovine serum (FBS) (Atlanta Biologicals, Lawerenceville, GA) and 1% antibiotic/antimycotic mixture (Sigma-Aldrich, St. Louis MO). Murine melanoma B16F10 cells (ATCC, Manassas, VA, USA) were cultured in Minimum essential medium (Invitrogen, Carlsbad, CA), supplemented with 5% heat-inactivated Hyclone FBS (Thermo Scientific, Rockford, IL), 1% antibiotic-antimycotic mixture (Sigma-Aldrich, St. Louis MO), 1% Mem-sodium pyruvate (Invitrogen, Carlsbad, CA), 1% Mem-vitamin (Invitrogen, Carlsbad, CA), L-Glutamine (2mM final concentration) (Invitrogen, Carlsbad, CA), and 1% Mem NEAA (Invitrogen, Carlsbad, CA). All cell lines were authenticated by ATCC by short tandem repeat profiling. Cultures were maintained to 80-90% confluency at 37°C in a humidified atmosphere containing 5% CO₂. Compounds were dissolved in dimethyl sulfoxide (DMSO) (Sigma-Aldrich, St. Louis, MO) to make a stock solution of 20 mM. Compound solutions were freshly prepared by diluting stocks with cell culture medium before use.

Cytotoxicity assay

A375, M14, and RPMI7951 were seeded in 96-well plates at a concentration of 1,000–5,000 cells per well, depending on growth rate of the cell line. After overnight incubation, the media was replaced and cells were treated with the test compounds at 10 concentrations ranging from 0.03 nM to 1 μM plus a vehicle control for 72 h in four

replicates. Following treatment, the MTS reagent (Promega, Madison, WI) was added to the cells and incubated in dark at 37°C for at least 1 hour. Absorbance at 490 nm was measured using a plate reader (DYNEX Technologies, Chantilly VA). Percentages of cell survival versus drug concentrations were plotted, and the IC₅₀ (concentration that inhibited cell growth by 50% of untreated control) values were obtained by nonlinear regression analysis using GraphPad Prism (GraphPad Software, San Diego, CA).

Chemistry

Our proposed synthetic strategy for RABI analogues is illustrated in **Scheme 4-1**. To construct the RABI scaffold, we resort to Suzuki coupling reaction using boronic esters and bromides. The bromides are afforded by Grignard reactions, in which 4-bromoimidazole is treated with benzoyl chlorides.

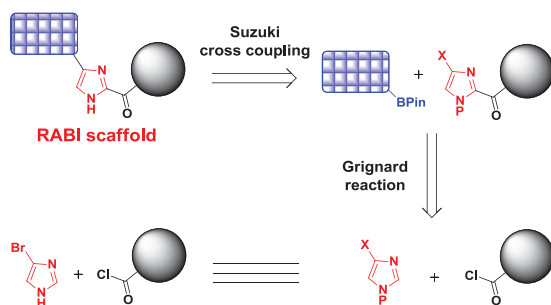
Preparation of the boronic esters was carried out according to reported procedures [205-207] as outlined in **Scheme 4-2**. In brief, bromides were protected with Boc or benzenesulfonyl, followed by Miyaura borylation in the presence of Pd(dppf)₂ in complex with CH₂Cl₂ and potassium acetate to provide boronates **6a-6d** and **7-11**.

RABI analogues **15a-15k** were accomplished by following the synthetic approach as depicted in **Scheme 4-3**. Commercially available 4-bromoimidazole reacted with SEMCl in the presence of sodium hydride to provide SEM protected product **12** in 86% yield. Treatment of **12** with Grignard reagent *i*-PrMgCl(LiCl) and 3,4,5-trimethoxybenzoyl chloride provided **13** in 24% yield. Suzuki cross-coupling of **13** with pinacol boronic esters in the presence of Pd₂(dba)₃ and 2-dicyclohexylphosphino-2',4',6'-triisopropylbiphenyl afforded compounds **14a-14k**. **14a-14k** were subjected to the deprotection of benzenesulfonyl, Boc and 2-(Trimethylsilyl)ethoxymethyl to furnish target RABI analogues **15a-15k**. Cleavage of the protecting groups of 2-(Trimethylsilyl)ethoxymethyl and boc in **15a-15k** can be simultaneously achieved using trifluoroacetic acid while benzenesulfonyl group can be removed by refluxing in sodium hydroxide solution.

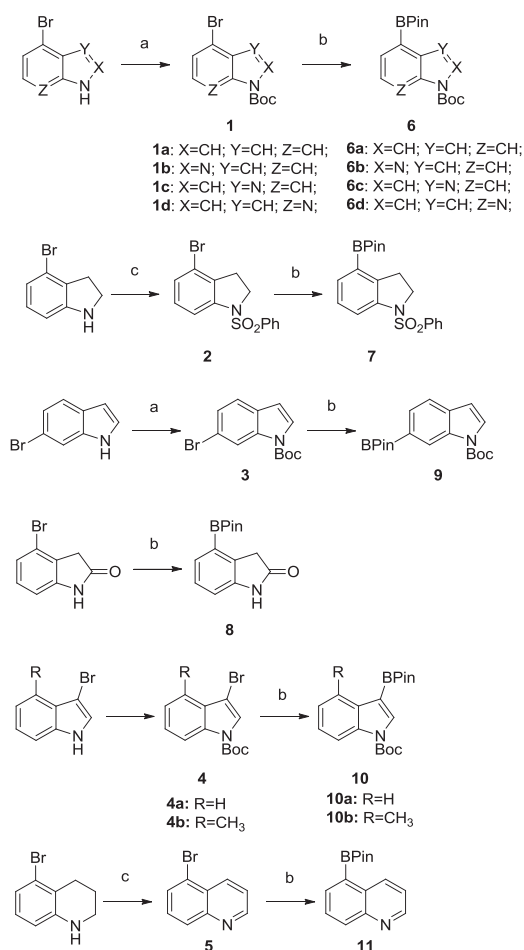
Analogue **18** was obtained in a similar manner to that of **15a-15k**. Its synthesis was outlined in **Scheme 4-4**. The synthesis of the starting material 3-methoxy[4,5]dioxene benzoyl chloride was described in Chapter 3.

Results

All new RABI analogues were evaluated for their cytotoxicity in human melanoma cell lines including A375, M14 and RMPI7951. Colchicine was used as a positive control. The antiproliferative effects of all the compounds were evaluated using MTT assay. IC₅₀s were reported in nM and calculated from at least three independent experiments, each of which were performed in duplicates. The *in vitro* assay result was

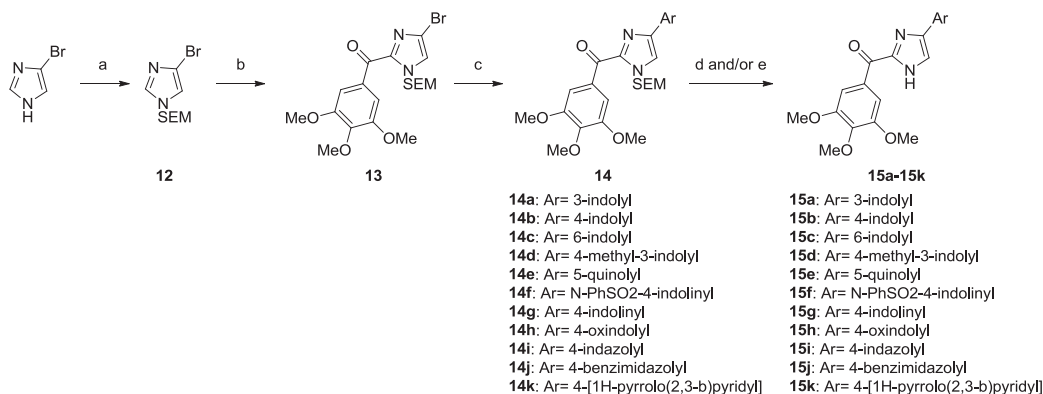


Scheme 4-1. Retrosynthetic analysis of RABI analogues



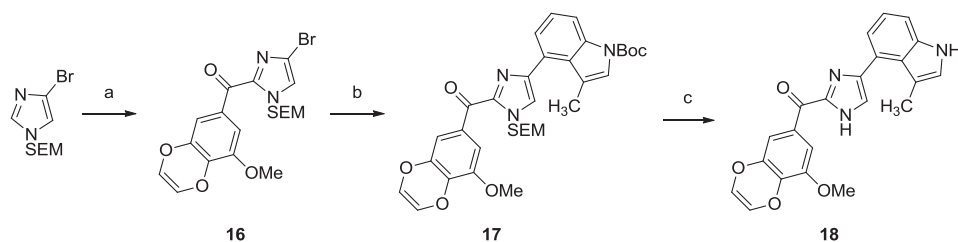
Scheme 4-2. Synthesis of boronic esters

Reagents and conditions: (a): Boc₂O, DMAP, DCM, rt; (b): bis(pinacolato)diboron, Pd(dppf)₂.CH₂Cl₂, KOAc, dioxane, 80°C; (c): PhSO₂Cl, NaH, THF, 0°C to rt.



Scheme 4-3. Synthesis of RABI analogues 15a-15k

Reagents and conditions: (a): SEMCl, NaH, THF, 0°C to rt; (b): 3,4,5-trimethoxybenzoyl chloride, *i*-PrMgCl(LiCl), THF, rt; (c): Pd₂(dba)₃, 2-dicyclohexylphosphino-2',4',6'-triisopropylbiphenyl, Na₂CO₃, toluene-MeOH-H₂O (20:4:1), reflux; (d): NaOH(40% in H₂O), MeOH, reflux; (e): TFA, DCM, rt.



Scheme 4-4. Synthesis of RABI analog 18

Reagents and conditions: (a): 3-methoxy[4,5]dioxene benzoyl chloride, *i*-PrMgCl(LiCl), THF, rt; (b): Pd₂(dba)₃, 2-dicyclohexylphosphino-2',4',6'-triisopropylbiphenyl, Na₂CO₃, toluene-MeOH-H₂O (20:4:1), reflux; (c): TFA, DCM, rt.

shown in **Table 4-1**.

In our previously disclosed RABI series, the most potent analogue MX-RABI had an average IC_{50} of 14nM against a panel of melanoma and prostate cancer cell lines. When the benzene moiety in MX-RABI was replaced with a 3-indolyl group, compound **15a** was resulted in. **15a** was 2.5-fold less active than the MX-RABI. Our previous SAR study of ABI-231 in Chapter 2 showed that rotation of the indole ring or introduction of small substituents to the indole ring in ABI-231 can significantly improve antitubulin activity. To further develop SAR, we synthesized 4-indolyl, 6-indolyl and 4-methyl-3-indolyl RABI analogues **15b**, **15c** and **15d**. It turned out that neither altering the 3-indolyl to 6-indolyl (**15c**) nor adding a 4-methyl group to 3-indolyl (**15d**) was beneficial to the antiproliferative activity. **15b**, an analogue resulted from alteration of the 3-indolyl to 4-indolyl, exhibited greatly enhanced antiproliferative activity and had an average IC_{50} of 3.5 nM. **15b** was 4-fold and ~2-fold more cytotoxic than MX-RABI and ABI-231, respectively. Having shown that a 4-indolyl moiety significantly improved the antiproliferative activity, we shifted our effort to investigate SAR by replacing 4-indole with structurally similar bicyclic heterocycles. With this aim in mind, we have synthesized analogues **15e-15k**. When the 4-indolyl was enlarged to 5-quinolyl (**15e**), antiproliferative activity was markedly lost, suggesting the crucial role of the NH in 4-indolyl. Replacement of the N-PhSO₂ in **15f** with N-H (**15g**) restored the activity from micromolar range to 21 nM, which supported the significance of the free NH in 4-indoline. Analogue **15h** with a 4-oxindolyl substructure showed equipotent activity to MX-RABI and had an average IC_{50} of 13.7 nM. Adding extra nitrogen to the 4-indolyl analogue (**15b**) formed a 4-indazolyl analogue **15i**. **15i** had an average IC_{50} of 0.8 nM. It was >4-fold more cytotoxic than **15b**; its antiproliferative activity increased by approximately 18-fold compared to that of MX-RABI; its activity enhanced by nearly an order of magnitude when compared to that of ABI-231. Encouraged by this observation, we have synthesized another two analogues **15j** and **15k**. **15j** shifted the nitrogen on the 2-position of indazole to the 3-position while **15k** relocated that to the 7-position. **15j** and **15k** both were significantly less active than **15i** although showed potent activities with IC_{50} s in double-digit nanomolar range.

Discussion

RABI compounds structurally resulted from the rotation of imidazole in ABI scaffold. RABIs are potent tubulin inhibitors with antiproliferative activities in double-digit nanomolar range. In our continuing effort on improving the biological activities of RABIs, we hypothesize that replacing the benzene moiety in MX-RABI with indoles can improve its inhibitory activity.

In our initial attempt to establish the RABI scaffold, we followed the synthetic method reported previously [185] and have tried the Debus-Radziszewski imidazole synthesis as shown in **Figure 4-3**. The tested reaction involved indolyl 3-glyoxal and 3,4,5-trimethoxyphenyl glyoxal as reactants. Disappointingly, only the product with two

Table 4-1. *In vitro* growth inhibitory effects (nM) of RABI analogues (n=3)

Compound	A375	M14	RMPI7951
15a	26.8 ± 1.0	29.1 ± 1.2	49.9 ± 3.2
15b	3.2 ± 0.2	2.3 ± 0.2	5.1 ± 0.3
15c	37.9 ± 2.0	38.5 ± 3.8	85.2 ± 7.0
15d	101.4 ± 2.4	99.7 ± 3.4	134.4 ± 5.9
15e	>1000.0	>1000.0	>1000.0
15f	>1000.0	>1000.0	>1000.0
15g	16.3 ± 0.7	21.0 ± 1.7	25.7 ± 1.6
15h	12.7 ± 0.8	13.4 ± 0.6	15.0 ± 0.7
15i	0.7 ± 0.1	0.7 ± 0.1	1.1 ± 0.1
15j	34.6 ± 2.1	38.5 ± 2.4	43.1 ± 2.9
15k	18.7 ± 1.1	18.4 ± 0.8	32.0 ± 1.4
18	281.8 ± 23.7	249.1 ± 19.9	376.2 ± 65.7

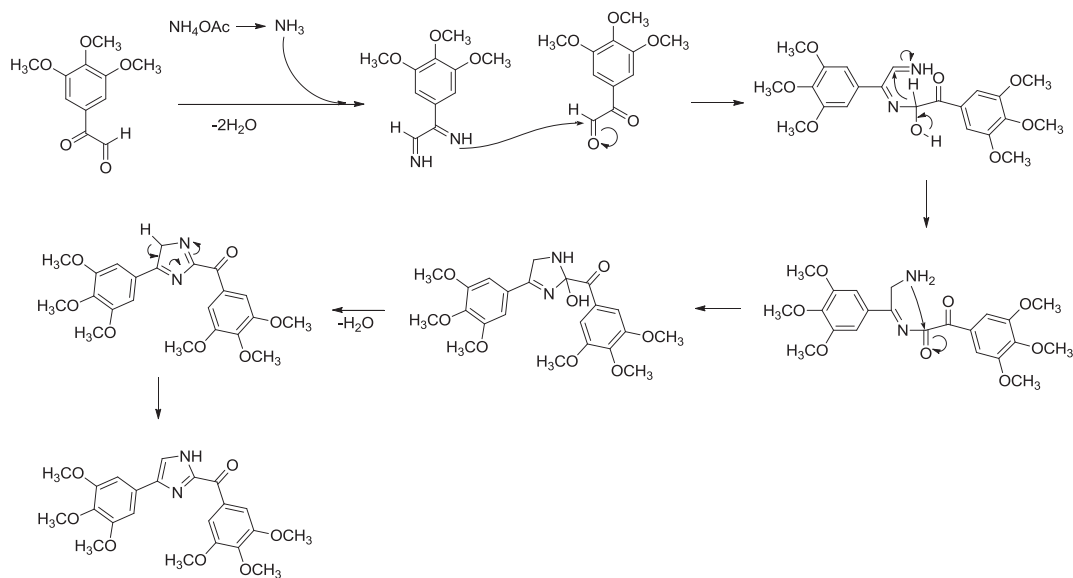
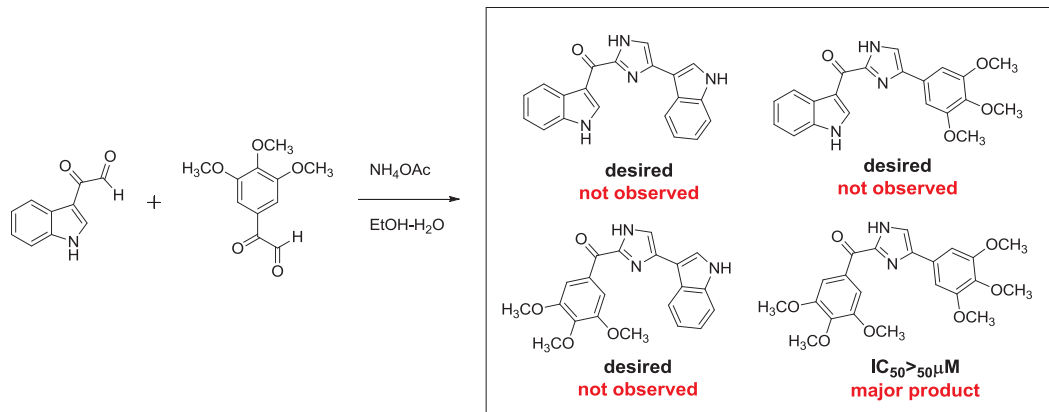


Figure 4-3. Synthesis of RABI scaffolds and proposed mechanism toward the observed major product

3,4,5-TMP moieties was observed while the other three products were absent. This might be because that (1) 3,4,5-trimethoxyphenyl glyoxal is more active than indolyl 3-glyoxal to form diimine intermediate (2) 3,4,5-trimethoxyphenyl glyoxal is more active than indolyl 3-glyoxal to react with the formed diimine intermediate. The possible mechanism is illustrated in **Figure 4-3**.

During our exploration of a synthetic method to establish ABI-231 analogues modifying the 3,4,5-TMP moiety, a reaction as depicted in **Figure 4-4** was conducted. In this reaction, we expected the occurrence of magnesium-halogen exchange to form the target product. However, the targeted product was not obtained. Instead, a moiety of the RABI scaffold was generated. The possible explanation is that the proton on the 2-position of imidazole was more susceptible (too acidic ?) than the bromo to *i*-PrMgCl(LiCl). Despite this, this unexpected reaction provided us an opportunity to investigate the SAR of MX-RABI by modifying the 3,4,5-TMP and the benzene moieties.

Among the twelve RABI analogues, **15a**, an ABI-231 based RABI analogue, showed less potent antiproliferative activity than ABI-231. According to the co-crystal structure of the 4-methyl-3-indole ABI-231 analogue reported in Chapter 2, NH on the imidazole formed an H-bond interaction with the α -Thr179 residue. The observed decreased activity in **15a** might be due to the absence of an H-bond interaction between NH on the imidazole of **15a** and the α -Thr179 residue (**Figure 4-5**). Analogues **15b** with a 4-indole moiety and **15i** with a 4-indazole moiety exhibited markedly improved anticancer activities; they had average IC₅₀s of 3.5 and 0.8 nM, respectively. Compared to MX-RABI, **15b** and **15i** displayed 4-fold and 17.5-fold improvements of antiproliferative activities, respectively. The difference in the activity of **15b** and **15i** may suggest an extra H-bond interaction is formed between nitrogen on the 2-position of indazole with nearby residue (**Figure 4-5**). We are currently exerting effort on obtaining a co-crystal structure of **15i** in complex with tubulin protein to rationalize its strong activity.

In conclusion, we have established a concise synthetic method for RABI scaffold and have synthesized twelve new RABI analogues. The most potent analogue **15i** has an average IC₅₀ of 0.8 nM. **15i** represents the first CBSI with sub-nM activity in the related scaffold.

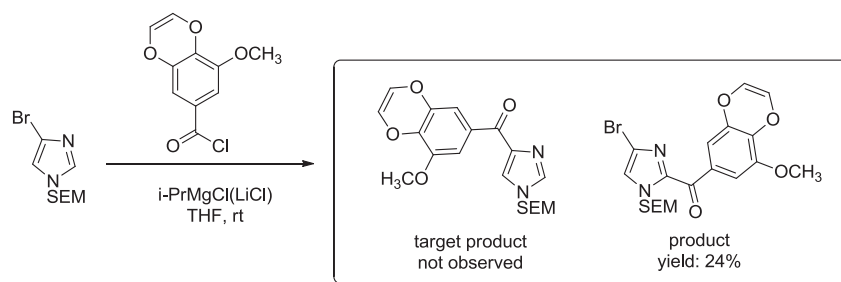


Figure 4-4. Synthesis of an intermediate for ABI-231 analogue

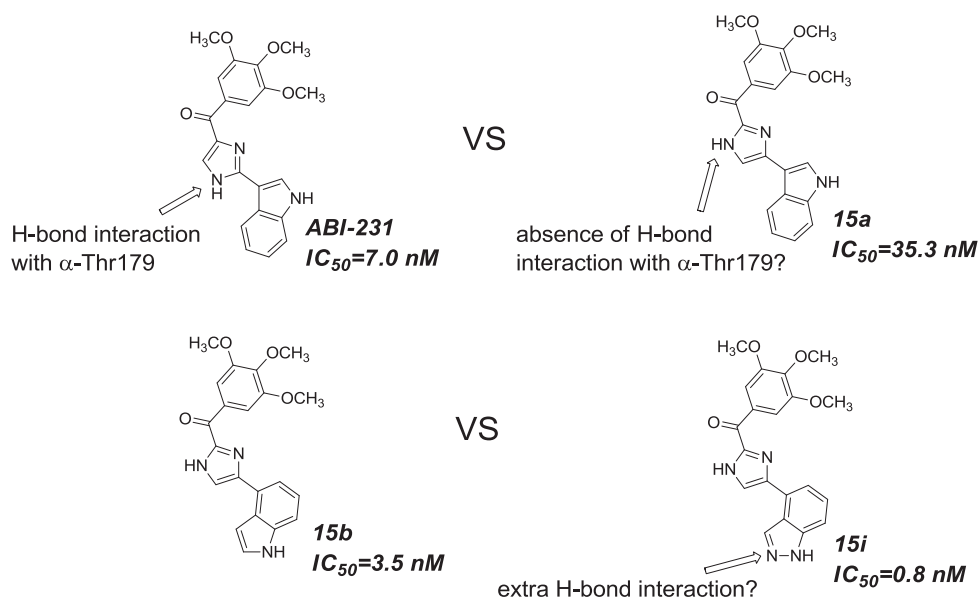


Figure 4-5. Structure and IC_{50} comparisons between ABI-231 and 15a, 15b and 15i

CHAPTER 5. DESIGN, SYNTHESIS AND STRUCTURE-ACTIVITY RELATIONSHIP STUDY OF NOVEL UC-112 ANALOGUES

Introduction

Survivin is the smallest member in the family of the Inhibitor of Apoptosis Protein (IAP). It is almost absent in healthy tissues while is highly overexpressed in tumors [105]. Survivin is therefore considered as a cancer specific biomarker [106]. Regardless of the apparent role of survivin in anti-apoptosis, the biological mechanism how survivin promotes anti-apoptosis remains debatable. On one hand, it is demonstrated that survivin can directly bind to the caspases and subsequently block their apoptotic activities [107, 108]. On the other hand, survivin is reported to exert its anti-apoptotic function by indirectly binding to caspases. Evidence has shown that survivin interacts with XIAP and HBXIP, another two members of the IAP family [109]; these interactions can protect XIAP or HBXIP from ubiquitination and thereafter block activation of caspase-9. Alternatively, survivin may bind to the mitochondrial protein SMAC to antagonized its pro-apoptotic ability [110]. Besides its role in anti-apoptosis, survivin is also responsible for multidrug resistance and radiation resistance [111, 112]. The tumor cells with high expression of survivin are shown to develop resistance more easily to cisplatin and vincristine than the tumor cells with low expression of survivin [113]. Due to its specific expression in tumor cells and important role in regulating cellular functions, survivin is regarded as a promising therapeutic target for the development of anticancer therapy [104].

Selective expression of survivin in tumor cells has been validated thus down-regulating survivin expression to treat cancer may be effective. Many strategies have been applied to block the anti-apoptotic ability of survivin. These strategies include but are not limited to introducing recombinant cell-permeable dominant-negative survivin protein [114, 115], obstructing protein translation using antisense oligonucleotides [116], and small-molecule based survivin antagonists [117, 118]. The crystal structure of human survivin was revealed in the early of this century, indicating this protein is an unusual bow tie-shape dimer [130]. Targeting survivin by employing small-molecule survivin inhibitors is challenging because no binding pocket in survivin has been identified. The challenge in developing survivin specific small-molecule inhibitor also lies in that survivin interacts with many other molecules such as P53, STAT3, caspases and notch signaling pathway to mediate apoptosis and mitosis [208-211]; it is therefore difficult to specify the drug target and evaluate the drug efficacy. A number of survivin inhibitors have been released so far, including YM155, FL118, shepherdin, 5-deazaflavin analogues, panepoxydone, terameprocol and MK2206; only YM155, LY2181308 and SPC3042 have successfully reached clinical trials [212], however, none of them has been granted an approval by the FDA. YM155 was discovered by Astellas Pharma in 2007, it has an IC_{50} in sub-nanomolar range against several types of cancer cell lines [125]. In clinical trials, YM155 was evaluated as monotherapy or combinational forms for many cancer types including blood cancer and solid tumors [213]. YM155 was withdrawn in phase II clinical trial due to its systemic toxicity.

In our previous exploration, we have disclosed the identification of [5-((benzyloxy)methyl)-7-(pyrrolidin-1-ylmethyl)quinolin-8-ol] (UC-112, the structure is shown in **Figure 5-1**) through virtual screening [126]. UC-112 is a potent and selective survivin inhibitor. UC-112 promoted apoptosis by mechanistically lowering the level of survivin protein and activating caspases 3/7 and 9. UC-112 is demonstrated to be effective for the P-gp overexpressed multidrug-resistant cancer cell lines. Subsequent SAR study of UC-112 results in MX-106 (**Figure 5-1**), which shows a significant effect in suppressing survivin expression. The *in vivo* efficacy of MX-106 to inhibit tumor growth is also demonstrated by using an A375 human melanoma xenograft model [214]. The SAR result indicates that both the 8-hydroxyquinoline and the pyrrolidine in UC-112 are essential for maximum activity; hydrophobic substituent on the benzene is beneficial to activity. Based on this SAR result, we hypothesize that (1): the benzyloxy moiety in UC-112 is amicable to modify; (2) the benzyloxy moiety is too flexible in this molecule; reducing the flexibility of the benzyloxy moiety can improve the activity (**Figure 1-8**). With these hypotheses in mind, we herein show our extensive effort on modifying the benzyloxy moiety in UC-112. Thirty-six UC-112 analogues are synthesized and evaluated for activities.

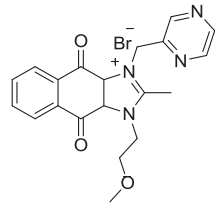
Experimental Section

General chemistry

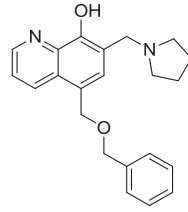
Tetrahydrofuran was distilled from sodium-benzophenone. All other solvents and chemical reagents were obtained from commercial sources and directly used without further purification. Glassware was oven-dried before use. All reactions were performed under an argon atmosphere. TLC was performed on silica gel 60 GF254 and monitored under UV light or visualized using phosphomolybdic acid reagent. Flash chromatography was performed on 230-400 mesh silica gel (Fisher Scientific). Melting points were recorded on a MPA100 Automated Melting Point Apparatus. NMR spectra were obtained on a Bruker Ascend 400 (Billerica, MA) spectrometer or a Varian Inova-500 spectrometer (Agilent Technologies, Santa Clara, CA). HR-MS were obtained on Waters Acquity UPLC linked to Waters Acquity Photodiode Array Detector and Waters Acquity Single Quadrupole Mass Detector. Chemical shifts are given in ppm with tetramethylsilane (TMS) as an internal reference. All coupling constants (*J*) are given in Hertz (Hz).

Chemical synthesis

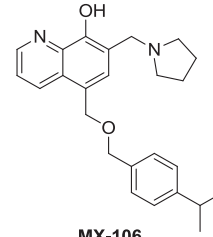
General procedure for synthesis of 1a-1g, 9a-9y. To a stirred suspension of 5-chloromethyl-8-quinolinol hydrochloride (1.0 mmol, 230 mg), sodium carbonate (6.0 mmol, 636 mg) and amine or indole (1.1 mmol) in acetonitrile (10 mL) was added



YM155



UC-112



MX-106

Figure 5-1. Example of reported survivin inhibitors

potassium iodide (0.3 mmol, 50 mg). The mixture was refluxed for 6 hr and then filtered; the residue was washed with acetonitrile. The combined solution was evaporated under vacuum to give the crude which was purified with flash chromatography on silica. Elution with hexane/ethyl acetate (10:1-1:1) gave desired compounds **1a-1g**, **9a-9g** (yield: 21-72%).

5-((5-fluoro-1H-indazol-1-yl)methyl)quinolin-8-ol (1a). ¹H NMR (400 MHz, DMSO-d₆) δ 10.08 (s, 1H), 8.87 (dd, J = 4.2, 1.5 Hz, 1H), 8.67 (dd, J = 8.6, 1.6 Hz, 1H), 8.39 (d, J = 0.9 Hz, 1H), 7.67 (ddt, J = 9.3, 4.7, 0.9 Hz, 1H), 7.64 – 7.51 (m, 2H), 7.40 (ddd, J = 9.6, 2.5, 0.7 Hz, 1H), 7.22 – 7.05 (m, 2H), 6.05 (s, 2H).

5-((1H-benzo[d][1,2,3]triazol-1-yl)methyl)quinolin-8-ol (1b). ¹H NMR (400 MHz, DMSO-d₆) δ 10.09 (s, 1H), 8.84 (dd, J = 4.1, 1.6 Hz, 1H), 8.72 (dd, J = 8.6, 1.6 Hz, 1H), 8.01 (dt, J = 8.3, 1.0 Hz, 1H), 7.80 (dt, J = 8.4, 1.0 Hz, 1H), 7.64 (d, J = 7.9 Hz, 1H), 7.59 (dd, J = 8.6, 4.2 Hz, 1H), 7.45 (ddd, J = 8.2, 6.9, 1.0 Hz, 1H), 7.32 (ddd, J = 8.1, 6.9, 1.0 Hz, 1H), 7.11 (d, J = 7.8 Hz, 1H), 6.37 (s, 2H).

1-((8-hydroxyquinolin-5-yl)methyl)-2,3-dihydroquinolin-4(1H)-one (1d). ¹H NMR (400 MHz, DMSO-d₆) δ 9.83 (s, 1H), 8.92 (dd, J = 4.2, 1.5 Hz, 1H), 8.50 (dd, J = 8.6, 1.6 Hz, 1H), 7.76 (dd, J = 7.9, 1.7 Hz, 1H), 7.63 (dd, J = 8.6, 4.1 Hz, 1H), 7.51 – 7.28 (m, 2H), 7.04 (d, J = 7.8 Hz, 1H), 6.86 (d, J = 8.6 Hz, 1H), 6.72 (t, J = 7.4 Hz, 1H), 4.95 (s, 2H), 3.54 (dd, J = 7.7, 6.2 Hz, 2H), 2.62 (dd, J = 7.8, 6.2 Hz, 2H).

5-(((1-phenyl-1H-benzo[d]imidazol-2-yl)amino)methyl)quinolin-8-ol (1e). ¹H NMR (400 MHz, Acetone-d₆) δ 8.79 (dd, J = 4.2, 1.6 Hz, 1H), 8.75 – 8.64 (m, 1H), 8.61 (dd, J = 8.6, 1.6 Hz, 1H), 7.53 – 7.41 (m, 2H), 7.34 (d, J = 7.8 Hz, 1H), 7.19 (td, J = 6.7, 5.8, 3.1 Hz, 3H), 7.12 – 7.04 (m, 3H), 7.00 (dd, J = 7.7, 2.3 Hz, 2H), 6.91 (td, J = 7.6, 1.2 Hz, 1H), 6.41 (t, J = 5.5 Hz, 1H), 5.27 (s, 2H), 5.07 (d, J = 5.1 Hz, 2H).

Tert-butyl (R)-(1-(((8-hydroxyquinolin-5-yl)methyl)amino)-1-oxo-3-(phenylthio)propan-2-yl)carbamate (1f). ¹H NMR (400 MHz, Chloroform-d) δ 8.79 (dd, J = 4.2, 1.5 Hz, 1H), 8.33 (dd, J = 8.6, 1.5 Hz, 1H), 7.46 (dd, J = 8.6, 4.2 Hz, 1H), 7.38 (d, J = 7.8 Hz, 1H), 7.26 – 7.15 (m, 5H), 7.09 (d, J = 7.8 Hz, 1H), 6.43 (s, 1H), 5.22 (s, 1H), 4.77 (d, J = 5.5 Hz, 2H), 4.19 (d, J = 6.1 Hz, 1H), 3.75 – 3.59 (m, 2H), 2.88 (dd, J = 13.9, 5.8 Hz, 1H), 2.74 (dd, J = 13.8, 6.8 Hz, 1H), 1.35 (s, 9H).

5-((1H-indol-1-yl)methyl)quinolin-8-ol (9a). ¹H NMR (400 MHz, Methanol-d₄) δ 8.68 (dd, J = 4.2, 1.6 Hz, 1H), 8.34 (dd, J = 8.6, 1.6 Hz, 1H), 7.46 (dt, J = 8.0, 1.0 Hz, 1H), 7.32 (dt, J = 8.1, 1.0 Hz, 1H), 7.30 – 7.24 (m, 2H), 7.08 (ddd, J = 8.2, 6.9, 1.1 Hz, 1H), 7.00 (d, J = 7.8 Hz, 1H), 6.96 (ddd, J = 8.0, 7.0, 1.0 Hz, 1H), 6.70 (d, J = 1.1 Hz, 1H), 4.34 (s, 2H).

5-((2-methyl-1H-indol-1-yl)methyl)quinolin-8-ol (9b). ¹H NMR (400 MHz, DMSO-d₆) δ 10.84 (s, 1H), 9.55 (s, 1H), 8.84 (dd, J = 4.1, 1.6 Hz, 1H), 8.58 (dd, J = 8.6, 1.6 Hz, 1H), 7.54 (dd, J = 8.6, 4.1 Hz, 1H), 7.27 (d, J = 8.0 Hz, 1H), 7.18 (d, J = 7.8 Hz,

1H), 7.11 (d, J = 7.9 Hz, 1H), 7.01 – 6.90 (m, 2H), 6.82 (ddd, J = 8.0, 7.0, 1.1 Hz, 1H), 4.35 (s, 2H), 2.33 (s, 3H).

5-((2-ethyl-1H-indol-1-yl)methyl)quinolin-8-ol (9c). ¹H NMR (400 MHz, Chloroform-d) δ 8.84 (s, 1H), 8.57 (d, J = 8.6 Hz, 1H), 8.30 (s, 1H), 7.96 (s, 1H), 7.59 – 7.33 (m, 3H), 7.24 – 7.00 (m, 4H), 4.46 (s, 2H), 2.75 (t, J = 7.5 Hz, 2H), 1.25 (d, J = 7.9 Hz, 3H).

5-((4-fluoro-1H-indol-1-yl)methyl)quinolin-8-ol (9d). ¹H NMR (400 MHz, DMSO-d₆) δ 11.14 (s, 1H), 9.61 (s, 1H), 8.85 (dd, J = 4.1, 1.6 Hz, 1H), 8.55 (dd, J = 8.6, 1.6 Hz, 1H), 7.55 (dd, J = 8.6, 4.1 Hz, 1H), 7.23 (dd, J = 19.3, 8.0 Hz, 2H), 7.15 – 6.95 (m, 2H), 6.88 (d, J = 2.4 Hz, 1H), 6.72 (dd, J = 11.5, 7.7 Hz, 1H), 4.50 (s, 2H).

5-((4-nitro-1H-indol-1-yl)methyl)quinolin-8-ol (9e). ¹H NMR (400 MHz, Acetone-d₆) δ 10.91 (s, 1H), 8.86 – 8.81 (m, 1H), 8.52 (dd, J = 8.5, 1.6 Hz, 1H), 7.85 (d, J = 8.1 Hz, 1H), 7.79 (d, J = 7.8 Hz, 1H), 7.54 (dd, J = 8.5, 4.1 Hz, 1H), 7.29 (t, J = 8.0 Hz, 1H), 7.15 (d, J = 7.8 Hz, 1H), 7.07 (d, J = 2.3 Hz, 1H), 7.01 (t, J = 7.3 Hz, 1H), 4.58 (s, 2H).

5-((5-fluoro-1H-indol-1-yl)methyl)quinolin-8-ol (9f). ¹H NMR (400 MHz, Chloroform-d) δ 8.76 (dd, J = 4.2, 1.5 Hz, 1H), 8.32 (dd, J = 8.5, 1.6 Hz, 1H), 7.95 (s, 1H), 7.41 – 7.33 (m, 2H), 7.30 – 7.20 (m, 2H), 7.11 (d, J = 7.7 Hz, 1H), 6.96 (td, J = 9.0, 2.5 Hz, 1H), 6.70 (dt, J = 2.4, 1.1 Hz, 1H), 4.38 (s, 2H).

5-((5-chloro-1H-indol-1-yl)methyl)quinolin-8-ol (9g). ¹H NMR (400 MHz, Chloroform-d) δ 8.79 (dd, J = 4.2, 1.5 Hz, 1H), 8.38 (s, 1H), 8.09 (dd, J = 8.6, 1.5 Hz, 1H), 7.61 (d, J = 2.0 Hz, 1H), 7.41 (dd, J = 8.5, 4.2 Hz, 1H), 7.30 (d, J = 8.7 Hz, 1H), 7.21 – 7.13 (m, 2H), 7.09 (d, J = 7.9 Hz, 1H), 6.95 (d, J = 3.2 Hz, 1H), 6.43 (dd, J = 3.2, 0.8 Hz, 1H), 5.58 (s, 2H).

1-((8-hydroxyquinolin-5-yl)methyl)-1H-indole-5-carbonitrile (9h). ¹H NMR (400 MHz, Chloroform-d) δ 8.82 (dd, J = 4.2, 1.5 Hz, 1H), 8.40 (s, 1H), 8.09 (dd, J = 8.5, 1.5 Hz, 1H), 7.99 (t, J = 1.1 Hz, 1H), 7.48 – 7.39 (m, 3H), 7.21 – 7.14 (m, 1H), 7.11 (d, J = 7.9 Hz, 1H), 7.06 (d, J = 3.3 Hz, 1H), 6.57 (d, J = 3.2 Hz, 1H), 5.65 (s, 2H).

5-((5-nitro-1H-indol-1-yl)methyl)quinolin-8-ol (9i). ¹H NMR (400 MHz, DMSO-d₆) δ 9.91 (s, 1H), 8.90 (dd, J = 4.2, 1.5 Hz, 1H), 8.61 (d, J = 2.3 Hz, 1H), 8.52 (dd, J = 8.6, 1.6 Hz, 1H), 8.03 (dd, J = 9.1, 2.4 Hz, 1H), 7.76 (d, J = 9.1 Hz, 1H), 7.70 – 7.54 (m, 2H), 7.15 – 6.93 (m, 2H), 6.80 (d, J = 3.2 Hz, 1H), 5.93 (s, 2H).

Ethyl 1-((8-hydroxyquinolin-5-yl)methyl)-1H-indole-5-carboxylate (9j). ¹H NMR (400 MHz, Acetone-d₆) δ 10.43 (s, 1H), 8.82 (dt, J = 4.2, 1.1 Hz, 1H), 8.58 (dt, J = 8.6, 1.1 Hz, 1H), 8.35 (d, J = 1.5 Hz, 1H), 7.84 (dd, J = 8.8, 1.6 Hz, 1H), 7.53 (dd, J = 8.6, 4.3 Hz, 1H), 7.48 (d, J = 8.6 Hz, 1H), 7.44 (d, J = 7.7 Hz, 1H), 7.10 (d, J = 7.8 Hz, 1H), 7.04 (d, J = 1.3 Hz, 1H), 4.63 – 4.41 (m, 2H), 4.33 (dd, J = 7.1, 0.8 Hz, 2H), 1.36 (td, J = 7.1, 0.8 Hz, 3H).

5-((6-fluoro-1H-indol-1-yl)methyl)quinolin-8-ol (9k). ¹H NMR (400 MHz, Chloroform-d) δ 8.80 (dd, J = 4.2, 1.5 Hz, 1H), 8.44 (s, 1H), 8.12 (dd, J = 8.5, 1.5 Hz, 1H), 7.57 (dd, J = 8.7, 5.4 Hz, 1H), 7.42 (dd, J = 8.6, 4.2 Hz, 1H), 7.21 – 7.15 (m, 1H), 7.11 (d, J = 7.8 Hz, 1H), 7.07 (dd, J = 9.8, 2.3 Hz, 1H), 6.96 – 6.89 (m, 2H), 6.48 (dd, J = 3.2, 0.9 Hz, 1H), 5.54 (s, 2H).

5-((6-chloro-1H-indol-1-yl)methyl)quinolin-8-ol (9l). ¹H NMR (400 MHz, Methanol-d₄) δ 8.77 (dd, J = 4.2, 1.6 Hz, 1H), 8.46 (dd, J = 8.6, 1.6 Hz, 1H), 7.46 – 7.40 (m, 2H), 7.36 – 7.30 (m, 2H), 7.04 (d, J = 7.8 Hz, 1H), 6.95 (dd, J = 8.5, 1.9 Hz, 1H), 6.80 (d, J = 1.1 Hz, 1H), 4.43 (s, 2H).

5-((6-bromo-1H-indol-1-yl)methyl)quinolin-8-ol (9m). ¹H NMR (400 MHz, Chloroform-d) δ 8.80 (dd, J = 4.2, 1.5 Hz, 1H), 8.38 (dd, J = 8.4, 1.8 Hz, 1H), 8.09 (dd, J = 8.5, 1.5 Hz, 1H), 7.56 (dt, J = 1.5, 0.6 Hz, 1H), 7.53 – 7.48 (m, 1H), 7.41 (dd, J = 8.6, 4.2 Hz, 1H), 7.25 – 7.22 (m, 1H), 7.17 – 7.12 (m, 1H), 7.09 (d, J = 7.8 Hz, 1H), 6.88 (d, J = 3.3 Hz, 1H), 6.45 (dd, J = 3.2, 0.9 Hz, 1H), 5.54 (s, 2H).

5-((6-nitro-1H-indol-1-yl)methyl)quinolin-8-ol (9n). ¹H NMR (400 MHz, Chloroform-d) δ 8.74 (ddt, J = 7.8, 3.6, 1.8 Hz, 1H), 8.47 – 8.14 (m, 1H), 7.46 – 7.20 (m, 3H), 7.09 (ddd, J = 9.8, 7.7, 3.0 Hz, 1H), 6.97 (dddd, J = 9.5, 7.8, 4.7, 2.3 Hz, 1H), 6.92 – 6.82 (m, 1H), 6.71 – 6.64 (m, 1H), 4.49 – 4.33 (m, 2H).

5-((6-methoxy-1H-indol-1-yl)methyl)quinolin-8-ol (9o). ¹H NMR (400 MHz, Chloroform-d) δ 8.75 (dd, J = 4.2, 1.5 Hz, 1H), 8.35 (dd, J = 8.5, 1.5 Hz, 1H), 7.78 (s, 1H), 7.46 (d, J = 8.7 Hz, 1H), 7.40 – 7.34 (m, 2H), 7.10 (d, J = 7.8 Hz, 1H), 6.86 (d, J = 2.1 Hz, 1H), 6.79 (dd, J = 8.6, 2.3 Hz, 1H), 6.54 (dt, J = 2.3, 1.2 Hz, 1H), 4.40 (s, 2H), 3.85 (s, 3H).

5-((7-fluoro-1H-indol-1-yl)methyl)quinolin-8-ol (9p). ¹H NMR (400 MHz, Chloroform-d) δ 8.83 (dd, J = 4.2, 1.5 Hz, 1H), 8.45 (dd, J = 1.8, 1.0 Hz, 1H), 8.08 (ddd, J = 15.1, 8.7, 1.8 Hz, 2H), 7.70 (dd, J = 8.8, 0.5 Hz, 1H), 7.46 (dd, J = 8.6, 4.2 Hz, 1H), 7.25 – 7.21 (m, 1H), 7.19 (d, J = 3.2 Hz, 1H), 7.13 (d, J = 7.9 Hz, 1H), 6.59 (dd, J = 3.2, 0.9 Hz, 1H), 5.71 (d, J = 0.9 Hz, 2H).

5-((7-methyl-1H-indol-1-yl)methyl)quinolin-8-ol (9q). ¹H NMR (400 MHz, Acetone-d₆) δ 9.97 (s, 1H), 8.80 (dd, J = 4.2, 1.6 Hz, 1H), 8.65 (s, 1H), 8.55 (dd, J = 8.5, 1.6 Hz, 1H), 7.49 (dd, J = 8.6, 4.2 Hz, 1H), 7.42 (d, J = 7.7 Hz, 2H), 7.09 (d, J = 7.9 Hz, 1H), 7.05 – 6.78 (m, 3H), 4.47 (s, 2H), 2.49 (s, 3H).

5-((2,3-dimethyl-1H-indol-1-yl)methyl)quinolin-8-ol (9r). ¹H NMR (400 MHz, Chloroform-d) δ 8.86 (dd, J = 4.2, 1.5 Hz, 1H), 8.40 (dd, J = 8.5, 1.5 Hz, 1H), 7.66 – 7.51 (m, 2H), 7.22 – 7.06 (m, 3H), 6.95 (d, J = 7.9 Hz, 1H), 6.55 – 6.38 (m, 1H), 5.62 (d, J = 1.2 Hz, 2H), 2.35 (s, 3H), 2.27 (s, 3H).

5-((5-methoxy-2-methyl-1H-indol-1-yl)methyl)quinolin-8-ol (9s). ¹H NMR (400 MHz, DMSO-d₆) δ 10.70 (s, 1H), 9.60 (s, 1H), 8.86 (dd, J = 4.1, 1.6 Hz, 1H), 8.60 (dd, J = 8.6, 1.6 Hz, 1H), 7.56 (dd, J = 8.6, 4.2 Hz, 1H), 7.17 (dd, J = 15.5, 8.3 Hz, 2H), 7.01 (d, J = 7.8 Hz, 1H), 6.71 (d, J = 2.4 Hz, 1H), 6.64 (dd, J = 8.7, 2.4 Hz, 1H), 4.34 (s, 2H), 3.61 (s, 3H), 2.31 (s, 3H).

5-((2-ethyl-5-fluoro-1H-indol-1-yl)methyl)quinolin-8-ol (9t). ¹H NMR (400 MHz, Acetone-d₆) δ 10.97 (s, 1H), 8.84 (dd, J = 4.2, 1.5 Hz, 1H), 8.76 (dd, J = 8.6, 1.5 Hz, 1H), 8.61 (s, 1H), 7.60 (dd, J = 8.6, 4.2 Hz, 1H), 7.55 (ddd, J = 8.9, 4.5, 0.7 Hz, 1H), 7.19 (dt, J = 7.9, 1.1 Hz, 1H), 7.15 – 7.10 (m, 1H), 7.10 – 7.05 (m, 1H), 7.03 (d, J = 7.9 Hz, 1H), 4.92 (d, J = 1.0 Hz, 2H), 4.36 (q, J = 7.1 Hz, 2H), 1.26 (t, J = 7.1 Hz, 3H).

1-((8-hydroxyquinolin-5-yl)methyl)-6-methoxy-1H-indole-3-carbonitrile (9u). ¹H NMR (400 MHz, DMSO-d₆) δ 10.72 (s, 1H), 9.74 (s, 1H), 8.86 (dd, J = 4.1, 1.5 Hz, 1H), 8.53 (dd, J = 8.5, 1.5 Hz, 1H), 7.57 (dd, J = 8.6, 4.1 Hz, 1H), 7.44 (d, J = 8.6 Hz, 1H), 7.19 (d, J = 7.9 Hz, 1H), 7.05 (d, J = 7.8 Hz, 1H), 6.81 (d, J = 2.3 Hz, 1H), 6.71 (dd, J = 8.6, 2.3 Hz, 1H), 4.48 (s, 2H), 3.73 (s, 3H).

5-((4,5-difluoro-1H-indol-1-yl)methyl)quinolin-8-ol (9v). ¹H NMR (400 MHz, DMSO-d₆) δ 10.97 (s, 1H), 9.58 (s, 1H), 8.83 (dd, J = 4.0, 1.6 Hz, 1H), 8.53 (dd, J = 8.6, 1.6 Hz, 1H), 7.52 (dd, J = 8.6, 4.1 Hz, 1H), 7.43 (dd, J = 11.5, 8.0 Hz, 1H), 7.38 (d, J = 7.8 Hz, 1H), 7.32 (dd, J = 11.3, 7.0 Hz, 1H), 7.06 (d, J = 2.4 Hz, 1H), 7.02 (d, J = 7.8 Hz, 1H), 4.37 (s, 2H).

5-((5,6-difluoro-1H-indol-1-yl)methyl)quinolin-8-ol (9w). ¹H NMR (400 MHz, Acetone-d₆) δ 10.24 (s, 1H), 8.79 (dd, J = 4.2, 1.6 Hz, 1H), 8.52 (dd, J = 8.6, 1.6 Hz, 1H), 7.48 (dd, J = 8.6, 4.2 Hz, 1H), 7.44 – 7.35 (m, 2H), 7.31 (dd, J = 11.2, 7.0 Hz, 1H), 7.08 (d, J = 7.8 Hz, 1H), 7.05 – 6.99 (m, 1H), 4.43 (d, J = 1.0 Hz, 2H).

5-((6-chloro-5-fluoro-1H-indol-1-yl)methyl)quinolin-8-ol (9x). ¹H NMR (400 MHz, Acetone-d₆) δ 10.28 (s, 1H), 8.80 (dd, J = 4.2, 1.6 Hz, 1H), 8.53 (dd, J = 8.6, 1.6 Hz, 1H), 7.54 – 7.47 (m, 2H), 7.41 (t, J = 8.6 Hz, 2H), 7.12 – 7.05 (m, 2H), 4.45 (s, 2H).

5-((5,6-dichloro-1H-indol-1-yl)methyl)quinolin-8-ol (9y). ¹H NMR (400 MHz, DMSO-d₆) δ 11.30 – 10.99 (m, 1H), 9.63 (s, 1H), 8.84 (dd, J = 4.1, 1.4 Hz, 1H), 8.52 (dd, J = 8.5, 1.6 Hz, 1H), 7.72 (s, 1H), 7.60 (s, 1H), 7.53 (dd, J = 8.5, 4.1 Hz, 1H), 7.37 (d, J = 7.8 Hz, 1H), 7.13 (d, J = 2.3 Hz, 1H), 7.04 (d, J = 7.7 Hz, 1H), 4.40 (s, 2H).

General procedure for synthesis of 2a-2f, 6a-6f, 8 and 10a-10y. To a stirred suspension of **1a-1g** or **5a-5g** or **7** or **9a-9y** (0.5 mmol) and paraformaldehyde (0.5 mmol, 15 mg) in ethanol (6 mL) was added pyrrolidine (0.45 mmol, 32 mg). The mixture was refluxed for 1-5 hr and solvent was evaporated under reduced pressure to give the crude which was purified with flash chromatography on silica. Elution with dichloromethane-methanol (10:0-10:1) gave desired compounds **2a-2f, 6a-6f, 8 and 10a-10y** (34-81% yield).

5-((5-fluoro-1H-indazol-1-yl)methyl)-7-(pyrrolidin-1-ylmethyl)quinolin-8-ol (2a). ¹H NMR (400 MHz, Chloroform-d) δ 8.84 (dd, J = 4.1, 1.6 Hz, 1H), 8.74 (dd, J = 4.2, 1.7 Hz, 1H), 8.19 (dd, J = 8.6, 1.6 Hz, 1H), 7.68 (ddt, J = 9.2, 4.6, 1.0 Hz, 1H), 7.64 (d, J = 0.9 Hz, 1H), 7.38 – 7.29 (m, 2H), 7.10 – 6.99 (m, 2H), 5.87 (s, 2H), 4.02 (s, 2H), 2.84 – 2.62 (m, 4H), 1.88 (p, J = 3.3 Hz, 4H).

5-((1H-benzo[d][1,2,3]triazol-1-yl)methyl)-7-(pyrrolidin-1-ylmethyl)quinolin-8-ol (2b). ¹H NMR (400 MHz, Chloroform-d) δ 10.42 (s, 1H), 8.78 (dd, J = 4.2, 1.6 Hz, 1H), 8.44 (dd, J = 8.6, 1.6 Hz, 1H), 7.96 (dt, J = 7.9, 1.2 Hz, 1H), 7.44 – 7.17 (m, 5H), 6.11 (s, 2H), 3.95 (s, 2H), 2.64 (td, J = 5.6, 4.5, 2.3 Hz, 4H), 1.81 (p, J = 3.4 Hz, 4H).

5-((6-chloro-9H-purin-9-yl)methyl)-7-(pyrrolidin-1-ylmethyl)quinolin-8-ol (2c). ¹H NMR (400 MHz, Chloroform-d) δ 8.83 (s, 1H), 8.79 (dd, J = 4.2, 1.5 Hz, 1H), 8.69 (s, 1H), 8.60 (dd, J = 8.6, 1.5 Hz, 1H), 8.46 (s, 1H), 7.49 (dd, J = 8.6, 4.2 Hz, 1H), 5.80 (s, 2H), 4.45 (s, 2H), 3.30 (s, 4H), 2.16 – 2.11 (m, 4H).

1-((8-hydroxy-7-(pyrrolidin-1-ylmethyl)quinolin-5-yl)methyl)-2,3-dihydroquinolin-4(1H)-one (2d). ¹H NMR (400 MHz, Chloroform-d) δ 8.95 (d, J = 4.1 Hz, 1H), 8.31 (dd, J = 8.5, 2.2 Hz, 1H), 8.05 – 7.96 (m, 1H), 7.50 – 7.37 (m, 2H), 7.23 (s, 1H), 6.93 – 6.78 (m, 2H), 4.82 (s, 2H), 4.01 (d, J = 1.9 Hz, 2H), 3.46 (t, J = 6.7 Hz, 2H), 2.73 (d, J = 6.1 Hz, 4H), 2.65 (t, J = 6.9 Hz, 2H), 1.90 (p, J = 3.3, 2.6 Hz, 4H).

5-(((1-phenyl-1H-benzo[d]imidazol-2-yl)amino)methyl)-7-(pyrrolidin-1-ylmethyl)quinolin-8-ol (2e). ¹H NMR (400 MHz, Chloroform-d) δ 8.84 (dd, J = 4.2, 1.6 Hz, 1H), 8.21 (dd, J = 8.5, 1.6 Hz, 1H), 7.60 (dt, J = 7.8, 0.9 Hz, 1H), 7.29 (dd, J = 8.5, 4.1 Hz, 1H), 7.19 (ddd, J = 9.9, 5.3, 2.3 Hz, 5H), 7.12 – 7.07 (m, 2H), 7.06 – 7.01 (m, 2H), 5.05 (s, 2H), 5.01 – 4.92 (m, 2H), 4.21 (s, 1H), 3.96 (s, 2H), 2.81 – 2.58 (m, 4H), 1.88 (p, J = 3.3 Hz, 4H).

Tert-butyl (R)-(1-(((8-hydroxy-7-(pyrrolidin-1-ylmethyl)quinolin-5-yl)methyl)amino)-1-oxo-3-(phenylthio)propan-2-yl)carbamate (2f). ¹H NMR (400 MHz, Chloroform-d) δ 8.81 (s, 1H), 8.41 (d, J = 8.6 Hz, 1H), 7.88 (s, 1H), 7.52 (s, 1H), 7.32 – 7.07 (m, 5H), 5.96 (s, 1H), 4.97 (s, 1H), 4.68 (d, J = 15.4 Hz, 1H), 4.47 (s, 1H), 4.39 – 4.16 (m, 2H), 3.75 (d, J = 2.0 Hz, 2H), 3.21 (s, 4H), 3.03 – 2.88 (m, 2H), 2.10 (s, 4H), 1.41 (s, 9H).

N-((8-hydroxy-7-(pyrrolidin-1-ylmethyl)quinolin-5-yl)methyl)-2-(3,4,5-trimethoxyphenyl)acetamide (6a). ¹H NMR (400 MHz, Methanol-d₄) δ 8.78 (d, J = 4.1 Hz, 1H), 8.33 (d, J = 8.3 Hz, 1H), 7.40 (dd, J = 8.5, 4.2 Hz, 1H), 7.31 (s, 1H), 6.55 (s, 2H), 4.74 (s, 1H), 3.97 (s, 2H), 3.75 (s, 3H), 3.70 (s, 6H), 3.45 (s, 2H), 3.37 (d, J = 1.7 Hz, 2H), 2.72 (s, 4H), 1.89 (s, 4H).

N-((8-hydroxy-7-(pyrrolidin-1-ylmethyl)quinolin-5-yl)methyl)-2-(4-nitrophenyl)acetamide (6b). ¹H NMR (400 MHz, DMSO-d₆) δ 8.85 (dd, J = 4.1, 1.5 Hz, 1H), 8.66 (t, J = 5.6 Hz, 1H), 8.37 (dd, J = 8.5, 1.6 Hz, 1H), 8.23 – 8.12 (m, 2H), 7.60 –

7.47 (m, 3H), 7.39 (s, 1H), 4.64 (d, J = 5.5 Hz, 2H), 3.78 (s, 2H), 3.64 (s, 2H), 2.51 (dt, J = 3.7, 1.8 Hz, 4H), 1.73 (p, J = 3.0 Hz, 4H).

2-(4-fluorophenyl)-N-((8-hydroxy-7-(pyrrolidin-1-ylmethyl)quinolin-5-yl)methyl)acetamide (6c). ¹H NMR (400 MHz, DMSO-d₆) δ 8.92 (dd, J = 4.1, 1.5 Hz, 1H), 8.60 (t, J = 5.5 Hz, 1H), 8.43 (dd, J = 8.6, 1.6 Hz, 1H), 7.70 – 7.49 (m, 2H), 7.36 – 7.23 (m, 2H), 7.18 – 7.04 (m, 2H), 4.63 (d, J = 5.5 Hz, 2H), 4.25 (s, 2H), 3.47 (s, 2H), 3.04 (s, 4H), 1.89 (p, J = 3.4 Hz, 4H).

N-((8-hydroxy-7-(pyrrolidin-1-ylmethyl)quinolin-5-yl)methyl)-2-(4-(trifluoromethyl)phenyl)acetamide (6d). ¹H NMR (400 MHz, Chloroform-d) δ 8.86 (dd, J = 4.1, 1.6 Hz, 1H), 8.20 (dd, J = 8.6, 1.6 Hz, 1H), 7.61 – 7.51 (m, 2H), 7.44 – 7.30 (m, 3H), 7.15 (s, 1H), 5.76 (s, 1H), 4.75 (d, J = 5.4 Hz, 2H), 3.95 (s, 2H), 3.61 (s, 2H), 2.71 (td, J = 5.4, 4.4, 2.3 Hz, 4H), 1.88 (p, J = 3.3 Hz, 4H).

N-(8-hydroxy-7-(pyrrolidin-1-ylmethyl)quinolin-5-yl)-2-(4-nitrophenyl)acetamide (6e). ¹H NMR (400 MHz, Methanol-d₄) δ 8.93 (dd, J = 4.2, 1.6 Hz, 1H), 8.34 (dd, J = 8.6, 1.6 Hz, 1H), 8.32 – 8.22 (m, 2H), 7.80 – 7.67 (m, 5H), 7.64 (dd, J = 8.6, 4.2 Hz, 1H), 7.60 (s, 1H), 7.40 – 7.29 (m, 3H), 4.58 (s, 2H), 4.02 (s, 2H), 3.49 – 3.40 (m, 4H), 3.37 (s, 1H), 2.11 (p, J = 4.0 Hz, 4H).

N-(8-hydroxy-7-(pyrrolidin-1-ylmethyl)quinolin-5-yl)-2-(4-(trifluoromethyl)phenyl)acetamide (6f). ¹H NMR (400 MHz, Methanol-d₄) δ 8.88 (dd, J = 4.2, 1.6 Hz, 1H), 8.27 (dd, J = 8.5, 1.6 Hz, 1H), 7.68 (q, J = 8.4 Hz, 4H), 7.62 – 7.52 (m, 2H), 7.49 (d, J = 3.3 Hz, 2H), 4.33 (s, 2H), 3.95 (s, 2H), 3.57 (s, 1H), 3.19 – 3.05 (m, 4H), 2.07 – 1.94 (m, 4H).

1-(4-bromobenzyl)-3-((8-hydroxy-7-(pyrrolidin-1-ylmethyl)quinolin-5-yl)methyl)urea (8). ¹H NMR (400 MHz, Methanol-d₄) δ 8.83 (dd, J = 4.2, 1.6 Hz, 1H), 8.50 (dd, J = 8.6, 1.6 Hz, 1H), 7.53 (dd, J = 8.6, 4.2 Hz, 1H), 7.50 – 7.41 (m, 2H), 7.35 (s, 1H), 7.29 – 7.14 (m, 2H), 4.71 (s, 2H), 4.32 (s, 2H), 4.06 (s, 2H), 3.00 – 2.64 (m, 4H), 1.92 (p, J = 3.3 Hz, 4H).

5-((1H-indol-1-yl)methyl)-7-(pyrrolidin-1-ylmethyl)quinolin-8-ol (10a). ¹H NMR (400 MHz, Acetone-d₆) δ 9.88 (s, 1H), 8.63 (dd, J = 4.1, 1.5 Hz, 1H), 8.37 (dd, J = 8.6, 1.6 Hz, 1H), 7.43 (dt, J = 7.9, 1.0 Hz, 1H), 7.39 (s, 1H), 7.30 (dd, J = 8.5, 4.1 Hz, 1H), 7.23 (dt, J = 8.1, 0.9 Hz, 1H), 6.94 (ddd, J = 8.2, 7.1, 1.2 Hz, 1H), 6.84 (ddd, J = 8.0, 7.0, 1.0 Hz, 1H), 6.79 (p, J = 1.1 Hz, 1H), 4.33 (s, 2H), 3.73 (s, 2H), 2.48 – 2.35 (m, 4H), 1.61 (p, J = 3.2 Hz, 4H).

5-((2-methyl-1H-indol-1-yl)methyl)-7-(pyrrolidin-1-ylmethyl)quinolin-8-ol (10b). ¹H NMR (400 MHz, Chloroform-d) δ 10.51 (s, 1H), 9.06 – 8.84 (m, 1H), 8.70 – 8.31 (m, 2H), 7.55 – 7.25 (m, 3H), 7.21 – 7.08 (m, 1H), 7.01 (t, J = 7.5 Hz, 1H), 6.96 (s, 1H), 4.39 (s, 2H), 3.86 (s, 2H), 2.63 (d, J = 6.1 Hz, 4H), 1.99 – 1.64 (m, 4H).

5-((2-ethyl-1H-indol-1-yl)methyl)-7-(pyrrolidin-1-ylmethyl)quinolin-8-ol (10c). ¹H NMR (400 MHz, Chloroform-d) δ 8.90 (dd, J = 4.2, 1.5 Hz, 1H), 8.46 (dd, J = 8.6, 1.5 Hz, 1H), 8.15 (s, 1H), 7.39 (dd, J = 8.5, 4.1 Hz, 1H), 7.34 (dt, J = 8.0, 1.3 Hz, 2H), 7.17 – 7.10 (m, 1H), 7.05 – 6.99 (m, 1H), 6.95 (s, 1H), 4.42 (s, 2H), 3.88 (s, 2H), 2.73 – 2.61 (m, 6H), 1.84 (h, J = 3.2 Hz, 4H), 1.19 (t, J = 7.6 Hz, 3H).

5-((4-fluoro-1H-indol-1-yl)methyl)-7-(pyrrolidin-1-ylmethyl)quinolin-8-ol (10d). ¹H NMR (400 MHz, Chloroform-d) δ 8.75 (dd, J = 4.1, 1.6 Hz, 1H), 8.35 – 8.24 (m, 1H), 8.22 (d, J = 16.3 Hz, 1H), 7.26 (dd, J = 8.5, 4.1 Hz, 1H), 7.19 (d, J = 4.0 Hz, 2H), 7.14 – 6.96 (m, 2H), 6.69 (ddd, J = 11.2, 7.4, 1.3 Hz, 1H), 6.43 (s, 1H), 4.48 (s, 2H), 3.98 (s, 2H), 2.75 (t, J = 5.3 Hz, 4H), 1.83 (p, J = 3.3 Hz, 4H).

5-((4-nitro-1H-indol-1-yl)methyl)-7-(pyrrolidin-1-ylmethyl)quinolin-8-ol (10e). ¹H NMR (400 MHz, Chloroform-d) δ 9.42 (s, 1H), 8.71 (dd, J = 4.1, 1.6 Hz, 1H), 8.15 (dd, J = 8.5, 1.6 Hz, 1H), 7.76 (dd, J = 7.9, 0.9 Hz, 1H), 7.56 (dd, J = 8.1, 0.9 Hz, 1H), 7.23 – 7.16 (m, 2H), 7.13 (t, J = 8.0 Hz, 1H), 6.98 (s, 1H), 6.50 (s, 1H), 4.43 (s, 2H), 3.86 (s, 2H), 2.60 (q, J = 5.0, 4.0 Hz, 4H), 1.75 (p, J = 3.2 Hz, 4H).

5-((5-fluoro-1H-indol-1-yl)methyl)-7-(pyrrolidin-1-ylmethyl)quinolin-8-ol (10f). ¹H NMR (400 MHz, Methanol-d₄) δ 8.76 (dd, J = 4.2, 1.6 Hz, 1H), 8.47 (dd, J = 8.6, 1.6 Hz, 1H), 7.43 (dd, J = 8.6, 4.2 Hz, 1H), 7.33 – 7.24 (m, 2H), 7.09 (dd, J = 9.9, 2.5 Hz, 1H), 6.88 (s, 1H), 6.83 (td, J = 9.1, 2.5 Hz, 1H), 4.41 (s, 2H), 3.98 (s, 2H), 2.79 – 2.62 (m, 4H), 1.86 (p, J = 3.3 Hz, 4H).

5-((5-chloro-1H-indol-1-yl)methyl)-7-(pyrrolidin-1-ylmethyl)quinolin-8-ol (10g). ¹H NMR (400 MHz, Chloroform-d) δ 8.89 (dd, J = 4.1, 1.6 Hz, 1H), 8.05 (dd, J = 8.5, 1.6 Hz, 1H), 7.62 (dd, J = 2.1, 0.5 Hz, 1H), 7.35 (dd, J = 8.6, 4.1 Hz, 1H), 7.31 (dt, J = 8.7, 0.7 Hz, 1H), 7.17 (dd, J = 8.7, 2.0 Hz, 1H), 6.97 – 6.91 (m, 2H), 6.43 (dd, J = 3.2, 0.8 Hz, 1H), 5.58 (d, J = 0.8 Hz, 2H), 3.93 (s, 2H), 2.67 (d, J = 6.3 Hz, 4H), 1.87 (p, J = 3.3 Hz, 4H).

1-((8-hydroxy-7-(pyrrolidin-1-ylmethyl)quinolin-5-yl)methyl)-1H-indole-5-carbonitrile (10h). ¹H NMR (400 MHz, Chloroform-d) δ 8.90 (dd, J = 4.2, 1.6 Hz, 1H), 8.05 – 7.98 (m, 2H), 7.46 (d, J = 1.1 Hz, 2H), 7.37 (dd, J = 8.6, 4.1 Hz, 1H), 7.05 (d, J = 3.3 Hz, 1H), 6.97 (s, 1H), 6.57 (d, J = 3.3 Hz, 1H), 5.63 (d, J = 0.8 Hz, 2H), 3.95 (s, 2H), 2.78 – 2.59 (m, 4H), 1.88 (p, J = 3.3 Hz, 4H).

5-((5-nitro-1H-indol-1-yl)methyl)-7-(pyrrolidin-1-ylmethyl)quinolin-8-ol (10i). ¹H NMR (400 MHz, Chloroform-d) δ 10.95 (s, 1H), 8.90 (dd, J = 4.1, 1.6 Hz, 1H), 8.59 (d, J = 2.2 Hz, 1H), 8.11 (dd, J = 9.1, 2.2 Hz, 1H), 8.03 (dd, J = 8.6, 1.6 Hz, 1H), 7.43 (d, J = 9.1 Hz, 1H), 7.36 (dd, J = 8.6, 4.1 Hz, 1H), 7.08 (d, J = 3.3 Hz, 1H), 6.97 (s, 1H), 6.66 (dd, J = 3.3, 0.8 Hz, 1H), 5.71 – 5.52 (m, 2H), 3.94 (s, 2H), 2.68 (td, J = 5.8, 4.9, 2.5 Hz, 4H), 1.94 – 1.77 (m, 4H).

Ethyl 1-((8-hydroxy-7-(pyrrolidin-1-ylmethyl)quinolin-5-yl)methyl)-1H-indole-5-carboxylate (10j). ¹H NMR (400 MHz, Chloroform-d) δ 10.22 (s, 1H), 9.53 (s,

1H), 8.82 (dd, J = 4.1, 1.5 Hz, 1H), 8.43 (d, J = 1.5 Hz, 1H), 8.25 (dd, J = 8.6, 1.6 Hz, 1H), 7.91 (dd, J = 8.6, 1.6 Hz, 1H), 7.35 (d, J = 8.6 Hz, 1H), 7.33 – 7.25 (m, 1H), 7.15 (s, 1H), 6.64 (s, 1H), 4.86 – 4.35 (m, 4H), 3.94 (s, 2H), 2.68 (d, J = 6.1 Hz, 4H), 2.15 – 1.72 (m, 4H), 1.42 (t, J = 7.1 Hz, 3H).

5-((6-fluoro-1H-indol-1-yl)methyl)-7-(pyrrolidin-1-ylmethyl)quinolin-8-ol (10k). ¹H NMR (400 MHz, Chloroform-d) δ 8.89 (dd, J = 4.1, 1.6 Hz, 1H), 8.06 (dd, J = 8.6, 1.6 Hz, 1H), 7.55 (dd, J = 8.7, 5.4 Hz, 1H), 7.35 (dd, J = 8.6, 4.1 Hz, 1H), 7.07 (dd, J = 10.0, 2.3 Hz, 1H), 6.98 (s, 1H), 6.94 – 6.84 (m, 2H), 6.46 (dd, J = 3.3, 0.9 Hz, 1H), 5.52 (s, 2H), 3.94 (s, 2H), 2.84 – 2.54 (m, 4H), 1.87 (p, J = 3.3 Hz, 4H).

5-((6-chloro-1H-indol-1-yl)methyl)-7-(pyrrolidin-1-ylmethyl)quinolin-8-ol (10l). ¹H NMR (400 MHz, Chloroform-d) δ 8.89 (dd, J = 4.2, 1.6 Hz, 1H), 8.06 (dd, J = 8.6, 1.6 Hz, 1H), 7.55 (dd, J = 8.5, 0.6 Hz, 1H), 7.44 – 7.33 (m, 2H), 7.19 – 7.03 (m, 2H), 6.93 (d, J = 3.2 Hz, 1H), 6.46 (dd, J = 3.3, 0.9 Hz, 1H), 5.56 (d, J = 0.8 Hz, 2H), 4.03 (s, 2H), 2.79 (s, 4H), 1.91 (s, 4H).

5-((6-bromo-1H-indol-1-yl)methyl)-7-(pyrrolidin-1-ylmethyl)quinolin-8-ol (10m). ¹H NMR (400 MHz, Chloroform-d) δ 10.37 (s, 1H), 8.88 (dd, J = 4.1, 1.6 Hz, 1H), 8.02 (dd, J = 8.5, 1.6 Hz, 1H), 7.60 – 7.53 (m, 1H), 7.50 (d, J = 8.4 Hz, 1H), 7.34 (dd, J = 8.5, 4.1 Hz, 1H), 7.23 (dd, J = 8.4, 1.7 Hz, 1H), 6.95 (s, 1H), 6.87 (d, J = 3.2 Hz, 1H), 6.44 (dd, J = 3.3, 0.9 Hz, 1H), 5.51 (s, 2H), 3.93 (s, 2H), 2.68 (p, J = 3.9, 3.5 Hz, 4H), 1.86 (p, J = 3.3 Hz, 4H).

5-((6-nitro-1H-indol-1-yl)methyl)-7-(pyrrolidin-1-ylmethyl)quinolin-8-ol (10n). ¹H NMR (400 MHz, Chloroform-d) δ 9.54 (s, 1H), 8.91 (dd, J = 4.1, 1.6 Hz, 1H), 8.44 (d, J = 1.9 Hz, 1H), 8.03 (ddd, J = 10.6, 8.7, 1.8 Hz, 2H), 7.68 (d, J = 8.8 Hz, 1H), 7.36 (dd, J = 8.5, 4.1 Hz, 1H), 7.18 (d, J = 3.1 Hz, 1H), 7.07 (s, 1H), 6.57 (dd, J = 3.2, 0.9 Hz, 1H), 5.68 (s, 2H), 3.97 (s, 2H), 2.80 – 2.58 (m, 4H), 1.88 (p, J = 3.3 Hz, 4H).

5-((6-methoxy-1H-indol-1-yl)methyl)-7-(pyrrolidin-1-ylmethyl)quinolin-8-ol (10o). ¹H NMR (400 MHz, Chloroform-d) δ 8.84 (dd, J = 4.1, 1.6 Hz, 1H), 8.27 (dd, J = 8.5, 1.6 Hz, 1H), 7.90 (s, 1H), 7.46 (d, J = 8.7 Hz, 1H), 7.28 (dd, J = 8.6, 4.1 Hz, 1H), 7.15 (s, 1H), 6.84 (d, J = 2.2 Hz, 1H), 6.78 (dd, J = 8.6, 2.3 Hz, 1H), 6.48 (dt, J = 2.4, 1.2 Hz, 1H), 4.37 (s, 2H), 3.94 (s, 2H), 3.84 (s, 3H), 2.78 – 2.57 (m, 4H), 1.85 (p, J = 3.2 Hz, 4H).

5-((7-fluoro-1H-indol-1-yl)methyl)-7-(pyrrolidin-1-ylmethyl)quinolin-8-ol (10p). ¹H NMR (400 MHz, DMSO-d₆) δ 11.34 (s, 1H), 8.81 (dd, J = 4.2, 1.5 Hz, 1H), 8.53 (dd, J = 8.6, 1.6 Hz, 1H), 7.65 – 7.40 (m, 2H), 7.40 – 7.24 (m, 1H), 7.12 (s, 1H), 7.02 – 6.68 (m, 2H), 4.41 (s, 2H), 3.80 (s, 2H), 2.50 (d, J = 6.3 Hz, 4H), 1.68 (h, J = 3.2 Hz, 4H).

5-((7-methyl-1H-indol-1-yl)methyl)-7-(pyrrolidin-1-ylmethyl)quinolin-8-ol (10q). ¹H NMR (400 MHz, Chloroform-d) δ 9.74 (s, 1H), 8.84 (dd, J = 4.2, 1.6 Hz, 1H), 8.28 (dd, J = 8.6, 1.6 Hz, 1H), 8.18 (s, 1H), 7.50 (d, J = 7.7 Hz, 1H), 7.30 – 7.24 (m, 1H),

7.19 (s, 1H), 7.11 – 6.99 (m, 2H), 6.57 (d, J = 2.0 Hz, 1H), 4.41 (s, 2H), 3.95 (s, 2H), 2.82 – 2.62 (m, 4H), 2.47 (s, 3H), 1.97 – 1.78 (m, 4H).

5-((2,3-dimethyl-1H-indol-1-yl)methyl)-7-(pyrrolidin-1-ylmethyl)quinolin-8-ol (10r). ¹H NMR (400 MHz, Chloroform-d) δ 10.57 (s, 1H), 8.94 (dd, J = 4.2, 1.6 Hz, 1H), 8.28 (dd, J = 8.6, 1.6 Hz, 1H), 7.57 (dd, J = 8.2, 1.7 Hz, 1H), 7.45 (dd, J = 8.5, 4.2 Hz, 1H), 7.20 – 6.97 (m, 3H), 6.27 (s, 1H), 5.54 (d, J = 1.2 Hz, 2H), 3.75 (s, 2H), 2.72 – 2.46 (m, 4H), 2.33 (s, 3H), 2.24 (s, 3H), 1.79 (p, J = 3.2 Hz, 4H).

5-((5-methoxy-2-methyl-1H-indol-1-yl)methyl)-7-(pyrrolidin-1-ylmethyl)quinolin-8-ol (10s). ¹H NMR (400 MHz, Chloroform-d) δ 10.18 (s, 1H), 8.87 (dd, J = 4.2, 1.5 Hz, 1H), 8.41 (dd, J = 8.5, 1.6 Hz, 1H), 8.20 (s, 1H), 7.36 (dd, J = 8.5, 4.1 Hz, 1H), 7.23 – 7.07 (m, 1H), 6.93 (s, 1H), 6.74 (dt, J = 3.9, 1.9 Hz, 2H), 4.32 (s, 2H), 3.85 (s, 2H), 3.69 (s, 3H), 2.84 – 2.41 (m, 4H), 2.22 (s, 3H), 1.93 – 1.70 (m, 4H).

5-((2-ethyl-5-fluoro-1H-indol-1-yl)methyl)-7-(pyrrolidin-1-ylmethyl)quinolin-8-ol (10t). ¹H NMR (400 MHz, Chloroform-d) δ 9.11 (s, 1H), 8.89 (dd, J = 4.1, 1.6 Hz, 1H), 8.50 (dd, J = 8.6, 1.7 Hz, 1H), 7.50 – 7.40 (m, 1H), 7.39 – 7.31 (m, 1H), 7.10 – 6.92 (m, 3H), 4.83 (s, 2H), 4.39 (q, J = 7.1 Hz, 2H), 3.92 (s, 2H), 2.81 – 2.57 (m, 4H), 1.85 (p, J = 3.2 Hz, 4H), 1.28 (t, J = 7.1 Hz, 3H).

1-((8-hydroxy-7-(pyrrolidin-1-ylmethyl)quinolin-5-yl)methyl)-6-methoxy-1H-indole-3-carbonitrile (10u). ¹H NMR (400 MHz, DMSO-d₆) δ 10.73 (s, 1H), 8.83 (dd, J = 4.1, 1.5 Hz, 1H), 8.46 (dd, J = 8.5, 1.6 Hz, 1H), 7.51 (dd, J = 8.5, 4.1 Hz, 1H), 7.45 (d, J = 8.5 Hz, 1H), 7.27 (s, 1H), 6.82 (d, J = 2.3 Hz, 1H), 6.71 (dd, J = 8.6, 2.3 Hz, 1H), 4.48 (s, 2H), 4.01 (s, 2H), 3.79 (s, 2H), 3.73 (s, 3H), 2.65 – 2.36 (m, 4H), 1.66 (h, J = 3.1 Hz, 4H).

5-((4,5-difluoro-1H-indol-1-yl)methyl)-7-(pyrrolidin-1-ylmethyl)quinolin-8-ol (10v). ¹H NMR (400 MHz, Chloroform-d) δ 8.86 (dd, J = 4.1, 1.5 Hz, 1H), 8.50 (s, 1H), 8.27 (dd, J = 8.6, 1.6 Hz, 1H), 7.37 – 7.31 (m, 1H), 7.29 (d, J = 2.2 Hz, 1H), 7.19 (s, 1H), 7.15 (dd, J = 10.6, 6.5 Hz, 1H), 6.69 (s, 1H), 4.35 (s, 2H), 4.01 (s, 2H), 2.75 (q, J = 5.3, 4.6 Hz, 4H), 2.13 – 1.81 (m, 4H).

5-((5,6-difluoro-1H-indol-1-yl)methyl)-7-(pyrrolidin-1-ylmethyl)quinolin-8-ol (10w). ¹H NMR (400 MHz, Chloroform-d) δ 8.91 – 8.63 (m, 1H), 8.42 – 8.15 (m, 1H), 7.46 – 6.98 (m, 4H), 6.66 (d, J = 21.3 Hz, 1H), 4.45 – 4.21 (m, 2H), 3.98 – 3.78 (m, 2H), 2.81 – 2.51 (m, 4H), 1.99 – 1.69 (m, 4H).

5-((6-chloro-5-fluoro-1H-indol-1-yl)methyl)-7-(pyrrolidin-1-ylmethyl)quinolin-8-ol (10x). ¹H NMR (400 MHz, DMSO-d₆) δ 11.04 (s, 1H), 8.80 (dd, J = 4.2, 1.5 Hz, 1H), 8.50 (dd, J = 8.6, 1.6 Hz, 1H), 7.64 – 7.44 (m, 3H), 7.40 (d, J = 10.3 Hz, 1H), 7.18 (d, J = 1.7 Hz, 1H), 4.38 (s, 2H), 3.80 (s, 2H), 2.60 – 2.40 (m, 4H), 1.69 (q, J = 3.7, 3.3 Hz, 4H).

5-((5,6-dichloro-1H-indol-1-yl)methyl)-7-(pyrrolidin-1-ylmethyl)quinolin-8-ol (10y). ¹H NMR (400 MHz, DMSO-d₆) δ 11.15 (s, 1H), 8.82 (d, J = 4.2 Hz, 1H), 8.52 (d, J = 8.5 Hz, 1H), 7.67 (s, 1H), 7.59 (s, 1H), 7.55 – 7.38 (m, 2H), 7.22 (s, 1H), 4.41 (s, 2H), 3.82 (s, 2H), 2.51 (d, J = 6.7 Hz, 4H), 1.76 – 1.45 (m, 4H).

General procedure for synthesis of 5a-5f. To a stirred solution of compound 4 (1.0 mmol, 140 mg) or 5-amino-8-hydroxyquinoline dihydrochloride and carboxylic acid (1.2 mmol) in DMF-H₂O (1:5) were added oxyma (2.0 mmol, 284 mg), EDCI (2.0 mmol, 310 mg), and NaHCO₃ (6.0 mmol, 636 mg). After stirring at room temperature for 12 hr, the solution was extracted with EtOAc. The combined organic layers were washed with brine (3 ml), and then dried over Na₂SO₄. Concentration of organic phase gave crude product which was purified with flash chromatography on silica. Elution with dichloromethane/methanol (10:0-10:1) gave desired compounds **5a-5f** (yield: 27-59%).

N-((8-hydroxyquinolin-5-yl)methyl)-2-(3,4,5-trimethoxyphenyl)acetamide (5a). ¹H NMR (400 MHz, Chloroform-d) δ 8.79 (dd, J = 4.2, 1.5 Hz, 1H), 8.34 (dd, J = 8.5, 1.5 Hz, 1H), 7.46 (dd, J = 8.6, 4.2 Hz, 1H), 7.32 (d, J = 7.8 Hz, 1H), 7.06 (d, J = 7.8 Hz, 1H), 6.37 (s, 2H), 5.71 (s, 1H), 4.78 (d, J = 5.6 Hz, 2H), 3.80 (s, 3H), 3.72 (s, 6H), 3.52 (s, 2H).

N-((8-hydroxyquinolin-5-yl)methyl)-2-(4-nitrophenyl)acetamide (5b). ¹H NMR (400 MHz, DMSO-d₆) δ 9.78 (s, 1H), 8.87 (dd, J = 4.1, 1.6 Hz, 1H), 8.64 (t, J = 5.5 Hz, 1H), 8.39 (dd, J = 8.6, 1.6 Hz, 1H), 8.23 – 8.12 (m, 2H), 7.60 – 7.49 (m, 3H), 7.41 (d, J = 7.8 Hz, 1H), 7.04 (d, J = 7.8 Hz, 1H), 4.64 (d, J = 5.5 Hz, 2H), 3.64 (s, 2H).

2-(4-fluorophenyl)-N-((8-hydroxyquinolin-5-yl)methyl)acetamide (5c). ¹H NMR (400 MHz, DMSO-d₆) δ 9.76 (s, 1H), 8.87 (dd, J = 4.1, 1.6 Hz, 1H), 8.52 (t, J = 5.6 Hz, 1H), 8.40 (dd, J = 8.6, 1.6 Hz, 1H), 7.55 (dd, J = 8.6, 4.1 Hz, 1H), 7.39 (d, J = 7.8 Hz, 1H), 7.32 – 7.23 (m, 2H), 7.16 – 7.06 (m, 2H), 7.03 (d, J = 7.8 Hz, 1H), 4.62 (d, J = 5.5 Hz, 2H), 3.44 (s, 2H).

N-((8-hydroxyquinolin-5-yl)methyl)-2-(4-(trifluoromethyl)phenyl)acetamide (5d). ¹H NMR (400 MHz, DMSO-d₆) δ 9.79 (s, 1H), 8.87 (dd, J = 4.1, 1.5 Hz, 1H), 8.61 (t, J = 5.6 Hz, 1H), 8.39 (dd, J = 8.6, 1.6 Hz, 1H), 7.66 (d, J = 8.0 Hz, 2H), 7.55 (dd, J = 8.6, 4.1 Hz, 1H), 7.48 (d, J = 8.0 Hz, 2H), 7.40 (d, J = 7.8 Hz, 1H), 7.03 (d, J = 7.8 Hz, 1H), 4.64 (d, J = 5.5 Hz, 2H), 3.57 (s, 2H).

N-(8-hydroxyquinolin-5-yl)-2-(4-nitrophenyl)acetamide (5e). ¹H NMR (400 MHz, DMSO-d₆) δ 10.12 (s, 1H), 9.83 (s, 1H), 8.88 (dd, J = 4.1, 1.6 Hz, 1H), 8.32 (d, J = 1.6 Hz, 1H), 8.30 – 8.16 (m, 2H), 7.87 – 7.67 (m, 2H), 7.60 (dd, J = 8.6, 4.1 Hz, 1H), 7.46 (d, J = 8.2 Hz, 1H), 7.06 (d, J = 8.2 Hz, 1H), 3.97 (s, 2H).

N-(8-hydroxyquinolin-5-yl)-2-(4-(trifluoromethyl)phenyl)acetamide (5f). ¹H NMR (400 MHz, DMSO-d₆) δ 10.10 (s, 1H), 9.83 (s, 1H), 8.88 (dd, J = 4.1, 1.6 Hz, 1H), 8.30 (dd, J = 8.5, 1.6 Hz, 1H), 7.74 (d, J = 8.2 Hz, 2H), 7.64 (d, J = 8.0 Hz, 2H), 7.60 (dd,

$J = 8.6, 4.1$ Hz, 1H), 7.46 (d, $J = 8.2$ Hz, 1H), 7.56-7.40 (m, 1H), 7.06 (d, $J = 8.2$ Hz, 1H), 3.90 (s, 2H).

Synthesis of 5-(azidomethyl)quinolin-8-ol (3). To a stirred solution of 5-chloromethyl-8-quinolinol hydrochloride (10 mmol, 2.3 g) in acetone (20 ml) were added sodium azide (30 mmol, 1.95 g) at room temperature. After refluxed for 20 hr, the mixture was filtered and the residue was washed with acetone. Combined organic solvent was removed under reduced pressure to give crude product which was purified with flash chromatography on silica. Elution with hexanes/ethylacetate (10:1-1:1) gave desired compound **3** (1.54 g, 77%). $^1\text{H NMR}$ (400 MHz, $\text{DMSO-}d_6$) δ 10.04 (s, 1H), 8.92 (dd, $J = 4.1, 1.6$ Hz, 1H), 8.50 (dd, $J = 8.6, 1.6$ Hz, 1H), 7.67 (dd, $J = 8.6, 4.1$ Hz, 1H), 7.55 (d, $J = 7.8$ Hz, 1H), 7.08 (d, $J = 7.8$ Hz, 1H), 4.83 (s, 2H).

Synthesis of 5-(aminomethyl)quinolin-8-ol (4). A suspension of azide **3** (2.00 g, 10 mol) and 10% Pd/C (0.15 g) in ethylacetate (15 ml) was hydrogenated overnight, the reaction mixture was filtered off and washed with dichloromethane-methanol (1:1). The combined filtration was evaporated under vacuum to give the oily crude which was purified with flash chromatography on silica. Compound **4** was eluted out with dichloromethane/methanol (15:0-10:1) (1.18 g, 68%). $^1\text{H NMR}$ (400 MHz, $\text{DMSO-}d_6$) δ 8.86 (dd, $J = 4.1, 1.6$ Hz, 1H), 8.57 (dd, $J = 8.6, 1.6$ Hz, 1H), 7.58 (dd, $J = 8.5, 4.1$ Hz, 1H), 7.44 (dd, $J = 7.8, 0.9$ Hz, 1H), 7.02 (d, $J = 7.8$ Hz, 1H), 4.10 (d, $J = 0.8$ Hz, 2H),.

Synthesis of 1-(4-bromobenzyl)-3-((8-hydroxyquinolin-5-yl)methyl)urea (7). To a stirred solution of compound **4** (1.0 mmol, 140 mg) and 4-bromobenzyl isocyanate (1.0 mmol, 212 mg) in anhydrous dichloromethane (5ml) were added catalytic amount of trimethylamine (0.1 mmol, 10.1 mg). After stirring at room temperature for 5 hr, solvent was removed under reduced pressure to give crude product which was purified with flash chromatography on silica. Elution with hexanes/ethylacetate (10:1-1:1) gave desired compounds **7** (220 mg, 57%). $^1\text{H NMR}$ (400 MHz, $\text{DMSO-}d_6$) δ 9.71 (s, 1H), 8.88 (dd, $J = 4.1, 1.5$ Hz, 1H), 8.52 (dd, $J = 8.6, 1.6$ Hz, 1H), 7.60 (dd, $J = 8.6, 4.2$ Hz, 1H), 7.56 – 7.46 (m, 2H), 7.38 (d, $J = 7.8$ Hz, 1H), 7.30 – 7.14 (m, 2H), 7.03 (d, $J = 7.8$ Hz, 1H), 6.44 (t, $J = 5.8$ Hz, 1H), 6.39 (t, $J = 6.1$ Hz, 1H), 4.60 (d, $J = 5.7$ Hz, 2H), 4.21 (d, $J = 6.1$ Hz, 2H), 3.18 (d, $J = 5.1$ Hz, 1H).

Cell culture and reagents

Human melanoma A375, M14, WM164, RPMI7951, M14/MDR1 and B16F101 cell lines were purchased from ATCC (American Type Culture Collection, Manassas, VA, USA), and cultured in DMEM media (Mediatech, Inc., Manassas, VA) at 37°C in a humidified atmosphere containing 5% CO₂. The culture media were supplemented with 10% fetal bovine serum (Atlanta Biologicals, Lawrenceville, GA) and 1% antibiotic-antimycotic mixture (Sigma-Aldrich, St. Louis, MO). Compounds were dissolved in dimethylsulfoxide (DMSO; Sigma-Aldrich) to make a stock solution of 10 mM. Compound solutions were freshly prepared by diluting stocks with cell culture medium before use (final solution contained less than 0.5% DMSO). 5000 cells in logarithm

growing phase were seeded overnight into each well of a 96-well plate. Then the cells were continuously incubated for 48 h with sequential diluted compound solution (100 μ M to 3 nM, 100 μ l per well) in cell culture medium. The cell viability was determined in MTS assay and IC₅₀ was calculated (n = 4), following similar procedures as described previously [215-218]. Dulbecco's modified Eagle's Medium (DMEM), fetal bovine serum (FBS), penicillin/streptomycin and trypsin 0.25% were purchased from Hyclone (GE Healthcare Life Science, Pittsburgh, PA). Phosphate buffered saline (PBS) was purchased from Invitrogen GIBCO (Grand Island, NY). Dimethyl sulfoxide (DMSO) and 3-(4,5-dimethylthiazole-2-yl)-2,5-biphenyl tetrazolium bromide (MTT) were purchased from Sigma Chemical Co (St. Louis, MO). The P-glycoprotein (P-gp) overexpressing KB-C2 cell line was established from a parental human epidermoid carcinoma cell line KB-3-1, by a step-wise selection of KB-3-1 in increasing concentrations of colchicine up to 2 μ g/ml[219]. SW620/Ad300, which is also a P-gp overexpressing drug resistant cell line, was established by stepwise exposure of the parental human colon cancer cell line SW620 to increasing concentrations of doxorubicin up to 300 ng/ml[220]. The SW620 and SW620/Ad300 cell lines were kindly provided by Dr. Susan E. Bates and Dr. Robert W. Robey (NCI, NIH, Bethesda, MD, USA). All the cell lines were grown in DMEM supplemented with 10% FBS and 100 unit/ml penicillin/streptomycin in a humidified incubator containing 5% CO₂ at 37 °C.

Cytotoxicity assay

A375, M14, WM164, RPMI7951, M14/MDR1 and B16F101 were seeded in 96-well plates at a concentration of 1,000–5,000 cells per well, depending on growth rate of the cell line. After overnight incubation, the media was replaced and cells were treated with the test compounds at 10 concentrations ranging from 0.03 nM to 1 μ M plus a vehicle control for 72 h in four replicates. Following treatment, the MTS reagent (Promega, Madison, WI) was added to the cells and incubated in dark at 37°C for at least 1 hour. Absorbance at 490 nm was measured using a plate reader (DYNEX Technologies, Chantilly VA). Percentages of cell survival versus drug concentrations were plotted, and the IC₅₀ (concentration that inhibited cell growth by 50% of untreated control) values were obtained by nonlinear regression analysis using GraphPad Prism (GraphPad Software, San Diego, CA).

Cytotoxicity against P-gp overexpressed cell lines by MTT assay

The MTT colorimetric assay was used to measure the sensitivity of the cells against the synthesized compounds. The assay detects the formazan product formed from the reduction of MTT in active cells thus assesses the cell viability[221]. Cells were seeded in 96-well plates at 5000 cells/well (KB-3-1 or KB-C2 cells) or at 7000 cells/well (SW620 or SW620/Ad300 cells) in 180 μ l completed medium and cultured overnight. Then various concentrations of the compounds (20 μ l) were added to the designated wells. After 72 h continuous drug incubation, 20 μ l of MTT reagent (5 mg/ml) was added to each well and the plates were incubated at 37 °C for 4 h. Subsequently, the medium

was removed and 100 μ l of DMSO were added to dissolve the formazan crystals in each well. The absorbance was determined at 570 nm by the accuSkan™ GO UV/Vis Microplate Spectrophotometer (Fisher Sci., Fair Lawn, NJ). The IC₅₀ values of each compound on each cell line were calculated from the survival curves to represent the cytotoxicity of the compounds. The fold of drug resistance was calculated by dividing the IC₅₀ of the P-gp overexpressing cells by that of the parental cells. Two known P-gp substrates, YM155 and paclitaxel, were used as positive controls for P-gp overexpressing cell lines. On the other hand, cisplatin, which is not a substrate of P-gp, was used as negative control.

Liver microsomes stability assay

Liver microsomes stability assay was conducted following literature reports [222, 223]. The NADPH regenerating agent solutions A (catalog#: 451220) and B (catalog#: 451200) and mouse liver microsomes (CD-1, mixture of male, catalog#:452701, and female, catalog#: 452702) were obtained from BD Gentest (Woburn, MA). For each test compound, the mouse liver microsomal solution was prepared by adding 0.058 mL of concentrated mouse liver microsomes (20 mg/mL protein concentration) to 1.756 mL of 0.1 M potassium phosphate buffer (pH 7.4) containing 5 μ L of 0.5 M EDTA to make a 0.6381 mg/mL (protein) microsomal solution. Each test compound (2.2 μ L of 10 mM DMSO solution) was added directly to 1.79 mL of mouse liver microsomal solution and 90 μ L was transferred to wells in 96-well plates (0, 0.25, 0.5, 1, 2, and 4 h time points each in triplicate). The NADPH regenerating agent was prepared by mixing 0.113 mL of NADPH regenerating agent Solutions A, 0.023 mL of solution B and 0.315 mL of 0.1 M potassium phosphate buffer (pH 7.4) for each tested compound. To each well of the 96-well plate, 22.5 μ L of the NADPH regenerating agent was added to initiate the reaction, and the plate was incubated at 37 °C for each time point (0, 0.25, 0.5, 1, 2, and 4 h time points each in triplicate). The reaction was quenched by adding 225 μ L of cold acetonitrile containing warfarin (4 mg/ml) as internal control to each well. All of the plates were centrifuged at 4000 rpm for 20 min and the supernatants (100 μ L) were transferred to another 96-well plates for analysis on UPLC–MS (Waters Acquity UPLC linked to Waters Acquity Photodiode Array Detector and Waters Acquity Single Quadrupole Mass Detector) on Acquity UPLC BEH C18 1.7 mm (2.1x50 mm) column by running 90–5% gradient for water (+0.1% formic acid) and acetonitrile (+0.1% formic acid) in 2 minutes. The area under the single ion recording (SIR) channel for the test compound divided by the area under the SIR for internal control at 0 time concentration was considered as 100% to calculate remaining concentration at each time point. The terminal phase rate constant (ke) was estimated by linear regression of logarithmic transformed concentration versus the data, where ke = slope x(-ln10). The half life t_{1/2} was calculated as ln2/ke. The intrinsic clearance (CL_{int,app})= (0.693/in vitro t_{1/2}) x (1ml incubation volume/0.5 mg of microsomal protein) x (45 mg microsomal protein/gram of liver) x (55 g of liver/kg body weight) [224, 225].

Chemistry

Scheme 5-1 showed the synthetic method to access UC-112 analogues **2a-2f**. Starting material 5-chloromethyl-8-quinolinol hydrochloride was synthesized by following a reported procedure [214]. 5-chloromethyl-8-quinolinol hydrochloride was treated with commercially available amines in the presence of sodium hydride or sodium carbonate and potassium iodide to give **1a-1f**. **1a-1f** refluxed with paraformaldehyde and pyrrolidine in ethanol to provide analogues **2a-2f**.

Scheme 5-2 depicted the synthesis to obtain analogues **6a-6f** and **8**. To synthesize amide and urea analogues **6a-6d** and **8**, 5-chloromethyl-8-quinolinol hydrochloride was refluxed with sodium azide in acetone to yield azide compound **3**. **3** was subsequently hydrogenated in the presence of a catalytic equivalent of 10% Pd/C to provide amine **4**. With **4** in hand, treatment of it with carboxylic acids, EDCI and oxyma was able to form amide **5a-5d**. Refluxing the mixture of **5a-5d**, paraformaldehyde and pyrrolidine in ethanol gave the amide analogues **6a-6d**. Syntheses of another two amide analogues **6e** and **6f** were carried out using commercially available 5-amino-8-hydroxyquinoline dihydrochloride by following the same method. Treatment of amine **4** using a catalytic equivalent of triethylamine generated the urea intermediate **8**, which was subjected to Mannich reaction to give urea analogue **9**.

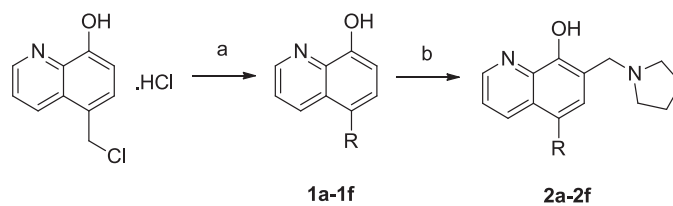
Indole analogues **10a-10y** with either mono-substitution or di-substitution were prepared by following **Scheme 5-3**. In brief, 5-chloromethyl-8-quinolinol hydrochloride was refluxed together with indoles in the presence of sodium carbonate and a catalytic amount of potassium iodide in acetonitrile to generate intermediate **9a-9y**. Treatment of **9a-9y** with paraformaldehyde and pyrrolidine under reflux condition subsequently furnished analogues **10a-10y**.

Results

All analogues of UC-112 were evaluated for their cytotoxicity in human melanoma cell lines including A375, WM1641, M14, RPMI, M14/MDR1 and B16F10. The antiproliferative effects of the compounds were evaluated by MTT assay. IC₅₀s were reported in μM and calculated from at least three independent experiments, each performed in duplicates.

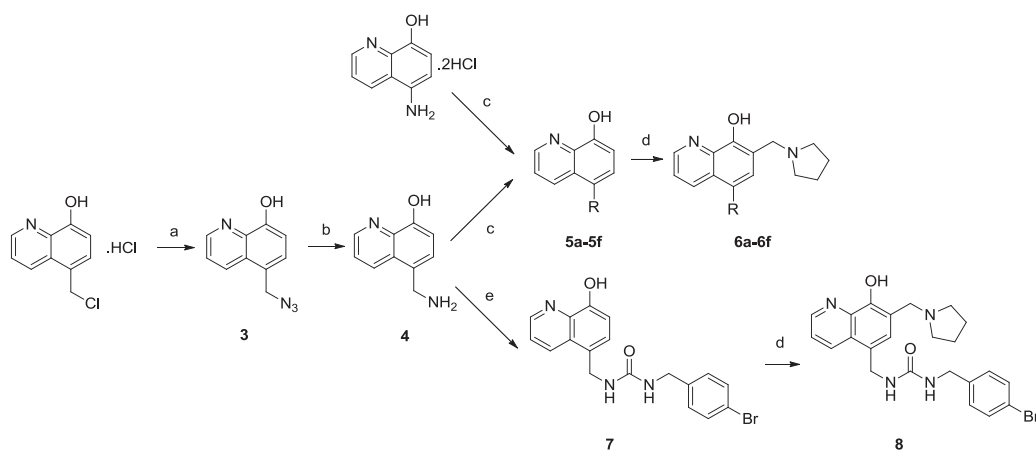
***In vitro* growth inhibitory effects of UC-112 analogues with modification of benzyloxy moiety**

As a continuation of our effort to develop selective survivin inhibitor based on UC-112, we initiated the SAR investigation by replacing the benzyloxy with a variety of different moieties. The structures and *in vitro* assay result for analogues **2a-2f**, **6a-6f**, **8** and **10a** were shown in **Figure 5-2** and **Table 5-1**. Compared to the reference compound MX-106, analogues **2a** with a 5-fluoroindazole moiety, **2b** with a benzotriazole moiety



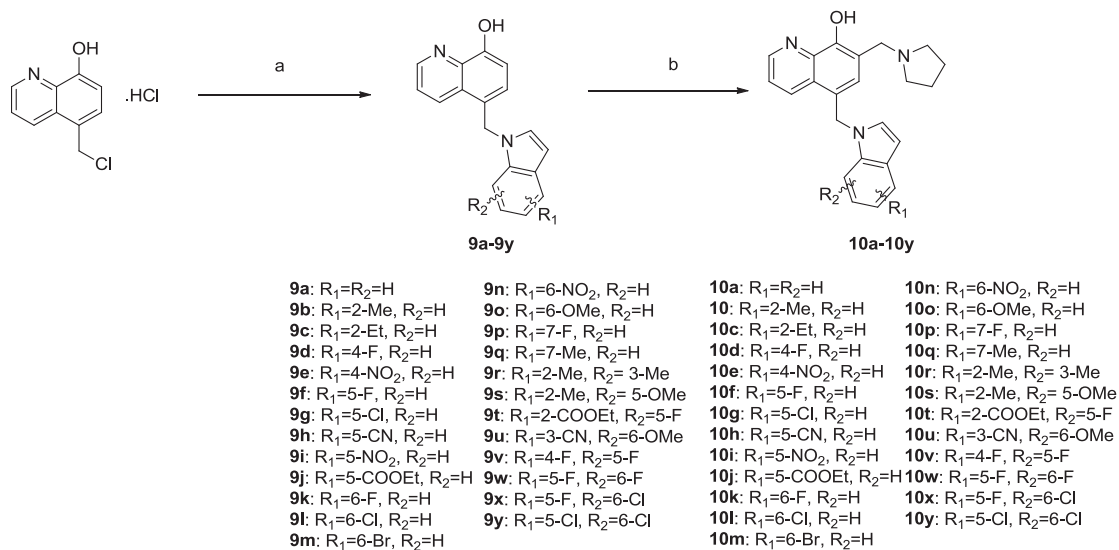
Scheme 5-1. Synthesis of 2a-2f

Reagents and conditions: (a) NaH, DMF or KI, Na₂CO₃, MeCN, reflux; (b) paraformaldehyde, pyrrolidine, ethanol, reflux;



Scheme 5-2. Synthesis of 6a-6f and 8

Reagents and conditions: (a) NaN₃, acetone, reflux; (b) H₂, Pd/C(10%), ethyl acetate, rt; (c) Et₃N, DCM, 0°C to rt; (d): paraformaldehyde, pyrrolidine, ethanol, reflux; (e) Oxyma, EDCI, NaHCO₃, DMF-H₂O, rt.



Scheme 5-3. Synthesis of 10a-10y

Reagents and conditions: (a) NaH, DMF or KI, Na₂CO₃, MeCN, reflux; (b) paraformaldehyde, pyrrolidine, ethanol, reflux.

Compound	R	Compound	R	Compound	R	Compound	R
1a/2a		1e/2e		5c/6c		7/8	
1b/2b		1f/2f		5d/6d		9a/10a	
1c/2c		5a/6a		5e/6e			
1d/2d		5b/6b		5f/6f			

Figure 5-2. Structures of UC-112 analogues with modification of benzyloxy moiety

Table 5-1. *In vitro* growth inhibitory effects (μM) of UC-112 analogues with modification of benzyloxy moiety (n=3)

Compound	A375	WM164	M14	RPMI	M14/MDR1	B16F10
2a	3.6±0.2	8.6±1.1	5.4±0.3	11.1±0.7	7.0±0.1	>30.0
2b	1.9±0.1	>30.0	2.3±0.1	6.5±0.2	3.1±0.1	22.5±1.2
2c	3.9±0.1	56.4±1.1	4.1±0.2	17.4±1.2	7.9±0.1	34.9±1.1
2d	14.1±0.7	33.9±1.1	11.5±0.4	21.0±0.4	14.3±0.2	22.6±0.3
2e	3.1±0.2	>30.0	15.9±0.6	1.3±0.2	0.9±0.1	4.7±0.1
2f	7.6±0.1	24.5±0.4	16.7±0.1	23.8±0.6	22.0±0.3	>30.0
6a	>30.0	13.0±0.5	>30.0	>30.0	>30.0	>30.0
6b	4.7±0.2	3.7±0.3	5.1±0.1	26.2±6.2	10.7±1.2	8.5±3.6
6c	3.5±0.3	2.8±0.2	8.6±0.2	18.4±0.3	7.4±1.2	2.7±0.1
6d	1.5±0.1	1.6±0.1	>30.0	12.9±0.2	12.2±0.2	>30.0
6e	6.0±1.3	24.9±1.0	6.7±0.3	25.3±2.4	12.2±0.5	11.6±11.6
6f	2.9±0.15	ND	2.4±0.1	6.8±0.6	3.3±0.2	ND
8	>30.0	20.18±0.49	>30.0	17.3±0.3	8.7±0.2	6.7±0.2
10a	0.8±0.1	0.9±0.1	0.8±0.1	4.4±0.3	2.1±0.1	8.2±0.7

ND: not determined

and **2c** with a 4-chloropurine moiety exhibited 3~5-fold reduced activities. Replacement of the benzyloxy with other moieties as shown in compounds **2d**, **2e** and **2f** resulted in significant reduction of inhibitory effects (> 3-fold). Replacing the benzyloxy with phenyl acetamides (analogues **6a-6d**) was detrimental to the antiproliferative activities. Shortening the linkage by one methylene in **6b** and **6d** resulted in analogues **6e-6f**, which showed similar activities to that of **6b** and **6d**. The introduction of a benzylurea was revealed to be significantly detrimental for antiproliferative activity. Among all the analogues in this series, analogue **10a** had an indole moiety; it exhibited the most potent activity and had an average IC₅₀ of 0.9 μM, which was comparable to that of MX-106.

After discovered an equipotent scaffold to MX-106, we turned our effort to investigate the substitutional effect on the indole ring. Analogues with mono-substituent **10b-10q** and analogues with di-substituents **10r-10y** were then synthesized.

***In vitro* growth inhibitory effects of UC-112 analogues with mono-substitution on the indole moiety**

The *in vitro* assay result for analogues having mono-substituent (**10a-10q**) was shown in **Table 5-2**. For the 2-position substituted analogues, **10b** with a methyl group and **10c** with an ethyl group showed slightly reduced activities compared to **10a**. Introducing substituents to the 4-position on the indole diminished the antiproliferative activity, which was demonstrated by analogues **10d** and **10e**. For analogues that had substituents on the 5-position of indole, they generally displayed comparable activities to that of **10a**; for example, compounds **10f**, **10h** and **10i** had IC₅₀s ranging from 0.7 to 1.1 μM; analogues **10g** and **10j**, which had chloro and bulky ester functional group, showed ~2-fold reduced activity in comparison with MX-106. In the series of analogues with substituents on the 6-position of the indole (**10k-10o**), they were generally equipotent to MX-106 and **10a**; **10k-10o** had IC₅₀s as low as 0.7 μM. Analogues having substituents on the 7-position of indole were slightly less potent than corresponding 5- or 6-position substituted counterparts.

***In vitro* growth inhibitory effects of UC-112 analogues with di-substituents on the indole moiety**

Eight di-substituted indole analogues were synthesized in this series and their *in vitro* assay result was shown in **Table 5-3**. All the eight analogues did not show any improvement of activity compared to their mono-substituted counterparts. **10t-10y** were designed based on the most potent mono-substituted analogues **10f**, **10l** and **10o**. Incorporation of a secondary substituent to 5-fluoroindole or 6-methoxyindole generally was not beneficial to activity; for example, 5-fluoroindole analogues **10t**, **10v**, **10w** and **10x** had 2-ethylester, 4-fluro, 6-fluro and 6-chloro as the secondary functional group, respectively; they showed reduced cytotoxicities compared to **10f** and had IC₅₀s of >1.5 μM; the 3-cyano-6-methoxy indole analogue **10u** was less potent than the mono-

Table 5-2. *In vitro* growth inhibitory effects (μM) of UC-112 analogues with mono-substituent on the indole moiety (n=3)

Compound	A375	WM164	M14	RPMI7951	M14/MDR1	B16F10
10a	0.8 \pm 0.1	0.9 \pm 0.1	0.8 \pm 0.1	4.4 \pm 0.3	2.1 \pm 0.1	8.2 \pm 0.7
10b	2.2 \pm 0.2	7.5 \pm 1.2	1.4 \pm 0.2	2.2 \pm 0.2	0.7 \pm 0.1	5.7 \pm 0.8
10c	2.0 \pm 0.1	8.9 \pm 1.4	1.5 \pm 0.2	3.2 \pm 0.4	1.1 \pm 0.1	11.5 \pm 0.9
10d	1.6 \pm 0.3	6.5 \pm 0.6	1.2 \pm 0.2	2.2 \pm 0.2	0.8 \pm 0.1	8.9 \pm 1.7
10e	1.8 \pm 0.1	7.0 \pm 0.3	2.1 \pm 0.1	0.6 \pm 0.1	0.6 \pm 0.1	6.8 \pm 0.2
10f	0.7 \pm 0.2	0.7 \pm 0.2	1.9 \pm 0.4	ND	ND	ND
10g	1.8 \pm 0.2	1.6 \pm 0.2	4.0 \pm 0.4	6.4 \pm 0.6	0.8 \pm 0.1	1.7 \pm 0.2
10h	1.0 \pm 0.1	1.1 \pm 0.1	5.1 \pm 0.3	ND	ND	ND
10i	0.7 \pm 0.1	0.8 \pm 0.1	5.6 \pm 0.4	3.7 \pm 0.3	2.2 \pm 0.1	1.3 \pm 0.1
10j	1.9 \pm 0.2	4.7 \pm 0.6	2.4 \pm 0.2	1.5 \pm 0.1	0.8 \pm 0.1	6.0 \pm 0.1
10k	0.9 \pm 0.1	0.7 \pm 0.1	1.3 \pm 0.1	2.7 \pm 0.5	1.3 \pm 0.1	0.6 \pm 0.1
10l	0.9 \pm 0.4	0.9 \pm 0.4	0.8 \pm 0.4	7.7 \pm 0.5	3.8 \pm 0.1	25.5 \pm 2.4
10m	0.9 \pm 0.1	1.4 \pm 0.2	3.5 \pm 0.3	5.3 \pm 0.6	0.7 \pm 0.1	1.4 \pm 0.2
10n	0.9 \pm 0.1	0.7 \pm 0.1	2.8 \pm 0.2	4.3 \pm 0.7	2.8 \pm 0.2	1.1 \pm 0.2
10o	0.8 \pm 0.2	0.7 \pm 0.1	0.9 \pm 0.4	6.2 \pm 0.4	2.8 \pm 0.1	>30.0
10p	1.7 \pm 0.2	1.9 \pm 0.2	2.6 \pm 0.4	ND	ND	ND
10q	2.0 \pm 0.2	11.5 \pm 0.8	1.4 \pm 0.1	2.6 \pm 0.2	0.9 \pm 0.1	9.7 \pm 0.8

ND: not determined

Table 5-3. *In vitro* growth inhibitory effects (μM) of UC-112 analogues with di-substituents on the indole moiety (n=3)

Compound	A375	WM164	M14	RPMI7951	M14/MDR1	B16F10
10r	1.9 \pm 0.2	7.1 \pm 0.8	1.5 \pm 0.2	8.2 \pm 0.6	1.0 \pm 0.1	2.3 \pm 0.3
10s	1.9 \pm 0.2	4.6 \pm 0.1	2.0 \pm 0.1	2.1 \pm 0.1	1.0 \pm 0.1	4.3 \pm 0.1
10t	2.0 \pm 0.2	8.5 \pm 0.8	1.3 \pm 0.1	3.6 \pm 0.4	1.0 \pm 0.1	8.5 \pm 1.4
10u	1.7 \pm 0.1	16.7 \pm 0.5	1.6 \pm 0.1	3.7 \pm 0.1	1.9 \pm 0.1	ND
10v	1.2 \pm 0.1	2.8 \pm 0.1	2.1 \pm 0.1	0.8 \pm 0.1	0.6 \pm 0.1	2.4 \pm 0.1
10w	1.5 \pm 0.1	3.2 \pm 0.1	2.6 \pm 0.1	1.3 \pm 0.0	0.7 \pm 0.1	3.1 \pm 0.1
10x	2.0 \pm 0.2	4.5 \pm 0.2	2.0 \pm 0.2	1.7 \pm 0.1	1.0 \pm 0.1	2.1 \pm 0.1
10y	0.7 \pm 0.1	0.9 \pm 0.1	8.5 \pm 0.2	9.3 \pm 1.1	2.2 \pm 0.1	ND

ND: not determined

substituted counterpart **10o**; 5,6-dichloroindole analogue **10y** showed cytotoxicity comparable to that of 5-chloroindole analogue **10l**.

Inhibitory effect against P-gp overexpressed cell lines

Multidrug resistance protein 1 (MDR1) or P-gp belongs to the family of ATP-binding cassette (ABC) transporters and is encoded by ABCB1 gene. P-gp is responsible for the decline of concentrations of extensive anticancer drugs in multidrug resistant cells. Therefore, the ability to overcome P-gp mediated drug-resistance is a favorable property for drug candidates.

Other than M14 melanoma cell line, drug-resistant cell line M14/MDR1 was also tested to evaluate the ability of new analogue to overcome P-gp mediated drug-resistance. The result was shown in **Table 5-4**. 71% of the new indole analogues had RIs less than 1, indicating that most of the new indole analogues exhibited more potent inhibitory effects against P-gp overexpressed M14/MDR1 cell line than non-resistant M14 cell line. It is worthy noting that all the di-substituted indole analogues have RIs less than 1, implying that a secondary substituent on the indole is beneficial for the ability to overcome P-gp overexpression.

Besides melanoma cell lines, cervical and colorectal carcinoma cell lines were also tested to evaluate abilities of the new analogues to surmount P-gp overexpression. The result was summarized in **Table 5-5**. The small-molecular survivin inhibitor YM-155 showed remarkable cytotoxicity against KB-3-1 and SW620 cell lines with IC₅₀s of 5 nM and 4 nM, respectively. YM155 however displayed significantly reduced activities against the P-gp overexpressed cell lines KB-C2 and SW620/Ad300, having IC₅₀s of more than 20 μM. Similarly, paclitaxel, a notable substrate of P-gp, was not effective to P-gp overexpressed cell lines. In contrast, our indole analogues **10f**, **10i**, **10l**, **10o** and the previously reported MX-106 showed remarkably stronger inhibitory effects against P-gp overexpressed cell lines than non-resistant parent cell lines. In the non-resistant KB-3-1 cell line, four compounds **10f**, **10i**, **10l** and **10o** exhibited micromolar range activities (from 1.3 to 1.7 μM); their IC₅₀s were in sub-μM range (from 0.2 to 0.4 nM) against P-gp overexpressed KB-C2 cell line. **10f**, **10i**, **10l** and **10o** had IC₅₀s ranging from 0.2 to 0.3 μM against non-resistant SW620 cell line while their activities in P-gp overexpressed KB-C2 cell line were 3-6.7 folds more potent with IC₅₀s ranging from 0.03 to 0.01 μM. Collectively, our new indole analogues of UC-112 can overcome drug-resistance mediated by P-gp overexpression.

***In vitro* metabolic stability study**

Prior to *in vivo* study, the *in vitro* metabolic stabilities of analogues **10f**, **10i**, **10l** and **10o** were examined by measuring their half-life upon incubation with mouse, rat, and human liver microsomes in the presence of an NADPH regeneration system. The results

Table 5-4. *In vitro* growth inhibitory effects of indole analogues in P-gp overexpressed cell line M14/MDR1 (n=3)

Compound	M14	M14/MDR1	RI
10a	0.8 ±0.1	2.1±0.1	2.6
10b	1.4 ±0.2	0.7±0.1	0.5
10c	1.5 ±0.2	1.1±0.1	0.7
10d	1.2 ±0.2	0.8±0.1	0.7
10e	2.1 ±0.1	0.6±0.1	0.3
10f	1.9±0.4	ND	ND
10g	4.0 ±0.4	0.8±0.1	0.2
10h	5.1±0.3	ND	ND
10i	5.6 ±0.4	2.2±0.1	ND
10j	2.4±0.2	0.8±0.1	0.3
10k	1.3±0.1	1.3±0.1	1.0
10l	0.8±0.4	3.8±0.1	4.8
10m	3.5±0.3	0.7±0.1	0.2
10n	2.8±0.2	2.8±0.2	1.0
10o	0.9±0.4	2.8±0.1	3.1
10p	2.6±0.4	ND	ND
10q	1.4±0.1	0.9±0.1	0.6
10r	1.5±0.2	1.0±0.1	0.7
10s	2.0±0.1	1.0±0.1	0.5
10t	1.3 ±0.1	1.0±0.1	0.7
10u	1.6 ±0.1	1.9±0.1	1.2
10v	2.1±0.1	0.6±0.1	0.3
10w	2.6±0.1	0.7±0.1	0.3
10x	2.0 ±0.2	1.0±0.1	0.5
10y	8.5±0.2	2.2±0.1	0.3

ND: not determined; RI: resistance index, calculated by $IC_{50}(M14/MDR1)/IC_{50}(M14)$.

Table 5-5. *In vitro* growth inhibitory effects of 10f, 10i, 10l and 10o in P-gp overexpressed cell lines (n=3)

Compound	IC ₅₀ ± SD (μM)		RI	IC ₅₀ ± SD (μM)		RI
	KB-3-1	KB-C2		SW620	SW620/Ad300	
10f	1.4 ± 0.2	0.2 ± 0.0	0.14	0.2 ± 0.0	0.03 ± 0.00	0.15
10i	1.4 ± 0.4	0.2 ± 0.0	0.14	0.2 ± 0.0	0.06 ± 0.02	0.30
10l	1.7 ± 0.2	0.3 ± 0.0	0.18	0.23 ± 0.1	0.05 ± 0.03	0.22
10o	1.3 ± 0.2	0.4 ± 0.1	0.31	0.3 ± 0.0	0.10 ± 0.04	0.33
MX-106	1.3 ± 0.1	0.3 ± 0.1	0.23	0.2 ± 0.0	0.03 ± 0.01	0.15
YM-155	0.005 ± 0.000	37.3 ± 4.0	7460.00	0.004 ± 0.001	23.4 ± 2.4	5850
Paclitaxel	0.0005 ± 0.0001	0.3 ± 0.0	600.00	0.03 ± 0.00	2.0 ± 0.4	66.7
Doxorubicin	0.4 ± 0.1	1.7 ± 0.4	4.25	0.21 ± 0.03	15.2 ± 2.9	72.4
Cisplatin	1.1 ± 0.1	1.7 ± 0.1	1.55	1.8 ± 0.1	5.1 ± 0.6	2.83

RI: resistance index, which is calculated by $IC_{50}(KB-C2)/IC_{50}(KB-3-1)$ or $IC_{50}(SW620/Ad300)/IC_{50}(SW620)$.

were summarized in **Table 5-6**. All compounds possessed acceptable stability profile in three microsome species. Four compounds were more stable in human microsome than in mouse and rat microsomes. Among the four analogues, **10f** with a 5-fluoro was the most stable against mouse and rat microsomes. Therefore, **10f** will be chosen for future *in vivo* animal study.

Discussion

UC-112 was previously discovered through a virtual screening program from a library of drug-like compounds [126]. UC-112 selectively lowered the protein level of survivin without affecting other members of the IAP family. In a subsequent SAR study of UC-112, a series of analogues were synthesized and evaluated for their antiproliferative activities in a panel of melanoma cell lines [214]. The result demonstrated that: (1) 8-hydroxyl group and the nitrogen in 8-hydroxyquinoline were essential for exerting maximum inhibitory effect; (2) modifications of the pyrrolidine ring to other heterocycles were unsuccessful to improve activities; (3) modification of the benzyloxy was feasible to increase the activity. Based on this SAR result, we hypothesize that the benzyloxy moiety in UC-112 is too flexible; replacing the benzyloxy moiety with rigid moieties can improve the inhibitory activity.

In this chapter, we replaced the benzyloxy in UC-112 with other substructures to decrease the flexibility. Within the series of analogues modifying the benzyloxy moiety (**Figure 5-2** and **Table 5-1**), analogue **10a** which had an indole moiety was found to exert the most potent antiproliferative activity against a panel of melanoma cell lines. Further structural optimization of **10a** was focused on introducing mono-substituent and di-substituents. The result showed that many substituted indole analogues exhibited comparable potencies to that of MX-106 and UC-112. Importantly, while YM155 was significantly less cytotoxic in resistant cell lines than in non-resistant cell lines, the new UC-112 analogues were more potent against several types of P-gp overexpressed cancer cell lines than non-resistant cell lines. 71% of the indole analogues had RIs less than 1 in melanoma cell lines (M14 vs M14/MDR1). **10f**, **10i**, **10l** and **10o** were >3-fold more cytotoxic against P-gp overexpressed cervical and colorectal carcinoma cell lines (KB-C2 and SW620/Ad300) than non-resistant cervical and colorectal carcinoma cell lines (KB-3-1 and SW620). **10f**, **10i**, **10l** and **10o** exhibit significant cytotoxicity against SW620/Ad300 cell line with IC₅₀ as low as 30 nM. The new analogues showed favorable microsomal stability profile. Currently, the *in vivo* efficacy evaluation of the 5-F indole analogue (**10f**) in a subcutaneous mouse xenograft model with human A375 melanoma is undergoing.

In conclusion, we herein have synthesized thirty-six new UC-112 analogues modifying the benzyloxy moiety. Several new analogues showed equipotency to that of MX-106 in melanoma cell lines. New analogues showed significant cytotoxicity against colorectal carcinoma cell line with IC₅₀ as low as 0.2 μM. New UC-112 analogues also exhibited the ability to surmount P-gp mediated drug-resistance.

Table 5-6. *In vitro* microsomal stabilities of compounds 10f, 10i, 10l and 10o

Compound	Mouse		Rat		Human	
	$t_{1/2}$ (hr)	Clint (mL/Min/Kg)	$t_{1/2}$ (hr)	Clint (mL/Min/Kg)	$t_{1/2}$ (hr)	Clint (mL/Min/Kg)
Verapamil	1.44±0.12	39.7	3.81±0.48	12.3	1.57±0.17	13.3
10f	1.36±0.06	42.1	1.29±0.03	36.1	4.59±0.39	4.5
10i	1.17±0.06	48.7	1.20±0.05	39.0	2.16±0.19	9.6
10l	1.20±0.07	47.8	1.62±0.10	29.0	3.50±0.36	5.9
10o	0.88±0.06	65.1	1.26±0.06	37.0	2.80±0.18	7.4

CHAPTER 6. TOTAL SYNTHESIS OF BIOLOGICAL ACTIVE 20S-HYDROXYVITAMIN D3*

Introduction

25-hydroxylase (CYP2R1 or CYP27A1) in the liver and 1α -hydroxylase (CYP27B1) in the kidney are the enzymes responsible for sequential metabolism of vitamin D3 to produce bioactive $1\alpha,25$ -dihydroxyvitamin D3 [$1,25(\text{OH})_2\text{D}_3$, calcitriol] [226, 227]. $1,25(\text{OH})_2\text{D}_3$ activates nuclear vitamin D receptor (VDR). VDR is found in almost all tissues of the body and triggers numerous cellular effects including but not limited to stimulation of cell differentiation and/or apoptosis, inhibition of cell proliferation, regulation of secretory and immune factors of many cells, and cell protective functions, in a context dependent fashion [228-232]. Therefore, active forms of vitamin D can be used in therapy of cancer, hyperproliferative, autoimmune and metabolic disorders [233-235]. The applications are however limited by hypercalcemic (toxic) effect of calcitriol at pharmacological concentrations [144]. This side effect has led to the development of more than 3,000 synthetic vitamin D3 analogs showing low calcemic activity [236]. Some of these analogs such as paricalcitol, oxacalcitriol, falecalcitriol, tacalcitol and doxercalciferol were used to treat secondary hyperparathyroidism and psoriasis [233, 237]. Calcipotriol is also a promising agent for the treatment of pancreatic cancer and is currently undergoing human clinical trial [238] (Figure 6-1).

Mammalian cytochrome P450 side-chain cleavage enzyme (P450_{scc} or CYP11A1) not only cleaves the side chain of cholesterol to produce pregnenolone (precursor of all steroids) [145, 146] but also hydroxylates vitamin D3 in a sequential fashion [146-150] starting from C20 to form 20S-hydroxyvitamin D3 [20S-(OH)D3] (**1, Figure 6-1**). This intermediate is subsequently converted to di- and trihydroxy metabolites [147, 149-152]. Functional studies showed that 20S-(OH)D3 not only stimulated keratinocyte differentiation program but also inhibited NF- κ B activity in human keratinocytes [153]. In addition, it has shown anti-inflammatory activities, strong anti-proliferative effects, anti-leukemia and tumorostatic effects [153-157], protective effects against ultra-violet B (UVB) induced damage [158], as well as antifibrotic activity *in vivo* [159]. These activities are mediated either through activation of the VDR [153, 160] or inhibition of ROR α and ROR γ transcriptional activities [161]. More importantly, while having comparable anti-proliferative potency with $1,25(\text{OH})_2\text{D}_3$ which has strong hypercalcemic toxicity at a concentration of $1\mu\text{g}/\text{kg}$, 20S-(OH)D3 is not hypercalcemic at concentrations as high as $60\mu\text{g}/\text{kg}$ [154, 156, 158, 162].

*Modified with permission. Qinghui Wang, Zongtao Lin, Tae-Kang Kim, Andrzej T. Slominski, Duane D. Miller, Wei Li. Total synthesis of biologically active 20S-hydroxyvitamin D3. *Steroids*, 2015, 104: 153-162

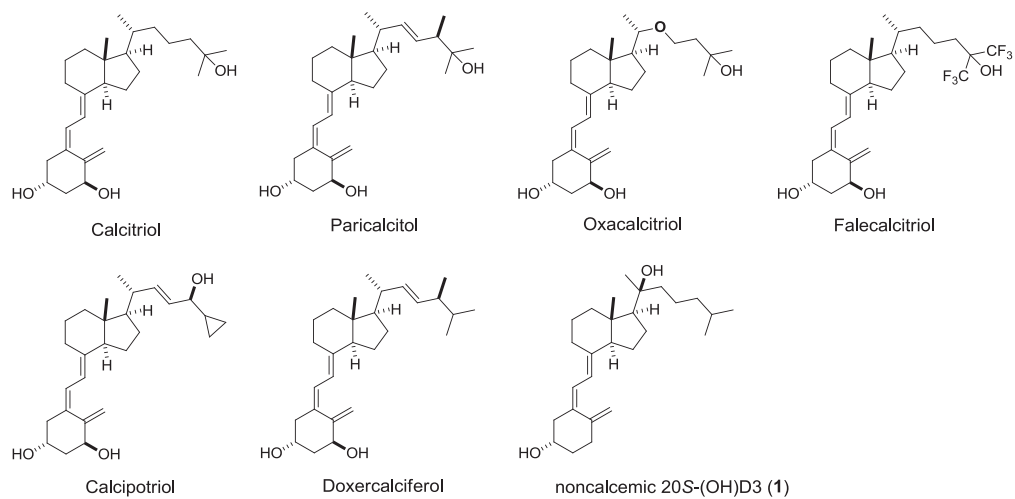


Figure 6-1. Marketed vitamin D analogs and noncalcemic 20S-(OH)D3

In-depth evaluation of the biological activity for 20*S*-(OH)D₃ or its analogs was hampered by lack of an efficient synthetic method of its production [239] without using costly enzymatic approaches [150, 151, 240]. 20*S*-(OH)D₃ was first chemically synthesized from pregnenolone acetate via Grignard reaction and low yielding UVB irradiation to afford low milligram scale of 20*S*-(OH)D₃ stereo-specifically. However, this method also generated structurally similar and physicochemically active by-products including previtamin D₃, lumisterol and tachysterol which presented a significant challenge in the purification of 20*S*-(OH)D₃ even through preparative HPLC [239]. Due to these disadvantages, scope of synthesis through UVB irradiation of 5,7-dienal precursor, 20*S*-(OH)-7-dehydrocholesterol was confined to very few derivatives, if not to almost exclusive production of 20*S*-(OH)D₃. Therefore, an approach that could easily generate large quantity of 20*S*-(OH)D₃ with high quality (> 98% purity) would facilitate further modifications on the side chain to determine the structure-activity relationships of this promising 20*S*-hydroxyl scaffold. Herein, we report an efficient total synthetic route for stereospecific 20*S*-(OH)D₃.

Experimental Section

General chemistry

Tetrahydrofuran was distilled from sodium-benzophenone. All other solvents and chemical reagents were obtained from commercial sources and directly used without further purification. Ergocalciferol was purchased from Chem Impex International Inc. Glassware was oven-dried before use. All reactions were performed under an argon atmosphere. TLC was performed on silica gel 60 GF254 and monitored under UV light or visualized using phosphomolybdic acid reagent. Flash chromatography was performed on 230-400 mesh silica gel (Fisher Scientific). Preparative TLC was performed on Analtech TLC Uniplates (250 μm). Melting points were recorded on a MPA100 Automated Melting Point Apparatus. NMR spectra were obtained on a Bruker Ascend 400 (Billerica, MA) spectrometer or a Varian Inova-500 spectrometer (Agilent Technologies, Santa Clara, CA). HR-MS were obtained on Waters Acquity UPLC linked to Waters Acquity Photodiode Array Detector and Waters Acquity Single Quadrupole Mass Detector. Chemical shifts are given in ppm with tetramethylsilane (TMS) as an internal reference. All coupling constants (*J*) are given in Hertz (Hz).

Chemical synthesis

(4*R*,7*aR*)-1-((2*R*,5*R*,*E*)-5,6-dimethylhept-3-en-2-yl)-4-((*R*,*Z*)-1-hydroxy-2-((*S*)-5-hydroxy-2-methylenecyclohexylidene)ethyl)-7*a*-methyloctahydro-1*H*-inden-4-ol (2). Following a reported procedure [241], to a solution of ergocalciferol (20 g, 50.5 mmol) in ethanol (2 L) at -45 °C was added dropwise solution of potassium permanganate (9.0 g, 58.7 mmol) in water (300 mL), the mixture was stirred for half an hour and further 1 hour at -15 °C and then warmed to room temperature. After 3 hours,

the precipitate was filtered off and the solution was evaporated to give yellowish crude oil. The crude oil was purified on silica gel column chromatography eluting with hexane/ethyl acetate (3:1) to give pure triol compound **2** as white solid (10.5 g, 65%) and unreacted starting material (5.1 g). Mp: 170-172 °C (MeOH). ¹H NMR (400 MHz, CD₃OD): δ 5.52 (dd, *J* = 9.9, 1.7 Hz, 1H, 6-H), 5.30 – 5.09 (m, 2H, 22/23-H), 5.02 – 4.98 (m, 2H, 7/19-H), 4.90 (d, *J* = 9.9 Hz, 1H, 19-H), 3.65 (m, 1H, 3-H), 2.55 (ddd, *J* = 12.4, 4.5, 1.9 Hz, 1H), 2.49 – 2.38 (m, 1H), 2.17 – 1.90 (m, 5H), 1.90 – 1.68 (m, 4H), 1.62 (m, 1H), 1.56 – 1.39 (m, 4H), 1.39 – 1.03 (m, 5H), 1.00 (d, *J* = 6.6 Hz, 3H, 21-H), 0.94 (d, *J* = 6.8 Hz, 3H, 28-H), 0.89 – 0.81 (t, *J* = 6.4 Hz, 9H, 18/26/27-H). ¹³C NMR (101 MHz, CD₃OD): δ 147.35, 140.78, 137.06, 133.12, 126.72, 111.72, 76.25 (C7), 71.42 (C8 or C3), 71.39 (C3 or C8), 61.04, 58.79, 47.60, 45.14, 44.36, 41.70, 41.53, 39.23, 37.21, 34.50, 34.38, 29.13, 22.87, 21.76, 21.29, 20.52, 20.12, 18.27, 13.59. ESI-HRMS: calculated for C₂₈H₄₆O₃Na [M+Na]⁺ 453.3345, found 453.3352.

(S,Z)-3-(2-hydroxyethylidene)-4-methylenecyclohexanol(3) and (4S,7aR)-1-((2R,5R,E)-5,6-dimethylhept-3-en-2-yl)-7a-methyloctahydro-1H-inden-4-ol (4). To a suspension of **2** (6.0 g, 13.9 mmol) and sodium carbonate (14.6 g, 138 mmol) in dichloromethane (50 mL) was added lead tetraacetate (6.7 g, 15.3 mmol) in portions at 0 °C. After 2 hours, the reaction was quenched with ethylene glycol and the mixture was vigorously stirred at 0 °C for 10 minutes. Water was then added and the mixture was extracted with dichloromethane for five times, washed with brine and dried with Na₂SO₄. The combined extracts were evaporated to give crude oil mixture, which was used for next step without further purification. To a solution of the above crude oily mixture in benzene (100 mL) at 0 °C under argon with stirring, Red-Al (28.7 mmol, 8.6 mL) was added dropwise and the mixture was stirred for 2 hours. On completion reaction was quenched with water. The mixture was filtered off and extracted with ethyl acetate, washed with brine and dried with anhydrous Na₂SO₄. Organic phase was evaporated to generate crude oil mixture which was purified by flash chromatography on silica. Elution with hexane/ethyl acetate (10:1) gave pure alcohol compound **4** as transparent oil (3.3 g, 86% for two steps), further elution with hexane/ethyl acetate (1:2) gave pure allylic alcohol **3** as colorless oil (0.91 g, 43% for two steps). compound **3**: ¹H NMR (400 MHz, CDCl₃): δ 5.45 (t, *J* = 6.6 Hz, 1H, 6-H), 4.97 (dd, *J* = 2.4, 1.3 Hz, 1H, 19-H), 4.59 (d, *J* = 2.3 Hz, 1H, 19-H), 4.25 (ddd, *J* = 12.7, 7.0, 1.2 Hz, 1H, 7-H), 4.14 (ddd, *J* = 12.6, 6.2, 1.3 Hz, 1H, 7-H), 3.94 (m, 1H, 3-H), 2.56 – 2.33 (m, 2H), 2.24 (dd, *J* = 13.2, 7.1 Hz, 1H), 2.19 – 2.06 (m, 1H), 1.87 (m, 1H), 1.75 – 1.60 (m, 1H). ¹³C NMR (101 MHz, CDCl₃): δ 144.51 (C10), 139.11 (C5), 125.95 (C6), 112.23 (C19), 68.64 (C3), 59.34 (C7), 44.82, 34.62, 31.45. ESI-HRMS: calculated for C₉H₁₁, [M-2H₂O+H]⁺ 119.0861, found 119.0861. compound **4**: ¹H NMR (400 MHz, CDCl₃): δ 5.25 – 5.02 (m, 2H, C22/23-H), 4.02 (d, *J* = 2.8 Hz, 1H, C8-H), 2.04 – 1.88 (m, 2H), 1.86 – 1.73 (m, 3H), 1.73 – 1.60 (m, 1H), 1.56 – 1.33 (m, 5H), 1.33 – 1.02 (m, 5H), 0.96 (d, *J* = 6.6 Hz, 3H, 22-H), 0.92 (s, 3H, C18-H), 0.89 (d, *J* = 11.2 Hz, 3H, 23-H), 0.80 (t, *J* = 6.6 Hz, 6H, C26/27-H). ¹³C NMR (101 MHz, CDCl₃): δ 135.59, 131.70, 69.14 (C8), 56.48, 52.72, 42.78, 41.65, 40.32, 39.75, 33.53, 33.00, 27.57, 22.46, 20.71, 19.88, 19.55, 17.57, 17.40, 13.61. ESI-HRMS: calculated for C₁₉H₃₃ [M-H₂O+H]⁺ 261.2582, found 261.2582.

(S,Z)-tert-butyl(2-(5-((tert-butyldimethylsilyl)oxy)-2-methylenecyclohexylidene)ethoxy)dimethylsilane (5). Imidazole (1.4 g, 21.2 mmol) and *tert*-butyldimethylsilyl chloride (4.8 g, 31.6 mmol) was sequentially added to a solution of compound **3** (0.82 g, 5.3 mmol) in dichloromethane (50 mL) in a round bottom flask with stirring. The resulting suspension was stirred for 2 hours. Water was then added and the mixture was extracted with dichloromethane, washed with brine and dried with anhydrous Na₂SO₄. Evaporation under vacuum gave the oily residue which was subjected to flash chromatography on silica. Elution with hexane/ethyl acetate (80:1) gave pure compound **5** as colorless oil (1.8 g, 88%). ¹H NMR (400 MHz, CDCl₃): δ 5.38 (ddt, *J* = 6.8, 5.3, 1.3 Hz, 1H, 6-H), 4.95 (p, *J* = 1.1 Hz, 1H, 19-H), 4.57 (dd, *J* = 2.4, 1.3 Hz, 1H, 19-H), 4.31 (ddt, *J* = 13.0, 7.2, 0.9 Hz, 1H, 7-H), 4.21 (ddd, *J* = 12.9, 5.3, 2.1 Hz, 1H, 7-H), 3.82 (tt, *J* = 8.9, 3.9 Hz, 1H, 3-H), 2.47 – 2.31 (m, 2H), 2.22 – 2.13 (m, 1H), 2.06 (m, 1H), 1.93 – 1.80 (m, 1H), 1.56 (m, 1H), 0.89 (d, *J* = 4.7 Hz, 18H, TBS), 0.08 – 0.03 (s, 12H, TBS). ¹³C NMR (101 MHz, CDCl₃): δ 144.89 (C10), 138.24 (C5), 126.29 (C6), 111.95 (C19), 70.11 (C3), 60.59 (C7), 45.93, 36.03, 32.15, 26.01 (TBS), 25.86 (TBS), 18.43, 18.18, -4.65 (TBS), -4.69 (TBS), -4.99 (TBS), -5.05 (TBS). ESI-HRMS: calculated for C₂₁H₄₂O₂Si₂Na [M+Na]⁺ 405.2621, found 405.2629.

(S,Z)-2-(5-((tert-butyldimethylsilyl)oxy)-2-methylenecyclohexylidene)ethanol (6). To a solution of compound **5** (1.7 g, 4.4 mmol) in anhydrous THF (20 mL) in a round bottom flask at -5 °C under nitrogen, *tetra-n*-butylammonium fluoride (1.0 M in THF, 4.8 mmol) was added dropwise with stirring. The resulting mixture was stirred for 3 hours, water was then added and the brown mixture was extracted with dichloromethane, washed with brine and dried with anhydrous Na₂SO₄. The combined extracts were evaporated under vacuum to give the oily residue which was purified with flash chromatography on silica. Pure allylic alcohol **6** was eluted out with hexane/ethyl acetate (50:1) as colorless oil (0.93 g, 78%). ¹H NMR (400 MHz, CDCl₃): δ 5.44 (ddt, *J* = 7.3, 5.9, 1.3 Hz, 1H, 6-H), 4.96 (d, *J* = 1.2 Hz, 1H, 19-H), 4.62 (t, *J* = 2.4 Hz, 1H, 19-H), 4.43 – 4.01 (m, 2H, 7-H), 3.84 (m, 1H, 3-H), 2.48 – 2.33 (m, 2H), 2.26 – 2.14 (m, 1H), 2.13 – 2.01 (m, 1H), 1.87 (m, 1H), 1.58 (m, 1H), 0.88 (s, 9H, TBS), 0.06 (d, *J* = 2.9 Hz, 6H, TBS). ¹³C NMR (101 MHz, CDCl₃): δ 144.83, 140.52, 124.88, 111.91, 70.11 (C3), 59.82 (C7), 46.02, 35.98, 32.26, 25.82 (TBS), 18.15, -4.67 (TBS), -4.71 (TBS). ESI-HRMS: calculated for C₁₅H₂₈O₂SiNa [M+Na]⁺ 291.1756, found 291.1755.

(S,Z)-(2-(5-((tert-butyldimethylsilyl)oxy)-2-methylenecyclohexylidene)ethyl)diphenylphosphine oxide (7). To a solution of the allylic alcohol **6** (0.81 g, 3.0 mmol) in anhydrous THF (20 mL) was added *n*-BuLi (2.5 M in hexanes, 30.0 mmol) under argon at 0 °C with stirring. After 5 minutes, a solution of *p*-tosyl chloride (598 mg, 3.15 mmol) dissolved in anhydrous THF (10 mL) was added to the allylic alcohol-BuLi solution. On the other side, to a solution of diphenylphosphine (1.02 mL, 6.0 mmol) in anhydrous THF (5 mL) under argon at 0 °C with stirring *n*-BuLi (2.5 M in hexanes, 2.2 mL, 5.7 mmol) was added dropwise to provide a red solution. After 10 minutes 4.1 mL of the red solution was then drawn to add to the solution of tosylate. The mixture was stirred for 30 minutes at 0 °C and quenched with H₂O (1 mL). Evaporation of the solution under vacuum gave a phosphine residue. To the phosphine residue in dichloromethane (15 mL) at 0 °C with stirring was added 10% H₂O₂ (1.1 mL).

Reaction was quenched with water, extracted with dichloromethane, washed with cold saturated sodium sulfite solution and brine and dried with Na₂SO₄. Organic solvent was removed under vacuum to give crude residue which was subjected to flash chromatography on silica for purification. Elution with hexane/ethyl acetate (3:1) gave pure phosphine oxide compound **7** as white solid (800 mg, 59%). Mp: 94-96 °C (EtOAc). ¹H NMR (400 MHz, CDCl₃): δ 7.71 (m, 4H, Ph), 7.56 – 7.36 (m, 6H, Ph), 5.35 (q, *J* = 7.2 Hz, 1H, 6-H), 4.92 (t, *J* = 1.9 Hz, 1H, 19-H), 4.68 (dd, *J* = 2.4, 1.3 Hz, 1H, 19-H), 3.52 (m, 1H, 3-H), 3.36 (m, 1H, 7-H), 3.20 (m, 1H, 7-H), 2.44 – 2.31 (m, 1H), 2.22 (dt, *J* = 13.3, 4.7 Hz, 1H), 2.15 – 2.05 (m, 1H), 1.81 – 1.71 (m, 1H), 1.66 (m, 1H), 1.47 (m, 1H), 0.83 (s, 9H, TBS), -0.00 (d, *J* = 2.0 Hz, 6H, TBS); ¹³C NMR (101 MHz, CDCl₃): δ 145.03, 145.01, 142.62, 142.50, 133.49, 132.99, 132.52, 132.00, 131.75, 131.73, 131.61, 131.58, 131.20, 131.11, 130.95, 130.86, 128.59, 128.48, 128.44, 128.32, 113.19, 113.11, 111.60, 111.59, 70.46 (C3), 70.43, 46.68, 46.66, 36.21, 32.48, 32.46, 31.44, 30.74, 25.82 (TBS), 18.12, -4.69 (TBS), -4.75 (TBS). ESI-HRMS: calculated for C₂₇H₃₇O₂PSiNa [M+Na]⁺ 475.2198, found 475.2203.

(4S,7aR)-1-((2R,5R,E)-5,6-dimethylhept-3-en-2-yl)-7a-methyloctahydro-1H-inden-4-yl acetate (8). Pyridine (1.3 mL, 16.1 mmol), 4-dimethylaminopyridine (352 mg, 2.88 mmol) and acetyl anhydride (0.98 mL, 104 mmol) was sequentially added to a solution of compound **4** (3.2 g, 11.5 mmol) in anhydrous dichloromethane (30 mL) in a round bottom flask under argon. The resulting mixture was stirred for 3 hours. Water was then added and the mixture was extracted with dichloromethane, washed with saturated NaHCO₃, 0.1 M HCl and brine and then dried with Na₂SO₄. Evaporation under vacuum gave the oily residue which was purified with flash chromatography on silica. Elution with hexane/ethyl acetate (30:1) gave pure compound **8** as colorless oil (3.4 g, 92%). ¹H NMR (400 MHz, CDCl₃): δ 5.31 – 5.00 (m, 3H, 8/22/23-H), 2.12 – 1.92 (m, 5H), 1.92 – 1.53 (m, 4H), 1.53 – 1.03 (m, 10H), 0.99 (d, *J* = 2.4 Hz, 3H, 22-H), 0.94 – 0.85 (m, 6H), 0.82 (t, *J* = 6.8 Hz, 6H, 26/27-H). ¹³C NMR (101 MHz, CDCl₃): δ 170.73 (acetyl), 135.47, 131.90, 71.35 (C8), 56.31, 51.41, 42.79, 41.82, 39.90, 39.84, 33.05, 30.50, 27.47, 22.61, 21.31, 20.77, 19.93, 19.60, 17.90, 17.60, 13.17. ESI-HRMS: calculated for C₂₁H₃₆O₂Na [M+Na]⁺ 343.2613, found 343.2614.

(4S,7aR)-1-((2S,3R,4R,5R)-3,4-dihydroxy-5,6-dimethylheptan-2-yl)-7a-methyloctahydro-1H-inden-4-yl acetate (9). To a solution of the compound **8** (3.3 g, 10.3 mmol) in acetone (40 mL) was added *N*-methylmorpholine *N*-oxide (6.0 g, 51.5 mmol) and 2.5% osmium tetroxide in *tert*-butanol (6.5 mL, 0.52 mmol) at room temperature with stirring. After 48 hours, water and ethyl acetate was added and the organic phase was separated, washed with brine and dried with Na₂SO₄. Evaporation under vacuum gave the oily residue which was purified with flash chromatography on silica. Elution with hexane/ethyl acetate (10:1) gave pure compound **9** as colorless oil (2.44 g, 67%). ¹H NMR (400 MHz, CDCl₃): δ 5.14 (d, *J* = 2.6 Hz, 1H, 8-H), 3.71 (dd, *J* = 2.4, 4.4 Hz, 1H, 22-H), 3.59 (t, *J* = 2.8 Hz, 1H, 23-H), 2.39 (s, 1H), 2.04 (s, 4H), 1.94 – 1.79 (m, 2H), 1.70 (m, 5H), 1.55 – 1.09 (m, 9H), 1.00 (d, *J* = 6.9 Hz, 3H, 21-H), 0.96 (d, *J* = 6.7 Hz, 3H, 28-H), 0.92 – 0.84 (m, 9H, 18/26/27-H). ¹³C NMR (101 MHz, CDCl₃): δ 170.80 (acetyl), 73.26 (C23), 71.19 (C8), 70.26 (C22), 53.02, 51.04, 44.11, 43.93, 42.45,

41.65, 40.00, 30.49, 29.89, 29.75, 26.91, 22.82, 21.44, 21.34, 18.94, 17.88, 13.91, 13.52, 12.83, 9.91. ESI-HRMS: calculated for $C_{21}H_{38}O_4Na$ $[M+Na]^+$ 377.2668, found 377.2668.

(4S,7aR)-7a-methyl-1-((S)-1-oxopropan-2-yl)octahydro-1H-inden-4-yl acetate (10). To a suspension of compound **9** (2.2 g, 6.2 mmol) in THF-H₂O (4:1, 10 mL), sodium periodate (1.45 g, 6.82 mmol) was added at 0 °C in portions with stirring. After 1 hour, the reaction was quenched with ethylene glycol and the mixture was stirred at 0 °C for 10 minutes. Water was then added and the mixture was extracted with ethyl acetate for three times, washed with brine and dried with Na₂SO₄. The combined extracts were evaporated to give crude oil, which was purified with flash chromatography on silica. Elution with hexane/ethyl acetate (5:1) gave pure compound **10** as transparent oil (1.03 g, 66%). ¹H NMR (400 MHz, CDCl₃): δ 9.57 (d, *J* = 3.2 Hz, 1H, CHO), 5.17 (d, *J* = 2.0 Hz, 1H, 8-H), 2.36 (m, 1H, 20-H), 2.05 (s, 3H), 1.97 (dt, *J* = 12.3, 3.3 Hz, 1H), 1.89 – 1.71 (m, 3H), 1.59 – 1.24 (m, 8H), 1.11 (d, *J* = 6.8 Hz, 3H, 21-H), 0.93 (s, 3H, 18-H). ¹³C NMR (101 MHz, CDCl₃): δ 204.78 (CHO), 170.70 (acetyl), 70.89 (C8), 51.37, 50.74, 49.17, 42.47, 39.75, 30.47, 26.00, 22.95, 21.32, 17.83, 13.42, 13.35. ESI-HRMS: calculated for $C_{15}H_{23}O_2$ $[M-H_2O+H]^+$ 235.1698, found 235.1696.

(1S,4S,7aS)-1-acetyl-7a-methyloctahydro-1H-inden-4-yl acetate (12). To a stirred solution of compound **10** (1.0 g, 3.9 mmol) in benzene (8 mL) was added morpholine (0.524 mL, 4.8 mmol) and *p*-toluenesulfonic acid (34mg, 0.195 mmol). The mixture was refluxed over a Dean-Stark water separator overnight. During the course of the reaction the theoretical amount of water (~70 mg) was separated. Upon completion as indicated by mass spectrum, the reaction mixture was cooled to room temperature and solvent was removed under vacuum to afford yellowish oil which was immediately used for next step. To a stirred solution of the above crude mixture in acetone (20 mL) was added alumina (481 mg, 4.72 mmol) supported potassium permanganate (616 mg, 3.9 mmol) in portions. The reaction mixture was filtered after 2 hours and washed with ethyl acetate. Solvents were removed under vacuum to afford crude oily product which was purified with flash chromatography on silica. Elution with hexane/ethyl acetate (6:1) gave pure compound **12** as colorless oil (659 mg, 70% for two steps). ¹H NMR (400 MHz, CDCl₃): δ 5.16 (d, *J* = 2.8 Hz, 1H, 8-H), 2.48 (dd, *J* = 10.0, 8.0 Hz, 1H, 17-H), 2.20 – 1.99 (m, 8H), 1.92 – 1.82 (m, 1H), 1.70 – 1.39 (m, 8H), 0.81 (s, 3H, 18-H). ¹³C NMR (101 MHz, CDCl₃): δ 208.52 (C20), 170.26 (acetyl), 70.27 (C8), 63.54, 51.15, 43.06, 38.85, 31.26, 30.08, 22.54, 21.46, 20.98, 17.64, 14.51 (C18). ESI-HRMS: calculated for $C_{14}H_{22}O_3Na$ $[M+Na]^+$ 261.1467, found 261.1467.

(1S,4S,7aS)-1-((S)-2-hydroxy-6-methylheptan-2-yl)-7a-methyloctahydro-1H-inden-4-ol (14). To a stirred suspension of magnesium (181 mg, 7.5 mmol) in anhydrous THF (10 mL) was added 1-bromo-4-methyl-pentane (0.733 mL, 5.0 mmol) under argon at room temperature. The mixture was then refluxed for 2 hours and cooled down in ice bath to give Grignard reagent **13** which was used without further purification. Compound **12** (100 mg, 0.42 mmol) in 2 mL THF was subsequently added to the reaction mixture which was warmed to room temperature after 30 minutes and stirred overnight. Cooled saturated NH₄Cl solution was added to quench the reaction and the mixture was extracted with ethyl acetate for three times, washed with brine and dried with Na₂SO₄. The

combined extracts were evaporated to give crude oil, which was purified with flash chromatography on silica. Elution with hexane/ethyl acetate (3:1) afforded pure compound **14** as colorless oil (94 mg, 80%). ¹H NMR (400 MHz, CDCl₃): δ 4.09 (d, *J* = 2.8 Hz, 1H, 8-H), 2.14 – 2.02 (m, 1H), 1.91 – 1.74 (m, 3H), 1.74 – 1.37 (m, 9H), 1.37 – 1.08 (m, 14H), 0.87 (dd, *J* = 6.7, 0.8 Hz, 6H, 26/27-H). ¹³C NMR (101 MHz, CDCl₃): δ 75.14 (C20), 69.41 (C8), 57.82, 52.55, 44.10, 42.52, 40.77, 39.56, 33.42, 27.92, 26.29, 22.71, 22.55, 22.21, 21.94, 21.30, 17.39, 15.44. ESI-HRMS: calculated for C₁₈H₃₁ [M-2H₂O+H]⁺ 247.2426, found 247.2430.

(1S,7aR)-1-((S)-2-hydroxy-6-methylheptan-2-yl)-7a-methylhexahydro-1H-inden-4(2H)-one (15). To a stirred solution of compound **14** (84 mg, 0.3 mmol) in dichloromethane (10 mL) was added pyridinium dichromate (225 mg, 0.6 mmol) at room temperature. The reaction mixture was stirred for 1 hour and filtered through celite. The celite was washed with dichloromethane and the combined solvent was removed under vacuum to give crude oily product which was purified with flash chromatography on silica. Elution with hexane/ethyl acetate (8:1) gave pure compound **15** as colorless oil (74 mg, 89%). ¹H NMR (400 MHz, CDCl₃): δ 2.43 (dd, *J* = 10.5, 6.9 Hz, 1H, 9-H), 2.33 – 2.13 (m, 3H, 9/12/14-H), 2.07 – 1.83 (m, 2H), 1.82 – 1.66 (m, 4H), 1.66 – 1.40 (m, 4H), 1.35 – 1.10 (m, 9H), 0.87 (d, *J* = 6.6 Hz, 6H, 26/27-H), 0.80 (s, 3H, 18-H). ¹³C NMR (101 MHz, CDCl₃): δ 211.99 (C8), 74.63 (C20), 62.10, 58.04, 49.84, 44.07, 40.80, 39.47, 39.26, 27.89, 26.53, 23.90, 22.67, 22.52, 21.95, 21.77, 18.73, 14.37. ESI-HRMS: calculated for C₁₈H₃₁O [M-H₂O+H]⁺ 263.2375, found 263.2377.

(1S,7aR)-1-((S)-2-(ethoxymethoxy)-6-methylheptan-2-yl)-7a-methylhexahydro-1H-inden-4(2H)-one (16). To a stirred solution of compound **15** (67 mg, 0.24 mmol), *N,N*-diisopropylethylamine (83 μL, 0.48 mmol) and 4-dimethylaminopyridine (12 mg, 0.096 mmol) in anhydrous dichloromethane (3 mL) was added chloromethyl ethyl ether (45 μL, 0.48 mmol) dropwise at ice temperature. The resulting mixture was stirred for overnight at room temperature. Water was then added and the reaction mixture was extracted with dichloromethane, washed with brine and dried with Na₂SO₄. The combined extracts were evaporated under vacuum to give the oily residue which was separated with flash chromatography on silica. Elution with hexane/ethyl acetate (30:1) gave pure compound **16** as colorless oil (73 mg, 90%). ¹H NMR (400 MHz, CDCl₃): δ 4.81 – 4.64 (m, 2H, EOM), 3.69 – 3.45 (m, 2H, EOM), 2.41 (dd, *J* = 11.5, 7.0 Hz, 1H), 2.32 – 2.06 (m, 3H), 2.03 – 1.43 (m, 11H), 1.31 (s, 3H, 21-H), 1.26 – 1.09 (m, 7H), 0.86 (dd, *J* = 6.6, 0.9 Hz, 6H, 26/27-H), 0.76 (s, 3H, 18-H). ¹³C NMR (101 MHz, CDCl₃): δ 212.17 (C8), 88.76 (EOM), 79.75 (C20), 63.20 (EOM), 62.19, 57.31, 49.72, 40.83, 40.26, 39.70, 39.40, 27.87, 23.92, 23.21, 22.70, 22.57, 22.50, 21.70, 18.74, 15.14, 14.66. ESI-HRMS: calculated for C₂₁H₃₈O₃Na [M+Na]⁺ 361.2719, found 361.2719.

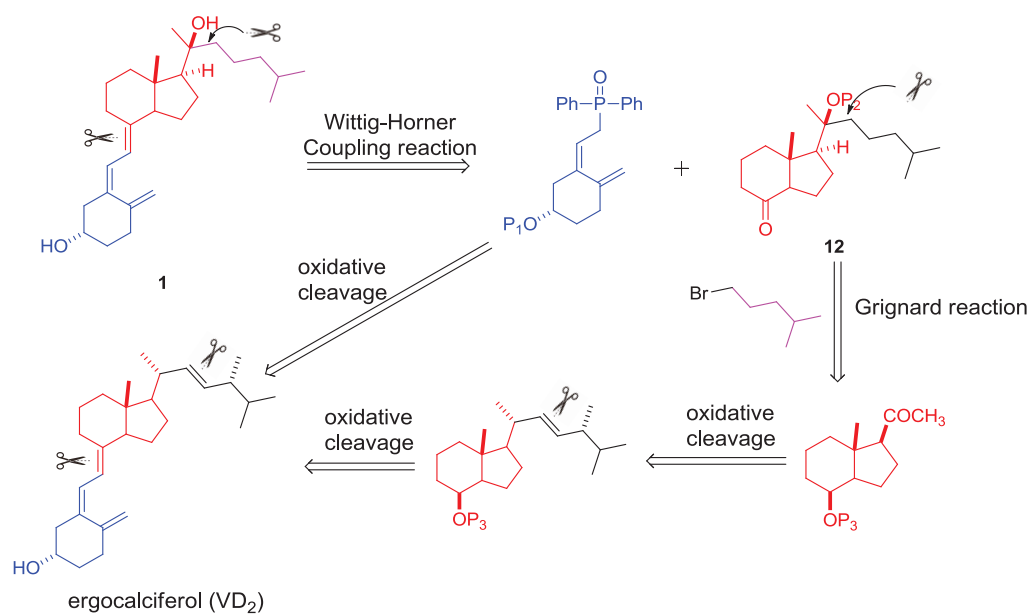
Tert-butyl(((1S,Z)-3-((E)-2-((1S,7aS)-1-((S)-2-(ethoxymethoxy)-6-methylheptan-2-yl)-7a-methylhexahydro-1H-inden-4(2H)-ylidene)ethylidene)-4-methylenecyclohexyl)oxy)dimethylsilane (17). To a stirred solution of compound **7** (51 mg, 0.15 mmol) in anhydrous THF (3 mL) was added phenyllithium (1.8 M in hexanes, 0.37 mmol) under argon at -78 °C. The mixture was stirred for another 30 minutes at this

temperature and was added precooled compound **16** (167 mg, 0.37 mmol) in 100 μ L anhydrous THF. Reaction was kept stirring at this temperature for 3 hours and further 12 hours at room temperature. Water was then added and the reaction mixture was extracted with ethyl acetate, washed with brine and dried with Na₂SO₄. The combined extracts were evaporated under vacuum to give the oily residue which was purified with flash chromatography on silica. Elution with hexane/ethyl acetate (30:1) gave pure compound **17** as colorless oil (45 mg, 52%). ¹H NMR (400 MHz, CDCl₃): δ 6.16 (d, *J* = 11.2 Hz, 1H, 6-H), 6.01 (d, *J* = 11.2 Hz, 1H, 7-H), 5.02 (s, 1H, 19-H), 4.85 – 4.64 (m, 3H, 19-H and EOM), 3.81 (m, 1H, H-3), 3.71 – 3.50 (m, 2H, EOM), 2.82 (d, *J* = 12.4 Hz, 1H, 9-H), 2.44 (dd, *J* = 13.0, 4.2 Hz, 1H), 2.36 (dt, *J* = 13.5, 4.8 Hz, 1H), 2.28 – 2.17 (m, 1H), 2.16 – 1.93 (m, 3H), 1.93 – 1.79 (m, 2H), 1.77 – 1.44 (m, 13H), 1.39 – 1.08 (m, 12H), 0.87 (d, *J* = 7.7 Hz, 15H, 26/27-H and TBS), 0.67 (s, 3H, 18-H), 0.06 (d, *J* = 2.2 Hz, 6H, TBS); ¹³C NMR (101 MHz, CDCl₃): δ 145.34 (C10), 141.18 (C8), 136.36 (C5), 121.32 (C6), 118.21 (C7), 112.13 (C19), 88.80 (EOM), 80.42 (C20), 70.54 (C3), 63.14 (EOM), 57.38, 56.63, 46.84, 45.73, 40.98, 40.30, 39.79, 36.34, 32.73, 28.80, 27.94, 25.99, 25.96, 25.91, 25.88, 23.32, 22.97, 22.77, 22.55, 21.98, 21.91, 18.18, 15.19, 14.15, -4.59 (TBS), -4.63 (TBS). ESI-HRMS: calculated for C₃₆H₆₄O₃SiNa [M+Na]⁺ 595.4522, found 595.4509.

(1S,Z)-3-((E)-2-((1S,7aS)-1-((S)-2-hydroxy-6-methylheptan-2-yl)-7a-methylhexahydro-1H-inden-4(2H)-ylidene)ethylidene)-4-methylenecyclohexanol (1). To a stirred solution of compound **17** (10 mg, 0.017 mmol) in MeOH-DCM (5:1, 3 mL) was added camphorsulfonic acid (4.3 mg, 0.020 mmol) at room temperature. The mixture was stirred for 3 hours and saturated NaHCO₃ was added. The mixture was extracted with dichloromethane, washed with brine and dried with Na₂SO₄. The combined extracts were evaporated under vacuo to give the oily residue which was purified with preparative TLC (hexane/ethyl acetate = 5:1) to afford pure compound **1** as colorless solid (2.6 mg, 37%). Mp: 91-93 °C (MeOH). ¹H NMR (400 MHz, CD₃OD): δ 6.22 (d, *J* = 11.2 Hz, 1H, 6-H), 6.02 (d, *J* = 11.2 Hz, 1H, 7-H), 5.08 – 5.00 (s, 1H, 19-H), 4.74 (d, *J* = 1.6 Hz, 1H, 19-H), 3.76 (m, 1H, 3-H), 2.85 (dd, *J* = 11.9, 4.0 Hz, 1H, 9-H), 2.58 – 2.48 (dd, 13.0, 4.2, 1H, 4-H), 2.40 (dt, *J* = 13.6, 4.9 Hz, 1H, 1-H), 2.25 – 1.91 (m, 5H), 1.81 – 1.62 (m, 5H), 1.61 – 1.43 (m, 6H), 1.43 – 1.09 (m, 11H), 0.89 (d, *J* = 6.6 Hz, 6H, 26/27-H), 0.69 (s, 3H, 18-H). ¹³C NMR (101 MHz, CD₃OD): δ 147.00 (C10), 142.30 (C8), 137.34 (C5), 122.61 (C6), 119.37 (C7), 112.65 (C19), 75.99 (C20), 70.55 (C3), 59.89, 57.80, 47.02, 45.11, 42.25, 40.95, 36.60, 33.59, 29.84, 29.17, 26.15, 24.44, 23.16, 23.06, 23.02, 22.97, 14.14. ESI-HRMS: calculated for C₂₇H₄₄O₂Na [M+Na]⁺ 423.3239, found 423.3235.

Chemistry

A retrosynthetic strategy was proposed as **Scheme 6-1**. The vitamin D3 scaffold could be established by Wittig-Horner coupling reaction between phosphine oxide **7** and C/D-ring fragment **16**. Due to steric effect of 18-methyl, stereoselective generation of 20*S*-hydroxy of **16** could be achieved using Grignard reagent **13** to attack **12**. In addition, introducing a relatively bulky protecting group on 8*S*-hydroxy was envisioned to assist the stereoselectivity of Grignard reaction. Conversion of VD2 to **7** and **12** could be

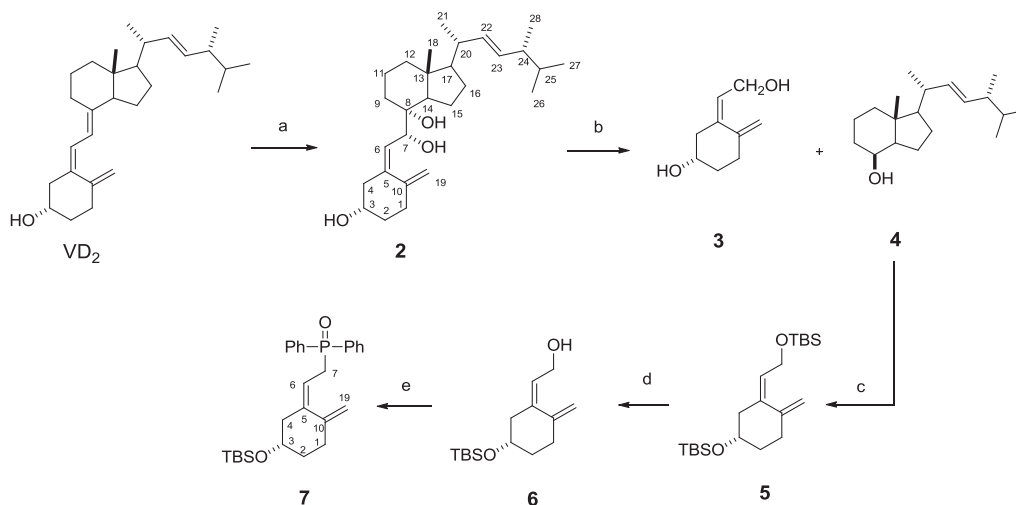


Scheme 6-1. Retrosynthetic analysis of 20S-(OH)D₃

carried out through oxidative cleavages.

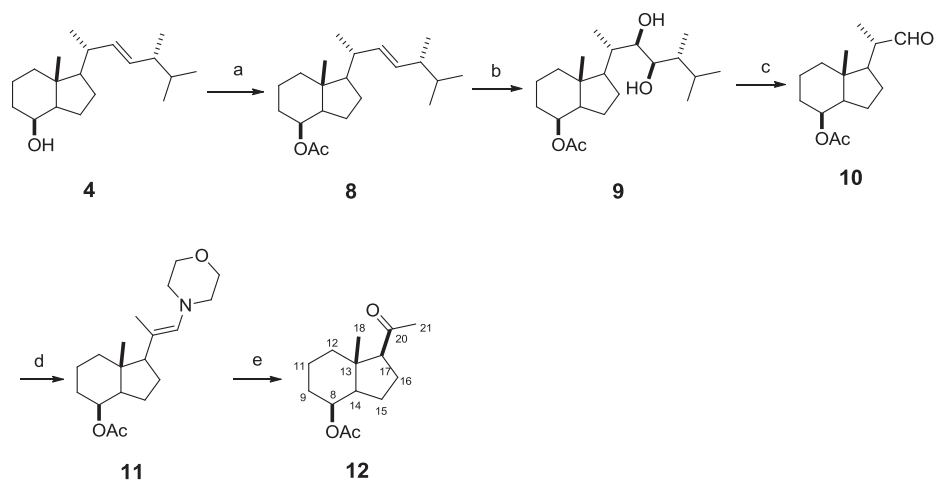
The synthesis of phosphine oxide **7** and protected C/D-ring ketone **12** were performed following literature reports [241, 242]. To prepare **7** and **12** in large scale so as to facilitate future structure-activity relationship studies, we modified the synthesis which were outlined as **Scheme 6-2** and **Scheme 6-3**. Initially, commercially available ergocalciferol was regioselectively dihydroxylated on the triene linkage to provide triol **2** with a yield of 65% when treating with potassium permanganate in ethanol at low temperature. Due to steric effect of 18-methyl, single 7*R*,8*R*-diastereoisomer was exclusively isolated over chromatography [241]. It is worth mentioning that when 3-OH was protected with TBS, dihydroxylation of the triene did not proceed. Subsequent treatment of vicinol **2** with lead tetraacetate in dichloromethane in the presence of sodium carbonate led to formation of corresponding C/D-ring ketone and A-ring allylic aldehyde. Although complete consumption of **2** was indicated on TLC, after workup procedures and purification using flash chromatography, A-ring allylic aldehyde ended up with poor yield (<20%) while C/D-ring ketone was obtained in 94% yield. We found that A-ring allylic aldehyde was unstable when exposed to air and moisture as clearly indicated by its spot on TLC and it should be used immediately. Thus, after quenching the oxidation reaction with ethylene glycol followed by simple workup procedure the crude mixture was directly used without purification to the following reduction step using excess equivalent of sodium bisaluminumhydride (65% in toluene) in benzene at 0 °C. Gratifyingly, these modified procedures afforded pure A-ring allylic alcohol **3** and C/D-ring alcohol **4** with yield of 43% and 86% for two steps after chromatography, respectively. It is worth noting that after TLC indicated completion of the oxidation reaction, quenching the reaction by adding ethylene glycol was crucial to prevent further oxidation of the aldehyde to carboxylic acid. In addition, compared with lithium aluminum hydride (LAH) and diisobutylaluminium hydride (DIBAL-H in toluene or tetrahydrofuran), Red-Al (>65% in toluene) was more efficient and regioselective to reduce only aldehyde rather than conjugated diene to form **3**. Compound **3** was subsequently protected with TBS to generate **5**, which underwent selective removal of TBS on the allylic moiety to produce alcohol **6** in 71% yield for two steps when stirring with *tetra-n*-butylammonium fluoride (TBAF) in THF under low temperature (-5 °C to ice temperature). The final A-ring intermediate phosphine oxide **7** was prepared following literature procedures in three steps with 59% overall yield [242].

Acetate **8** was produced when secondary alcohol **4** was treated with acetic anhydride and pyridine. Compound **8** was subjected to Upjohn reaction stirring with osmium tetroxide (0.5% wt in *t*-butanol) and *N*-methylmorpholine *N*-oxide in acetone at ambient temperature for 48 hr to form the major diastereoisomer **9** due to strong steric effect of 21- and 24-methyl groups. While TLC indicated existence of the other diastereomer as minor product, **9** was isolated in 67% yield. Cleavage of vicinol **9** in the presence of sodium periodate in H₂O-THF (1:4) provided aldehyde **10** in 66% yield. Aldehyde **10** was then refluxed in a Dean-Stark apparatus stirring with morpholine and catalytic amount of *p*-toluenesulfonic acid in benzene to form crude enamine **11** as, after dried on vacuum, slightly yellowish oil. Due to its instability and sensitivity to moisture,



Scheme 6-2. Synthesis of intermediate 7

Reagents and conditions: (a): KMnO_4 , $\text{EtOH-H}_2\text{O}$, rt; 65%; (b): i. $\text{Pb}(\text{OAc})_4$, Na_2CO_3 , DCM , 0°C ; ii. Red-Al, benzene, 0°C to rt; 43% for 3 and 86% for 4 in two steps; (c): TBSCl , Imidazole, DCM , rt; 88%; (d): TBAF , THF , rt; 78%; (e): i. $n\text{-BuLi}$, $p\text{-TsCl}$, THF , -78°C ; ii. $n\text{-BuLi}$, Ph_2PH , THF , -78°C ; iii. H_2O_2 , H_2O , DCM , rt; 59% in three steps.



Scheme 6-3. Synthesis of intermediate 12

Reagents and conditions: (a): Ac_2O , Pyr, DMAP, DCM, rt; 92%; (b): OsO_4 , NMO, Acetone/*t*-BuOH, rt; 67%; (c): NaIO_4 , H_2O -THF, 0°C ; 66%; (d): Morpholine, *p*-TsOH, PhH, reflux; (e): $\text{KMnO}_4/\text{Al}_2\text{O}_3$, Acetone, rt; 70% in two steps.

the crude enamine mixture was used for next step immediately without further purification. While the removal of C-22 on the chiron could be accomplished when treating **11** with singlet oxygen [242], this photo-oxygenation procedure was rather tedious. By referring to an alternative strategy [243], the yellowish oil was dissolved in acetone and treated with alumina supported potassium permanganate that was made prior to use, to provide the other key intermediate **12** in 70% for two steps after chromatography.

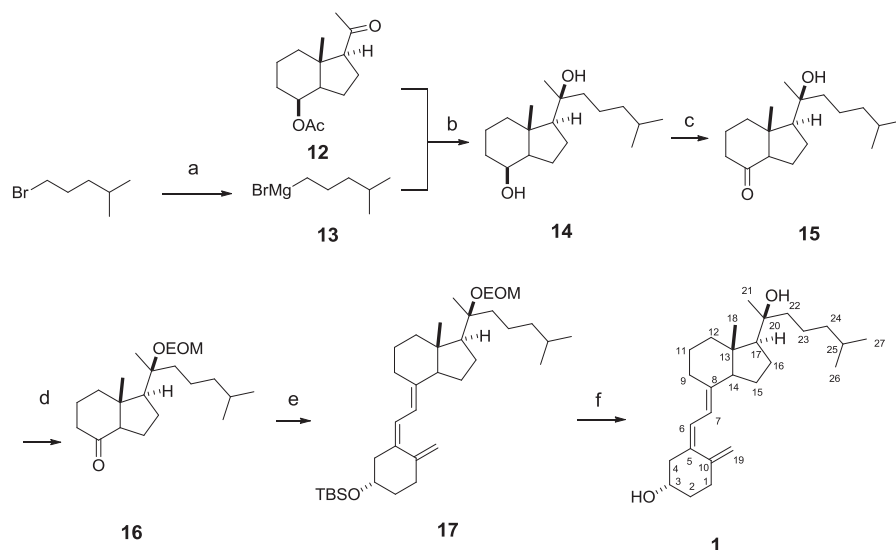
As shown in **Scheme 6-4**, Grignard reagent **13** was readily accessible by refluxing commercially available 1-bromo-4-methyl-pentane with magnesium in anhydrous THF. After 2 hours, **13** was immediately subjected to Grignard reaction to form the diol **14** with 80% yield. Similar to our previous studies [239], only the 20*S*-epimer was isolated over chromatography due to the steric effect of both 18-methyl and 8-acetyl. This stereospecificity is further supported by quantum mechanical calculations employing density functional theory (DFT) using Schrodinger Molecular Modeling Suite 2015. **Figure 6-2** shows the thermodynamically most stable and the preferred orientation of the acetyl group for the intermediate **12**. This conformational preference dictated the strongly favored back-side attack by the Grignard reagent **13** to form **14** with 20*S*-OH configuration. The attack from the front side to form 20*R*-OH configuration is sterically prohibited, consistent with what we found previously [239, 244]. Oxidation of diol **14** using Cornforth reagent pyridinium dichloromate (PDC) gave 20*S*-hydroxy Grundmann's ketone **15** in 89% yield. Compound **15** was subsequently introduced protecting group EOM on its tertiary alcohol to form ketone **16**, the other key intermediate for the final coupling step. With both C/D-ring fragment **16** and phosphine oxide **7** in hand, construction of the 20*S*-(OH)D₃ framework was successfully accomplished by employing Wittig-Horner reaction in the presence of phenyllithium (0.18 M, diluted from commercial source) in THF to form **17** in 52% yield. Simultaneously removal of EOM and TBS was achieved using camphorsulfonic acid (CSA) to produce the target compound 20*S*-(OH)D₃ in 37% yield.

Results

Figure 6-3 showed the comparison of ¹H-NMR of 20*S*-(OH)D₃s obtained from UVB irradiation and total synthesis. Clearly, similar to the one that was generated via UVB irradiation, 20*S*-(OH)D₃ obtained from total synthesis showed a desirable purity.

Discussion

20*S*-(OH)D₃, a noncalcemic vitamin D₃ analog, was enzymatically converted from vitamin D₃ by P450_{sec} and was first chemically synthesized via UVB irradiation [239]. However, this photochemical method also produces structurally similar and physicochemically active by-products that present a significant challenge for purification and further SAR studies for the promising 20*S*-hydroxyl scaffold. To overcome the



Scheme 6-4. Synthesis of 20S-(OH)D3

Reagents and conditions: (a): Mg, THF, reflux; (b): THF, reflux; 80% (c): PDC, DCM, rt; 89%; (d): EOMCl, DMAP, TEA, DCM, rt; 90%; (e): 7, PhLi, THF, -78°C to rt; 52%; (f): CSA, DCM-MeOH, rt; 37%.

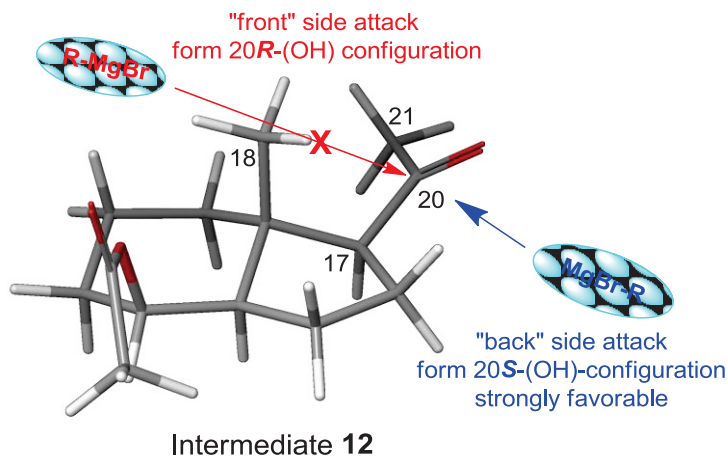


Figure 6-2. Preferred conformation of the intermediate (compound 12) calculated with density function theory with 6-31G** baseset

“Front” side attack by the bulky Grignard agent 13 to form 20R isomer of 14 is prohibited due to the steric hindrance from the 18-methyl and other moieties in compound 12, while the “back” side attack to form 20S isomer is strongly favored.

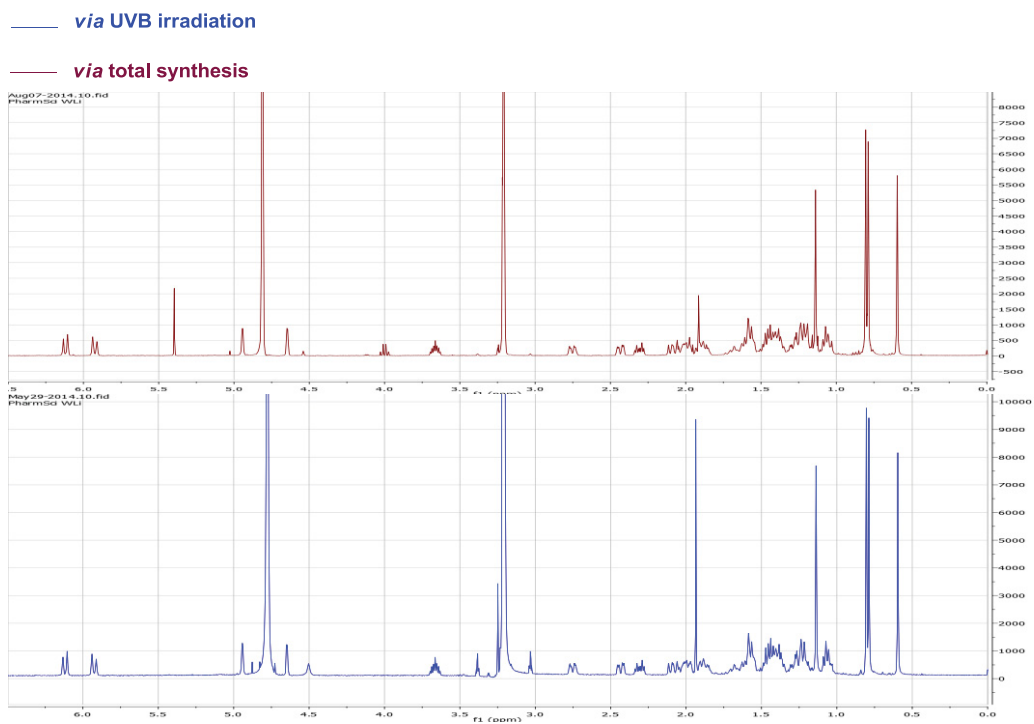


Figure 6-3. $^1\text{H-NMR}$ comparison of 20S-(OH)D3 obtained via UVB irradiation and total synthesis

deficiencies in current synthesis an alternative synthetic method was developed. The total synthetic strategy described in this report involves Wittig-Horner coupling and Grignard reaction and is successful in generating 20*S*-(OH)D₃ in 0.4% overall yield in 16 steps. A distinct advantage of this method over our previously reported method is that after we generate the two key intermediates phosphine oxide **7** and C/D-ring ketone **12** on gram scale from a common starting material vitamin D₂, we can efficiently make side chain derivatives for in-depth SAR studies of this 20*S*-hydroxyl scaffold.

CHAPTER 7. SUMMARY AND FUTURE DIRECTION

Cancer poses a tremendous challenge for public health in the 21st century. According to the statistics from the American Cancer Society, 1,688,780 new cases and 600,920 deaths are estimated to result from cancers in 2017. Melanoma is the least common but is the most lethal form of all skin cancers. About 80% deaths of patients with skin cancers are attributed to melanoma. Melanoma can spread to nearby lymph nodes and distant organ to eventually form advanced or metastatic melanoma. The overall 5-year survival rate for patients with advanced melanoma is as low as 5%. Encouragingly, targeted therapy and immunotherapy have achieved sensational success in the 2000s. Many BRAF inhibitors, MEK1/2 inhibitors, and immune checkpoint inhibitors have been approved by the FDA, vemurafenib, dabrafenib, trametinib, cobimetinib, nivolumab, pembrolizumab, Ipilimumab, for instance. These drugs are more effective to treat advanced melanoma than traditional chemotherapy (e.g., dacarbazine and temozolomide).

There are however problems within both targeted therapy and immune checkpoint inhibitors. For targeted therapy, patients are found to acquire drug-resistance after 6-month treatment with BRAF inhibitors vemurafenib or dabrafenib; the acquired resistance can markedly result in the resumption of tumor progression. Melanoma cancer cells develop drug-resistance to targeted therapy through many mechanisms; these mechanisms include but are not limited to: reactivation of the MAPK pathway by activating mutation of the downstream or upstream of BRAF; elevation of other RAF subtypes; BRAF amplification; ERK1/2 mutation; RTK upregulation; and PI3K pathway gene mutation. For immunotherapy, irAEs are significant problems. IrAEs if not treated in time, can be fatal.

Anticancer agents can be obtained from a natural source or through a medicinal chemistry program. Many of these agents are demonstrated to exhibit significant antitumor effects in preclinical and clinical trials, however, only a small portion of these agents are ultimately approved by the FDA for clinical cancer treatment. This is because that a large portion of antitumor agents are non-specific to tumor cells and can result in systemic toxicities to healthy cells. In the last decade, ADC is one of the most dynamic fields in drug discovery. ADC resorts to its antibody to selectively deliver cytotoxin to the target disease tissues or tumor cells. This can not only minimize the exposure of cytotoxins to healthy tissues but also maximize the concentration of cytotoxins to reach the tumors. Compared to cytotoxin alone, ADC generally has a broader therapeutic window.

ADC is composed of a potent cytotoxic chemical, a linker and an antibody. The roles of each portion of ADC are summarized well in excellent reviews published recently [166-168]. In general, all the three portions in ADC and the antigen localizing on the surface of tumor cell are vital for a successful ADC. The antigen should be highly expressed in the tumor instead of in the healthy tissue. This is because, on one hand, expression of antigen in the normal tissue can induce the ADC to move toward normal

cells and thereafter result in off-target toxicity; on the other hand, expression of antigen in the healthy tissue will reduce the availability of ADC to the tumor and lead to reduced antitumor effect [245]. In addition to the specificity in tumor, the antigen should have the ability to internalize the ADC upon its binding to the antibody; an inability of the antigen to recycle ADC to extracellular environment is also desirable in order to maintain the concentration of the free cytotoxic chemical in the cytoplasm of tumor cell. In ADC, the antibody is also critical. A favorable antibody should show not only high specificity and affinity to the antigen on the surface of tumor cell but also pharmacokinetic stability in circulating blood [246]. A stable antibody can increase the level of ADC to reach the antigen. Similarly, a stable linker in circulating blood also increases the opportunity for the ADC to bind to the antigen. Currently, linkers in ADCs can be divided into two groups: cleavable linkers (e.g., acid-labile linkers, protease cleavable linkers, and disulfide linkers) and non-cleavable linkers. The cleavable linkers are not only required to be stable in circulating blood but also should allow rapid release of cytotoxic chemical upon internalization to the cytoplasm of tumor cells [247, 248]. Cytotoxic chemical in ADC is named payload or warhead. A successful ADC highly depends on the payload. An ideal payload should have functional group(s) to conjugate to the linker; the new bond formed after conjugation should be stable in circulating blood. In addition to the conjugable site(s), the payload is strictly required to have significant potency (IC_{50} in sub-nanomolar range) [249].

The FDA has approved two ADCs for clinical uses. Brentuximab vedotin is approved in 2011 for the treatment of Hodgkin lymphoma and systemic anaplastic large cell lymphoma; trastuzumab emtansine is approved in 2013 for the treatment of HER2 positive breast cancer. There are approximately sixty ADCs in different stages of clinical trials currently. The payloads applied to the construction of ADCs are limited to mainly two categories: DNA-damaging agents and microtubule inhibitors. The challenges to broaden the pool of amenable payloads for ADCs development lie in: (1) the payload should be linkable; (2) the payload should be hydrophilic enough to prevent the antibody from aggregating; (3) the payload should overcome major drug-resistance mechanisms to prolong the therapeutic effect of ADC. Therefore, identification of payload with properties mentioned above is of importance.

ABI-231 is an anti-tubulin having potent antiproliferative activity (average IC_{50} = 5.2 nM) against a panel of cancer cell lines. ABI-231 binds to the colchicine binding site in tubulin and inhibits the tubulin polymerization. Importantly, ABI-231 can effectively overcome P-gp mediated drug-resistance and inhibit expression of tubulin β -III isotype. Its in-depth SAR study was however obstructed for many years due to an inefficient synthesis (0.28% over five steps).

In Chapter 2, we have established a novel synthetic method, which is amenable to SAR investigation and gram-scale synthesis of ABI-231. The synthetic strategy involves the synthesis of a diamine intermediate and imidazoline cyclization. Among the thirty new ABI-231 analogues, 4-methyl-3-indole and 4-indole analogues are the most potent and have average IC_{50} s of 2.2 and 3.0 nM, respectively. The co-crystal structure of 4-methyl-3-indole analogue in complex with tubulin reveals the existence of three H-bond

interactions between the ligand and receptor. *In vivo* efficacy evaluations of the most potent analogues in a subcutaneous mouse xenograft model with human A375 melanoma and an experimental lung metastasis model with B16F10 mouse melanoma are currently undergoing.

In a consecutive SAR study of ABI-231 as reported in Chapter 3, we modify the 3,4,5-TMP moiety in ABI-231. 3,4,5-TMP is one of the most common moieties in current tubulin inhibitors targeting the colchicine binding site. To the best of our knowledge, most structural modifications of CA-4 and its derivatives focus on either the double bond linkage or the 3-hydroxy-4-methoxy benzene moiety; rare modifications on the 3,4,5-TMP moiety is reported. In Chapter 3, we have established a concise synthetic method to overcome the limitation of a potentially explosive diazide intermediate. This novel method involves a Suzuki coupling and Grignard reaction strategy. Eight new ABI-231 analogues modifying the 3,4,5-TMP moiety are synthesized. Among these analogues, 3-methoxy-benzo[4,5]-dioxene analogue exhibits the most potent activity (average IC_{50} = 1.9 nM); 3-methoxy-benzo[4,5]-dioxole analogue shows equipotent activity (average IC_{50} = 4.9 nM) to ABI-231. To our best knowledge, 3-methoxy-benzo[4,5]-dioxene analogue represents the most successful instance modifying the 3,4,5-TMP moiety in CA-4 and its derivatives isosterically. Currently, mechanistic study and *in vivo* efficacy evaluation of these novel ABI-231 analogues are under investigation.

During our exploration of gram-scale synthesis of ABI-231 analogues, a reaction that can generate a substructure of RABI scaffold in 24% yield is observed. Based on this observation, a concise synthetic method involving a strategy of Grignard reaction/Suzuki coupling reaction is established to access twelve novel RABI analogues in Chapter 4. Among the twelve analogues, 4-indole RABI analogue (average IC_{50} = 3.5 nM) exhibits significantly more potent activity than that of MX-RABI; the strongest antiproliferative activity is observed in the 4-indazole RABI analogue, which has an average IC_{50} of 0.8 nM. The 4-indazole RABI analogue is the first CBSI showing sub-nanomolar range activity in the related scaffolds. Effort on investigating the mechanism of action and co-crystal structures in complex with tubulin protein for the potent 4-indazole RABI analogues is currently undergoing.

In Chapter 5, the SAR study of UC-112 is conducted by modifying the benzyloxy moiety. Thirty-six UC-112 analogues are synthesized. Several of the substituted indole analogues exhibit equipotency to that of UC-112 and MX-106. The novel indole analogues display significant abilities to overcome multidrug-resistance mediated by P-gp overexpression. In the future study, obtaining a co-crystal structure of one the indole analogues in complex with survivin protein is warranted to confirm the therapeutic target.

In Chapter 6, we have established an efficient total synthesis of biologically active 20S-(OH)D3. This method involves divergent generation of key intermediates from a common starting material VD2, stereoselective formation of the 20S-hydroxyl scaffold through Grignard reaction, as well as Wittig-Horner coupling to construct VD3 core structure. This synthetic strategy provides an alternative for the synthesis of 20S-(OH)D3 analogs rather than through UVB irradiations [250-253].

In Chapter 2-4, we have modified the indole and 3,4,5-TMP in ABI-231. We have discovered several novel ABI-231 analogues showing more potent activities than the prototype ABI-231. For future structural modification of the ABI-231 scaffold, it can commence with the imidazole moiety in ABI-231. The co-crystal structure of 4-methyl-3-indole analogue in complex with tubulin suggests the existence of a α -ASN101 residue nearby the imidazole moiety. By introducing functional groups such as amine, amide or heterocycles to the imidazole in ABI-231, it is potential to observe new H-bond interactions between these functional groups with α -Asn101 residue. Based on this hypothesis, two ABI-231 analogues with modifications of the imidazole moiety are proposed in **Figure 7-1**. A molecular modeling study of the proposed analogues has been performed on the platform Schrodinger 2015 molecular modeling suite (Schrodinger, Inc., New York, NY) using the co-crystal structure of 4-methyl-3-indole analogue in tubulin. The docking result is shown in **Figure 7-1**. 4-methyl-3-indole analogue shows a perfect conformational overlap with the original crystal structure and has a docking score of 12.0. The proposed analogues fit the pocket in a similar manner to that of 4-methyl-3-indole analogue. Except the H-bond interactions between the imidazole NH and carbonyl with nearby residues α -Thr179 and β -Asp249, the modeling result also reveals the existence of extra H-bond interactions between the newly introduced amino functional group on imidazole with nearby α -Asn101 and α -Thr 179 residues. Both proposed analogues have similar docking scores to that of 4-methyl-3-indole analogue.

One of the proposed analogues has been synthesized by following **Scheme 7-1** and its *in vitro* antiproliferative activity is tested. As shown in **Table 7-1**, the amino analogue **5** is equipotent to colchicine while two intermediates **3** and **4** exhibit slightly decreased activities. This suggests that the 4-position on the imidazole is tolerable for modification. Future structural optimization can commence with relatively larger functional groups such as amide or imidazole ring because the molecular modeling result indicates the pocket in the vicinity of imidazole is broad enough to accommodate bulkier groups.

Besides modification of the ABI-231 scaffold, RABI scaffold is also worthy investigating. An in-depth structural optimization of the most potent RABI analogue (**15i**, in Chapter 4) may provide a good chance to generate analogues having IC₅₀s within picomolar range. Obtaining the co-crystal structure of **15i** in complex with tubulin is therefore important and helpful for designing new generations of tubulin inhibitors.

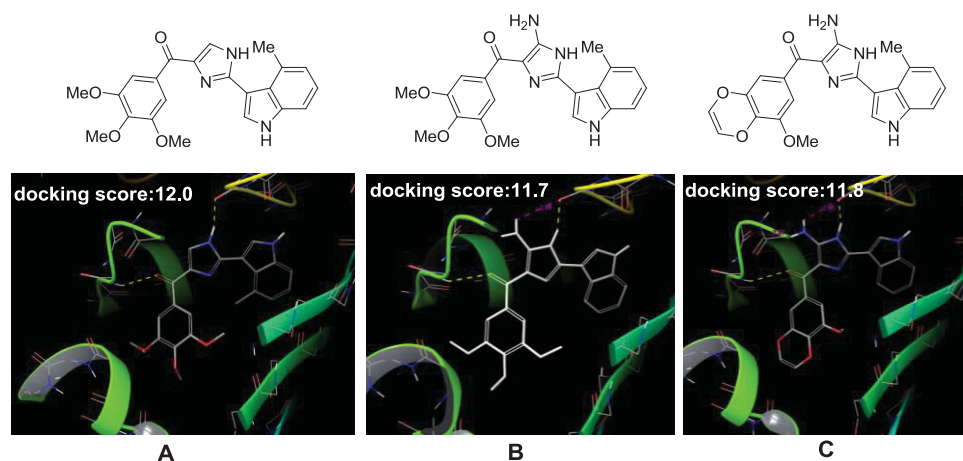
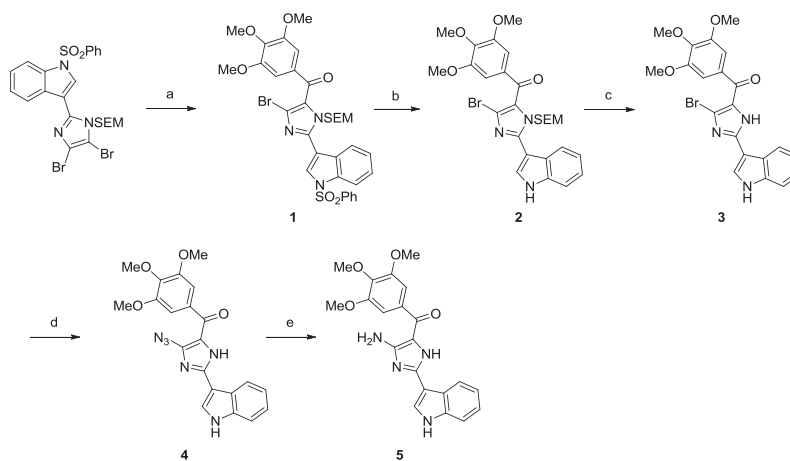


Figure 7-1. Docking study of proposed ABI-231 analogues in co-crystal structure of 4-methyl-3-indole analogue in complex with tubulin



Scheme 7-1. Synthesis of proposed ABI-231 analogue 5

Reagents and conditions: (a): 3,4,5-trimethoxybenzoyl chloride, *i*-PrMgCl(LiCl), THF, rt; (b): NaOH(40% in H₂O), MeOH, reflux; (c): TFA, DCM; (d): NaN₃, DMSO, reflux; (e): H₂, Pd/C, EtOAc-MeOH, rt (1:1).

Table 7-1. *In vitro* growth inhibitory effect of proposed analogue and its intermediates

Compound	A375	M14	RPMI7951
3	18.9±1.1	16.4±0.9	21.5±1.3
4	17.1±1.4	18.6±1.0	27.0±1.1
5	12.7±0.9	11.9±1.4	17.2±2.0
Colchicine	14.5±0.7	14.2±1.0	10.5±0.8

LIST OF REFERENCES

1. Siegel RL, Miller KD, Jemal A: **Cancer Statistics, 2017**. *Ca-Cancer J Clin* 2017, **67**(1):7-30.
2. Schachter J, Laish A, Mekhmandarov S, Feinmesser M, Fenig E, Tamir G, Gutman H: **Standard and nonstandard applications of sentinel node-guided melanoma surgery**. *World J Surg* 2000, **24**(4):491-495.
3. Sandru A, Voinea S, Panaitescu E, Blidaru A: **Survival rates of patients with metastatic malignant melanoma**. *Journal of medicine and life* 2014, **7**(4):572-576.
4. Nikolaou VA, Stratigos AJ, Flaherty KT, Tsao H: **Melanoma: New Insights and New Therapies**. *J Invest Dermatol* 2012, **132**(3):854-863.
5. McCubrey JA, Steelman LS, Chappell WH, Abrams SL, Wong EWT, Chang F, Lehmann B, Terrian DM, Milella M, Tafuri A *et al*: **Roles of the Raf/MEK/ERK pathway in cell growth, malignant transformation and drug resistance**. *Bba-Mol Cell Res* 2007, **1773**(8):1263-1284.
6. Liang H, Liu T, Chen FJ, Liu ZQ, Liu SJ: **A full-length 3D structure for MAPK/ERK kinase 2 (MEK2)**. *Sci China Life Sci* 2011, **54**(4):336-341.
7. Sacks DB: **The role of scaffold proteins in MEK/ERK signalling**. *Biochem Soc T* 2006, **34**:833-836.
8. Akinleye A, Furqan M, Mukhi N, Ravella P, Liu DL: **MEK and the inhibitors: from bench to bedside**. *J Hematol Oncol* 2013, **6**.
9. Strickland LR, Pal HC, Elmets CA, Afaq F: **Targeting drivers of melanoma with synthetic small molecules and phytochemicals**. *Cancer Lett* 2015, **359**(1):20-35.
10. Davies MA: **The Role of the PI3K-AKT Pathway in Melanoma**. *Cancer J* 2012, **18**(2):142-147.
11. Manning BD, Cantley LC: **AKT/PKB signaling: Navigating downstream**. *Cell* 2007, **129**(7):1261-1274.
12. Slipicevic A, Holm R, Nguyen MTP, Bohler PJ, Davidson B, Florenes VA: **Expression of activated Akt and PTEN in malignant melanomas - Relationship with clinical outcome**. *Am J Clin Pathol* 2005, **124**(4):528-536.
13. Karbowniczek M, Spittle CS, Morrison T, Wu H, Henske EP: **MTOR is activated in the majority of malignant melanomas**. *J Invest Dermatol* 2008, **128**(4):980-987.
14. Roskoski R: **RAF protein-serine/threonine kinases: Structure and regulation**. *Biochem Biophys Res Co* 2010, **399**(3):313-317.
15. Davies H, Bignell GR, Cox C, Stephens P, Edkins S, Clegg S, Teague J, Woffendin H, Garnett MJ, Bottomley W *et al*: **Mutations of the BRAF gene in human cancer**. *Nature* 2002, **417**(6892):949-954.
16. Karasarides M, Chiloehes A, Hayward R, Niculescu-Duvaz D, Scanlon I, Friedlos F, Ogilvie L, Hedley D, Martin J, Marshall CJ *et al*: **B-RAF is a therapeutic target in melanoma**. *Oncogene* 2004, **23**(37):6292-6298.

17. Hoeflich MP, Gray DC, Eby MT, Tien JY, Wong L, Bower J, Gogineni A, Zha ZP, Cole MJ, Stern HM *et al*: **Oncogenic BRAF is required for tumor growth and maintenance in melanoma models.** *Cancer research* 2006, **66**(2):999-1006.
18. Eggermont AMM, Spatz A, Robert C: **Cutaneous melanoma.** *Lancet* 2014, **383**(9919):816-827.
19. Tsai J, Lee JT, Wang W, Zhang J, Cho H, Mamo S, Bremer R, Gillette S, Kong J, Haass NK *et al*: **Discovery of a selective inhibitor of oncogenic B-Raf kinase with potent antimelanoma activity.** *P Natl Acad Sci USA* 2008, **105**(8):3041-3046.
20. Beck D, Niessner H, Smalley KSM, Flaherty K, Paraiso KHT, Busch C, Sinnberg T, Vasseur S, Iovanna JL, Driessen S *et al*: **Vemurafenib Potently Induces Endoplasmic Reticulum Stress-Mediated Apoptosis in BRAFV600E Melanoma Cells.** *Sci Signal* 2013, **6**(260).
21. Trunzer K, Pavlick AC, Schuchter L, Gonzalez R, McArthur GA, Hutson TE, Moschos SJ, Flaherty KT, Kim KB, Weber JS *et al*: **Pharmacodynamic Effects and Mechanisms of Resistance to Vemurafenib in Patients With Metastatic Melanoma.** *J Clin Oncol* 2013, **31**(14):1767-+.
22. Hallmeyer S, Hamid O, Sorof TA, Mun Y, Liu SY, Abhyankar S, Gibney GT, Puzanov I: **Phase II study of vemurafenib in patients with locally advanced, unresectable stage IIIc or metastatic melanoma and activating exon 15 BRAF mutations other than V600E.** *J Clin Oncol* 2014, **32**(15).
23. Schilling B, Sondermann W, Zhao F, Griewank KG, Livingstone E, Sucker A, Zelba H, Weide B, Trefzer U, Wilhelm T *et al*: **Differential influence of vemurafenib and dabrafenib on patients' lymphocytes despite similar clinical efficacy in melanoma.** *Ann Oncol* 2014, **25**(3):747-753.
24. Roskoski R, Jr.: **MEK1/2 dual-specificity protein kinases: structure and regulation.** *Biochem Biophys Res Commun* 2012, **417**(1):5-10.
25. Wu XY, Noh SJ, Zhou GC, Dixon JE, Guan KL: **Selective activation of MEK1 but not MEK2 by A-Raf from epidermal growth factor-stimulated Hela cells.** *The Journal of biological chemistry* 1996, **271**(6):3265-3271.
26. Marais R, Light Y, Paterson HF, Mason CS, Marshall CJ: **Differential regulation of Raf-1, A-Raf, and B-Raf by oncogenic ras and tyrosine kinases.** *The Journal of biological chemistry* 1997, **272**(7):4378-4383.
27. Neuzillet C, Tijeras-Raballand A, de Mestier L, Cros J, Faivre S, Raymond E: **MEK in cancer and cancer therapy.** *Pharmacol Therapeut* 2014, **141**(2):160-171.
28. Falchook GS, Lewis KD, Infante JR, Gordon MS, Vogelzang NJ, DeMarini DJ, Sun P, Moy C, Szabo SA, Roadcap LT *et al*: **Activity of the oral MEK inhibitor trametinib in patients with advanced melanoma: a phase 1 dose-escalation trial.** *Lancet Oncol* 2012, **13**(8):782-789.
29. Kim KB, Kefford R, Pavlick AC, Infante JR, Ribas A, Sosman JA, Fecher LA, Millward M, McArthur GA, Hwu P *et al*: **Phase II Study of the MEK1/MEK2 Inhibitor Trametinib in Patients With Metastatic BRAF-Mutant Cutaneous Melanoma Previously Treated With or Without a BRAF Inhibitor.** *J Clin Oncol* 2013, **31**(4):482-489.

30. Azijli K, Stelloo E, Peters GJ, Van den Eertwegh AJM: **New Developments in the Treatment of Metastatic Melanoma: Immune Checkpoint Inhibitors and Targeted Therapies.** *Anticancer research* 2014, **34**(4):1493-1505.
31. Flaherty KT, Robert C, Hersey P, Nathan P, Garbe C, Milhem M, Demidov LV, Hassel JC, Rutkowski P, Mohr P *et al*: **Improved Survival with MEK Inhibition in BRAF-Mutated Melanoma.** *New Engl J Med* 2012, **367**(2):107-114.
32. Signorelli J, Gandhi AS: **Cobimetinib: A Novel MEK Inhibitor for Metastatic Melanoma.** *Ann Pharmacother* 2017, **51**(2):146-153.
33. Adjei AA, Cohen RB, Franklin W, Morris C, Wilson D, Molina JR, Hanson LJ, Gore L, Chow L, Leong S *et al*: **Phase I pharmacokinetic and pharmacodynamic study of the oral, small-molecule mitogen-activated protein kinase kinase 1/2 inhibitor AZD6244 (ARRY-142886) in patients with advanced cancers.** *J Clin Oncol* 2008, **26**(13):2139-2146.
34. Yeh TC, Marsh V, Bernat BA, Ballard J, Colwell H, Evans RJ, Parry J, Smith D, Brandhuber BJ, Gross S *et al*: **Biological characterization of ARRY-142886 (AZD6244), a potent, highly selective mitogen-activated protein kinase kinase 1/2 inhibitor.** *Clin Cancer Res* 2007, **13**(5):1576-1583.
35. Friday BB, Yu CR, Dy GK, Smith PD, Wang L, Thibodeau SN, Adjei AA: **BRAF V600E disrupts AZD6244-Induced abrogation of negative feedback pathways between extracellular signal-regulated kinase and Raf proteins.** *Cancer research* 2008, **68**(15):6145-6153.
36. Kirkwood JM, Bastholt L, Robert C, Sosman J, Larkin J, Hersey P, Middleton M, Cantarini M, Zazulina V, Kemsley K *et al*: **Phase II, Open-Label, Randomized Trial of the MEK1/2 Inhibitor Selumetinib as Monotherapy versus Temozolomide in Patients with Advanced Melanoma.** *Clin Cancer Res* 2012, **18**(2):555-567.
37. Beadling C, Jacobson-Dunlop E, Hodi FS, Le C, Warrick A, Patterson J, Town A, Harlow A, Cruz F, Azar S *et al*: **KIT Gene Mutations and Copy Number in Melanoma Subtypes.** *Clin Cancer Res* 2008, **14**(21):6821-6828.
38. Todd JR, Scurr LL, Becker TM, Kefford RF, Rizos H: **The MAPK pathway functions as a redundant survival signal that reinforces the PI3K cascade in c-Kit mutant melanoma.** *Oncogene* 2014, **33**(2):236-245.
39. Guo J, Si L, Kong Y, Flaherty KT, Xu XW, Zhu YY, Corless CL, Li L, Li HF, Sheng XN *et al*: **Phase II, Open-Label, Single-Arm Trial of Imatinib Mesylate in Patients With Metastatic Melanoma Harboring c-Kit Mutation or Amplification.** *J Clin Oncol* 2011, **29**(21):2904-2909.
40. Hodi FS, Corless CL, Giobbie-Hurder A, Fletcher JA, Zhu MJ, Marino-Enriquez A, Friedlander P, Gonzalez R, Weber JS, Gajewski TF *et al*: **Imatinib for Melanomas Harboring Mutationally Activated or Amplified KIT Arising on Mucosal, Acral, and Chronically Sun-Damaged Skin.** *J Clin Oncol* 2013, **31**(26):3182-+.
41. Cho JH, Kim KM, Kwon M, Kim JH, Lee J: **Nilotinib in patients with metastatic melanoma harboring KIT gene aberration.** *Invest New Drug* 2012, **30**(5):2008-2014.

42. Lebbe C, Chevret S, Jouary T, Dalac S, Dalle S, Guillot B, Arnault JP, Avril MF, Bedane C, Bens G *et al*: **Phase II multicentric uncontrolled national trial assessing the efficacy of nilotinib in the treatment of advanced melanomas with c-KIT mutation or amplification.** *J Clin Oncol* 2014, **32**(15).
43. Drake CG, Jaffee E, Pardoll DM: **Mechanisms of immune evasion by tumors.** *Adv Immunol* 2006, **90**:51-81.
44. Eggermont AM, Chiarion-Sileni V, Grob JJ, Dummer R, Wolchok JD, Schmidt H, Hamid O, Robert C, Ascierto PA, Richards JM *et al*: **Ipilimumab versus placebo after complete resection of stage III melanoma: Initial efficacy and safety results from the EORTC 18071 phase III trial.** *J Clin Oncol* 2014, **32**(18).
45. Hodi FS: **Improved Survival with Ipilimumab in Patients with Metastatic Melanoma (vol 363, pg 711, 2010).** *New Engl J Med* 2010, **363**(13):1290-1290.
46. De Sousa SMC, Long GV, Tonks KT: **Ipilimumab-induced hypophysitis: early Australian experience.** *Med J Australia* 2014, **201**(4):198-199.
47. Camacho LH, Antonia S, Sosman J, Kirkwood JM, Gajewski TF, Redman B, Pavlov D, Bulanhagui C, Bozon VA, Gomez-Navarro J *et al*: **Phase I/II Trial of Tremelimumab in Patients With Metastatic Melanoma.** *J Clin Oncol* 2009, **27**(7):1075-1081.
48. Ribas A, Kefford R, Marshall MA, Punt CJA, Haanen JB, Marmol M, Garbe C, Gogas H, Schachter J, Linette G *et al*: **Phase III Randomized Clinical Trial Comparing Tremelimumab With Standard-of-Care Chemotherapy in Patients With Advanced Melanoma.** *J Clin Oncol* 2013, **31**(5):616-622.
49. Weber JS, D'Angelo SP, Minor D, Hodi FS, Gutzmer R, Neyns B, Hoeller C, Khushalani NI, Miller WH, Lao CD *et al*: **Nivolumab versus chemotherapy in patients with advanced melanoma who progressed after anti-CTLA-4 treatment (CheckMate 037): a randomised, controlled, open-label, phase 3 trial.** *Lancet Oncol* 2015, **16**(4):375-384.
50. Hamid O, Robert C, Daud A, Hodi FS, Hwu WJ, Kefford R, Wolchok JD, Hersey P, Joseph RW, Weber JS *et al*: **Safety and Tumor Responses with Lambrolizumab (Anti-PD-1) in Melanoma.** *New Engl J Med* 2013, **369**(2):134-144.
51. Ribas A, Wolchok JD, Robert C, Kefford R, Hamid O, Daud A, Hwu WJ, Weber JS, Joshua AM, Gangadhar TC *et al*: **Updated Clinical Efficacy of the Anti-Pd-1 Monoclonal Antibody Pembrolizumab (Mk-3475) in 411 Patients with Melanoma.** *Eur J Cancer* 2015, **51**:E24-E24.
52. Chapman PB, Hauschild A, Robert C, Haanen JB, Ascierto P, Larkin J, Dummer R, Garbe C, Testori A, Maio M *et al*: **Improved Survival with Vemurafenib in Melanoma with BRAF V600E Mutation.** *New Engl J Med* 2011, **364**(26):2507-2516.
53. Hauschild A, Grob JJ, Demidov LV, Jouary T, Gutzmer R, Millward M, Rutkowski P, Blank CU, Miller WH, Kaempgen E *et al*: **Dabrafenib in BRAF-mutated metastatic melanoma: a multicentre, open-label, phase 3 randomised controlled trial.** *Lancet* 2012, **380**(9839):358-365.

54. Shi HB, Hong AY, Kong XJ, Koya RC, Song CY, Moriceau G, Hugo W, Yu CC, Ng C, Chodon T *et al*: **A Novel AKT1 Mutant Amplifies an Adaptive Melanoma Response to BRAF Inhibition**. *Cancer Discov* 2014, **4**(1):69-79.
55. Rizos H, Menzies AM, Pupo GM, Carlino MS, Fung C, Hyman J, Haydu LE, Mijatov B, Becker TM, Boyd SC *et al*: **BRAF Inhibitor Resistance Mechanisms in Metastatic Melanoma: Spectrum and Clinical Impact**. *Clin Cancer Res* 2014, **20**(7):1965-1977.
56. Shi HB, Hugo W, Kong XJ, Hong A, Koya RC, Moriceau G, Chodon T, Guo RQ, Johnson DB, Dahlman KB *et al*: **Acquired Resistance and Clonal Evolution in Melanoma during BRAF Inhibitor Therapy**. *Cancer Discov* 2014, **4**(1):80-93.
57. Poulikakos PI, Persaud Y, Janakiraman M, Kong XJ, Ng C, Moriceau G, Shi HB, Atefi M, Titz B, Gabay MT *et al*: **RAF inhibitor resistance is mediated by dimerization of aberrantly spliced BRAF(V600E)**. *Nature* 2011, **480**(7377):387-U144.
58. Shi HB, Moriceau G, Kong XJ, Lee MK, Lee H, Koya RC, Ng C, Chodon T, Scolyer RA, Dahlman KB *et al*: **Melanoma whole-exome sequencing identifies B-V600E-RAF amplification-mediated acquired B-RAF inhibitor resistance**. *Nat Commun* 2012, **3**.
59. Carlino MS, Fung C, Shahheydari H, Todd JR, Boyd SC, Irvine M, Nagrial AM, Scolyer RA, Kefford RF, Long GV *et al*: **Preexisting MEK1(P124) Mutations Diminish Response to BRAF Inhibitors in Metastatic Melanoma Patients**. *Clin Cancer Res* 2015, **21**(1):98-105.
60. Wagle N, Van Allen EM, Treacy DJ, Frederick DT, Cooper ZA, Taylor-Weiner A, Rosenberg M, Goetz EM, Sullivan RJ, Farlow DN *et al*: **MAP Kinase Pathway Alterations in BRAF-Mutant Melanoma Patients with Acquired Resistance to Combined RAF/MEK Inhibition**. *Cancer Discov* 2014, **4**(1):61-68.
61. Johannessen CM, Boehm JS, Kim SY, Thomas SR, Wardwell L, Johnson LA, Emery CM, Stransky N, Cogdill AP, Barretina J *et al*: **COT drives resistance to RAF inhibition through MAP kinase pathway reactivation**. *Nature* 2010, **468**(7326):968-U370.
62. Welsh SJ, Rizos H, Scolyer RA, Long GV: **Resistance to combination BRAF and MEK inhibition in metastatic melanoma: Where to next?** *Eur J Cancer* 2016, **62**:76-85.
63. Amaral T, Sinnberg T, Meier F, Krepler C, Levesque M, Niessner H, Garbe C: **The mitogen-activated protein kinase pathway in melanoma part I - Activation and primary resistance mechanisms to BRAF inhibition**. *Eur J Cancer* 2017, **73**:85-92.
64. Sullivan RJ, Flaherty KT: **Resistance to BRAF-targeted therapy in melanoma**. *Eur J Cancer* 2013, **49**(6):1297-1304.
65. Wellbrock C: **MAPK pathway inhibition in melanoma: resistance three ways**. *Biochem Soc T* 2014, **42**:727-732.
66. Flaherty KT, Infante JR, Daud A, Gonzalez R, Kefford RF, Sosman J, Hamid O, Schuchter L, Cebon J, Ibrahim N *et al*: **Combined BRAF and MEK Inhibition in Melanoma with BRAF V600 Mutations**. *New Engl J Med* 2012, **367**(18):1694-1703.

67. Long GV, Weber JS, Infante JR, Kim KB, Daud A, Gonzalez R, Sosman JA, Hamid O, Schuchter L, Cebon J *et al*: **Overall Survival and Durable Responses in Patients With BRAF V600-Mutant Metastatic Melanoma Receiving Dabrafenib Combined With Trametinib.** *J Clin Oncol* 2016, **34**(8):871-+.
68. Nijenhuis CM, Haanen JBAG, Schellens JHM, Beijnen JH: **Is combination therapy the next step to overcome resistance and reduce toxicities in melanoma?** *Cancer Treat Rev* 2013, **39**(4):305-312.
69. Villadolid J, Amin A: **Immune checkpoint inhibitors in clinical practice: update on management of immune-related toxicities.** *Translational lung cancer research* 2015, **4**(5):560-575.
70. Sorger PK, Dobles M, Tournebize R, Hyman AA: **Coupling cell division and cell death to microtubule dynamics.** *Curr Opin Cell Biol* 1997, **9**(6):807-814.
71. Horio T, Murata T: **The role of dynamic instability in microtubule organization.** *Front Plant Sci* 2014, **5**.
72. Kavallaris M: **Microtubules and resistance to tubulin-binding agents.** *Nat Rev Cancer* 2010, **10**(4).
73. Kaur R, Kaur G, Gill RK, Soni R, Bariwal J: **Recent developments in tubulin polymerization inhibitors: An overview.** *European journal of medicinal chemistry* 2014, **87**:89-124.
74. Islam MN, Iskander MN: **Microtubulin binding sites as target for developing anticancer agents.** *Mini-Rev Med Chem* 2004, **4**(10):1077-1104.
75. Jordan A, Hadfield JA, Lawrence NJ, McGown AT: **Tubulin as a target for anticancer drugs: Agents which interact with the mitotic spindle.** *Med Res Rev* 1998, **18**(4):259-296.
76. Kumar S, Mahdi H, Bryant C, Shah JP, Garg G, Munkarah A: **Clinical trials and progress with paclitaxel in ovarian cancer.** *International journal of women's health* 2010, **2**:411-427.
77. Ornstein DL, Rigas JR: **Taxotere: Clinical Trials in Non-Small Cell Lung Cancer.** *The oncologist* 1998, **3**(2):86-93.
78. Vahdat LT: **Clinical studies with epothilones for the treatment of metastatic breast cancer.** *Seminars in oncology* 2008, **35**(2 Suppl 2):S22-30; quiz S40.
79. Krick EL, Cohen RB, Gregor TP, Salah PC, Sorenmo KU: **Prospective clinical trial to compare vincristine and vinblastine in a COP-based protocol for lymphoma in cats.** *Journal of veterinary internal medicine / American College of Veterinary Internal Medicine* 2013, **27**(1):134-140.
80. Ling V: **Multidrug resistance: molecular mechanisms and clinical relevance.** *Cancer chemotherapy and pharmacology* 1997, **40** Suppl:S3-8.
81. Kerb R, Hoffmeyer S, Brinkmann U: **ABC drug transporters: hereditary polymorphisms and pharmacological impact in MDR1, MRP1 and MRP2.** *Pharmacogenomics* 2001, **2**(1):51-64.
82. Doyle L, Ross DD: **Multidrug resistance mediated by the breast cancer resistance protein BCRP (ABCG2).** *Oncogene* 2003, **22**(47):7340-7358.
83. Sparreboom A, van Tellingen O, Nooijen WJ, Beijnen JH: **Nonlinear pharmacokinetics of paclitaxel in mice results from the pharmaceutical vehicle Cremophor EL.** *Cancer research* 1996, **56**(9):2112-2115.

84. Mozzetti S, Ferlini C, Concolino P, Filippetti F, Raspaglio G, Prislei S, Gallo D, Martinelli E, Ranelletti FO, Ferrandina G *et al*: **Class III beta-tubulin overexpression is a prominent mechanism of paclitaxel resistance in ovarian cancer patients.** *Clin Cancer Res* 2005, **11**(1):298-305.
85. Seve P, Dumontet C: **Is class III beta-tubulin a predictive factor in patients receiving tubulin-binding agents?** *Lancet Oncol* 2008, **9**(2):168-175.
86. Aoki D, Oda Y, Hattori S, Taguchi K, Ohishi Y, Basaki Y, Oie S, Suzuki N, Kono S, Tsuneyoshi M *et al*: **Overexpression of Class III beta-Tubulin Predicts Good Response to Taxane-Based Chemotherapy in Ovarian Clear Cell Adenocarcinoma.** *Clin Cancer Res* 2009, **15**(4):1473-1480.
87. Robinson MW, Trudgett A, Hoey EM, Fairweather I: **Triclabendazole-resistant Fasciola hepatica: beta-tubulin and response to in vitro treatment with triclabendazole.** *Parasitology* 2002, **124**:325-338.
88. Kavallaris M, Verrills NM, Hill BT: **Anticancer therapy with novel tubulin-interacting drugs.** *Drug Resist Update* 2001, **4**(6):392-401.
89. Seve P, Dumontet C: **Is class III beta-tubulin a predictive factor in patients receiving tubulin-binding agents?** *Lancet Oncol* 2008, **9**(2):168-175.
90. Wilson L, Panda D, Jordan MA: **Modulation of microtubule dynamics by drugs: A paradigm for the actions of cellular regulators.** *Cell Struct Funct* 1999, **24**(5):329-335.
91. Jordan MA, Wilson L: **Microtubules as a target for anticancer drugs.** *Nat Rev Cancer* 2004, **4**(4):253-265.
92. Verrills NM, Walsh BJ, Cobon GS, Hains PG, Kavallaris M: **Proteome analysis of Vinca alkaloid response and resistance in acute lymphoblastic leukemia reveals novel cytoskeletal alterations.** *The Journal of biological chemistry* 2003, **278**(46):45082-45093.
93. Verrills NM, Po'uha ST, Liu MLM, Liaw TYE, Larsen MR, Ivery MT, Marshall GM, Gunning PW, Kavallaris M: **Alterations in gamma-actin and tubulin-targeted drug resistance in childhood leukemia.** *J Natl Cancer I* 2006, **98**(19):1363-1374.
94. Stengel C, Newman SP, Leese MP, Potter BV, Reed MJ, Purohit A: **Class III beta-tubulin expression and in vitro resistance to microtubule targeting agents.** *British journal of cancer* 2010, **102**(2):316-324.
95. Mukhtar E, Adhami VM, Mukhtar H: **Targeting Microtubules by Natural Agents for Cancer Therapy.** *Molecular cancer therapeutics* 2014, **13**(2):275-284.
96. Ravelli RBG, Gigant B, Curmi PA, Jourdain I, Lachkar S, Sobel A, Knossow M: **Insight into tubulin regulation from a complex with colchicine and a stathmin-like domain.** *Nature* 2004, **428**(6979):198-202.
97. Finkelstein Y, Aks SE, Hutson JR, Juurlink DN, Nguyen P, Dubnov-Raz G, Pollak U, Koren G, Bentur Y: **Colchicine poisoning: the dark side of an ancient drug.** *Clin Toxicol* 2010, **48**(5):407-414.
98. Borisy GG, Taylor EW: **The mechanism of action of colchicine. Binding of colchicine-3H to cellular protein.** *The Journal of cell biology* 1967, **34**(2):525-533.

99. Kanthou C, Tozer GM: **Microtubule depolymerizing vascular disrupting agents: novel therapeutic agents for oncology and other pathologies.** *Int J Exp Pathol* 2009, **90**(3):284-294.
100. Stengel C, Newman SP, Leese MP, Potter BVL, Reed MJ, Purohit A: **Class III beta-tubulin expression and in vitro resistance to microtubule targeting agents.** *Brit J Cancer* 2010, **102**(2):316-324.
101. Wu XX, Wang QH, Li W: **Recent Advances in Heterocyclic Tubulin Inhibitors Targeting the Colchicine Binding Site.** *Anti-cancer agents in medicinal chemistry* 2016, **16**(10):1325-1338.
102. Lu Y, Chen JJ, Xiao M, Li W, Miller DD: **An Overview of Tubulin Inhibitors That Interact with the Colchicine Binding Site.** *Pharm Res-Dordr* 2012, **29**(11):2943-2971.
103. Ji YT, Liu YN, Liu ZP: **Tubulin Colchicine Binding Site Inhibitors as Vascular Disrupting Agents in Clinical Developments.** *Current medicinal chemistry* 2015, **22**(11):1348-1360.
104. Ryan BM, O'Donovan N, Duffy MJ: **Survivin: A new target for anti-cancer therapy.** *Cancer Treat Rev* 2009, **35**(7):553-562.
105. Altieri DC: **Opinion - Survivin, cancer networks and pathway-directed drug discovery.** *Nat Rev Cancer* 2008, **8**(1):61-70.
106. Duffy MJ, O'Donovan N, Brennan DJ, Gallagher WM, Ryan BM: **Survivin: A promising tumor biomarker.** *Cancer Lett* 2007, **249**(1):49-60.
107. Shin S, Sung BJ, Cho YS, Kim HJ, Ha NC, Hwang JI, Chung CW, Jung YK, Oh BH: **An anti-apoptotic protein human survivin is a direct inhibitor of caspase-3 and-7.** *Biochemistry-US* 2001, **40**(4):1117-1123.
108. Tamm I, Wang Y, Sausville E, Scudiero DA, Vigna N, Oltersdorf T, Reed JC: **IAP-family protein Survivin inhibits caspase activity and apoptosis induced by Fas (CD95), Bax, caspases, and anticancer drugs.** *Cancer research* 1998, **58**(23):5315-5320.
109. Hu DQ, Liu SW, Shi L, Li C, Wu LF, Fan ZS: **Cleavage of Survivin by Granzyme M Triggers Degradation of the Survivin-X-linked Inhibitor of Apoptosis Protein (XIAP) Complex to Free Caspase Activity Leading to Cytolysis of Target Tumor Cells.** *The Journal of biological chemistry* 2010, **285**(24):18326-18335.
110. Altieri DC: **Survivin in apoptosis control and cell cycle regulation in cancer.** *Progress in cell cycle research* 2003, **5**:447-452.
111. Chakravarti A, Zhai GG, Zhang M, Malhotra R, Latham DE, Delaney MA, Robe P, Nestler U, Song QH, Loeffler J: **Survivin enhances radiation resistance in primary human glioblastoma cells via caspase-independent mechanisms.** *Oncogene* 2004, **23**(45):7494-7506.
112. Cheung CHA, Chen HH, Kuo CC, Chang CY, Coumar MS, Hsieh HP, Chang JY: **Survivin counteracts the therapeutic effect of microtubule de-stabilizers by stabilizing tubulin polymers.** *Mol Cancer* 2009, **8**.
113. Pennati M, Folini M, Zaffaroni N: **Targeting survivin in cancer therapy: fulfilled promises and open questions.** *Carcinogenesis* 2007, **28**(6):1133-1139.

114. O'Connor DS, Grossman D, Plescia J, Li FZ, Zhang H, Villa A, Tognin S, Marchisio PC, Altieri DC: **Regulation of apoptosis at cell division by p34(cdc2) phosphorylation of survivin.** *P Natl Acad Sci USA* 2000, **97**(24):13103-13107.
115. Yan H, Thomas J, Liu T, Raj D, London N, Tandeski T, Leachman SA, Lee RM, Grossman D: **Induction of melanoma cell apoptosis and inhibition of tumor growth using a cell-permeable Survivin antagonist.** *Oncogene* 2006, **25**(52):6968-6974.
116. Talbot DC, Davies J, Callies S, Andre V, Lahn M, Ang J, De Bono JS, Ranson M: **First human dose study evaluating safety and pharmacokinetics of LY2181308, an antisense oligonucleotide designed to inhibit survivin.** *J Clin Oncol* 2008, **26**(15).
117. Xiao M, Li W: **Recent Advances on Small-Molecule Survivin Inhibitors.** *Current medicinal chemistry* 2015, **22**(9):1136-1146.
118. Roy K, Singh N, Kanwar RK, Kanwar JR: **Survivin Modulators: An Updated Patent Review (2011-2015).** *Recent Pat Anti-Canc* 2016, **11**(2):152-169.
119. Meli M, Pennati M, Curto M, Daidone MG, Plescia J, Toba S, Altieri DC, Zaffaroni N, Colombo G: **Small-molecule targeting of heat shock protein 90 chaperone function: Rational identification of a new anticancer lead.** *Journal of medicinal chemistry* 2006, **49**(26):7721-7730.
120. Huang K, Li LA, Meng YG, You YQ, Fu XY, Song L: **Arctigenin Promotes Apoptosis in Ovarian Cancer Cells via the iNOS/NO/STAT3/Survivin Signalling.** *Basic Clin Pharmacol* 2014, **115**(6):507-511.
121. Ling X, Cao SS, Cheng QY, Keefe JT, Rustum YM, Li FZ: **A Novel Small Molecule FL118 That Selectively Inhibits Survivin, Mcl-1, XIAP and cIAP2 in a p53-Independent Manner, Shows Superior Antitumor Activity.** *Plos One* 2012, **7**(9).
122. Xia WL, Bisi J, Strum J, Liu LH, Carrick K, Graham KM, Treece AL, Hardwicke MA, Dush M, Liao QY *et al*: **Regulation of survivin by ErbB2 signaling: Therapeutic implications for ErbB2-overexpressing breast cancers.** *Cancer research* 2006, **66**(3):1640-1647.
123. Agarwal E, Chaudhuri A, Leiphakpam PD, Haferbier KL, Brattain MG, Chowdhury S: **Akt inhibitor MK-2206 promotes anti-tumor activity and cell death by modulation of AIF and Ezrin in colorectal cancer.** *Bmc Cancer* 2014, **14**.
124. Iizuka D, Ogura A, Kuwabara M, Inanami O: **Purvalanol A induces apoptosis and downregulation of antiapoptotic proteins through abrogation of phosphorylation of JAK2/STAT3 and RNA polymerase II.** *Anti-Cancer Drug* 2008, **19**(6):565-572.
125. Nakahara T, Kita A, Yamanaka K, Mori M, Amino N, Takeuchi M, Tominaga F, Hatakeyama S, Kinoyama I, Matsuhisa A *et al*: **YM155, a Novel Small-Molecule Survivin Suppressant, Induces Regression of Established Human Hormone-Refractory Prostate Tumor Xenografts (vol 67, pg 8014, 2007).** *Cancer research* 2012, **72**(15):3886-3886.
126. Wang J, Li W: **Discovery of Novel Second Mitochondria-Derived Activator of Caspase Mimetics as Selective Inhibitor of Apoptosis Protein Inhibitors.** *The Journal of pharmacology and experimental therapeutics* 2014, **349**(2):319-329.

127. Wall NR, O'Connor DS, Plescia J, Pommier Y, Altieri DC: **Suppression of survivin phosphorylation on Thr(34) by flavopiridol enhances tumor cell apoptosis.** *Cancer research* 2003, **63**(1):230-235.
128. Chang CC, Heller JD, Kuo J, Huang RCC: **Tetra-O-methyl nordihydroguaiaretic acid induces growth arrest and cellular apoptosis by inhibiting Cdc2 and survivin expression.** *P Natl Acad Sci USA* 2004, **101**(36):13239-13244.
129. Arora R, Yates C, Gary BD, McClellan S, Tan M, Xi YG, Reed E, Piazza GA, Owen LB, Dean-Colomb W: **Panepoxydone Targets NF-kB and FOXM1 to Inhibit Proliferation, Induce Apoptosis and Reverse Epithelial to Mesenchymal Transition in Breast Cancer.** *Plos One* 2014, **9**(6).
130. Chantalat L, Skoufias DA, Kleman JP, Jung B, Dideberg O, Margolis RL: **Crystal structure of human survivin reveals a bow tie-shaped dimer with two unusual alpha-helical extensions.** *Mol Cell* 2000, **6**(1):183-189.
131. Cheng JB, Motola DL, Mangelsdorf DJ, Russell DW: **De-orphanization of cytochrome P450 2R1 - A microsomal vitamin D 25-hydroxylase.** *The Journal of biological chemistry* 2003, **278**(39):38084-38093.
132. Deeb KK, Trump DL, Johnson CS: **Vitamin D signalling pathways in cancer: potential for anticancer therapeutics.** *Nat Rev Cancer* 2007, **7**(9):684-700.
133. Washington MN, Kim JS, Weigel NL: **1alpha,25-dihydroxyvitamin D3 inhibits C4-2 prostate cancer cell growth via a retinoblastoma protein (Rb)-independent G1 arrest.** *The Prostate* 2011, **71**(1):98-110.
134. Akutsu N, Lin R, Bastien Y, Bestawros A, Enepekides DJ, Black MJ, White JH: **Regulation of gene Expression by 1alpha,25-dihydroxyvitamin D3 and Its analog EB1089 under growth-inhibitory conditions in squamous carcinoma Cells.** *Mol Endocrinol* 2001, **15**(7):1127-1139.
135. Bao BY, Hu YC, Ting HJ, Lee YF: **Androgen signaling is required for the vitamin D-mediated growth inhibition in human prostate cancer cells.** *Oncogene* 2004, **23**(19):3350-3360.
136. Diaz GD, Paraskeva C, Thomas MG, Binderup L, Hague A: **Apoptosis is induced by the active metabolite of vitamin D-3 and its analogue EB1089 in colorectal adenoma and carcinoma cells: Possible implications for prevention and therapy.** *Cancer research* 2000, **60**(8):2304-2312.
137. Motomura S, Kanamori H, Maruta A, Kodama F, Ohkubo T: **The Effect of 1-Hydroxyvitamin D3 for Prolongation of Leukemic Transformation-Free Survival in Myelodysplastic Syndromes.** *Am J Hematol* 1991, **38**(1):67-68.
138. Villaggio B, Soldano S, Cutolo M: **1,25-dihydroxyvitamin D3 downregulates aromatase expression and inflammatory cytokines in human macrophages.** *Clin Exp Rheumatol* 2012, **30**(6):934-938.
139. Kaler P, Augenlicht L, Klampfer L: **Macrophage-derived IL-1 beta stimulates Wnt signaling and growth of colon cancer cells: a crosstalk interrupted by vitamin D-3.** *Oncogene* 2009, **28**(44):3892-3902.
140. Ben-Shoshan M, Amir S, Dang DT, Dang LH, Weisman Y, Mabweesh NJ: **1 alpha,25-dihydroxyvitamin D-3 (Calcitriol) inhibits hypoxia-inducible factor-1/vascular endothelial growth factor pathway in human cancer cells.** *Molecular cancer therapeutics* 2007, **6**(4):1433-1439.

141. Chung I, Hang GZ, Seshadri M, Gillard BM, Yu WD, Foster BA, Trump DL, Johnson CS: **Role of Vitamin D Receptor in the Antiproliferative Effects of Calcitriol in Tumor-Derived Endothelial Cells and Tumor Angiogenesis In vivo.** *Cancer research* 2009, **69**(3):967-975.
142. Kovalenko PL, Zhang ZT, Cui M, Clinton SK, Fleet JC: **1,25 dihydroxyvitamin D-mediated orchestration of anticancer, transcript-level effects in the immortalized, non-transformed prostate epithelial cell line, RWPE1.** *Bmc Genomics* 2010, **11**.
143. Figueroa JA, De Raad S, Tadlock L, Speights VO, Rinehart JJ: **Differential expression of insulin-like growth factor binding proteins in high versus low Gleason score prostate cancer.** *J Urology* 1998, **159**(4):1379-1383.
144. Jones G: **Pharmacokinetics of vitamin D toxicity.** *The American journal of clinical nutrition* 2008, **88**(2):582S-586S.
145. Miller WL, Auchus RJ: **The molecular biology, biochemistry, and physiology of human steroidogenesis and its disorders.** *Endocrine reviews* 2011, **32**(1):81-151.
146. Tuckey RC: **Progesterone synthesis by the human placenta.** *Placenta* 2005, **26**(4):273-281.
147. Slominski AT, Li W, Kim TK, Semak I, Wang J, Zjawiony JK, Tuckey RC: **Novel activities of CYP11A1 and their potential physiological significance.** *The Journal of steroid biochemistry and molecular biology* 2014.
148. Slominski A, Zjawiony J, Wortsman J, Semak I, Stewart J, Pisarchik A, Sweatman T, Marcos J, Dunbar C, R CT: **A novel pathway for sequential transformation of 7-dehydrocholesterol and expression of the P450scc system in mammalian skin.** *European journal of biochemistry / FEBS* 2004, **271**(21):4178-4188.
149. Slominski A, Semak I, Wortsman J, Zjawiony J, Li W, Zbytek B, Tuckey RC: **An alternative pathway of vitamin D metabolism. Cytochrome P450scc (CYP11A1)-mediated conversion to 20-hydroxyvitamin D2 and 17,20-dihydroxyvitamin D2.** *The FEBS journal* 2006, **273**(13):2891-2901.
150. Slominski A, Semak I, Zjawiony J, Wortsman J, Li W, Szczesniewski A, Tuckey RC: **The cytochrome P450scc system opens an alternate pathway of vitamin D3 metabolism.** *The FEBS journal* 2005, **272**(16):4080-4090.
151. Tuckey RC, Li W, Zjawiony JK, Zmijewski MA, Nguyen MN, Sweatman T, Miller D, Slominski A: **Pathways and products for the metabolism of vitamin D3 by cytochrome P450scc.** *The FEBS journal* 2008, **275**(10):2585-2596.
152. Guryev O, Carvalho RA, Usanov S, Gilep A, Estabrook RW: **A pathway for the metabolism of vitamin D3: unique hydroxylated metabolites formed during catalysis with cytochrome P450scc (CYP11A1).** *Proceedings of the National Academy of Sciences of the United States of America* 2003, **100**(25):14754-14759.
153. Slominski AT, Kim TK, Li W, Yi AK, Postlethwaite A, Tuckey RC: **The role of CYP11A1 in the production of vitamin D metabolites and their role in the regulation of epidermal functions.** *The Journal of steroid biochemistry and molecular biology* 2014, **144 Pt A**:28-39.
154. Janjetovic Z, Zmijewski MA, Tuckey RC, DeLeon DA, Nguyen MN, Pfeffer LM, Slominski AT: **20-Hydroxycholecalciferol, product of vitamin D3**

- hydroxylation by P450scc, decreases NF-kappaB activity by increasing IkappaB alpha levels in human keratinocytes.** *PloS one* 2009, **4**(6):e5988.
155. Zbytek B, Janjetovic Z, Tuckey RC, Zmijewski MA, Sweatman TW, Jones E, Nguyen MN, Slominski AT: **20-Hydroxyvitamin D3, a product of vitamin D3 hydroxylation by cytochrome P450scc, stimulates keratinocyte differentiation.** *The Journal of investigative dermatology* 2008, **128**(9):2271-2280.
 156. Slominski AT, Janjetovic Z, Fuller BE, Zmijewski MA, Tuckey RC, Nguyen MN, Sweatman T, Li W, Zjawiony J, Miller D *et al*: **Products of vitamin D3 or 7-dehydrocholesterol metabolism by cytochrome P450scc show anti-leukemia effects, having low or absent calcemic activity.** *PloS one* 2010, **5**(3):e9907.
 157. Slominski AT, Janjetovic Z, Kim TK, Wright AC, Grese LN, Riney SJ, Nguyen MN, Tuckey RC: **Novel vitamin D hydroxyderivatives inhibit melanoma growth and show differential effects on normal melanocytes.** *Anticancer research* 2012, **32**(9):3733-3742.
 158. Chen J, Wang J, Kim TK, Tieu EW, Tang EK, Lin Z, Kovacic D, Miller DD, Postlethwaite A, Tuckey RC *et al*: **Novel vitamin D analogs as potential therapeutics: metabolism, toxicity profiling, and antiproliferative activity.** *Anticancer research* 2014, **34**(5):2153-2163.
 159. Slominski A, Janjetovic Z, Tuckey RC, Nguyen MN, Bhattacharya KG, Wang J, Li W, Jiao Y, Gu W, Brown M *et al*: **20S-hydroxyvitamin D3, noncalcemic product of CYP11A1 action on vitamin D3, exhibits potent antifibrogenic activity in vivo.** *The Journal of clinical endocrinology and metabolism* 2013, **98**(2):E298-303.
 160. Slominski AT, Kim TK, Janjetovic Z, Tuckey RC, Bieniek R, Yue J, Li W, Chen J, Nguyen MN, Tang EK *et al*: **20-Hydroxyvitamin D2 is a noncalcemic analog of vitamin D with potent antiproliferative and prodifferentiation activities in normal and malignant cells.** *American journal of physiology Cell physiology* 2011, **300**(3):C526-541.
 161. Slominski AT, Kim TK, Takeda Y, Janjetovic Z, Brozyna AA, Skobowiat C, Wang J, Postlethwaite A, Li W, Tuckey RC *et al*: **RORalpha and ROR gamma are expressed in human skin and serve as receptors for endogenously produced noncalcemic 20-hydroxy- and 20,23-dihydroxyvitamin D.** *FASEB journal : official publication of the Federation of American Societies for Experimental Biology* 2014, **28**(7):2775-2789.
 162. Kim TK, Wang J, Janjetovic Z, Chen JJ, Tuckey RC, Nguyen MN, Tang EKY, Miller D, Li W, Slominski AT: **Correlation between secosteroid-induced vitamin D receptor activity in melanoma cells and computer-modeled receptor binding strength.** *Mol Cell Endocrinol* 2012, **361**(1-2):143-152.
 163. Fedorenko IV, Gibney GT, Sondak VK, Smalley KSM: **Beyond BRAF: where next for melanoma therapy?** *Brit J Cancer* 2015, **112**(2):217-226.
 164. Wolchok JD, Kluger H, Callahan MK, Postow MA, Rizvi NA, Lesokhin AM, Segal NH, Ariyan CE, Gordon RA, Reed K *et al*: **Nivolumab plus Ipilimumab in Advanced Melanoma.** *New Engl J Med* 2013, **369**(2):122-133.
 165. Sznol M, Kluger HM, Callahan MK, Postow MA, Gordon RA, Segal NH, Rizvi NA, Lesokhin AM, Atkins MB, Kirkwood JM *et al*: **Survival, response**

- duration, and activity by BRAF mutation (MT) status of nivolumab (NIVO, anti-PD-1, BMS-936558, ONO-4538) and ipilimumab (IPI) concurrent therapy in advanced melanoma (MEL). *J Clin Oncol* 2014, **32**(18).
166. Beck A, Wurch T, Bailly C, Corvaia N: **Strategies and challenges for the next generation of therapeutic antibodies.** *Nat Rev Immunol* 2010, **10**(5):345-352.
 167. Panowski S, Bhakta S, Raab H, Polakis P, Junutula JR: **Site-specific antibody drug conjugates for cancer therapy.** *Mabs-Austin* 2014, **6**(1):34-45.
 168. Peters C, Brown S: **Antibody-drug conjugates as novel anti-cancer chemotherapeutics.** *Bioscience Rep* 2015, **35**.
 169. Chen JJ, Ahn S, Wang J, Lu Y, Dalton JT, Miller DD, Li W: **Discovery of Novel 2-Aryl-4-benzoyl-imidazole (ABI-III) Analogues Targeting Tubulin Polymerization As Antiproliferative Agents.** *Journal of medicinal chemistry* 2012, **55**(16):7285-7289.
 170. Mukhtar E, Adhami VM, Mukhtar H: **Targeting microtubules by natural agents for cancer therapy.** *Mol Cancer Ther* 2014, **13**(2):275-284.
 171. Heald R, Nogales E: **Microtubule dynamics.** *J Cell Sci* 2002, **115**(1):3-4.
 172. Kuppens IE: **Current state of the art of new tubulin inhibitors in the clinic.** *Current clinical pharmacology* 2006, **1**(1):57-70.
 173. Loong HH, Yeo W: **Microtubule-targeting agents in oncology and therapeutic potential in hepatocellular carcinoma.** *OncoTargets and therapy* 2014, **7**:575-585.
 174. McGuire S: **World Cancer Report 2014. Geneva, Switzerland: World Health Organization, International Agency for Research on Cancer, WHO Press, 2015.** *Adv Nutr* 2016, **7**(2):418-419.
 175. Orr GA, Verdier-Pinard P, McDaid H, Horwitz SB: **Mechanisms of Taxol resistance related to microtubules.** *Oncogene* 2003, **22**(47):7280-7295.
 176. Kavallaris M, Tait AS, Walsh BJ, He LF, Horwitz SB, Norris MD, Haber M: **Multiple microtubule alterations are associated with Vinca alkaloid resistance in human leukemia cells.** *Cancer research* 2001, **61**(15):5803-5809.
 177. Zagouri F, Sergentanis TN, Chrysikos D, Dimopoulos MA, Bamias A: **Epothilones in epithelial ovarian, fallopian tube, or primary peritoneal cancer: a systematic review.** *OncoTargets and therapy* 2015, **8**:2187-2198.
 178. Trendowski M: **Recent Advances in the Development of Antineoplastic Agents Derived from Natural Products.** *Drugs* 2015, **75**(17):1993-2016.
 179. Aseyev O, Ribeiro JM, Cardoso F: **Review on the clinical use of eribulin mesylate for the treatment of breast cancer.** *Expert Opin Pharmaco* 2016, **17**(4):589-600.
 180. Li CM, Wang Z, Lu Y, Ahn S, Narayanan R, Kearbey JD, Parke DN, Li W, Miller DD, Dalton JT: **Biological Activity of 4-Substituted Methoxybenzoyl-Aryl-Thiazole: An Active Microtubule Inhibitor.** *Cancer research* 2011, **71**(1):216-224.
 181. Lu Y, Li CM, Wang Z, Ross CR, Chen J, Dalton JT, Li W, Miller DD: **Discovery of 4-Substituted Methoxybenzoyl-aryl-thiazole as Novel Anticancer Agents: Synthesis, Biological Evaluation, and Structure-Activity Relationships.** *Journal of medicinal chemistry* 2009, **52**(6):1701-1711.

182. Chen JJ, Wang Z, Li CM, Lu Y, Vaddady PK, Meibohm B, Dalton JT, Miller DD, Li W: **Discovery of Novel 2-Aryl-4-benzoyl-imidazoles Targeting the Colchicines Binding Site in Tubulin As Potential Anticancer Agents.** *Journal of medicinal chemistry* 2010, **53**(20):7414-7427.
183. Chen JJ, Li CM, Wang J, Ahn S, Wang Z, Lu Y, Dalton JT, Miller DD, Li W: **Synthesis and antiproliferative activity of novel 2-aryl-4-benzoyl-imidazole derivatives targeting tubulin polymerization.** *Bioorganic & medicinal chemistry* 2011, **19**(16):4782-4795.
184. Alves FRD, Barreiro EJ, Fraga CAM: **From Nature to Drug Discovery: The Indole Scaffold as a 'Privileged Structure'.** *Mini-Rev Med Chem* 2009, **9**(7):782-793.
185. Xiao M, Ahn SJ, Wang J, Chen JJ, Miller DD, Dalton JT, Li W: **Discovery of 4-Aryl-2-benzoyl-imidazoles as Tubulin Polymerization Inhibitor with Potent Antiproliferative Properties.** *Journal of medicinal chemistry* 2013, **56**(8):3318-3329.
186. Lu Y, Chen JJ, Wang J, Li CM, Ahn S, Barrett CM, Dalton JT, Li W, Miller DD: **Design, Synthesis, and Biological Evaluation of Stable Colchicine Binding Site Tubulin Inhibitors as Potential Anticancer Agents.** *Journal of medicinal chemistry* 2014, **57**(17):7355-7366.
187. Fujioka H, Murai K, Kubo O, Ohba Y, Kita Y: **One-pot synthesis of imidazolines from aldehydes: detailed study about solvents and substrates.** *Tetrahedron* 2007, **63**(3):638-643.
188. Lee SH, Kohn H: **Cyclic disulfide C(8) iminoporfiromycin: Nucleophilic activation of a porfiromycin.** *J Am Chem Soc* 2004, **126**(13):4281-4292.
189. Guinchard X, Vallee Y, Denis JN: **Total synthesis of marine sponge bis(indole) alkaloids of the topsentin class.** *J Org Chem* 2007, **72**(10):3972-3975.
190. Hwang DJ, Wang J, Li W, Miller DD: **Structural Optimization of Indole Derivatives Acting at Colchicine Binding Site as Potential Anticancer Agents.** *Acs Med Chem Lett* 2015, **6**(9):993-997.
191. Etienne-Manneville S: **From signaling pathways to microtubule dynamics: the key players.** *Curr Opin Cell Biol* 2010, **22**(1):104-111.
192. Yue QX, Liu XA, Guo DA: **Microtubule-Binding Natural Products for Cancer Therapy.** *Planta Med* 2010, **76**(11):1037-1043.
193. Dong M, Liu F, Zhou H, Zhai S, Yan B: **Novel Natural Product- and Privileged Scaffold-Based Tubulin Inhibitors Targeting the Colchicine Binding Site.** *Molecules* 2016, **21**(10).
194. Chen J, Liu T, Dong XW, Hu YZ: **Recent Development and SAR Analysis of Colchicine Binding Site Inhibitors.** *Mini-Rev Med Chem* 2009, **9**(10):1174-1190.
195. van Otterlo WAL, Ngidi EL, de Koning CB: **Sequential isomerization and ring-closing metathesis: masked styryl and vinyloxyaryl groups for the synthesis of benzo-fused heterocycles.** *Tetrahedron Lett* 2003, **44**(34):6483-6486.
196. Robert C, Long GV, Brady B, Dutriaux C, Maio M, Mortier L, Hassel JC, Rutkowski P, McNeil C, Kalinka-Warzocho E *et al*: **Nivolumab in Previously Untreated Melanoma without BRAF Mutation.** *New Engl J Med* 2015, **372**(4):320-330.

197. Vinay DS, Ryan EP, Pawelec G, Talib WH, Stagg J, Elkord E, Lichtor T, Decker WK, Whelan RL, Kumara HMCS *et al*: **Immune evasion in cancer: Mechanistic basis and therapeutic strategies.** *Semin Cancer Biol* 2015, **35**:S185-S198.
198. Farkona S, Diamandis EP, Blasutig IM: **Cancer immunotherapy: the beginning of the end of cancer?** *Bmc Med* 2016, **14**.
199. Pellegrini F, Budman DR: **Review: Tubulin function, action of antitubulin drugs, and new drug development.** *Cancer Invest* 2005, **23**(3):264-273.
200. Stanton RA, Gernert KM, Nettles JH, Aneja R: **Drugs That Target Dynamic Microtubules: A New Molecular Perspective.** *Med Res Rev* 2011, **31**(3):443-481.
201. Liu YM, Chen HL, Lee HY, Liou JP: **Tubulin inhibitors: a patent review.** *Expert Opin Ther Pat* 2014, **24**(1):69-88.
202. Dong MQ, Liu F, Zhou HY, Zhai SM, Yan B: **Novel Natural Product- and Privileged Scaffold-Based Tubulin Inhibitors Targeting the Colchicine Binding Site.** *Molecules* 2016, **21**(10).
203. Klute K, Nackos E, Tasaki S, Nguyen DP, Bander NH, Tagawa ST: **Microtubule inhibitor-based antibody-drug conjugates for cancer therapy.** *Oncotargets and therapy* 2014, **7**.
204. Teicher BA, Chari RVJ: **Antibody Conjugate Therapeutics: Challenges and Potential.** *Clin Cancer Res* 2011, **17**(20):6389-6397.
205. Edfeldt F, Evenas J, Lepisto M, Ward A, Petersen J, Wissler L, Rohman M, Sivars U, Svensson K, Perry M *et al*: **Identification of indole inhibitors of human hematopoietic prostaglandin D-2 synthase (hH-PGDS).** *Bioorganic & medicinal chemistry letters* 2015, **25**(12):2496-2500.
206. Richardson TI, Clarke CA, Yu KL, Yee YK, Bleisch TJ, Lopez JE, Jones SA, Hughes NE, Muehl BS, Lugar CW *et al*: **Novel 3-Aryl Indoles as Progesterone Receptor Antagonists for Uterine Fibroids.** *Acs Med Chem Lett* 2011, **2**(2):148-153.
207. Zeng R, Dong GB: **Rh-Catalyzed Decarbonylative Coupling with Alkynes via C-C Activation of Isatins.** *J Am Chem Soc* 2015, **137**(4):1408-1411.
208. Hoffman WH, Biade S, Zilfou JT, Chen JD, Murphy M: **Transcriptional repression of the anti-apoptotic survivin gene by wild type p53.** *The Journal of biological chemistry* 2002, **277**(5):3247-3257.
209. Chandele A, Prasad V, Jagtap JC, Shukla R, Shastry PR: **Upregulation of survivin in G2/M cells and inhibition of caspase 9 activity enhances resistance in staurosporine-induced apoptosis.** *Neoplasia* 2004, **6**(1):29-40.
210. Wang HJ, Gambosova K, Cooper ZA, Holloway MP, Kassai A, Izquierdo D, Cleveland K, Boney CM, Altura RA: **EGF regulates survivin stability through the Raf-1/ERK pathway in insulin-secreting pancreatic beta-cells.** *Bmc Mol Biol* 2010, **11**.
211. Chen YQ, Li DM, Liu HL, Xu HB, Zheng HH, Qian F, Li W, Zhao CL, Wang ZH, Wang XJ: **Notch-1 signaling facilitates survivin expression in human non-small cell lung cancer cells.** *Cancer Biol Ther* 2011, **11**(1):14-21.

212. Coumar MS, Tsai FY, Kanwar JR, Sarvagalla S, Cheung CHA: **Treat cancers by targeting survivin: Just a dream or future reality?** *Cancer Treat Rev* 2013, **39**(7):802-811.
213. Rauch A, Hennig D, Schafer C, Wirth M, Marx C, Heinzl T, Schneider G, Kramer OH: **Survivin and YM155: How faithful is the liaison?** *Bba-Rev Cancer* 2014, **1845**(2):202-220.
214. Xiao M, Wang J, Lin ZT, Lu Y, Li ZM, White SW, Miller DD, Li W: **Design, Synthesis and Structure-Activity Relationship Studies of Novel Survivin Inhibitors with Potent Anti-Proliferative Properties.** *Plos One* 2015, **10**(6).
215. Wang J, Li W: **Discovery of novel second mitochondria-derived activator of caspase mimetics as selective inhibitor of apoptosis protein inhibitors.** *J Pharmacol Exp Ther* 2014, **349**(2):319-329.
216. Xiao M, Wang J, Lin Z, Lu Y, Li Z, White SW, Miller DD, Li W: **Design, Synthesis and Structure-Activity Relationship Studies of Novel Survivin Inhibitors with Potent Anti-Proliferative Properties.** *PLoS One* 2015, **10**(6):e0129807.
217. Wang J, Chen J, Miller DD, Li W: **Synergistic combination of novel tubulin inhibitor ABI-274 and vemurafenib overcome vemurafenib acquired resistance in BRAFV600E melanoma.** *Mol Cancer Ther* 2014, **13**(1):16-26.
218. Hwang DJ, Wang J, Li W, Miller DD: **Structural Optimization of Indole Derivatives Acting at Colchicine Binding Site as Potential Anticancer Agents.** *ACS Med Chem Lett* 2015, **6**(9):993-997.
219. Akiyama S, Fojo A, Hanover JA, Pastan I, Gottesman MM: **Isolation and genetic characterization of human KB cell lines resistant to multiple drugs.** *Somat Cell Mol Genet* 1985, **11**(2):117-126.
220. Robey RW, Shukla S, Finley EM, Oldham RK, Barnett D, Ambudkar SV, Fojo T, Bates SE: **Inhibition of P-glycoprotein (ABCB1)- and multidrug resistance-associated protein 1 (ABCC1)-mediated transport by the orally administered inhibitor, CBT-1((R)).** *Biochem Pharmacol* 2008, **75**(6):1302-1312.
221. Carmichael J, DeGraff WG, Gazdar AF, Minna JD, Mitchell JB: **Evaluation of a tetrazolium-based semiautomated colorimetric assay: assessment of chemosensitivity testing.** *Cancer Res* 1987, **47**(4):936-942.
222. Mahindroo N, Connelly MC, Punchihewa C, Yang L, Yan B, Fujii N: **Amide conjugates of ketoprofen and indole as inhibitors of Gli1-mediated transcription in the Hedgehog pathway.** *Bioorganic & medicinal chemistry* 2010, **18**(13):4801-4811.
223. Di L, Kerns EH, Li SQ, Petusky SL: **High throughput microsomal stability assay for insoluble compounds.** *Int J Pharm* 2006, **317**(1):54-60.
224. Davies B, Morris T: **Physiological-Parameters in Laboratory-Animals and Humans.** *Pharm Res-Dordr* 1993, **10**(7):1093-1095.
225. Lu C, Li P, Gallegos R, Uttamsingh V, Xia CQ, Miwa GT, Balani SK, Gan LS: **Comparison of intrinsic clearance in liver microsomes and hepatocytes from rats and humans: Evaluation of free fraction and uptake in hepatocytes.** *Drug Metab Dispos* 2006, **34**(9):1600-1605.

226. Cheng JB, Motola DL, Mangelsdorf DJ, Russell DW: **De-orphanization of cytochrome P450 2R1: a microsomal vitamin D 25-hydroxylase.** *The Journal of biological chemistry* 2003, **278**(39):38084-38093.
227. DeLuca HF: **Vitamin D: the vitamin and the hormone.** *Federation proceedings* 1974, **33**(11):2211-2219.
228. Pike JW: **Intracellular receptors mediate the biologic action of 1,25-dihydroxyvitamin D3.** *Nutrition reviews* 1985, **43**(6):161-168.
229. Korf H, Decallonne B, Mathieu C: **Vitamin D for infections.** *Current opinion in endocrinology, diabetes, and obesity* 2014, **21**(6):431-436.
230. Bikle DD: **Vitamin D receptor, a tumor suppressor in skin.** *Canadian journal of physiology and pharmacology* 2015, **93**(5):349-354.
231. Chiang KC, Chen TC: **The anti-cancer actions of vitamin D.** *Anti-cancer agents in medicinal chemistry* 2013, **13**(1):126-139.
232. Li YC: **Vitamin D receptor signaling in renal and cardiovascular protection.** *Seminars in nephrology* 2013, **33**(5):433-447.
233. Plum LA, DeLuca HF: **Vitamin D, disease and therapeutic opportunities.** *Nat Rev Drug Discov* 2010, **9**(12):941-955.
234. Kulie T, Groff A, Redmer J, Hounshell J, Schrage S: **Vitamin D: an evidence-based review.** *Journal of the American Board of Family Medicine : JABFM* 2009, **22**(6):698-706.
235. Cheung FS, Lovicu FJ, Reichardt JK: **Current progress in using vitamin D and its analogs for cancer prevention and treatment.** *Expert review of anticancer therapy* 2012, **12**(6):811-837.
236. Stein MS, Wark JD: **An update on the therapeutic potential of vitamin D analogues.** *Expert opinion on investigational drugs* 2003, **12**(5):825-840.
237. Leyssens C, Verlinden L, Verstuyf A: **The future of vitamin D analogs.** *Frontiers in physiology* 2014, **5**:122.
238. Sherman MH, Yu RT, Engle DD, Ding N, Atkins AR, Tiriach H, Collisson EA, Connor F, Van Dyke T, Kozlov S *et al*: **Vitamin d receptor-mediated stromal reprogramming suppresses pancreatitis and enhances pancreatic cancer therapy.** *Cell* 2014, **159**(1):80-93.
239. Li W, Chen J, Janjetovic Z, Kim TK, Sweatman T, Lu Y, Zjawiony J, Tuckey RC, Miller D, Slominski A: **Chemical synthesis of 20S-hydroxyvitamin D3, which shows antiproliferative activity.** *Steroids* 2010, **75**(12):926-935.
240. Tuckey RC, Janjetovic Z, Li W, Nguyen MN, Zmijewski MA, Zjawiony J, Slominski A: **Metabolism of 1 alpha-hydroxyvitamin D3 by cytochrome P450scc to biologically active 1 alpha,20-dihydroxyvitamin D3.** *J Steroid Biochem* 2008, **112**(4-5):213-219.
241. Kutner A, Zhao H, Fitak H, Wilson SR: **Synthesis of Retiferol Rad(1) and Rad(2), the Lead Representatives of a New Class of Des-Cd Analogs of Cholecalciferol.** *Bioorg Chem* 1995, **23**(1):22-32.
242. Posner GH, Crawford K, Siu-Caldera ML, Reddy GS, Sarabia SF, Feldman D, van Etten E, Mathieu C, Gennaro L, Vouros P *et al*: **Conceptually new 20-epi-22-oxa sulfone analogues of the hormone 1alpha,25-dihydroxyvitamin D(3): synthesis and biological evaluation.** *Journal of medicinal chemistry* 2000, **43**(19):3581-3586.

243. Harris CE, Chrisman W, Bickford SA, Lee LY, Torreblanca AE, Singaram B: **Enamine oxidations .2. Selective oxidative cleavage of beta,beta-disubstituted enamines using alumina supported permanganate. Synthesis of one-carbon dehomologated carbonyl compounds from enamines.** *Tetrahedron Lett* 1997, **38**(6):981-984.
244. Lu Y, Chen J, Janjetovic Z, Michaels P, Tang EK, Wang J, Tuckey RC, Slominski AT, Li W, Miller DD: **Design, synthesis, and biological action of 20R-hydroxyvitamin D3.** *Journal of medicinal chemistry* 2012, **55**(7):3573-3577.
245. Teicher BA: **Antibody-Drug Conjugate Targets.** *Curr Cancer Drug Tar* 2009, **9**(8):982-1004.
246. Wang W, Wang EQ, Balthasar JP: **Monoclonal Antibody Pharmacokinetics and Pharmacodynamics.** *Clin Pharmacol Ther* 2008, **84**(5):548-558.
247. Carter PJ, Senter PD: **Antibody-drug conjugates for cancer therapy.** *Cancer J* 2008, **14**(3):154-169.
248. Feld J, Barta SK, Schinke C, Braunschweig I, Zhou YY, Verma AK: **Linked-In: Design and Efficacy of Antibody Drug Conjugates in Oncology.** *Oncotarget* 2013, **4**(3):397-412.
249. Pietersz GA, Krauer K: **Antibody-Targeted Drugs for the Therapy of Cancer.** *J Drug Target* 1994, **2**(3):183-215.
250. Lin ZT, Marepally SR, Ma DJ, Kim TK, Oak ASW, Myers LK, Tuckey RC, Slominski AT, Miller DD, Li W: **Synthesis and Biological Evaluation of Vitamin D3 Metabolite 20S,23S-Dihydroxyvitamin D3 and Its 23R Epimer.** *Journal of medicinal chemistry* 2016, **59**(10):5102-5108.
251. Lin Z, Marepally SR, Kim TK, Janjetovic Z, Oak ASW, Postlethwaite AE, Myers LK, Tuckey RC, Slominski AT, Miller DD *et al*: **Design, Synthesis and Biological Activities of Novel Gemini 20S-Hydroxyvitamin D-3 Analogs.** *Anticancer research* 2016, **36**(3):877-886.
252. Lin ZT, Marepally SR, Ma DJ, Myers LK, Postlethwaite AE, Tuckey RC, Cheng CYS, Kim TK, Yue JM, Slominski AT *et al*: **Chemical Synthesis and Biological Activities of 20S,24S/R-Dihydroxyvitamin D3 Epimers and Their 1 alpha-Hydroxyl Derivatives.** *Journal of medicinal chemistry* 2015, **58**(19):7881-7887.
253. Lu Y, Chen JJ, Janjetovic Z, Michaels P, Tang EKY, Wang J, Tuckey RC, Slominski AT, Li W, Miller DD: **Design, Synthesis, and Biological Action of 20R-Hydroxyvitamin D3.** *Journal of medicinal chemistry* 2012, **55**(7):3573-3577.

VITA

Qinghui Wang was born in Fuzhou, Jiangxi Province, China in 1985. He graduated from Jiang University of Traditional Chinese Medicine with a Bachelor of Engineering in 2007. He entered Peking University Health Science Center in 2008 and obtained his Master of Science (advisor: Dr. Mingying Shang) in Pharmacognosy. Starting from August 2011, he studied at The University of Tennessee Health Science Center and joined Dr. Wei Li's lab in Spring 2014. He is the recipient of Robert A. Magarian Outstanding Podium Presentation Award in the 43rd annual MALTO Medicinal Chemistry-Pharmacognosy Meeting-in-Miniature hold in Houston.